BEHAVIOUR AND EFFICIENCY OF PERIMETER PILE GROUPS

by

Alexis Victoria Rose

A dissertation submitted for the Degree of

Doctor of Philosophy

City University London

Geotechnical Engineering Research Group

School of Engineering and Mathematical Sciences

January 2012

Contents

List of Tables

List of Figures

List of Symbols

Soil properties

α	Adhesion factor
β	Failure angle through clay
c	Apparent cohesion
δ	Angle of friction between pile and soil
D_{50}	Mean particle size
E	Young's Modulus
ϕ	Friction angle
G_s	Specific gravity
γ	Unit weight
μ	Coefficient of friction
ν	Poisson's ratio
s_u	Undrained shear strength
s_{ut}	Undrained shear strength at pile toe
τ_f	Shear strength at failure
τ_s	Shear strength of shaft
W_L	Liquid limit
W_P	Plastic limit

Soil stresses

K	Earth pressure coefficient
K_o	Earth pressure at rest
OCR	Overconsolidation ratio
p'	Mean normal effective stress
p_o	Vertical overburden pressure
q'	Deviator stress
σ	Total stress
σ'	Effective stress
σ_h	Horizontal total stress
σ_v	Vertical total stress
t	Load applied to pile head
z	Settlement of pile head

Pile references

A	Pile area
B	Pile group breadth
d	Pile diameter
FoS	Factor of safety
G	Group factor

η	Efficiency
L, l	Pile length, embedded pile length
λ	Pile group length (plan)
N	Bearing capacity factor
n	Number of piles
n_c	Number of piles in a column
n_r	Number of piles in a row
P	Pile perimeter
P_c	Contact pressure
Q	Capacity
Q_a	Allowable capacity
Q_b	Pile base capacity
Q_{calc}	Capacity from calculation
Q_s	Pile shaft capacity
Q_{test}	Capacity from test
Q_{ult}	Ultimate capacity
R_{cs}	Cross sectional ratio
s	Pile spacing

Centrifuge properties

a_i	Inertial radial acceleration
g	Gravity
h_m	Depth in model
h_p	Depth in prototype
N_g	Gravity scaling factor
r	Radius from centre of rotation
r_o	Ratio of over-stress
r_u	Ratio of under-stress
R	Radius from centre of rotation
R_e	Effective centrifuge radius for the model
R_t	Radius to the top of the model
σ_{vm}	Vertical stress in model
σ_{vp}	Vertical stress in prototype
ω	Angular velocity (radians/seconds)

Acknowledgements

I owe most of my acknowledgements of thanks to my Supervisor, Professor Neil Taylor, who managed to make the many complications of centrifuge testing seem just about accessible to me. I am extremely appreciative of all his contributions, support and advice throughout my research, and for being a wonderful friend with such inspiring intelligence. I am also grateful to various members of the Geotechnical Research Group at City University; in particular Dr Richard Goodey for patiently helping me with so many of my early centrifuge tests. Also thanks to our talented technicians, Melvyn Hayes and Keith Osbourne, along with Professor Sarah Stallebrass and "the boys", who helped out along the way.

Many people contributed towards my Thesis in a variety of ways: Firstly, Ceri Hobbs, for making me aware of the project and persuading me I was capable of completing the PhD, also for his encouragement. I would like to thank John Atkinson for checking a number of chapters and his valuable comments; to Chris Raison, Dinesh Patel and Jim Martin for helping me along the right path, in terms of the approach and practical applications. The funding from EPSRC was gratefully received, and I should also acknowledge GCG and Hugh St John for their financial support and for the initial concept of the research project.

The Cannon Place redevelopment in London was an interesting aspect of this research and I was assisted by a number of people: first and foremost I wish to thank Tony Taylor, for his enthusiasm and for taking the time to explain the project to me. I would also like to thank Jim Fraser and Foggo Associates for their financial contributions and allowing me access to all the data; as well as Angela Beckwith for taking me on many site visits during construction.

My experience in Canada at the University of Western Ontario was exceptional. For that, I would like to thank my Canadian Supervisor, Dr Hesham El Naggar for all his assistance, both with my research and with making the trip happen. I would also like to extend my most sincere gratitude to Erol Tas, Zeyad El Sherbiny and Ahmed Abd Elaziz for all their time and efforts in helping me get to grips with Abaqus. Furthermore, I am hugely grateful to Arul Britto, for all his online help from Cambridge University. In addition, I wish to thank Nadir Ansari and Mary Ellen Bruce, for their tireless encouragement and for supporting my trip to Canada and assisting my attendance at invaluable events to showcase my research in the UK, Canada and America.

My final, most heartfelt thanks are for my parents, who gave support in every way possible.

Declaration

I grant powers of discretion to the University Librarian to allow this dissertation to be copied in whole or in part without further reference to me. This permission covers only single copies made for study purposes, subject to normal conditions of appropriate acknowledgement.

Abstract

Groups of piles are commonly used as high capacity foundations. It is recognised that the load distribution among piles in a group will vary and it is thought that the inner piles are likely to make a relatively small contribution to the total load carried. The essence of the research undertaken is to establish the relative effectiveness of pile groups with either no inner piles (perimeter group) or a single central pile (target group) when compared to the more commonly used grid group arrangement. Pile groups in which the central piles were omitted were used for the Cannon Place redevelopment in London and provided the impetus for the research project.

The main research technique used is geotechnical centrifuge modelling. Samples of overconsolidated kaolin clay were prepared and tested on the centrifuge at City University London. This provided a firm clay into which pile groups could be installed in a wide variety of arrangements. Three or four different pile groups were located in each centrifuge model and loaded to failure using a strain-rate controlled load actuator. The individual model piles were made of 5 mm diameter aluminium rod placed in holes pre-drilled in the consolidated kaolin prior to the centrifuge test. All piles extended to a depth 250 mm in the clay giving an l/d ratio of 50. The ranges of pile groups tested are linear, circular and square perimeter, circular and square target and square grid. Single pile tests provided the reference pile capacities used to normalise the data from the 23 centrifuge models tested.

The experimental work was complemented by a parametric numerical modelling study using the finite element programme Abaqus. This gave insight into the pile-soil interaction and permitted a more meticulous analysis of the soil stresses and displacements. In addition, the numerical modelling enabled extension to the original variables tested as part of the centrifuge experiments and the soil shear strength and l/d ratio were varied.

The pile groups failed in one of two ways: either as individual piles with the piles settling into the ground with no noticeable settlement of the soil surrounding a pile, or as a block with the soil contained within the outer ring of piles settling by the same or

similar amount as the piles. The change from block failure to individual pile failure often occurred at a pile centre-to-centre spacing of about two pile diameters though variables such as number of piles, the presence of a target pile and the strength of the soil all had an effect.

The efficiency of a pile group is defined as the load capacity of a pile group expressed as a ratio of the number of the piles in the group multiplied by the load capacity of a single isolated pile. It was demonstrated that a grid group arrangement was the least efficient of the groups tested, whereas a perimeter group arrangement could achieve higher efficiencies of greater than unity and the inclusion of a target pile could further enhance the group efficiency. It has been shown that a target group comprised of 17 piles (16 piles plus one central pile) has a significantly higher efficiency than a 5x5 grid group comprised of 25 piles, such that the capacity at lower settlements is the same for both groups.

1 Introduction

1.1 Background

> *"...Construction of groups of piles can be an effective and practical means of forming high capacity foundations in confined spaces. However, the inner piles within a group of uniformly and closely spaced piles may make little contribution to the group performance. In this case, the group capacity becomes dependent upon the geometry of the envelope rather than the capacity of the single piles. Under these conditions the most efficient group may be one which comprises a ring of piles around the periphery of the area defining the group, with all central piles omitted..."*
>
> *[discussions of initial concept, 2008]*

The research is linked to a construction project in the City of London. The foundations for part of the Cannon Place redevelopment incorporate 11 pile groups arranged as square and rectangular 'perimeter groups'. This foundation design solution was adopted principally because of the numerous site constraints, but has gone on to win awards for the degree of ingenuity involved. More details of the project are given in Chapter 3.

The purpose of this project was to explore characteristics of pile groups that are installed in a perimeter group arrangement, which can be described as a group where the piles are closely spaced around the perimeter only, leaving a body of soil in the centre (see Figures 1.01 and 1.02). Such pile groups may be installed when it is necessary to carry large loads in confined spaces but there is currently little experience of the performance that could be expected. It has been suggested that central piles within a group may contribute little to the overall capacity, and this research aims to answer this supposition. The main issues concern the geometry of the group; the

number of piles, the spacing and the shape in which they are arranged. These properties will affect the soil-pile interaction and consequently the overall behaviour of the group, and thus its efficiency.

Initially, the capacity of a line of piles, such as in a bored pile wall, was investigated. The capacity is usually assumed to be based on the geometry of an envelope comprising the planes to the rear and front tangential to the wall and the base area between them (see Figure 1.03). This approach needed to be compared with the capacity of the individual piles and requires an understanding of how the installation of piles in close proximity to each other affects the capacity of the pile group and how the soil in between the piles responds when the piles are loaded. With an initial insight into the behaviour and the mechanisms by which the piles fail, the work was then expanded to more complex group arrangements, as well as forming a baseline comparison with traditional 'grid' group layouts. A key feature of the experiments was to use single pile correlation and a reliable system for measuring the shear strength of the clay so that each model, which comprised a number of pile group tests, could be compared with all other models, regardless of the soil sample in which it was tested.

1.2 Synopsis

This centrifuge research project was aimed at exploring the behaviour of perimeter pile groups in firm/stiff clay. The number of piles, pile spacing and group geometry were varied, whilst the pile diameter and pile length remained constant. The pile dimensions represent the highest length/diameter (l/d) ratio (l/d = 50) that was practicably possible for modelling purposes using the centrifuge facility at City University London. A high l/d ratio was sought to best represent the equivalent prototype.

Apparatus was specifically developed to allow centrifuge testing of a number of perimeter groups within a single clay sample and to allow the installation of piles with high positional accuracy. Aluminium model piles were installed in overconsolidated kaolin clay; they were loaded under monotonic axial loading conditions and tested to failure. Each of the initial tests comprised four groups of five piles in a linear

arrangement and at a variety of pile to pile spacing ranging from 1.0 to 3.0 pile diameters, d. The main purpose of the linear group tests was to ascertain if there is a relationship between pile spacing and load capacity. The subsequent tests aimed to investigate the geometry of perimeter groups and how the pile arrangement affects the failure mechanism, the group capacity and thus the pile group efficiency. The properties under investigation are summarised in Table 1.01.

It is reasonably widely accepted that pile groups in clay have an efficiency of less than one, which means that the group capacity is less than nQ, where n is the number of piles in the group and Q is the capacity of a single isolated pile. Efficiency is defined and discussed fully in the literature review, in Section 2.3. However, the definitions given are more specifically the solution for groups installed in a grid arrangement and the same rule does not necessarily apply to perimeter groups. There is often confusion and contradiction surrounding the design of pile groups and how the capacity of each given pile is affected by each neighbouring pile. The research was aimed to further the understanding of the behaviour of pile groups and to see how this knowledge can then be applied to practical situations.

1.3 Actions and objectives

The research involved a series of physical model tests supported by numerical analyses and was, where possible, related to the monitoring that was carried out in connection with the work on site at Cannon Place. The main objective of the research was to provide an understanding of the behaviour and efficiency of perimeter pile groups. To achieve this, the principal actions were:

- Design and commission of apparatus
- Establish a repeatable test method
- Determine the capacity of a single pile
- Evaluate the relationship between pile spacing and group capacity for linear groups
- Assess the likelihood of block failure for perimeter groups
- Compare the efficiency of grid groups with previous publications

- Observe the relationship between pile spacing, group size and geometry
- Suggest a solution for the design of pile groups, in terms of efficiency

1.4 Thesis summary

➢ Chapter 2: Literature Review

The literature review is divided into five relevant sections as follows: design of piles in clay soil; pile spacing and group efficiency; pile-soil interaction under axial load; centrifuge testing of pile groups in clay; and existing research into perimeter pile groups. A whole range of information sources has been researched and reviewed, including journal papers, conference proceedings, books, design codes, theses, along with several other engineering publications.

➢ Chapter 3: Cannon Place Redevelopment

An introduction to the construction project at Cannon Place is explained. This redevelopment was the initial driver behind the research project and includes 11 perimeter groups. A summary of the pile design, the construction of the pile groups and the related monitoring is included (comparisons have been made between Cannon Place monitoring data and the centrifuge and numerical modelling in following chapters).

➢ Chapter 4: Centrifuge Modelling Theory

The chapter begins with an introduction to centrifuge modelling, the principles and associated scaling laws. There are a number of sources of error concerned with this test method, which are discussed. A précis is given of the specific centrifuge facility at City University London.

➢ Chapter 5: Centrifuge Testing

The entire process of centrifuge testing from clay preparation to test completion is explained. It includes a description of all the apparatus components, the preparation of the soil sample and a detailed step-by-step procedure of the model creation. The

instrumentation involved in recording the data is presented, along with an explanation of the test methodology.

- Chapter 6: Centrifuge Analysis

This chapter is concerned with describing, discussing and analysing all of the tests completed. Twenty-three tests were undertaken, which includes approximately 50 successful pile group tests, incorporating a wide variety of arrangements. Those tests that were deemed unsuccessful are also discussed, along with the lessons learned and consequent modifications.

- Chapter 7: Numerical Modelling

The numerical modelling was undertaken using the software programme Abaqus. This chapter gives an introduction to Abaqus, along with a description of each aspect of the model that was constructed and the various modifications that were made between tests.

- Chapter 8: Numerical Analysis and Comparison

This chapter continues on from the description in the previous chapter. The results of the modelling are described and analysed and a comparison is made with the results from the centrifuge modelling. In addition, the modelling allowed an insight into soil movements and stresses and also permitted efficient testing of different variables.

- Chapter 9: Discussion

These few pages are a discussion of all relevant facets of the research, which need to be revisited and embellished before the final conclusions are drawn.

- Chapter 10: Conclusions and Further Work

This aim of this chapter is to summarise all the pertinent findings and conclude with what has been learned from this research and indicates what other work could lead to further understanding of this topic.

2 Literature Review

2.1 Introduction

The literature review has been divided into the following five sections:

- Design of piles in clay soil
- Pile spacing and group efficiency
- Pile-soil interaction under axial load
- Centrifuge testing of pile groups in clay
- Existing research into perimeter pile groups

Publications from a wide range of sources have been studied and their significance to this research topic and the proposed model tests is discussed. Sections 2.2 to 2.6 present the key information that has been discovered; Section 2.7 goes on to summarise and critique these findings in the context of the research project.

2.2 Design of piles in clay soil

2.2.1 Pile design equations

The first established journal paper on the design of single piles in clay was written by Skempton and published in 1959. Since then, little of the fundamental design has changed, but this first paper has been supplemented by much additional research.

Skempton stated that current pile design requires calculation of end bearing capacity, shaft capacity and the working load calculated by applying a factor of safety (FoS), as well as a reduction factor applied where piles have been placed in a group.

The basic equation for ultimate pile capacity, Q_{ult}, originally stated by Skempton becomes:

$$Q_{ult} = s_u P \alpha L + s_{ut} N A \qquad \text{(Equation 2.1)}$$

Where $s_u P \alpha L$ is the shaft friction component and $s_{ut} NA$ is the end bearing component and the equation is comprised of the following parameters:

s_u	undrained shear strength (average over the effective length of the pile)
P	pile perimeter
α	adhesion factor
L	pile length (effective)
s_{ut}	shear strength at the pile toe
N	bearing capacity factor
A	pile cross-sectional area

The equation is limited for use with piles loaded under undrained conditions. For circular piles loaded at depth within a mass of clay, N is generally considered to be equal to 9. The evidence for this is given by Skempton (1951) but the two principal theories are those of Mott, later developed by Gibson (1950) and Meyerhof (1951). The allowable capacity, Q_a, is given by the equation:

$$Q_a = (GQ_{ult}) / FoS \qquad \text{(Equation 2.2)}$$

Skempton explains that the factor of safety is applied partly to minimise settlements and partly to allow for any unknowns. The value adopted is usually dependent on pile testing and information available from the ground investigation; where little information is available, a value of 3.0 is commonly used. The group factor, G, is equal to 1 for an isolated pile, but where the piles are closely spaced G is less than 1. Whitaker (1957) reports on an experimental investigation and found that for piles spaced at 3.0 d, G lies between 0.7 and 0.8 depending on the number of piles and the slenderness ratio. However, it should be noted that his tests were carried out using very soft clay. Whitaker's paper is discussed in more detail in Section 2.3.

The ultimate capacity of a pile is reached when the pile first continues to settle at a steady rate under constant load (or the maximum load in a constant rate of strain test). At lower loads the rate of settlement decreases with time and eventually becomes zero. Pile loading tests (Skempton, 1959) have shown that for piles between

300 to 600 mm diameter, the settlement at the ultimate capacity is approximately 0.085 d. The findings of Skempton, which relate to the design of bored piles in London Clay have remained the cornerstone of bored pile design. The formula of pile capacity has gone virtually unchanged and the findings are still generally as outlined in his original paper.

2.2.2 The adhesion factor

Skempton (1959) analysed records of loading tests on bored piles in London Clay from 10 sites. The ratio, α, of adhesion developed on the shaft, to the average undisturbed shear strength of the clay, s_u, was found to be about 0.45. This value of α applies a factor to the s_u value to take account of the different friction at the pile-soil interface compared with the soil-soil interface. The value of less than unity was felt to be largely because the clay immediately adjacent to the pile shaft absorbs water during drilling and also from the wet concrete used to form the pile. A range of α values were calculated and were found to be as high as 0.6 and as low as 0.3, depending on the geology, method of installation and workmanship. However, since this publication, piling techniques have advanced and higher values are now more common, as discovered by Burland (1973). In 1959, bored piling methods using winch operated tripod piling rigs were common for installing replacement piles and the construction duration would have led to extended softening of the clay, compared with modern methods of replacement pile installation.

Burland gives a wider range of values that α may take; between 0.3 and 1.5 depending on soil and type of pile. However, in practice, it is considered ill-advised and virtually unheard of to use an α value of greater than unity. Following a large number of tests it has been possible to develop correlations of values to particular types of pile in various ground conditions (e.g. Tomlinson 1963 and 1971). Generally, the α value reduces from unity for piles in clay of low strength, down to 0.5 or less for clay of strength greater than 100 kPa.

The relationship that exists between s_u and α is often presented in a graphical format such as is shown in Figure 2.01. Each of the three graphs shows the relationship for

different stratigraphy, and further differentiates for different l/d ratios. Generally speaking, the lower the s_u, the higher the value of α and the higher the rate of change of the α value.

2.2.3 Alternative design methods

Burland (1973) outlined an approach to calculating the shaft resistance of piles in clay. Whereas Skempton's method used the undrained strength of the clay, Burland's method used effective stress principles. Burland states that failure of the soil usually takes place some distance beneath the base of the pile and therefore much of the soil involved in shearing will not have suffered disturbance during installation. However, this is only really significant for large diameter piles with a relatively low slenderness ratio. In the long term, the soil beneath the base will normally experience an increase in effective stress and so an increase in strength. Therefore, the undrained bearing capacity represents a safe lower limit. As stated by Burland, using undrained strength to calculate end bearing seems justified, but there is little reason for using undrained strength to calculate shaft adhesion when the major shear distortion is confined to a thin zone (Cooke & Price, 1973) and drainage will take place rapidly.

The shear strength of soils is largely determined by the frictional forces arising during slip at the contact between the soil particles. This is a function of the stress transmitted by the soil skeleton rather than the total normal stress. The maximum shear resistance on a plane through the soil is often given by:

$$\tau_f = c' + \sigma' \tan\phi' \qquad \text{(Equation 2.3)}$$

τ_f shear strength (peak)

c' effective apparent cohesion

σ' normal effective stress

ϕ' effective friction angle

The effective stress approach to shaft friction in stiff clay is more complex. The approach described is similar to that outlined by Chandler (1966, 1968). The following

equation is still assumed to apply (although less so for driven piles) but there is a problem estimating the value of K.

$$\tau_s = p_o' K \tan\delta \qquad \text{(Equation 2.4)}$$

τ_s shaft friction

p_o' vertical effective overburden pressure

K earth pressure coefficient

δ angle of friction between pile and soil

According to Burland, the value of K can be greater than 3 near the surface and less than 1 at depth. Therefore, the first step is to estimate the shaft friction corresponding to $K = K_o$, an 'ideal pile' where initial stress conditions are not altered during installation. Values of K_o at various depths in London Clay have been deduced from laboratory tests by Skempton (1961) and others. Failure will be in the remoulded soil and for London Clay, $\phi' = 22^\circ$ (remoulded drained angle of friction).

Fleming et al (1992) agree that provided the pile is formed promptly after excavation of the shaft, little change in the in-situ effective stress state in the soil should occur, and Equation 2.4 may be applied. In heavily overconsolidated soil, some allowance for stress relaxation should be made with a reduction in K value. The friction angle to be used for Equation 2.4 is debatable. The surface for most bored piles will be sufficiently rough to ensure failure takes place in the soil around the pile rather than exactly at the interface. However, it has been suggested (for example, by Burland & Twine, 1988) that a residual angle of friction is appropriate, particularly for piles in stiff heavily overconsolidated clay.

Fleming (1992) states that the long-term, drained (effective) end-bearing capacity of a pile in clay will be considerably more than the undrained capacity. However, that the settlements required to mobilise the drained capacity would be far too large to be tolerated by most structures. It is known that pile capacity can increase with time, particularly for driven piles in clay (or fine grained) soils. The change in capacity is brought about by pore pressures, which are in excess during pile installation, but then

dissipate and the soil will consolidate. Therefore the water content of the soil will decrease and so the shear strength will increase.

In summary, the effective stress method is good for soft clays, but for stiff clays the approach is more difficult. For London Clay values of K_o have been estimated and used to obtain a relationship between τ_s and the mean depth for an 'ideal pile'. Comparison with pile test results appears to confirm that this ideal relationship gives an upper limit of τ_s for bored piles and a lower limit for driven piles (Burland, 1973).

2.2.4 Components of capacity: Q_s and Q_b

Burland & Cooke (1974) detail a method for determining Q_s (Equation 2.2) for piles with a wide range of dimensions. In fine grained soils, the frictional component is generally much greater than the end bearing, unless the pile has been constructed with an enlarged base (underreamed). The significance of the geometry was not appreciated until Whitaker and Cooke (1966) carried out tests separating the shaft and base components of the load capacity of the pile. Their results show that the two components of load capacity are mobilised at different magnitudes of settlement, as shown in Figure 2.02.

The frictional resistance develops rapidly and linearly with settlement and is generally fully mobilised at 0.5 % of the pile diameter (0.05 d) and thereafter it remains constant, with no load increase. Whereas the base resistance is rarely fully mobilised until settlement reaches 10 to 20 % of the base diameter (0.10 to 0.20 d). This value is slightly higher than that suggested by Skempton. The load vs settlement behaviour of a pile is normally far from linear, although it is often convenient to assume it is linear for loads of less than one third of the ultimate base resistance.

Some settlement caused by consolidation will invariably occur and the movement will cause further load capacity to be mobilised at the base. If the total load is unchanged during this time, the load transferred to the soil by the shaft must fall to the same extent as the base load increases. So, the components will change, but the overall factor of safety will remain constant (Whitaker & Cooke, 1966).

Fleming et al (2009) comment that the shaft capacity is mobilised at typically 0.5 to 2 % of the pile diameter (0.005 to 0.02 d), whereas the base capacity may require displacements as large as 5 to 10 % of the pile base diameter (0.05 to 0.10 d) for full mobilisation. Once the pile shaft capacity has been fully mobilised, the 'stiffness' of the pile-soil system reduces to that of the pile base and then the displacements start to increase rapidly.

2.2.5 Design of pile groups in clay soil

Piles are often installed in groups and tied together by means of a pile cap. Failure of this pile group may occur either by failure of the individual piles, or failure of the overall block of soil. Section 2.3 goes on to discuss the concept of pile group efficiency, so all that will be said for now is that in certain situations, the capacity of a pile within the group may be reduced by comparison to a single isolated pile. This is especially likely in the case of driven piles into sensitive or soft clays.

Fleming et al (1992) provide details on the design of pile groups. They state that in the case of block failure, soil between the piles may move with the piles, resulting in failure planes that follow the periphery of the group, or in some cases, localised rows of failure may occur (see Figure 2.03). In general, block failure is associated with close spacing of piles, although quite what constitutes a 'close spacing' is mostly undefined in literature, or at least, cannot be agreed upon. Fleming instructs that independent calculations should be made of both the block capacity and the individual pile capacities, to ensure that there is an adequate factor of safety against both modes of failure.

Fleming, along with numerous other Authors, explains that the axial capacity of a group failing as a block may be calculated the same way as for a single pile (using Equation 2.1), but now using parameters: perimeter, P, and area, A, for the whole block, rather than a single pile, which assumes that the full shear strength of the soil is mobilised around the perimeter of the block. In addition, the bearing capacity factor needs to be recalculated accordingly, from the equation:

$$N = 5(1+0.2B/\lambda) \cdot [1+(l/12B)] \qquad \text{(Equation 2.5)}$$

B group breadth (plan)

λ group length (plan)

l embedded pile length

It should be noted that the settlement needed to mobilise the base capacity of the block will usually be very large (e.g. 5 to 10 % the width of the group). Since the end-bearing pressure would be much more significant than the skin friction, block failure only becomes more likely than the failure of the individual piles where the increase in base area is offset by a substantial decrease in surface area, therefore piles with a higher slenderness ratio are less likely to fail in this way.

Pile group settlement and load-distribution under pile caps and piled rafts is discussed in great detail in the literature, most notably by Randolph and Poulos. However, these complex and extensive subjects are beyond the focus of the research and will not be discussed in this review, with the exception of a short paragraph on load distribution in Section 2.3.3.

2.3 Pile spacing and group efficiency

2.3.1 Pile spacing

Whitaker (1957) carried out a series of experiments on groups of model piles investigating the effect that neighbouring piles have on each other. The experiments were carried out in soft remoulded London Clay, with a shear strength of between 4 and 9 kPa and groups of piles in a grid layout, 3x3, 5x5, 7x7 and 9x9 were tested. Two modes of failure of the pile groups were observed; block failure where the central soil is incorporated and the group appears to behave as one large foundation; and individual failure where the piles fail as separate entities. It was found that the transition from block failure to individual pile failure occurred at a spacing of 1.75 d for piles 24 d long in a 5x5 group; whereas the transition occurred at 2.25 d for piles 48 d long in a 9x9 group. Graphs of all these results are shown in Figures 2.04 and 2.05. This behavioural transition (the pile spacing where block failure shifts to individual failure) was at progressively closer spacing for shorter piles and smaller groups. The transition

found by Cooke (1974) is slightly higher than that found by Whitaker, although this could be due to a number of factors, for example the method of pile installation or the shear strength of the clay. The values are generally in agreement with each other.

Barden and Monckton (1970) advanced the work undertaken by Whitaker and included tests in soft and stiff clay, with undrained shear strengths of 7 and 106 kPa respectively. The tests involve the consolidation of powdered clay (at a water content of 1.5 x W_L) using a Rowe consolidation cell and the installation of groups of driven piles. Steel rods of 3.2 mm diameter and 102 mm in length were driven 63 mm into the clay in square groups of 3x3 and 5x5. The piles were connected by a rigid cap, which was well clear of the clay and the groups were left 24 hours between driving and starting the tests. The results indicated that block failure occurs for pile spacing less than 2.0 d in both soft and stiff clay, which is slightly less, although concurrent, with the results of Whitaker (1957) and Cooke (1974).

A peak capacity was found at a pile spacing of 2.0 d and there was then a drop in capacity with increased pile spacing, before a final increase in capacity, as the spacing further increased (see Figure 2.06). The Authors put the increase in capacity down to local strengthening of the clay in the region of the closely spaced groups, following the dissipation of the pore pressures induced by pile driving. However, this is unlikely to be true in the case of bored piles, so it is probable that a different pattern of results will be observed from such tests. The possibility of clay strengthening greatly complicates the application of the simple efficiency formulae such as the Converse-Labarre equation, which is discussed in Section 2.3.2.

Cooke (1974) discusses the subject of pile spacing and group efficiency. It is noted that piles forming a group are frequently installed at close pile spacing, typically 2.0 to 4.0 d. Cooke specifically defines the efficiency as the ratio of the average load per pile in a group when failure occurs (continued settlement at constant load), to the ultimate bearing capacity of a comparable single pile. The settlement ratio is best defined as the settlement of a pile group divided by the settlement of a single pile when both carry the same proportion of their ultimate load. Cooke's model experiments concluded with the following observations:

- Increased efficiency with increased spacing
- Maximum settlement ratio at 2.5 d, falling with increased spacing (for a constant number of piles)
- Block failure common where spacing is less than 2.5 d
- Rigid cap on ground surface increases capacity at pile spacing of more than 2.5 d (at the expense of greater settlement)

The block capacity of a group may be less than the sum of the individual pile capacities. De Mello (1969) summarised data for pile groups of up to 9x9 piles and showed that block failure did not become pronounced until the pile spacing is less than 2.0 to 3.0 d (again, in keeping with previous research). Full scale tests on a 3x3 pile group in stiff clay (O'Neill, 1983) confirm that the pile group capacity may be estimated with good accuracy as the sum of the individuals (the same as $\eta = 1$). Various findings from research carried out on pile group efficiency in clay have been summarised and are shown in Figure 2.07. Fleming (1992) also suggests a series of efficiency factors, which take into account pile slenderness ratio, pile stiffness ratio, pile spacing ratio, soil homogeneity and Poisson's ratio. However, Fleming et al (2009) postulate that the concept of 'efficiency' of a group is more appropriately used in respect of the stiffness of the foundation, rather than the capacity.

It is agreed by many Authors that the two modes, of individual pile and block failure, should be appraised independently. Large pile groups designed conventionally may have very low efficiencies, which has highlighted the need to improve design methods for such groups, optimising the quantity and location of the piles.

Piles that have a diameter of 300 mm or less and have a relatively high slenderness ratio (50, or higher) are often referred to in practice as minipiles or micropiles. Advice and guidelines relating to the design of pile groups formed with piles of these dimensions are numerous. The British Standard for 'Execution of special geotechnical works – Micropiles' (BS EN 14199:2005) makes the following two statements with regard to spacing:

- The spacing of micropiles shall be considered in relation to micropile type, micropile diameter, length of micropile, the ground conditions, and their group performance.
- The possible interference of one micropile with another during installation should be considered when determining micropile spacing, orientation and installation sequence.

The 'Micropile design and construction guidelines' issued in June 2000 by the US Department of Transportation Federal Highway Administration (FHWA) give slightly differing comments. For friction piles in cohesive soils they recommend a reduction factor of 0.7 where pile spacing is less than 3.0 d, because it is considered that if piles are too closely spaced they will have a negative interaction that will result in a reduced capacity of the group. For gravity grouted piles, they recommend that the soil type and installation method be examined for impact to the effective stress of the soil surrounding the piles, and the impact to the capacity of the pile group.

Despite the slight variation within these two national micropile design guidelines, it is somewhat clear that there has been a recent move away from the fallacy that piles should be spaced at more than 3.0 d and that it comes down to a matter of judgement, which should be based on the particular site in question. What is also apparent is the lack of commitment to any specific advice; generally the guidance is rather vague.

2.3.2 Efficiency design and equations

The efficiency of a pile group is defined as follows:

$$\eta = \text{capacity of pile group} / (n \,.\, \text{capacity of an isolated pile}) \qquad \text{(Equation 2.6)}$$

where n is the number of piles in the pile group.

The Converse-Labarre equation (Bolin, 1941) is an efficiency formula, which calculates the efficiency of pile groups. The equation can be written as follows:

$$\eta = 1 - \{[\arctan (d/s)] / (\pi/2)\} \,.\, \{2-(1/n_c)-(1/n_r)\} \qquad \text{(Equation 2.7)}$$

η efficiency

d pile diameter

s centre-to-centre spacing

n_c number of piles in a column

n_r number of piles in a row

The equation is restricted to pile groups installed in a grid formation and cannot be directly applied to a group installed in a perimeter group arrangement. In addition, it does not take into account variations for installation technique, slenderness ratio or soil type. However, a modification of the formula, with partial factors to allow for the aforementioned variations, may prove a reasonable starting place for a pile group design formula.

Terzaghi and Peck (1948) consider that the use of efficiency formulae is contrary to good design, since no consideration is given to the wide range of varying factors, for example: pile type, ground conditions and l/d ratio. However, in 1967 they put forward their own method, suggesting that the group capacity is the lesser of the sum of the ultimate capacities of the individual piles, or the ultimate capacity of the block, which is given by:

$$Q_{(block)} = B_g L_g s_u N + 2L(B_g + L_g)s_u \qquad \text{(Equation 2.8)}$$

B_g plan width of pile group

L_g plan length of pile group

L pile length

s_u undrained shear strength

N bearing capacity factor

Feld (1943) used the idea of interference and suggested a rule whereby the calculated bearing value of a pile in a group is reduced by one-sixteenth for each adjacent pile. So, for example, in a 5x5 square group the corner piles are reduced by three-sixteenths, and the central pile is reduced by half. Thus, Feld's rule would state that the efficiency of the 5x5 group is the same, whether the central pile is present or not.

Kerisel (1967) put forward a series of reduction factors, which he suggests apply to closely spaced pile groups in clay. The factors are such that a group of piles spaced at 2.5 d centres would be reduced by 45 %, at 4.0 d centres by 25 %, and only at a spacing of 10 d centres did he consider that there would be no reduction factor. It is a surprise to learn that these reduction factors are conjured up from "some codes of practice", which are unexplained and unreferenced in the publication (Kerisel, 1967).

2.3.3 Load distribution

The experiments on load distribution (Whitaker, 1957) showed that for a large range of loading, the corner piles take the largest and the centre piles the smallest proportion of load and the proportion of load taken increases with distance from centre of the group. As a function of test conditions, these results may be of restricted use in their application to the behaviour of piles in stiff clays.

It is known that for a stiff pile cap, load is highest at the corners and also along the edges. For a flexible pile cap, the load is distributed more evenly, but often at the cost of higher settlements at the centre caused by a dishing effect of the pile cap.

Cooke (1974) demonstrated how interaction between piles within a group caused a significant reduction in the load carried by the inner piles, particularly when closely spaced. In a 25-pile square group at pile spacing of 2.0 d, each of the corner piles was found to carry five times as much load as the centre pile; other piles carried loads roughly proportional to their distance from the centre. This raised questions as to whether many of the piles installed within such groups are really necessary, but of course, if a reduction in the numbers of piles increases settlements then the significance needs to be examined carefully.

2.4 Pile-soil interaction under axial load

2.4.1 Load transfer analysis

Cooke & Price (1973) have progressed advances in the subject of strain and displacement around friction piles. They comment that important knowledge has been gained in understanding the manner in which friction piles transfer load to the

supporting soil using instrumented piles but that relatively little attention had been paid to the behaviour of the soil surrounding the piles. They reference the theoretical studies by Butterfield & Banerjee (1971) and Poulos & Davis (1968) and their discoveries showing how settlement and load transfer are related to soil properties and pile dimensions. However, Cooke & Price note that before these findings can be applied to design, the underlying assumptions (in particular the effect of installation on the shear modulus of the clay) need to be verified by field experiments.

A test involving a steel tubular pile installed in London Clay showed that movements were greatest within a distance of about 2.0 d (horizontally) of the shaft surface, but were measurable at distances greater than 10 d from the shaft. The clay within about 1.0 d from the shaft was considerably disturbed during installation and the shear modulus in this zone was reduced significantly. The load transfer from the pile to the soil increased with depth at a greater rate than the shear strength of the clay.

Motta (1994) presented an elastic perfectly plastic solution in a closed form for axially loaded single piles under design loads based on the method of the t-z (load vs settlement) curves. The solution allowed the prediction of vertical pile movements with depth. Different from elastic solutions, the method can take into account (to some extent) the non-linear behaviour of the t-z curve. An analytical t-z curve that gives results in good agreement with the experimental ones is the hyperbola proposed by Chin (1972). The Chin method is very simple and widely used. Chin observed that the plot of the settlement, versus the ratio settlement/capacity very frequently results in a linear relationship when the pile approached failure. If this curve is conveniently modified into an elastic perfectly plastic t-z curve, it enables a closed-form solution to be used to predict the pile settlement and load distribution. It has been expressed in the form:

$$z / t = mz + C \qquad \text{(Equation 2.9)}$$

- z — the pile head total settlement
- t — the applied load on the pile head
- m — the slope of the linear plot

C a constant (corresponding to the initial slope of the t-z curve)

Thus, if z/t is plotted against an abscissa of z, a linear plot is obtained and the inverse of the slope (1/m) gives an asymptotic limiting value of t. It is often reported that the Chin method leads to over predictions, but at the same time, it is accepted that the linear functions predict pile performance very well. Fleming's CEMSET method (1992) is generally considered an advancement of Chin's method and as a result it usually gives more accurate predictions. The improvement is principally because Fleming's model can distinguish the two components of shaft friction and base resistance; also, it can predict elastic shortening. Brinch Hansen's 80 % criterion (1963) is an alternative method, whereby the pile capacity is defined as the load that gives four times the movement of the pile head as obtained for 80 % of that load.

Coyle & Reese (1966) observe that the ratio of load transfer to soil shear strength (percentage shear strength developed) is a function of pile movement and depth. A relationship is established between load transfer, soil shear strength and pile movement which can be used to calculate theoretical t-z curves. However, strictly speaking the relationship is limited for use with steel tubular piles.

Most piles exhibit some shaft compression at working loads, which should be accounted for in estimating pile deflection. The extent of compression will reduce with depth and will form a component of the total settlement. Also, the load will vary down the pile as the load is shed into the surrounding soil and so it can be shown that very little load reaches the base of long piles, although this less so for groups of piles. Compression of the pile head may lead to a large relative movement between the pile shaft and the soil, which may result in a reduction in shear transfer from a peak value of shaft friction to a residual value. However, strain softening behaviour can also have consequences for the ultimate capacity of long piles, where a form of progressive failure becomes possible.

2.4.2 Numerical methods

The response of piles under axial load has been examined extensively using numerical methods, in particular integral equation or boundary element methods (BEM). Such

methods show how the settlement of a pile depends on parameters such as pile geometry, pile stiffness and soil stiffness.

Randolph (1994) commented that the most rigorous treatment of piles and pile groups is provided by the BEM as described by Poulos & Davis (1980), Banerjee & Butterfield (1981) and Poulos (1989). Randolph noted that pile design was still centred around the axial capacity of isolated piles and the performance of the group was assessed through the use of interaction factors and group efficiencies derived from elastic theory. In order to be accurate, attention must be paid to the non-linear response of the soil. However, for most conventional pile groups the non-linear effects are only significant at very high load levels.

Finite element and boundary element analyses of the response of friction piles have shown that the load is transferred from the pile shaft by shear stresses generated in the soil on vertical and horizontal planes. A pile may be considered as surrounded by concentric cylinders of soil, with shear stresses on each cylinder. For vertical equilibrium, the magnitude of the shear stress on each cylinder must decrease inversely with the surface area of the cylinder (Cooke, 1974). However, resulting deflections decrease with the logarithm of distance from the pile axis, and so significant deflections extend some distance away from the pile, up to about one pile length (Fleming et al, 2009).

Numerical techniques are readily available to analyse the detailed response of the piles and the pile cap. One approach is to consider the area occupied by the pile group as a region of reinforced soil. Often, the primary aim of pile foundations is to limit settlements to acceptable levels, in particular differential settlements (the main source of structural damage). In general, but depending on exact structural loading, the main pile support is best placed towards the centre of the foundation, preventing the normal tendency of the foundation to dish in the centre. Randolph shows from an example calculation that even for a fully flexible raft a few piles located at the centre of a raft can reduce differential settlements by a factor of two, compared to a conventional pile group extending beneath the complete raft.

2.5 Centrifuge testing of pile groups in clay

Al-Mhaidib (2005) describes the results of an experimental study investigating the influence of loading rate on the behaviour of pile groups in clay. The pile groups tested were 2x1, 3x1, 2x2, 2x3 and 3x3 with a spacing of 3.0 or 9.0 d. The load vs settlement, axial capacity and group efficiency were investigated.

The loading rate had a significant influence on the load vs displacement response, where the faster loading resulted in a stronger soil response. The influence on magnitude of the pile head displacement at failure was negligible. The rate of loading was found to affect markedly the axial capacity; the increase in capacity caused by a 100-fold change in loading rate was about 30 %. The relationship between logarithm of loading rate and axial capacity was linear. The Author makes observations that the effect of loading rate on the efficiency of the pile group is insignificant and for the same pile spacing the group efficiency decreases with an increase in the number of piles in the group. The efficiency values obtained are in good agreement with those calculated from the Converse-Labarre equation.

Saffery and Tate (1961) carried out model tests in remoulded London Clay and found that the faster the rate of loading, the higher the recorded load at failure. They also observed that the settlement at failure did not noticeably change for different loading rates. The experiments also investigated the influence of the sequence of pile driving, which involved varying the order of installation in two 3x3 pile groups. In group A, the central pile was driven first and a corner pile driven last; in group B, a corner pile was driven first and the central pile driven last. In group A, the capacity of the central pile was 60 N and the corner pile 90 N; in group B, the capacity of the central pile was 100 N and the corner pile was 60 N. This result would strongly indicate that the installation sequence has a significant impact on the capacity of the individual piles. The total capacity of the nine piles in group B was only 90 % of the capacity of group A; although it is uncertain whether this occurred as a result of the driving sequence or if this was caused by another factor.

Xu et al (2006) document tests carried out in the geotechnical drum centrifuge at the University of Western Australia. Kaolin clay slurry was prepared to a water content of 120 % and, once consolidated, groups of five piles were jacked in to the sample at a constant rate of 1 mm/s. The results of this research provide useful insights into the significant influence of pile tip area ratio, Ar, and spacing ratio on the stiffness and capacity of single and pile groups in clay. Closed-ended piles (Ar = 1) were used in addition to open thick-walled (Ar = 0.46) and open thin-walled (Ar = 0.13) piles. It was found that shaft friction tended to increase in proportion to Ar, but that pile group efficiency was 0.8 for the closed-ended piles and increased closer to unity for thin-walled pipe piles.

The pile group stiffness efficiency is defined as the axial stiffness of the pile group, divided by the number of piles multiplied by the axial stiffness of a single pile. Stiffness efficiency for thin-walled pipe piles was significantly higher and is such that the overall group stiffness is relatively independent of the pile end condition. It was considered that this research validates the effectiveness of concrete pipe piles.

2.6 Existing research into perimeter pile groups

The FOREVER project (FOundations REinforced VERtically) was a French national project on micropiles, which began in 1993 and concluded in 2001. It had a goal of promoting the use of micropiles, in particular in groups or networks, by establishing an experimental and theoretical basis for their specific characteristics and applications. The pile groups were generally arranged as a square grid of various size and a range of spacings were tested. Pile spacing of pile groups in sand had previously been documented by Lo (1967), Vesic (1969), O'Neill (1983) and numerous others.

Results have shown a positive group effect for groups consisting of a large number of slender piles, which is most likely due to 'soil confinement'; this appears to be at an optimum value for spacing between 2.5 and 4.0 d. Below this value, block failure occurs and above this value the piles behave independently. These results in sand are of limited significance to the current research.

In addition to the groups, networks of piles were tested; a network is defined as a set of closely spaced micropiles in which the majority of elements are inclined in an interlocking manner. The report highlighted that installation technique was an important parameter, but was outside the scope of the study. It was found that in loose to medium dense granular soils a positive network effect could be obtained, but that in dense granular soils it could not. Pile networks are beyond the scope of the current research.

Yetginer, White and Bolton (2006) carried out a series of tests on push-in piles in a 'cell' arrangement, which comprised jacked piles installed at close centres in sand around an enclosed soil block. Two cell foundations, each comprising 12 steel tubular piles were installed and maintained load tests were subsequently carried out. The Authors commented that the most notable feature of the load test results was the very high stiffness and that the response was significantly stiffer than was found for driven or bored piles.

Perimeter pile groups were installed in kaolin clay as part of a research project conducted by Begaj-Qerimi (2009). The work was akin to a field test that was done as part of the Re-Use of Foundations for Urban Sites project (RUFUS), which is funded by the European Union and aims to provide ways of overcoming problems for the re-use of foundations for sustainable development. Eight bored minipiles were installed at 3.0 d pile spacing around the existing foundation, although their capacity was not recorded since the main interest of the project was limited to the effect the group had on the central existing pile. However, the experiments did show that when an existing pile is 'reinforced' with a ring of minipiles, the capacity of the pile is enhanced.

2.7 Literature critique

2.7.1 Design of piles in clay soil

The work carried out by Skempton in 1957 still underpins the basis of pile design in clay soils and generally yields reliable answers. To allow the load carrying capacity of the groups to be better understood, an α value for the model tests has to be determined. The undrained shear strength of the modelling clay (kaolin) will be

measured at the end of each test using a Pilcon hand shear vane. Then, using the capacity found from centrifuge tests on single piles, the Skempton equation (Equation 2.1) can be used to back calculate a value of α for the clay-pile interface.

The rate of loading in the centrifuge tests will be relatively quick and will therefore represent undrained conditions. As a consequence, Skempton's method will be used primarily in the analysis of results, as opposed to Burland's effective stress methods. The kaolin used in the model tests will be a firm clay, with a shear strength of approximately 60 kPa. The phenomenon of increasing capacity with time will not be considered since the piles will be tested relatively quickly after installation.

Pile loading tests overseen by Skempton have shown that (for piles between 300 and 600 mm diameter), the settlement at the ultimate capacity is approximately 0.085 d. On the other hand, Burland and Cooke (1974) argue that the frictional resistance is usually fully mobilised at 0.05 d and the base resistance is considered to be fully mobilised when settlement reaches 0.10 to 0.20 d. Finally, Fleming et al (2009) suggest that the shaft capacity is mobilised at typically 0.005 to 0.02 d, whereas the base capacity may require displacements as large as 0.05 to 0.10 d for full mobilisation.

Skempton, Burland and Cooke, and Fleming, clearly have slightly conflicting views regarding the degree of settlement at which the different components of capacity are mobilised. Also, these 'rules' have generally been generated from field tests, which are significantly different from centrifuge tests. In addition, they are often the results from piles with relatively low l/d ratios, which will take up load differently from piles with higher l/d ratios. In conclusion, the centrifuge tests may well have different outcomes, and the value of settlement suggested by these Authors should only be seen as a guide for what will be used for the centrifuge tests.

Fleming states that in the case of block failure of a pile group, soil between the piles may move with the piles, resulting in failure planes which follow the periphery of the group. He instructs that independent calculations should be made of both the block capacity and the individual pile capacities, to ensure that there is an adequate factor of safety against both modes of failure. The axial capacity of a group failing as a block

may be calculated the same way as for a single pile but now using parameters perimeter, P, and area, A, for the whole block. It should be noted that the settlement needed to mobilise the base capacity of the block will usually be very large (e.g. 5 to 10 % the width of the group).

2.7.2 Pile spacing and group efficiency

Research into pile spacing and group efficiency has been fairly extensive, yet it is still somewhat inconclusive. The experiments carried out by Whitaker (1957) are of great interest because of their numerous similarities to this research. However, fundamental differences such as soil strength, installation technique and test methodology mean that they cannot be directly compared. The same is true for the tests conducted by Barden and Monckton. Numerous tests were done around this time (1950's to 1970's) to try and grasp the influence of pile spacing and its effect on efficiency. However, in more recent years there has been a transition back to the original advice given by Terzaghi and Peck (1948), who argued that devising generalised efficiency equations and rules relating to pile spacing was a step in the wrong direction and that each site should be assessed independently.

Comparisons between this research and previous experiments of other Authors will be critical to the apparent success of these tests. If the experiments can be correlated it will have more stature and will result in an increased confidence in the work. Of course, such comparisons can only be made between groups of the same kind, i.e. grid groups.

The findings of Whitaker, with regard to load distribution are of course only of interest to the square groups, since it can be assumed that the piles within a circular group will share the load equally. Unfortunately, an investigation into load distribution falls outside the scope of the research, but nevertheless is an important factor to consider. Whitaker's results may be applicable to some extent, but again, there are a number of significant differences. This discovery of the partial redundancy of the inner piles is a fundamental part of this research.

The settlement required to mobilise the base capacity of a grid group as a block is known to be large. Therefore, if the benefits of any base capacity can be exploited in perimeter groups then it is probable that these settlements will also be large. These predicted increased settlements may limit the application of perimeter groups to less sensitive structures.

2.7.3 Pile-soil interaction under axial load

Cooke & Price's pile installation test using driven steel tubes found that soil movements were greatest within about 2.0 d (horizontally) of the shaft surface and clay within about 1.0 d from the shaft was considerably disturbed. They also found that the load transfer increases with depth at a greater rate than the shear strength of the clay. These findings may be of some relevance to the model tests, because although the piles are not driven steel tubes, the clay will be cut with a steel tube, which is driven into the clay before the model pile is installed.

Motta's elastic perfectly plastic solution in a closed form for axially loaded single piles under design loads gives results in good agreement with the experimental ones is the hyperbola proposed by Chin (1972). Fleming's CEMSET method (1992) is considered an advancement of Chin's method and has been widely adopted.

Relative movements between the pile shaft and the soil, caused by pile head compression, may result in a reduction in shear transfer to a residual value. Such strain softening may be significant and can also have consequences for the ultimate capacity of long piles, where a form of progressive failure becomes possible. The load will vary down the pile as the load is shed into the surrounding soil and minimal load will reach the base of long piles at the commencement of loading, although this less so for groups of piles.

Numerical analyses have shown that the load is transferred from the pile shaft by shear stresses generated in the soil on vertical and horizontal planes. As reasoned previously, for vertical equilibrium, only soil very close to the pile is ever highly stressed. These findings are very relevant to the current research and further support suggestions by some other Authors that only the soil in the immediate vicinity of the

pile shaft is detrimentally stressed or disturbed, thus questioning the need for piles to be spaced far apart.

Randolph (1994) confirms that group design is based on single pile design with the necessary factors applied and he also shows that 'central piles' can significantly reduce settlements, which was also discussed by Cooke (1974). An interesting advancement of the perimeter groups, which could also be viewed as middle ground between perimeter groups and grid groups, would be perimeter group with a single central pile. The term 'target group' will be coined for such a group.

2.7.4 Centrifuge testing of pile groups in clay

Al-Mhaidib (2005) showed that the loading rate had a significant influence on the load vs settlement response, where the faster loading resulted in a stronger soil response. However, he found that the effect of loading rate on the efficiency of the pile group is insignificant. Saffery and Tate (1961) also found that the faster the rate of loading, the higher the recorded load at failure. In addition, he discovered that the installation sequence has a significant impact on the capacity of the individual piles.

The loading rate of the actuator in the model tests will aim to replicate the speed of loading in a real situation, with scale and acceleration accounted for suitably. The installation sequence will follow a similar pattern as far as possible, for every test.

2.7.5 Existing research into perimeter pile groups

A number of previous research projects have involved investigations into pile group arrangements that are in some ways similar to the perimeter groups involved in this research. Despite this, there are no answers to questions regarding the behaviour or efficiency that may be expected for bored pile groups in clay. Therefore, the research is essential to the understanding of these pile groups.

3 Cannon Place Redevelopment

3.1 Introduction

The research is linked to a £360M construction project in the City of London. The site was previously a 15-storey office block built in the 1960s, which is currently being transformed into a new futuristic-style 8-storey office and retail complex. The Cannon Place redevelopment began in July 2008 and took approximately three years to complete.

The piled foundations for the redevelopment are a combination of old and new and are a complex range of dimensions and pile types. The structural columns in the northern half of the site reuse the existing under-ream piles, supplemented by new settlement reducing piles. The columns in the southern half of the site are founded on new under-ream and large diameter piles where there is sufficient headroom to use a larger rig, and on perimeter pile groups where headroom is restricted. The original design involved hand dug caissons, but this idea was unpopular and eventually rejected on the basis of health and safety concerns. The idea was then modified and developed into this inventive perimeter pile group solution.

The development includes 11 perimeter groups each in a square or rectangular arrangement, comprising between 16 and 24 piles, with each group capable of supporting the 16 MN load imposed. A summary of the pile groups is given in Table 3.01. The piles were 305 mm diameter and approximately 30 m long, therefore with a l/d ratio of about 100. The pile spacing is 500 mm, or 1.64 pile diameters, which was dictated by site constraints as well as the structural capacity requirements and geotechnical limitations. The pile groups will support around one third of the columns. The external group dimensions range from about 2.3 m x 2.3 m to 2.8 m x 3.3 m. The pile layout drawing is shown in Figures 3.01a and 3.01b.

The closely spaced piles will work in conjunction with the virgin London Clay that they enclose and is contained by a 1.5 m thick concrete pile cap. The piling site is

constrained in 2.6 m of headroom and also within a Victorian multi-arch brick viaduct. In addition, the ancient walls and floor slabs of a Roman Governor's Palace, which is a scheduled ancient monument, created further restrictions with regard to positioning of new foundations. The piles were installed through a pre-assembled timber frame containing steel tubes as guides to aid with verticality of the 30 m long piles. This method enabled the 1 in 200 verticality tolerances to be either achieved or bettered.

It was agreed that in lieu of a SIMBAT or similar dynamic test on the existing piles, a system of ground movement monitoring points would be set up whilst the building is constructed and the loads are being applied. The monitoring comprised a system of precise levelling and a number of extensometer installations.

Finally, it should be emphasised that whilst the research project is linked to the foundations at Cannon Place, it is not intended for the centrifuge tests to replicate them. The tests are aimed at giving a broader impression of the behaviour that may be expected for this type of pile group arrangement.

3.2 Pile design

The pile design was a collaborative effort between two specialist geotechnical engineering consultants, one employed by the project design engineers and the other employed by the contractor.

The site is underlain by Made Ground, overlying drift deposits of River Terrace Gravels to a depth of approximately 4.0 m below ground level. The underlying solid geology in which the foundations are cast is comprised of London Clay only. The undrained shear strength of the London Clay around the site can be summarised as $s_u = 80 + 5.13\ z$ kN/m^2, where z is the depth below the top of the clay.

A comprehensive preliminary pile test programme was undertaken as a consequence of the new and original nature of the pile group design. In addition, a number of SIMBAT dynamic pile tests were completed once the concrete had achieved sufficient strength. These tests were done as an alternative to integrity testing, which is not

suitable on piles with high l/d ratios. Analysis of the test pile results showed the range of α values to be between 0.38 and 0.59.

Two initial designs were considered; design A, where the piles fail individually; and design B, where the piles behave as a block and fail around the group perimeter. An α of 0.4 was adopted in design A, which is low compared to the average of the tests but is explained by the phenomenon of so-called 'progressive debonding'. In essence, as the pile approaches its ultimate capacity, the upper section of the shaft will have moved about 10 % of the pile diameter relative the ground, whereas the base of the pile will have moved very little, if at all. This will cause progressive debonding at the top of the pile shaft leaving only residual friction, which will extend down the pile as the applied load increases (Martin el al, 2010). In design B a higher α of approximately 0.7 could be used, since much of the failure plane is through the clay itself. The shaft area is reduced (for these more closely spaced groups) when considering the block as opposed to the sum of the individuals, but the base area of the block is much larger because the central soil is included, which gives higher calculated failure load albeit with larger settlement.

The pile group analysed in the final design (a conservative combination of designs A and B) acts predominantly in skin friction, mobilised on the outer perimeter of the pile group. The corresponding settlement was calculated to be small, with less than 10 mm immediate settlement. With the addition of long-term settlement and elastic shortening of the pile, the overall settlement was expected to be no greater than 20 mm. The stiffness of the perimeter group to a column load acting on it was therefore not expected to differ significantly from a single solid pile of equivalent capacity. In general, the perimeter group ultimate capacity was found to be about 10 % below the single pile ultimate capacity and this is thought to be as a result of ground relaxation caused by construction of adjacent piles (Martin et al, 2010). Axisymmetric finite element analysis was carried out, in addition to 3D analysis, which used the boundary element method.

A programme of precise levelling was put in place and includes measurements on all the main structural columns. This enabled the response of the pile groups to be

monitored during and after building construction. The findings are presented in Section 3.4.

3.3 Construction

A total of 190 micropiles were installed between June and November 2008. On average, two piles were completed per day and were installed using either a Hutte 202 rig, or, where headroom was more restricted, a Klemm 702 rig with a 2.2 m mast. The drilling of the London Clay was undertaken using nominal 0.75 m lengths of 305 mm diameter segmental augers. Good drilling by an experienced operative was crucial to achieve high accuracy installation, in particular concerning the pile verticality.

Temporary casing was installed prior to drilling; the area was excavated to pile cap formation level and the casing placed before backfilling around the casing with dry bentonite gravel mix, which would be easy to remove after piling and was suitable as a piling platform. After pile installation, the temporary casing and backfill was excavated back down to pile cap formation level. The casing worked as a guide over the top few metres and helped achieve excellent verticality.

Following drilling, every borehole was checked visually by shining a light to the base of the borehole. The verticality was also checked using a laser and was found to be exceptionally good; in all but three cases was better than 1 in 200 and the average was 1 in 580.

The piles were always concreted the same day as they were bored and a slump check was always performed prior to accepting the concrete. The specified fluidity was essential to ensure good pumpability and to allow the mixture to flow around the reinforcement cage; after concreting, a 6H16 reinforcement cage was installed over the top 12 m section of the pile.

A pictorial summary of the installation of the pile groups is shown in Figures 3.02 to 3.11, beginning from the process of pile boring and concluding with the placement of the structural column. Figure 3.11 shows the new structural column in place, which allows transfer of load from the new superstructure to the new pile group, bypassing

an old Victorian arch. Every pile group had a structural column installed onto its pile cap, some of which required this technique.

3.4 Monitoring

A programme of precise levelling was designed and implemented to monitor the movements of the main structural columns supported by the pile groups. The programme was, in part, to satisfy the requirements imposed by London Underground Ltd. The limited space and regularly changing foundation areas meant that the monitoring stations had to move location a number of times during the life of the construction project, which has lead to some inconsistency in the results. In general, the monitoring requirements stated that each of the main structural columns needed to be monitored via a total station system. Figure 3.12 shows the load vs settlement curves of two monitoring points on pile caps 4 and 10. Both pile caps have settled approximately 4 mm. It is difficult to tell from the shape of the curves, but both responses appear to be on the initial linear section of a normal load vs settlement curve, which is what would be expected.

4 Centrifuge Modelling Theory

4.1 Principles of centrifuge modelling

One of the advantages of centrifuge testing is that a wide variety of prototype scenarios can be tested relatively quickly and cheaply and under the same controlled test conditions. However, thoughtful planning is required and careful execution to minimise the errors inherent in centrifuge modelling techniques, as discussed in more detail in Section 4.3.

The fundamental principle of centrifuge modelling is that the stress distribution can be reproduced at homologous points in a small scale model as in the full scale prototype. The physics behind the concept is based on Newton's first law of motion, which is sometimes referred to as the law of inertia. If a payload is placed on a platform with its centre of mass at a distance, r, from the centre of rotation and then accelerated to a constant angular velocity, ω, during the test, a condition known as uniform circular motion imposes a radial acceleration, a_i, onto the payload. Or, to put it another way, the law states that pulling a mass out of a straight path into a radial path of radius r, the centrifuge will impose an inward acceleration, a_i, on the mass towards the axis of rotation. The acceleration is a function of the angular velocity and radius from the centre of rotation.

$$a_i = \omega^2 r \qquad \text{(Equation 4.1)}$$

a_i inertial radial acceleration

ω angular velocity

r radius from centre of rotation

Soil behaviour is governed by the stress level and stress history to which the soil has been subjected. The model will be subjected to similar stress history to that assumed for the prototype. As a consequence there is a need to model in situ stresses that change with depth to reproduce the strength and stiffness aspects of soil behaviour.

Physical modelling using a centrifuge involves accelerating a model contained in a strongbox (either rectangular or cylindrical) at the end of centrifuge arm to create an inertial radial acceleration field many times greater than the Earth's gravity. In the model, stress increases rapidly with depth from zero at the surface to values at depth that are determined by the soil density and radial acceleration.

4.2 Scaling laws

4.2.1 Stress

The model is a reduced scale version of the prototype, which need to be related by appropriate scaling laws. Soil behaviour is dominated by the frictional forces between particles and their relationship with the volumetric state of the soil, which is expressed as voids ratio, or specific volume. To enable a centrifuge model to be compared with the prototype, the soil (in the same relative positions) must be at the same stress level. As stated earlier the fundamental principle behind centrifuge testing is the reproduction of the stress distribution of the prototype.

$$\sigma_{vm} = \sigma_{vp} \qquad \text{(Equation 4.2)}$$

For the prototype with material of density ρ, at depth h_p, the vertical stress σ_{vp} is:

$$\sigma_{vp} = \rho g h_p \qquad \text{(Equation 4.3)}$$

Therefore if the density of the material in the prototype is the same as that in the model - and central to the theory of centrifuge modelling is the fact that the acceleration of N_g times the Earth's gravity is applied - then the vertical stress σ_{vm} acting at depth h_m in the model is given by:

$$\sigma_{vm} = \rho g_m h_m \qquad \text{(Equation 4.4)}$$

Where g_m is equivalent to the gravities applied in the centrifuge. From Equation 4.2, Equation 4.5 can be obtained:

$$\rho g h_p = \rho g_m h_m \qquad \text{(Equation 4.5)}$$

And therefore:

$$h_p = N_g h_m \qquad \text{(Equation 4.6)}$$

Where N_g is the number of times greater the gravitational field is in the model compared with Earth's gravity (prototype scale). This allows creation of a small model, which makes testing much more manageable. When tested at inertial acceleration field of N_g times Earth's gravity, the vertical stress at depth h_m in the model should be the same as at depth h_p in the prototype. Figures 4.01a and 4.01b illustrate how inertial stresses in the model correspond to the gravitational stresses in the prototype.

Since the effect of the radial acceleration is to increase the self weight of the model in the direction of its base, with careful choice of model dimensions and radial acceleration, prototype stress profiles which vary with depth can be simulated closely.

4.2.2 Length

The scaling law for length is $1:N_g$ and it affects the geometrical properties of all components used in the model. However, from Equation 4.1 it can be seen that the radial acceleration varies with radius, thus the scale factor is only correct at one particular location in the model. This problem is relatively minor if care is taken to select the radius at which the gravity scale factor is determined, and in doing so reducing areas of under-stress and over-stress. Taylor (1995) quantified the error and showed it is generally less than 3 % if the level of acceleration is chosen at the radius R_e, which is found at a depth of h/3, where h is the model depth from the top of the soil.

4.2.3 Mass

The effect that a mass has on a model is a combination of the increase in force it exerts due to the increase in acceleration level (N_g) and the reduction in soil or foundation area on which it acts ($1/N_g^2$). The combination gives an effective scale factor for mass of $1/N_g^3$.

4.2.4 Force and time

The scaling law for force and time is the same; $1:1/N_g^2$. The application of the scaling law for force is used in the numerical modelling, where the prototype is modelled, rather than the centrifuge scale. The scaling law for time is applied where discussing the rate at which the actuator should advance. This scaling factor is a significant advantage of centrifuge testing, because events such as consolidation and seepage can occur in a vastly reduced time scale.

A summary of the main properties that required application of scaling laws is given in Table 4.01.

4.3 Errors in centrifuge modelling

4.3.1 Acceleration

In trying to model a prototype event it is inevitable that errors will result from testing procedure and the artificial gravity field. The Earth's gravity is uniform for the purpose of problems encountered in civil engineering but the centrifuge generates a slightly variable acceleration throughout the model, Taylor (1995). This is because there is variation in radius over the height of the model causing variation in acceleration (see Figure 4.02). The following paragraphs identify the errors caused by the radial acceleration field in centrifuge model testing.

- Vertical acceleration field

As stated earlier, the stress distribution with depth in the model is non-linear (Taylor, 1995). The vertical stress at any point within the centrifuge model is calculated by taking the average acceleration acting upon the soil above. As acceleration varies linearly with radius this corresponds to the acceleration midway between the point under consideration and the model surface. Care must therefore be taken in model design to ensure that the over-stress at the model base and the under-stress near to the top are within acceptable limits.

Using expressions for the ratios of under-stress (r_u) and over-stress (r_o) to the prototype stress at the same depth and equating the two, it can be shown that the least relative variation is obtained when the required acceleration is set at ⅓ of model depth. Figure 4.03 shows the correct stress at ⅔ model depth and the stress variation with depth in a centrifuge model and its corresponding prototype. A convenient rule for minimising the error in stress distribution is derived by considering the relative magnitude of under and over-stress. By equating the ratios of maximum r_u and maximum r_o the following equation can be derived, where R_e is the effective centrifuge radius for the model and R_t is the radius to the top of the soil sample, as defined in Figures 4.03.

$$R_e = R_t + h_m / 3 \qquad \text{(Equation 4.7)}$$

- Radial acceleration error

The acceleration is also directed towards the centre of rotation. Stewart (1989) described the radial acceleration field that acts in a direction that passes through the axis of the centrifuge. Hence, in the horizontal plane there is a change in its direction relative to vertical across the width of the model. This means that there is an increasing component of lateral acceleration within the model as the distance from the centreline increases. This lateral acceleration will be greatest at the largest offset from the centreline i.e. boundaries at the soil surface.

Error is induced in the stress field due to a lateral acceleration caused by the geometry of most centrifuges and the shape of the model containers. In these tests the model container was positioned so as to minimise any effects caused by lateral acceleration.

4.3.2 Boundary effects

The range of scales at which the prototype may be modelled is controlled not only by the practicalities of instrumentation but also by the boundary effects imposed by the container. The box used for this research is manufactured from aluminium alloy and has internal dimensions of 200 x 550 mm with an internal height of 375 mm.

Phillips (1995) gives guidance on containers and states that side wall friction is always present to some extent and consequently, the model should be sufficiently wide so that it does not create significant problems. Craig (1995) suggests that a minimum distance of 5 pile diameters from the boundaries of the model container is sufficient to minimise these effects.

4.3.3 Modelling effects

The model soil sample was prepared in a consolidation press before the model was assembled and placed on the centrifuge arm. The sample was subjected to vertical pre-consolidation pressure from the loading ram, and after removal from the consolidation press there was no pressure on the sample until it was accelerated in the centrifuge. As a consequence, the soil sample has a different stress history and OCR to many firm/stiff in-situ clays.

Stallebrass (1990) showed that the soil bulk modulus and shear modulus are dependent on mean normal effective stress and overconsolidation ratio (p' and OCR together specify the current specific volume). There will therefore be a difference in the stiffness of the soil model, compared with many firm/stiff in-situ clays. This will also cause a variation in the undrained shear strength profile. Using laboratory and centrifuge tests, Nuñez (1989) determined a method for calculating the undrained shear strength profile of a centrifuge sample of kaolin clay:

$$s_u = 0.22\sigma_v'OCR^{0.62} \qquad \text{(Equation 4.8)}$$

A number of other Authors found similar relationships (Phillips, 1987; Springman, 1989 and Stewart, 1989) but the equation presented by Nuñez provided the best comparison to the measured data.

For Speswhite kaolin clay, permeability is a function of voids ratio (Al-Tabbaa, 1987). Hence, the reduction in permeability with depth may be different in the kaolin clay model compared to in-situ clays, because of differences in the variation of specific volume with depth in the model.

There is a potential problem with the scaling effects of the soil grains. In line with the scaling laws previously stated, the average grain size of the soil in the model should be reduced by $1/N_g$ for correct representation of the prototype grain size. However, since it is considered that the soil behaviour will remain the same and that clay will still behave as clay, regardless of its exact particle size, it is judged suitable to use Speswhite kaolin clay, which has been tested rigorously in the centrifuge and is well understood.

The ratio between the pile diameter, d and the mean particle size D_{50}, can have an effect on failure mechanism and thus may affect the behaviour of the pile. It has been shown that the problem of grain size related errors affecting pile capacity problems in centrifuge modelling can be considered negligible if the d/D_{50} ratio is greater than 30. The d/D_{50} ratio in these centrifuge tests is greater than 2000.

4.4 The geotechnical centrifuge

The Geotechnical Engineering Research Centre at City University uses the Acutronic 661 centrifuge shown in Figure 4.04. The arrangement of the centrifuge, the data acquisition systems and control room is shown schematically in Figure 4.05. It combines a swing radius of 1.8 m with maximum acceleration of 200 g. A package weight of 400 kg at 100 g can be accommodated and this capacity reduces linearly with acceleration to give a maximum 200 kg at 200 g; thus the centrifuge is a 40 g/tonne machine. The package is balanced by a 1450 kg counterweight that can be moved radially on a screw mechanism. The swing platform at one end of the rotor has overall dimensions of 500 mm x 700 mm with usable height of 960 mm in the central area between the arms.

Four strain gauged sensors are used to detect out-of-balance in the base. The signals from these sensors are monitored and if the out-of-balance exceeds the pre-set maximum of 15 kN then the machine is shut down automatically. The machine is situated in an aerodynamic shell which is surrounded by a block wall. This wall is in turn surrounded by a reinforced concrete containment shell. The control room is situated behind the block wall.

The cooling system involves water being supplied from a hydraulic slip ring, which is sprayed into the shell and subsequently evaporates. Electrical and hydraulic connections are available at the swing platform and are supplied through a stack of slip rings. Electrical slip rings are used to transmit transducer signals (which are amplified and converted from analogue to digital by the on-board computer prior to transmission in bits), to communicate closed circuit television signals, supply power for lights or operating solenoids or motors as necessary. The fluid slip rings may be used for water, oil or compressed air.

The data acquisition system features onboard signal amplification for the 64 data-logging channels using a variable gain of up to 1000. The amplifier unit is located close to the centrifuge axis, and together with an onboard PC, converts the analogue transducer signals to digital. The data-logging PC is located in the control room and software allows data to be displayed in real time either numerically or graphically.

5 Centrifuge Testing

5.1 Apparatus

5.1.1 Strongbox

The rectangular strongbox used to contain the model has the following internal dimensions: width = 200 mm, length = 550 mm, height = 375 mm. The walls and base are approximately 40 mm in thickness. The strongbox has a base drainage system consisting of a herringbone network of 3 mm deep grooves, connected to taps at either end of the box. Sample drainage is discussed in more detail in Section 5.2.4 and 5.3.5. The apparatus was designed to allow three or four pile groups to be tested in a single clay sample so that when four groups were tested, the groups would be evenly spaced at 110 mm centres, with a minimum distance of 50 mm between groups and 70 mm from the container boundaries. The geometry of the scale model is 1:60. An aluminium clay cutter was made specifically for the strongbox, to allow accurate cutting of the clay surface to obtain the exact required height of clay sample (see Figure 5.01).

5.1.2 Reference frame

All apparatus is positioned and connected to the strongbox via the reference frame. Figure 5.02 shows a long section of the strongbox highlighting the parts of the apparatus and Figure 5.03 shows two cross sections of the apparatus. The reference frame was initially designed to sit inside the top of the box, but when it was recognised that a greater distance was required between the toe of the piles and the base of the box, two spacers were introduced (one at either end of the box) which allowed the frame to sit on top of the box, 75 mm higher. Each guide plate is located via two pins on top of the reference frame and the pile cap holders are also located via two pins, 70 mm lower, on an internal step within the frame. All guides and holders were screwed down to the reference frame before pile installation took place.

5.1.3 Piles and pile caps

The piles and pile caps are made of aluminium. The piles are all identical in size, whereas the size of the pile cap varies depending on the size of the group, although they are all square in shape and 15 mm in thickness. The differing weight of pile caps is accounted for when calculating the capacity of the pile group, but the average pile cap dimension was approximately 65 x 65 mm. Alternative pile caps of dimension 65 x 20 mm were made for the linear group tests. Each pile cap had two platforms, one at either end, from where the settlement was measured and every hole within the pile cap had a 6 mm thread drilled into the top of the pile cap (see Figure 5.04). The guide plates and pile cap holders were made from 9.5 mm thick aluminium and the pile caps were attached to the pile cap holders via two screws.

The piles are 5 mm diameter aluminium rods, 270 mm long. The effective length of the pile, as far as the test is concerned, is 250 mm; an 11 mm length is exposed between the top of the clay and the base of the pile cap, and the remaining 9 mm is fixed within the pile cap. A thin walled steel cutter with an internal diameter of 5 mm was used to core the clay before pile insertion. The pile installation process is described in detail in Section 5.3. Aluminium is frequently and successfully used in centrifuge modelling (Klotz, 2000; McNamara, 2001) because of its good workability and its similar unit weight to concrete. However, the metallic surface is notably smoother than concrete, although this is not an issue when comparing relative data sets, rather than searching for absolute values.

5.1.4 Displacement transducer brackets

After pile installation, the guide plates and pile cap holders are removed and two displacement transducer brackets are located on the reference frame. The brackets are placed along the length of the strongbox and each support up to four displacement transducers, of type linear variable differential transformers (LVDTs). The LVDTs are connected to the brackets with D-clamps. Each pile cap has an LVDT monitoring settlement at either end to allow an average to be calculated. The purpose of this was to eradicate the effect of possible rotation about the shorter pile cap axis. Rotation

about the longer pile cap axis would not be detected via this method, although it is less likely to occur and its impact can be considered negligible.

5.1.5 Loading frame

The loading frame comprised a number of elements that allowed three or four groups of piles to be loaded at the same or similar times in the same soil model. A single force of up to 10 kN could be provided through the vertical lead screw of a Zimm worm-drive gearbox, having a reduction ratio of 4:1. This screw jack was driven by a horizontal spindle using a DC servo Maxon motor RE35 90W and associated gearhead. To allow for any misalignment, an Oldham coupler with acetal torque disc was used to connect the motor gearbox to the Zimm gearbox. The motor was fitted with an encoder that monitored its rotational speed. This linked to the DC servo amplifiers mounted on the centrifuge and with associated software on a computer in the centrifuge control room the motor could be controlled to an accurate predetermined speed independent of the force being delivered by the screw jack.

In the majority of experiments, the gearhead used had a reduction ratio of 43:1. The vertical descent of the screw jack was set at 0.25 mm/min which meant the Maxon motor was effectively operating at a low rotational speed. In some tests, it was found that the motor stalled and the gearhead was changed to one with a ratio of 156:1, which allowed better operation and control.

To assist assembly and alignment, the motor and screw jack were mounted on a 6 mm thick aluminium alloy plate. This in turn was mounted on a 12.7 mm plate that could span the centrifuge strong box. Stiffening beams were attached to the underside of this plate to minimise deflections of the whole load frame during centrifuge flight. Four 10 mm diameter bolts were used to attach the frame to the strong box.

A 35 mm deep steel beam was attached to the end of the lead screw. The beam was designed to be stiff and to have minimal deflection under estimated loading from the pile groups. Load cells were fastened into this beam at positions coincident with the centres of pile groups being tested. Two 12 mm silver steel guides were attached to the top of the loading beam and passed through plain bearings located in housings

attached to the top of the load frame. The intention was that the guide rods would restrict any tendency of the loading beam to rotate since the pile groups would each develop different loads depending on the numbers of piles, their arrangement and the stage at which a load cell came into contact with a pile cap. A drawing of the loading apparatus is shown in Figure 5.05.

5.2 Clay consolidation

5.2.1 Preparation

An aluminium extension of the same dimensions as the strongbox, except only 300 mm in height, was attached to the strongbox to allow a greater height of sample to be made. A rubber o-ring was fitted in a groove between the two boxes with silicone grease to ensure it was water-tight and in addition, both boxes had a thin coating of white lithium based water pump grease applied to reduce friction on the contact surface. A sheet of 3 mm porous plastic was cut with precision to fit inside the box directly above the base drainage system, to allow the water to flow out but prevent the drains becoming blocked with clay. A sheet of filter paper was then placed on top of the porous plastic sheet to ensure the clay did not get into the porous plastic and to prevent it from sticking.

5.2.2 Kaolin clay

The soil used was Speswhite kaolin clay, which has the following properties:

Specific gravity, $G_s = 2.62$

Liquid limit, $w_L = 65\ \%$

Plastic limit, $w_P = 30\ \%$

London Clay is unfavourable for use in model testing due to its extremely low permeability. Models for clay soils are usually prepared from kaolin owing to its relatively high permeability; the reduced geometrical time scale in the model results in a dramatic speeding up of time related processes, in particular, clay consolidation. The time difference between conducting identical tests in the different soils is significant

and so warrants the use of kaolin clay over a clay that is more commonly encountered in the field.

The clay powder was mixed in a Winkworth industrial ribbon blade mixer to produce a volume of about 80 litres of slurry by adding distilled water until the clay reached a moisture content of 110 %. Approximately 74 litres of the slurry was then slowly poured into the strongbox from a minimal height of not more than 100 mm taking care not to allow the build up of air pockets. Additionally, the slurry was stirred at regular intervals with a palette knife to ensure removal of any air bubbles that may have become trapped during pouring. The clay was then levelled using the palette knife and a sheet of filter paper was placed on top of the clay with a second sheet of tight fitting porous plastic placed above.

5.2.3 Consolidation press

Consolidation took place in a computer controlled hydraulic press. The computer programme combined with a specific PC interface card processed data from the instrumentation and updated voltage output to the convertors controlling air pressure to the hydraulic pump. The elevated pressures required for consolidation are obtained using a pump which amplifies air pressure into oil pressure at a ratio of 1:36.

The sample underwent consolidation in a hydraulic press to a maximum pressure of 500 kPa; the pressure was applied in increments over a 10 day period and consolidation of the sample was monitored by plotting a graph of settlement against time (see Figure 5.06). Once consolidation was complete and the maximum pressure of 500 kPa had been maintained for a minimum of 72 hours, the pressure was then reduced to 250 kPa and the sample was allowed to swell for 24 hours. A given thickness of clay with these properties and under this pattern of pressure changes will consolidate to approximately 55 % of the initial thickness. There have been many clay samples tested by the City University Research Group using the same stress history (e.g. McNamara, 2001; Begaj-Qerimi, 2009). The same stress history was repeated for these experiments, since it was known it would produce a reliable firm clay sample of the required consistency.

5.2.4 Drainage

Drainage took place at the top of the sample, through the holes in the loading plate of the press; and at the bottom of the sample, through the two-way drainage system. A tube was connected to each of the drainage taps and then placed in a container of water, which prevented air from getting back into the system. Once the load began being applied to the sample the taps were opened, which expelled water through the tubes and was collected in the water container. These taps are only closed again immediately prior to removing the sample from the press; this helps minimise swelling by reducing the dissipation of negative pore water pressures.

5.2.5 Pore pressures

Up to four pore pressure transducers (PPTs) were installed in the clay sample during the swelling process. The installation method has been used with success in previous similar research studies (e.g. McNamara, 2001; Begaj-Qerimi, 2009). The PPTs each have a porous stone fitted in front of the transducer and prior to installation the porous stones are de-aired in water, which is subjected to an absolute pressure of between 0.05 and 0.1 atmospheres using a vacuum pump.

Blanking screws were removed from the back of the strongbox at predefined access locations and a guide tube of 60 mm length was then fitted in their place. The strongbox had access ports at depths of 110, 170, 230 and 250 mm from the top and these depths were chosen to give a range over the height of the sample with two readings at the base of the piles. The clay was cored to the centre line of the box using a thin walled cutter; the cutter was placed through the guide to ensure the clay was cored perfectly horizontally. The PPT was then inserted to just beyond the centre point to ensure complete contact between the porous stone and the clay. The void behind the PPT was backfilled with clay slurry placed with a syringe and the threaded plugs along with the rubber washer were fitted into the back wall of the box to give a watertight seal around the PPT lead.

5.3 Model creation

5.3.1 Sample height

After taking the sample out of the press and removing the filter paper and porous plastic sheet the clay was trimmed. The blade of the clay cutter can be adjusted to allow the clay to be cut to the correct height and this was done in increments of about 3 to 5 mm, for ease of operation.

In the preliminary test, 1a, the gap between the base of the pile cap and the top of the clay was only 4 mm, which proved to be insufficient as the clay heaved during the equilibrium phase in the centrifuge and then during loading the pile caps came into contact with the surface of the clay. The gap was subsequently increased to 10 mm to allow sufficient room for the clay to heave and for the settlement of the pile caps under loading without contacting the clay.

In the phase 1 linear group tests, a distance of 33 mm existed between the toe of the piles and the bottom of the box, which was considered acceptable in terms of eliminating boundary effects (because the distance was more than five pile diameters). However, for test phases 2 to 5, with mainly circular or square groups, it was decided that a greater distance should be allowed, so this gap was increased to over 100 mm by using a deeper sample of clay. In the phase 1 tests, the clay surface was cut to a height of 283 mm, 92 mm below the top of the box. For all other tests, the clay was cut to a height of 355 mm, 20 mm below the top of the box.

5.3.2 Clay boring

The model pile foundations were installed in the clay at 1 g prior to placing the assembled model on to the centrifuge arm. This was done as quickly as possible to minimise changes to the soil stress profile. Installation at 1 g, rather than in-flight, is considered acceptable since the analysis of results will focus on the relative load capacity values, rather than the absolute values. Craig (1984) found that when piles are installed at 1 g the effects on subsequent behaviour are less pronounced in clay than in sand, although the real impact and their effects remain a little uncertain.

The clay was cut and extracted using a thin walled stainless steel hypodermic tube with an external diameter of 5 mm, which was pushed through the guide plate then through the pile cap located approximately 75 mm lower (see Figure 5.07). The cutter was pushed in with no torque applied, but once at required depth, the handle was rotated 180 degrees to ensure the clay was fully sheared. This process was adopted to maintain a good verticality. During the preliminary test it was decided that silicone oil would be sprayed inside the cutting tube before the first cut on each pile to reduce friction and further enhance recovery. The cutting was repeated and the clay excavated in five sections for each pile to enhance clay recovery. As the number of piles in a test was set to almost double between the fourth and fifth tests, it was decided to reduce the number of cuts per pile to three, thus reducing the time between taking the sample out of the press, to accelerating the completed model on the centrifuge arm. Unfortunately, the reduction in model construction time was accompanied by a reduction in clay recovery during the coring process; reducing from approximately 85 to 60 % (see Figures 5.08 and 5.09).

5.3.3 Pile installation

The model pile was a 5 mm diameter and 270 mm long aluminium rod, which was pushed into the clay bore. A grub screw, which provided reaction at the top of the pile was tightened into the top of the pile cap. The pile was pushed 5 mm into the pile cap and then the 6 mm grub screw was installed, which meant that the pile was pushed down a further final millimetre. This method ensured contact between the pile and the grub screw, and therefore the pile cap. There was a gap of 11 mm between the base of the pile cap and the top of the clay, thus the toe of each pile was 250 mm below the surface of the clay model. See Figure 5.10 for a photograph of the set-up and Figure 5.11 for a schematic and description of the pile installation process. The piles were always installed in a clockwise order around the group, and where a central pile was included, this was installed last. In the case of grid groups, the piles were installed left to right, one row at a time.

After pile installation the guide plates and pile cap holders were removed and two displacement transducer brackets were located on the reference frame. The brackets

were placed perpendicular to the orientation of the guide plates and each support four displacement transducers, so each pile group therefore has a displacement transducer monitoring settlement on opposite ends of the pile cap to allow an average to be calculated.

5.3.4 Loading apparatus

A 10 kN motor driven screw jack load actuator (Figure 5.12) was bolted to the strongbox, which applied a vertical force to each pile group via a guided stiff load beam. Load cells were connected to the load beam, allowing individual measurement of the force applied to each pile group. Each pile group has a loading guide held in place in a central position on top of the pile cap and this encourages the loading pins (that were attached to the load cells) to apply the load to the centre point of the pile cap. Refer back to Figure 5.05 for a drawing of the apparatus, where the various components are labelled.

5.3.5 Water

Once the pile groups were constructed and the instrumentation connected, the model was placed on the centrifuge arm. The instrumentation and actuator were then connected to the centrifuge control box and a standpipe was connected to the strongbox base drain. The height of the standpipe was calculated so as to model a water table just below ground level. The height was initially 288 mm from the base of the clay sample (when the sample was 283 mm in thickness); but a 360 mm height standpipe was required once the clay sample was increased to a thickness of 355 mm. The standpipe had an overflow pipe surrounding it with a PPT at the base to act as a constant reference to check the height of water in the standpipe was correct.

The top and the bottom boundaries of the clay model control the equilibrium pore water pressure conditions. The model clay layer has an impermeable surface, as it is sealed with silicone oil to prevent the clay from drying out, and a hydrostatically increasing pore pressure with depth. The upper 10 mm layer of the clay is in suction. The drainage base plate was connected to the standpipe. The average water table is at

10 mm below the surface level, but varying from the centre to the sides and ends of the box.

Immediately before accelerating the model, the base drain was flushed out and 350 ml of silicone oil was poured on the clay surface to prevent it from drying out. A number of techniques have been used to try and prevent the oil seeping down between the clay bore and the pile shaft. The most successful proved to be the use of a thin brass ring bund around the outside of the group, 20 mm high and pressed 9 mm into the clay (see Section 5.6). These brass rings were installed before pile installation and the load guide was then located in the centre of the pile cap. The differing effect of these numerous methods was calculated, but since they were found to be so minimal, no adjustment was made to the results.

5.3.6 Acceleration

An acceleration field of 60 g was applied so the model then corresponded to an equivalent prototype pile of 300 mm diameter and 15 m long with an l/d ratio equal to 50. The completed model, including all instrumentation, is weighed, and the counterweight is set accordingly. The weight varied a little between tests, as a function of the groups tested, but generally the weight was about 170 kg, which corresponded to a counterweight offset of 214 mm. In general, for the tests which had more piles, and were therefore more labour-intensive, there was a time lapse of approximately 8 hours between taking the model out of the press and commencing the acceleration of the centrifuge. Ideally, this time period would have been reduced, but this would have come at the cost of the quality of the model, which would not have been acceptable.

The centrifuge gains speed at approximately 3 rpm/s; at 60 g the centrifuge is spinning at about 180 rpm. This complete sequence of events allowed a test to be undertaken within a two week period, as detailed in Table 5.01.

5.4 Instrumentation

5.4.1 Pore pressure transducers

The pore pressure transducers used were Druck type PDCR 81. They are fitted with a porous ceramic front element. The same type of transducer without a porous stone was used to monitor the water level in the standpipe. PPTs were calibrated using arm mounted junction boxes with filters, amplification and a logging system and were calibrated against a pressure transducer which was regularly calibrated in turn against a dead weight system.

5.4.2 Load cells

The load cells were stainless steel, sub-miniature tension or compression Omega load cells and part of the LCMFD series. They are capable of very precise readings of high resolution and the internal design provides excellent stability and minimises the effects of small off-axis loads. The main body of the unit is 25 mm x 14 mm. They have a maximum capacity of 5 kN and were calibrated with a Budenberg deadweight calibration rig numerous times over the duration of the testing programme. The calibration involved using centrifuge mounted junction boxes with filters, amplification and a logging system.

5.4.3 Linear variable differential transformers

Settlements of the piles were measured using linear variable differential transformers (LVDTs). They were Solartron DC 15 mm and were calibrated using a micrometer scale, also involving the centrifuge junction boxes with filters, amplification and a logging system. Like the load cells, they are capable of very precise readings of high resolution, but in reality the accuracy of the readings was limited by the positioning errors of the apparatus, which was in the order of +/- 0.5 mm.

5.4.4 Camera

For the final three tests (5c, 5d and 5e) a camera was installed on the loading apparatus, to allow the movement of the actuator to be monitored. A scale was

marked onto one of the vertical loading beam guides and the end of the motor was also marked to allow an easy assessment of whether it was rotating. With hindsight, the camera should have been present in every test to allow much easier determination of problems relating to the actuator.

5.5 Test methodology

5.5.1 Pore pressure equilibrium

Once the acceleration has been initiated the water feed was opened, which starts supplying water to the model via the standpipe. The PPTs all recorded negative values, implying suction, which is normal at this stage of the test. On the whole, the PPTs recorded data that would be expected, suggesting that equilibrium of the pore pressures had been reached via a regular-shaped pressure vs time graph. However, on a number of occasions there were problems with one or more transducers and the expected behaviour was not observed. Possible reasons for this are given in Section 5.6.

Before the load could be applied, the pore pressures within the clay sample were required to stabilise and reach equilibrium, which took approximately 40 hours.

5.5.2 Loading

Once in equilibrium, the loading actuator was advanced at a constant rate of 0.25 mm/minute. The rate the piles were loaded was intended to reflect loading rates at prototype scale. Assuming the maximum load is achieved in the centrifuge at a displacement of 1 mm, equal to a time period of four minutes, then at prototype scale this time is approximately equal to 10 days, since the scaling relationship is $1:1/N_g^2$. Loading rates at prototype scale can be hugely variable, from a dynamic pile load test at one end of the spectrum, to a lengthy construction period at the other. However, 10 days was considered to be reasonable. Axial loading was continued until no additional load could be sustained by the pile groups.

5.5.3 Post centrifuge test

Immediately after stopping the centrifuge, undrained shear strengths of the clay were measured at a range of depths using a Pilcon hand vane, which was operated in accordance with BS 1377-9. The hand vane gives a very good indication of the undrained shear strength and its accuracy, when used with care, is believed to be about +/- 2 kPa. A full description of the soil strengths that were obtained is given in Section 6.2. Generally, the profiles show a consistent trend, although the shear strengths varied between tests. Anomalies occurred occasionally where surface oil had been lost and the sample began drying out in the centrifuge. Moisture contents were also measured at four staggered depths in every sample. Clay was extracted using a thin walled steel cutter inserted the full depth of the sample and upon extracted the clay was cut into four pieces, recording the location of where each one was taken from. The mean average moisture content for all tests was 46 % and always within the range of 43 and 49 %.

For phase 5 tests, a method was introduced to try and determine with accuracy whether or not the central soil had in fact settled relative to the surrounding soil. In many tests, where no obvious shear surface had formed, indicating definite block failure, there was uncertainty about whether or not the central clay may have settled very slightly. Before testing, the height of the clay surface was measured at a range of locations surrounding each group. The measurements were made on a grid system around the brass ring, which could be easily relocated post-test, as shown in Figure 5.13. Once the model had been taken off the centrifuge arm, the pile caps were removed and the clay height was re-measured at the same locations. In several instances, this showed that the central soil had moved down fractionally further than the surrounding soil, indicating that a type of block failure had occurred. This is discussed further in Section 6.5.6 and 6.6.5.

5.5.4 Model excavation

To help ensure repeatable tests and accurate placement of the reference frame, it would have been undesirable to take the box apart after every test, since the box was machined with precision as a single piece before any experimental work began.

Therefore the clay had to be excavated from the top, whilst taking care not to disturb any of the pile groups or the PPTs. The clay was excavated around the front and sides with a 20 mm diameter thin walled steel tube, the PPTs were then removed with care and the remaining clay sliced into two or three pieces. These clay blocks were then lifted out of the strongbox and the pile groups were carefully exposed using a thin steel wire clay cutter (see Figures 5.14 and 5.15). Upon excavation, it was revealed that the verticality of the piles was exceptionally good. Almost every group showed equal and consistent spacing down the length of each of the piles (see Figure 5.16). The only exception to this was the circular group of 12 piles spaced at 1.25 d. In test 4a, whilst the arrangement appeared flawless at the top, at the base of the group about four of the piles were out of alignment; a similar problem, but to a lesser extent occurred for the same group in test 4b.

The groups were excavated with considerable care to get the best possible view of the clay-pile contact surface and to check the groups had been formed accurately. This careful process allowed early detection of silicone oil that had entered the bore, and in places preventing contact between the pile and the clay. This problem was then remedied, as explained fully in Section 5.6. A range of test photos are shown in Figures 5.17 to 5.21 and are summarised as follows:

- 5.17 – completed model prior to testing
- 5.18 – loading beam and load cell in place above loading point and pile cap
- 5.19 – pile groups in strongbox post test
- 5.20 – plan view of TC18_1.50 showing shear surface
- 5.21 – cross sectional view of PS20_1.50 showing shear surface

5.6 Problems and errors

➢ Oil between clay and pile

Silicone oil found its way down between the pile and the clay bore in all of the early tests, but to slightly differing extents (see Figure 5.22). The problem was initially overcome by creating a clay bund prior to pile installation, and shown in Figure 5.23, although this did not completely eliminate the presence of oil. The problem was finally,

and successfully, overcome by introducing brass rings as shown in Figure 5.24. The rings are 0.5 mm thick by 20 mm high brass shim, cut specifically for each pile group. Each brass ring is pressed 9 mm into the clay with a thick layer of silicone grease pasted around the outside.

Test 1a, the first test, saw no oil prevention methods; tests 1b and 1c used just silicone grease pasted around the piles post installation; tests 2a, 2b, 2c and 2d used clay bunds; all other tests utilised the brass rings. The issue of the presence of oil between the pile and the clay in the earlier tests did cause problems with unquantifiable reductions in capacity. Test results that had to be discarded as a result of this problem are identified in Sections 6.3 and 6.4.

- Loss of surface oil

In a number of tests the surface silicone oil was lost as a result of less than perfect contact between the clay and the sides of the strongbox. Prior to the test going in the centrifuge, every effort was made to ensure good contact, by pressing the clay against the strongbox walls and then applying a silicone grease all around the edge to help prevent oil getting between the clay and the walls. However, despite this, in some cases oil was still lost. In four tests (1d, 3b, 4a and 4c) the oil was lost completely leaving a dry clay surface; which in the most severe case (test 3b) led to small cracks propagating out from the brass rings. The loss of surface oil led to a reduction in moisture content and an increase in shear strength, which produced test samples with different soil profiles from the standard narrow range. However, in the most part, this effect could be nullified by normalising all results against the capacity of a single pile, which was tested a number of times and then back-calculated using the shear strength of the soil and a calculated α value. This is discussed in detail in Section 6.3.4.

- PPTs not registering predicted pressures

This was a recurring problem throughout the duration of testing, for which no reliable solution was found. The cause could have been a number of factors surrounding the preparation and installation, for example: the porous stones were not de-aired properly, the void created to install the PPTs was not backfilled fully or that there was

poor contact between the porous stone and the clay. Occasionally, dissipation of suction to about half the value predicted from an idealised stress path was indicated. Grant (1998) and McNamara (2001) experienced similar problems and it is clear that it is difficult to remedy the problem. Therefore, so long as two of the transducers were registering reasonable predicted pressures, the test was continued and the clay was assumed to be a normal sample. This was confirmed later from the vane strength and water content measurements.

- Loading beam not horizontal

The issue of the loading beam not moving downwards perfectly horizontally became a problem during the phase 2 tests, where pile groups of significantly different sizes were tested within the same sample. For the phase 1 linear groups this was less of a problem because the load sustained by each pile group within the sample was of a similar magnitude. This same issue became a problem again and was modified a second time after test 4a. A yoke comprising a 15 mm deep aluminium alloy plate connected the tops of the two guide rods. This introduced additional stiffness to the loading beam arrangement to restrict potential rotation when the beam was loaded unevenly by pile groups developing significantly different capacities.

- Actuator malfunction (1)

Tests 1a, 1b and 1c were the first three tests completed, all containing 20 piles. The following test, test 2a, contained 36 piles. The larger force required to load all the pile groups within test 2a to failure led to slipping in the friction clamps of the drive coupling, which limited the maximum force that could be applied to the loading beam. The problem was eventually resolved by adding a mechanical shear connector in the coupling, although by this stage the results of a number of phase 2 tests had been affected. The groups that had to be discarded as a result of this actuator malfunction are discussed in Section 6.5.2.

- Actuator malfunction (2)

This problem occurred only in test 4d. There was an electrical fault that caused the actuator to move downwards significantly faster than intended (see Figure 5.25). Within a matter of seconds from initiating the actuator, the load cells had made rapid impact with the pile caps and proceeded to force them into the clay, to a depth of approximately 50 mm. As a consequence, the test yielded no usable data and all pile groups were discarded.

- Actuator malfunction (3)

Fortunately, this problem did not cause any data to be lost or lead to any further pile groups to be discarded, but it did have some effect on the results of test 5c, although the extent of the effect is unknown. After some investigation it was thought that the failed component belonged to the DC servo motor. The consequence was that the movement translated to the loading beam was a little erratic and not a smooth motion like it had been previously. Once the pile groups had taken up some initial load and the associated settlements had reached approximately 0.5 mm, the loading mechanism failed and would not load the pile groups any further. In response, the centrifuge was stopped and the loading recommenced, at the same rate, but at 1 g. The pile groups settled a little further before the mechanism failed once again. This time it was decided to load the groups at an increased rate of strain, rather than abort the test without knowing if the pile groups had reached their ultimate capacity. The strain rate was increased gradually until it finally began working again, at a rate of 20 mm/s, which is 80 times faster than the normal speed.

Following this problem, a different motor was used for the remaining tests. Whilst reasonable data was generated from test 5c and no pile groups were discarded, the results are treated with a degree of caution since for the latter stages of the test, the loading rate was significantly faster. From the literature review, it was revealed that a faster loading rate caused pile groups to appear to have higher capacities.

6 Centrifuge Analysis

6.1 Introduction

6.1.1 Nomenclature

In total, 23 centrifuge tests were done. They were completed in five phases, listed as follows:

- Phase 1: 1a, 1b, 1c, 1d
- Phase 2: 2a, 2b, 2c, 2d, 2e
- Phase 3: 3a, 3b, 3c, 3d
- Phase 4: 4a, 4b, 4c, 4d, 4e
- Phase 5: 5a, 5b, 5c, 5d, 5e

The separation into phases had no particular significance other than to split the work into manageable packages. The tests were carried out in the order listed, with one exception; test 1d was in fact completed after test 2c and before test 2d. All tests will be referred to by the two character reference. A summary of the test programme is given in Table 6.01.

Each group has a seven character reference, which can be described as follows:

For example, PC14_1.75;

- P group type (Perimeter, Target, Grid, Linear)
- C group shape (Circle, Square, Triangle, Line)
- 14 number of piles (ranging from 05 to 25)
- 1.75 centre to centre pile spacing, in pile diameters (ranging from 1.00 to 4.00)

The single pile tests are not specifically referred to, but are simply named as Sx1, Sx2 or Sx3 in Table 6.01, depending on whether the test included 1, 2 or 3 single piles (as explained further in Section 6.3).

6.1.2 Testing overview

The majority of tests included four groups, which were evenly spaced within the model. The first three tests (1a, 1b and 1c) were all linear groups, but when the first perimeter groups were tested it was thought that four groups would be a little too cramped within the box and so the number of groups was reduced to three. The two original positions in the middle were exchanged for one central position. The following eight tests included only three groups: 2a, 2b, 2c, 2d, 2e, 3b, 4a and 4b. Following test 4b the earlier decision was reversed and it was decided that four groups could be installed within the same sample without having a significant influence on neighbouring groups, and that this additional group per test would be very beneficial in maximising data output. Whilst it cannot be ruled out that there may be a limited impact because of the increased proximity, the closest the groups were spaced in any of the four-group tests was 50 mm, which equates to 10 pile diameters.

6.1.3 Failed tests

Of the 23 tests completed, five were considered failures, which meant all of the results were discarded and most of the groups involved in the failed tests were then retested:

- Test 1a – discarded because of the proximity of the clay surface to the pile caps
- Test 1b – discarded because of silicone oil getting between the clay and piles
- Test 1c - discarded because of silicone oil getting between the clay and piles
- Test 2c – discarded because of an actuator malfunction
- Test 4d – discarded because of an actuator malfunction

A number of individual groups within the 18 remaining tests were also excluded because of isolated problems, but the test itself was not discarded. Following a relatively unsuccessful series of phase 2 tests (2a – 2e), the apparatus was taken apart and reassembled for phase 3, along with minor adjustments and reinforcing of the loading frame. Of the 15 groups that made up phase 2, only a few were considered successful. The three groups that comprised test 2c were excluded, as stated above, and further individual groups were excluded from the remaining four tests. Four were discounted because the actuator failed to displace the groups by more than 1 mm and

a further few were discounted because an abnormally high load was apparently generated, which could not be explained. The error may have been caused by a problem within the data logging system although this cannot be confirmed. At this stage it was decided to exclude the triangular groups because of the limited number of test results. In doing so, this reduced the scope of the work and allowed focus on the circular and square groups. In consequence, further groups were excluded and of the five phase 2 tests, only test 2b and 2e yielded any good results, which meant that in fact seven of the 23 centrifuge tests were regarded as unsuccessful.

Phases 3, 4 and 5 were rather more successful and apart from the outright exclusion of test 4d, only a further four groups were discarded. As a summary, each test phase is listed below, along with the total number of groups tested, the number of successful groups and the corresponding success rate:

• Phase 1	4 tests	16 groups	1 usable	6 % success
• Phase 2	5 tests	15 groups	3 usable	20 % success
• Phase 3	4 tests	15 groups*	10 usable	67 % success
• Phase 4	5 tests	18 groups	11 usable	61 % success
• Phase 5	5 tests	20 groups	20 usable	100 % success

*Phase 3 included three groups where the piles were a composite material as opposed to solid aluminium. The inclusion of these tests would correspond to an 87 % success rate. The results of these composite pile tests are denoted by "(A)" in Table 6.01 are discussed in Section 6.8.

6.1.4 Data analysis

The pile cap weight was an important factor that needed to be included in the analysis because each group had some initial load imposed upon it by the pile cap, which was significant under the gravity field of 60 g. Therefore, each pile cap with the grub screws and the loading point used was weighed, then multiplied by 60 and divided by the number of piles in the group. Therefore, each pile had a value that was added to the output from the load cells, which is the reason why the load begins at greater than zero (in the graphs) when the settlement begins at zero. In theory, the multiplication

factor should have been slightly lower than 60, since the pile cap is at a smaller radius than the average R_e for the centrifuge model.

In general, the capacities that will be compared are those that are achieved by the group at a settlement of 1 mm, or 0.20 d, which has been calculated to be approximately 99 % of the peak capacity. In the rare cases where the peak capacity is markedly different from the '0.20 d capacity', then this will be referred to as well. This matter is discussed in more detail in the following sections, but it should be understood that the default capacity is the capacity at 0.20 d settlement, with the exception of single piles which is discussed in Section 6.3.2.

It is realised that this is in slight contradiction to the advice given in Section 2.7.1, where other Authors had found from field tests that the ultimate capacity was expected at lower settlements. However, the tests are noticeably different and therefore it is reasoned acceptable to consider a different value. In addition, Whitaker (1957) revealed that he had struggled to specify a consistent settlement at which ultimate capacity was achieved during his model experiments, which is somewhat reassuring. However, it is very important to note that these values of capacity (achieved at 0.20 d settlement) will not be used for the purposes of establishing a design value, since they are too high. A settlement of 0.20 d would be considered incorrect for pile design and a lower value should be selected, which corresponds to a lower point on the load vs settlement curve. A reasonable design value will be reconsidered in Chapter 8 when the centrifuge work will be analysed together with the results of the numerical modelling.

The reason 0.20 d is considered appropriate for comparing the centrifuge tests is because of the very small dimensions involved, coupled with the allowance of the distance it takes for groups to 'settle down' at the start of the test. It should be noted that the difference between the readings of the two LVDTs per pile cap, was generally in the order of 0.5 mm, but occasionally up to a difference of 1 mm. Whilst it would be preferable for the discrepancy to be smaller, the method of averaging two readings should mean there is minimal affect on the quality of the results.

6.2 Soil strength

The undrained shear strength, s_u, was measured using a Pilcon hand vane as soon as possible after the centrifuge had stopped. Measurements were taken at depths of 50, 100, 150, 200, 250 and 300 mm, and are shown in Figure 6.01. It was intended to keep the s_u of each soil sample exactly the same (with the exception of test 5b, which will be discussed in the following paragraph). However, there was some inevitable variation between tests, with the average s_u over the length of the pile ranging from 47 to 65 kPa. The mean average s_u overall was 53 kPa and of the 15 tests being considered out of the total 23 tests (excluding test 5b because of its reduced strength, the five discarded tests and two unsuccessful tests), 14 fell within an average s_u range of 12 kPa, from 47 to 58 kPa. The variation was caused by a number of factors: differences in initial moisture content, inconsistency in increasing the pressure, differences in model making time, surface oil loss and length of time in the centrifuge. Whilst every effort was made to keep these factors consistent, this was not always possible.

It was decided to create a soil sample with a lower strength by way of comparison. This idea was driven by the observation of a contrasting failure mechanism for an identical group arrangement, which was installed in two separate tests of differing s_u (as discussed in Section 6.6.3). The intention was for this softer soil to have a strength of approximately two thirds of the regular soil. Consequently, the soil was consolidated to a maximum pressure of 350 kPa and the result was a soil sample with average s_u of 33 kPa and an s_u variation of 9 kPa. The s_u variation is the difference between the s_u at the top of the pile and the s_u at the toe of the pile.

Not only was the s_u of the soil measured after every test, but the data were correlated with existing relationships proposed by a variety of Authors (refer to Section 4.3.3). These Authors have made connections between undrained shear strength, effective vertical stress and the overconsolidation ratio. A number of suggested relationships were investigated and the best fit to the measured data was with the relationship proposed by Nuñez (1989), which states that:

$$s_u = 0.22\sigma'_v OCR^{0.62}$$ [from Section 4.3, Equation 4.8]

The line of this equation is shown in Figure 6.02. The relationship slightly under predicts the strength at the top and over predicts the strength at the base. This is what would be expected since there will have been a drying effect at the top of the sample (during model making but especially so if the sample lost silicone oil from the surface), leading to an increased strength. Also, the base of the sample would have undergone some softening leading to a reduced strength.

The variation of s_u within each of the 16 centrifuge tests ranged from 0 to 26 kPa and the samples where the variation in s_u is particularly small are more prone to inconsistent results. However, 11 out of the 16 tests under consideration had a reasonable variation of s_u, of between 19 to 26 kPa.

6.3 Single piles

6.3.1 Arrangement

The capacity of a single pile was tested eleven times. Three single pile tests were included in test 1d, with further experiments carried out in test 3a, 3c, 4c, 4d, 5a, 5b, 5c and 5d. The location of the single pile test was varied so either two or three were done at each of the four locations within the model. For reference, the locations shall be referred to as the channel number used by the load cell (as indicated in the left hand column of Table 6.01 and shown in Figures 6.03a and 6.03b), which were numbered 29 to 32, from left to right when facing the box with the PPTs at the back. In tests with only three groups, channel 31 is removed and the new central location uses the load cell linked to channel 30. The linear group pile caps were used as part of the single pile tests.

In test 1d, two locations (29 and 32) each had a single pile installed at the central position of the five-pile linear group pile cap. The other test (location 31) had three piles installed in the pile cap with holes at 3.0 d spacing; the piles were installed at the two end positions and the central position and were therefore at 6.0 d centres.

For all other single pile tests, two piles were installed at the end locations of the 2.5 d pile cap, so the piles were always at 10 d centres. From test 1d, it was found that the single pile installed at the central position allowed the pile cap to rotate, and whilst a solution was found to hold it in position, it was not an ideal arrangement. In addition, it was considered that the group of three piles were perhaps too closely spaced, which was unnecessary. So in the subsequent single pile tests two piles were installed under each cap and therefore the total capacity was divided by two.

6.3.2 Capacity determination

The ultimate capacity was the peak capacity achieved by the pile(s). Ideally, the value would have been the capacity achieved at a certain settlement, in keeping with the notion that friction piles develop the majority of their capacity by a settlement corresponding to a small fraction of the pile diameter (typically 0.01 to 0.05 d). However, it was found that the single pile tests responded differently depending on the size of the other groups within the test and what order the pile groups started accumulating load. Naturally, the apparatus was designed with the intention that all groups would be perfectly level and begin to accumulate load at the same instant; in reality, there were slight differences in the heights of the groups, but generally no more than 0.5 mm. Nevertheless, it should be noted that even a difference of 0.1 mm between heights of groups would result in one being loaded 24 seconds ahead of the other. Also, this was further varied by the malfunctioning actuator (mainly in phase 2) and the ensuing modifications. It is perhaps not surprising that the response of a single pile is slightly affected by the other groups in the test and the order in which the groups pick up load. For example, if a single pile is located next to a large group, and picks up load first, the response may be different to a single pile that picked up load after the large group. This affect is likely to be most pronounced with the single piles and is caused by the fractional slowing of the loading system strain rate once a large pile group picks up load. This problem could possibly have been negated by a different loading system, one that did not load the groups via the same stiff loading beam, thus being affected by other groups within the test.

Figure 6.04 shows the graph of settlement vs time for the single pile, which further indicates the problem introduced above. The settlement of the pile groups with time is highly variable, for which the causes have been discussed. Groups that have a particularly pronounced variability are 5c-31 and 5d-29 (where the first two characters indicate the test number and the second two characters are the load cell channel number). In summary, the behaviour of the single piles was inconsistent, both in terms of settlement vs time and load vs settlement (see Figure 6.05). Consequently, it was decided to choose the peak values (up to a settlement of 5 mm, or a single pile diameter), regardless of the settlement at which they occurred. This method was demonstrably acceptable as later proven and discussed in Section 6.3.4.

6.3.3 Data omitted

Of the eleven groups tested, two of the groups from test 1d (1d-31 and 1d-32) were rejected because of possible excess oil on the piles, which resulted in reduced capacity. In addition, there was no usable data from test 4d, which had included a single pile test. The data from 5d-29 had shown an unusual response (as mentioned in the previous section) beyond a settlement of 1 mm, so the 'peak capacity' was taken as the capacity at 1 mm settlement. The remaining eight results were used to back-calculate α values. This was done by re-arranging Skempton's equation (Equation 2.1) in terms of α and using Q_{test} (the peak capacity from the centrifuge test) for the parameter, Q_{ult}; from this, the graph of α vs s_u was plotted (see Figure 6.06). Test 3a was then also rejected because it appeared to be an anomaly when compared against the other results. Therefore, seven results were used to calculate the equation of the αs_u trendline.

6.3.4 Single pile capacity

The mean average of the six results, which excludes test 5b, is 148 N. The range of capacities was between 140 and 157 N (shown by Q_{test} in Table 6.02), with a standard deviation of 6.0. A linear trendline was plotted through the data points and the equation of the line was calculated to be as follows:

$$\alpha = 1.1 - 0.008 s_u \qquad \text{(Equation 6.1)}$$

Whilst the relationship between α and s_u is not strictly linear over a wide range of shear strengths, it can be considered to be so between the relatively narrow limits of these tests. The trend line had an R^2 value of 0.957, where R^2 is the coefficient of determination; a number between 0 and 1 that reveals how closely the estimated values for the trend line correspond to the actual data. A trend line is more reliable the closer the value is to 1.

The calculated values of α allowed an equivalent single pile capacity to be calculated for all tests (shown as Q_{calc} in Table 6.02). For consistency, the calculated values were adopted for all further comparisons rather than the experimental result, for tests even where a single pile test had been included. In every case except one, the difference between the calculated and experimental single pile capacities was small, between 0 and 4 N. In test 3a, the difference was 16 N, which is significant and so the analysis of the results in this test was done with caution.

The calculated pile capacities ranged between 138 N (test 1c) and 156 N (test 4a); the capacity of test 5b was calculated to be 113 N, which happens to be identical to the experimental result.

The experimentation and calculation of the capacity of single piles allows the efficiency of group tests to be calculated. Eight of the eleven single pile tests were successful, and 38 of the groups tested were successful. These group tests are summarised in Table 6.03.

6.4 Linear groups

6.4.1 Arrangement

A total of 22 linear groups were tested and were incorporated in the following tests (the number in brackets represents the number of linear groups in that particular test): 1a (4), 1b (4), 1c (4), 1d (1), 3a (3), 3c (1), 3d (3), 4d (1) and 4e (1). The issue concerning the silicone oil preventing direct contact between the pile and the clay over the upper part of the pile caused problems with the data and unsurprisingly the loads sustained by these groups were low compared to similar groups tested once the problem had

been fixed. The issue was only satisfactorily resolved from test 1d onwards, and as a consequence the 12 results from tests 1a, 1b and 1c have been omitted from analysis. In addition, there were no usable data generated from test 4d. Two of the remaining nine groups were also omitted in some analyses because of dubious test results that were noticeably different to all others (1d-30 and 3d-32). The group LL05_1.00 showed an unusual staggered response and upon excavation of the group it is revealed that the piles were not vertical, which may have affected the reliability of the data. The results from this group are included in some of the analyses, where specified. All of these omissions left only six or seven groups available for analysis. A summary of these groups is given in Table 6.04.

6.4.2 Capacity determination

Load vs settlement curves for each of the six tests are plotted in Figure 6.07. Each curve shows the capacity per pile and is plotted up to 5 mm of settlement. Three of the curves had shown a settlement of approximately 1.5 mm before the load began increasing and this was likely to be caused by poor contact between either the pile cap and the piles or the loading point and the pile cap. For each of these curves the settlement has been reset to zero once there is uptake of load (denoted in the key of Figure 6.07 as "mod"). Resetting the x-axis to a maximum of 1 mm (Figure 6.08) confirms that there is little difference between the groups in terms of stiffness and initial response to loading and all curves have a similar shape.

The graph of settlement vs time for the nine groups is shown in Figure 6.09. As mentioned, in a number of tests the settlements began increasing before any uptake of load and in these situations the measured capacity is taken as the change in settlement from when the load starts increasing. With the exception of the three irregular lines, the remainder are reasonably consistent and suggest a good even response from the pile groups and between tests.

The capacity has been determined at the following stages: 0.1 mm, 0.25 mm, 0.5 mm and 1 mm, which represent 0.02, 0.05, 0.10 and 0.20 d. The peak capacity was also recorded. It has been calculated that at 0.05 d settlement, the groups have, on average, achieved 74 % of their peak capacity; at 0.10 d this value increases to 91 %,

and at 0.20 d the groups have attained 94 % of their peak capacity. However, by excluding the results from the group spaced at 1.0 d, these values increase to 78 %, 95 % and 99 % respectively. It should be noted that there are two results for LL05_2.00, since this group was tested twice, in test 3a and 4e. To calculate patterns in behaviour with respect to pile spacing, the average of the two tests is used.

6.4.3 Efficiency

Figure 6.10 shows the efficiency vs pile spacing at the stages of settlement discussed in the previous paragraph. The efficiency is derived from the capacity determined from the test, divided by the number of piles in the test (which assumes all piles carry the same load) divided by the calculated capacity of a single pile (as discussed in Section 6.3.4). The graph shows that at a settlement of 0.05 d the efficiencies are generally between 0.8 and 0.9, with the exception of pile spacing 1.0 d where this value is 0.5 and pile spacing 2.5 d where the value is 1.0. At a settlement of 0.10 d, the efficiencies are consistently between 1.0 and 1.1, with the exception of pile spacing 1.0 d where the efficiency is 0.6. The values of efficiency at 0.20 d are all approximately 1.1, which is very similar to the values at peak capacity, with the exception of pile spacing 1.0 d.

For groups where the piles are further apart, 2.5 d, 2.75 d, and to a lesser extent 2.0 d, the efficiencies at 0.10 d settlement and peak are all very similar. In contrast, where the piles are closer together, 1.25 d and 1.75 d, there is a more significant difference between the efficiency values. This suggests that over the range 1.25 d to 1.75 d, there is additional capacity created as the piles settle beyond 0.10 d, whereas for groups with piles spaced further apart, there is not. A pile spacing of 2.0 d appears to be a borderline case between these two effects. Comments and conclusions from this will be discussed in the following section.

6.4.4 Analysis

It is arguable as to whether a single line of piles can in fact behave as a block; there was no evidence of this at the surface but it is suggested that a 'block effect' failure mechanism may exist. The behaviour of the group is more complex where the piles are

spaced in between these 'close' and 'far' extremes, at the point of transition between the two failure modes. The idea of a 'block effect' is proposed, whereby there is a very slight suppression at the surface where the piles 'engage' some of the soil in between them, but this suppression is not visible to the naked eye via a shear surface. However, it would be difficult to devise apparatus to try and measure ground settlement at the surface between the piles in a linear group and this was not attempted.

A possible reasoning behind these results is that at a spacing of 1.0 d, the behaviour is a form of block failure, and the efficiency is lower than 1, since the capacity (specifically, the perimeter) of the 'block' is less than the capacity (perimeter) of the individual piles. When the spacing is increased, more clay in between the piles is incorporated creating a bigger 'block' and a higher capacity caused by more clay-clay failure. This type of failure predominates at a spacing of between 1.25 and 1.75 d and generates a peak in the data. This exact form of 'block effect' failure has not previously been suggested and is not well understood. As the spacing is further increased, the piles can no longer drag down the clay in between them and so they fail as individual piles. The question to be answered is why this central clay is engaged when it would be easier for the piles to fail individually because it would require less force. This proposed phenomenon is expanded upon in the following sections and in Chapter 9.

6.5 Perimeter groups

6.5.1 Arrangement

In total, 30 perimeter groups were tested. Tests 2a, 2b, 2c, 2d, 2e and 3b were comprised solely of perimeter groups, with three in each test, making a total of 18 tests. The following tests included some perimeter groups: 4a (2), 4b (1), 5a (1), 5c (1) and 5d (3) and test 5e comprised four perimeter group tests. Twenty tests had piles spaced at 2.0 d centres, with alternative pile spacing as follows: 1.25 (2), 1.5 (3), 1.75 (3), 3.0 (1) and 4.0 (1). Eleven groups were in square arrangements, 16 in circular arrangements, and the remaining three were triangular groups. The number of piles in each group was as follows: 8 (3), 9 (1), 10 (3), 12 (7), 14 (3), 16 (4), 18 (4) and 20 (5).

6.5.2 Test errors and failures

As previously mentioned, after the completion of the phase 2 tests and with only two successful results from the triangular groups, it was decided not to continue with this geometry, and keep the study focussed on just the square and circular groups. The triangular groups were also quite restrictive in the number of piles per group to allow an equilateral shape. The groups would be limited to 9, 12, 15 and 18 piles. An additional five groups had given unsatisfactory results in failing to achieve a settlement of 1 mm and four of these groups were part of the phase 2 tests. The failure of these four phase 2 groups was caused by the malfunction of the actuator. Three of the failures occurred in test 2c, making the test totally unsuccessful, and initiating design modifications to the actuator. A failure had also occurred in the previous test, test 2b, and was likely to be an onset of the more serious problem, which fully developed in test 2c.

The other failure occurred in test 4a and was caused by a loose bolt in the loading apparatus, which meant that the loading beam was not kept perfectly horizontal. The bolt was tightened and no further problems were encountered with tests 4b or 4c. Following the catastrophic failure of test 4d, the loading apparatus underwent a re-design, which included an improvement to the vertical guide system to further ensure the loading beam remained horizontal, as discussed in Section 5.6. The exclusion of various tests and groups means that of the 30 groups tested, only 16 will be used in the analysis, as highlighted in Table 6.05.

6.5.3 Capacity determination

The load vs settlement curves of the circular perimeter groups are shown in Figure 6.11. The curves show the load per pile, so the total group capacity is divided by the number of piles in the group. All groups appear to show a sensible and similar response at this scale. Figure 6.12 shows the same curves but this time the x-axis is set to a maximum of 1 mm, which highlights a range of responses over the initial gradient of the curve and indicates the stiffness of the groups. The least steep gradient, and therefore the group exhibiting the least stiff response is PC18_1.50, followed by PC12_1.50. The next groups showing a relatively 'soft' response are both PC12_1.25

groups, from test 4a and 4b. This suggests that groups with close spacing (which also fail as blocks, as discussed in the next section) show the least stiff responses, which means that the rate of build up of load is more gradual. This effect is more prominent in the bigger groups; i.e. PC18_1.50 shows a less steep curve than PC12_1.50. In contrast, the groups that display the stiffest responses are PC14_2.00 and PC12_3.00. In groups where the piles are placed further apart, it is expected that the interaction will be minimal and that they will fail is individual piles and therefore will show a stiff response. This is likely to be the case for PC12_3.00, but less so for PC14_2.00. Figure 6.13 is the same graph as Figure 6.12, but highlights the two different failure mechanisms. It can be seen that the groups failing via the block mechanism generally show a less stiff response.

In the case of the square groups, the pattern of load vs settlement is less clear, not helped by the availability of only five groups for comparison. Figure 6.14 shows the load vs settlement curves, which are displayed as the load per pile, assuming all piles carry equal load. The curve for PS20_1.50 is an erratic shape because of the problems that occurred in test 5c (refer to Section 5.6, 'actuator malfunction (3)'), although the overall shape of the curve can be considered a reasonable indication of its true behaviour. Group PS20_1.75 displays the highest peak; the ultimate capacity then falls to a similar value to that of groups PS08_2.00 and PS08_4.00. The groups with the lowest capacity per pile are PS10_2.00 and PS20_1.50. Figure 6.15 shows the load vs settlement curves for the first 1 mm of settlement. It should be noted that the curves of PS20_1.50 and PS08_4.00 have been slightly modified to create a clearer graph, but the overall pattern has not been affected.

The peak capacities were ascertained for each group, along with the capacities at 0.02, 0.05, 0.10 and 0.20 d settlement. A calculation was then made to determine the percentage of the peak capacity that had been attained at each of the four stages of settlement. It was found that at 0.02 d, 58 % of the peak capacity had been reached, at 0.05 d settlement, 79 % of the peak capacity had been reached; at 0.10 d settlement 93 % had been reached; and at 0.20 d, the capacity was 98 % of the peak capacity. These percentages are very similar to those calculated for the linear group tests

(summarised with all group types in Section 6.7.2). The data described in this section and in the following sections is summarised in Table 6.06.

6.5.4 Failure mechanism

Of the 16 groups under analysis, eight failed via the block mechanism, which meant that the central soil moved downwards with the piles, thus shearing with the soil outside the group perimeter. Groups that failed via the block mechanism generally, but not always, had lower efficiencies, as is discussed in Section 6.5.5.

It was noticed that where block failure had occurred, there was a prominent vertical shear surface over the top section of the group, which was only observable once the models had been deconstructed. Examples of this are shown in Figures 6.16 and 6.17. The full extents of these surfaces are unknown since they were rather irregular and were not measured. However, it can be said with confidence that this type of shear surface developed, to some extent, in all of the groups that underwent block failure. In addition, it is approximated that the depth of the surface is similar to the diameter of the group, with the exception of the groups PC12_1.25 (both in test 4a and 4b), where the surface seemed to extend a lot further down the group (Figure 6.17b). Whilst these surfaces were of notable interest and obvious significance, little more can be said about them since they were difficult to record and quantify accurately.

6.5.5 Efficiency

In this chapter, the efficiency of a group will generally be referring to the efficiency at a settlement of 0.20 d, which as mentioned previously is, on average, 98 % of the peak efficiency for perimeter groups. Four divisions have been identified:

- Low efficiency < 0.99
- Normal efficiency = 0.99 to 1.01
- Favourable efficiency = 1.02 to 1.09
- High/abnormal efficiency ≥ 1.10

The efficiency group "high/abnormal" is so called because it is important to keep in mind the possibility that these results are erroneous. Eight of the 16 perimeter groups

had a low efficiency; four had normal efficiencies, whilst the remaining quarter of groups had a favourable or high efficiency. The group with the highest efficiency was PC12_3.00 (Table 6.06). This group has a wider spacing than all groups, with the exception of PS08_4.00 (which incidentally had an efficiency of 1.01), but nevertheless it is believed that the result is slightly erroneous (this is discussed further at the end of Section 6.5.6). This particular group also responded with a higher efficiency at 0.05 and 0.10 d settlement than any other group, including linear groups and single piles. It is therefore thought that the result should be treated with a certain amount of caution.

Of the eight groups with low efficiencies, six of them have a pile spacing of less than 2.0 d. The two remaining groups that have a pile spacing of 2.0 d, are relatively small groups, both with just 10 piles. The cross sectional areas of the groups are expressed as the cross sectional ratio, R_{cs}, which is the area of the soil divided by the area of the piles. For these eight low efficiency groups, the range of R_{cs} values is 1.9 to 4.3.

Four groups have a normal efficiency, one is the group with 4.0 d pile spacing and another is a small group of just eight piles. The other two groups are relatively large, with cross sectional ratios of 6.5 and 8.1. The three groups with favourable efficiencies are summarised as follows:

- PC14_2.00; $R_{cs} = 5.7$; $\eta = 1.07$; individual failure
- PC16_1.75; $R_{cs} = 5.0$; $\eta = 1.09$; block failure
- PS20_1.75; $R_{cs} = 4.9$; $\eta = 1.09$; block failure

The two circular groups have very similar cross sectional areas and very similar efficiencies, yet the number of piles is different as is the pile spacing, and more crucially, the failure mechanism. Unfortunately, the central soil depression was not measured for the group PC14_2.00. However, it was measured for the group TC14_2.00 and was found to be 0.68 mm (as discussed later in Section 6.6.5) and so it is possible that even with the absence of the central pile, the soil would still have moved downwards to some extent. The square group has a slightly larger cross sectional area, approximately 23 % larger, but also has a greater number of piles, in fact 25 % more than the group of 16 piles, which has the same pile spacing. In truth, a

direct comparison between circular and square groups may not be apposite, but even so, there is a definite similarity between these groups. As an alternative way of comparing the size of the group, the diameter is calculated. For the circular groups the diameter is 44.6 mm and for the square group the (shortest) diameter is 43.8 mm, equalling a difference of just 0.8 mm.

Eleven circular groups and five square groups were tested, but as a result of the numerous unsuccessful tests there is only one group arrangement where it is possible to compare directly the influence of group shape. Group PC10_2.00 was calculated to have an efficiency of 0.93 and group PS10_2.00 had an efficiency of 0.84. This result indicates it is more efficient to utilise circular perimeter groups, although there is not enough data to confirm the suggestion. It would be expected that a circular group would have a higher efficiency, since the load distribution would be very similar, if not the same, on all piles. This is considered favourable in comparison to square groups where the load distribution is likely to be unequal and particularly high for the corner piles. Also, the area of soil encompassed by the piles is greater for circular groups, which can be important especially when block or 'block effect' failure occurs.

6.5.6 Central soil monitoring

A few initial rudimentary measurements were made in early tests to try and decipher whether or not the central core of soil was being affected when the piles were loaded. One of these measurements is shown in Figures 6.18a and 6.18b, which indicates the level of the soil on the outside of the group is about 21.5 mm, but on the inside of the piles the level is about 22.5 mm. In some cases it was reasonably convincing that the central soil had in fact moved down relative to the soil outside the pile group. However, movements were very small and unfortunately they were not properly recorded in these early tests.

The idea of measuring the movement of the central soil core was not revisited until test 5a. A bracket was fabricated that would fit across the width of the box and slide along the reference frame (see Figure 6.19). Three locations were drilled at 50 mm centres, which also had LVDT D-clamps located. The central LVDT was aligned in the middle location, which could measure the settlement in the centre of the groups. The

outer LVDTs measured just outside the groups. This monitoring was particularly useful for measuring movements that were not easy to see, for example, in test 5e the group PC20_2.00 did not show any visible settlement, but the results in Figure 6.20 clearly show that the central soil had settled relative to the soil outside the group, which would have otherwise gone undetected. It should be noted that this settlement measurement was 0.53 mm, which represents approximately 11 % of a single pile diameter. This method of measurement also allowed the possibility of central soil settlement to be dismissed for certain groups. In test 5a, a settlement of 0.14 mm was recorded for group PS08_4.00 and in test 5e a settlement of 0.16 mm was recorded for group PC12_3.00. Whilst both of these measurements represent approximately 3 % of the pile diameter, they are considered negligible as realistically they are beyond the level of accuracy possible, when bearing in mind the probable disturbances caused during the test.

It can be seen from the graph in Figure 6.20 (and the diagram in Figure 6.21) that the clay level at the front of the box (LVDT 43, see Figure 5.13) is always slightly higher than the back of the box (LVDT 41) and this is believed to be because of the increased protection offered by the loading apparatus. The loading beam is perfectly central, but the motor and gear box are located on a plate that is off centre and located towards the back of the box; this means the clay may swell slightly less on the other side of the box, where the wind effect was greater. The presence of the silicone oil on the surface should negate this effect, but it cannot be ruled out. It should be noted that all movements are relative to the model before loading on the centrifuge and the soil heaved 4 to 5 mm during the equilibrium phase. For groups PS08_4.00 and PC12_3.00, the graphs show an anomalous result for LVDT 43, which is caused by soil disturbance during hand vane testing. However, neither of these factors influence the central core of soil and its apparent depression.

One final, but important, observation is that the measurements from LVDT 42 show a lower clay level even on the outside of the group (i.e. the change in clay level is not a linear increase from the back of the box to the front), suggesting that there is interaction between groups. The group on the left-hand side of PC20_2.00 (nearest to data points "outside left") was PC18_1.50, which was 57 mm away; on the right-hand

side was PC12_3.00, which was 50 mm away. The graph shows that PC20_2.00 was more affected by the group in closest proximity, on the right-hand side. This subject is returned to in Section 6.6.5.

6.5.7 Analysis

Idealised proposed failure mechanisms are outlined in Figure 6.22 and show failure as; (a) individual piles, (b) partial block failure, and (c) complete block failure, which are shown as a function of pile spacing. At the furthest spacing the diagram shows the shear takes place along the clay-pile interface only; at the closest spacing the clay between the piles moves downwards with the pile, by the same amount and at the same rate. At the mid-way spacing, some shear takes place along the clay-pile interface, but additionally, some of the shearing takes place within the clay in between the piles. This generates clay-clay shearing, which is thought to occur more readily at higher displacements, compared to the displacement required to mobilise clay-pile shearing. It is this effect that may be resulting in an increased capacity at the transitional point between individual failure and block failure.

A similar apparent peak was commented upon by Whitaker (1957) initially and later by Barden and Monckton (1970), who suggest the peak efficiency is obtained at a spacing of 2.0 d. However, the reasoning suggested by Barden and Monckton was related to a strengthening of the clay post pile driving. Of course, in these tests the piles are bored, not driven, so this reasoning is not applicable.

Analysis has been completed to try and determine what failure surface a given group may have and whether the group would fail as individuals (failure surface is all clay-pile), as a block (failure surface is part clay-pile and part clay-clay), or somewhere between these two extremes. This analysis is explained with the aid of Figures 6.23 and 6.24. In plan view, the failure surface is denoted by the angle, β, which defines the location of this surface relative to the piles and the centre of the group. It is considered likely that block failures would generally occur with β angles in the range 30 to 90 °. A fundamental element of the analysis is the variation of β and that the clay-clay fraction (shown in orange) and the clay-pile fraction (shown in green) are considered

separately. Figure 6.24b shows an angle of 30 ° and (c) shows an angle of 90 °. Below 30 ° (a) a block mechanism would not be expected since the portion of pile circumference over which there is no clay-pile slip is too small. Beyond 90 ° (d) is thought to be an improbable mechanism since for this to occur, block failure would involve a high component of clay-clay shear relative to the clay-pile shear.

For each group, calculations were done to determine the exact area that would undergo clay-clay shear and also the area that would undergo clay-pile shear, and this was calculated for every angle between $\beta = 0$ and 100 °. The eleven circular perimeter groups were analysed, since the areas were more straightforward to calculate. The angle corresponding to the calculated capacity which was most similar to the capacity output from the centrifuge tests (at 0.20 d) was the β value assigned to that particular group. Two examples of the calculation spreadsheets are given in Tables 6.07 and 6.08, which are explained with the aid of Figure 6.25. A summary of the results from all groups is given in Table 6.09. Six of the groups had failed as blocks and these showed a range of calculated β values between 52 and 69 °, which fell well within the limits predicted (see "block shaft" column, Table 6.09).

Of the five groups that did not fail as blocks, two groups suggested that for the calculated capacity to correspond with the centrifuge capacity, β would have to equal 77 and 78 ° for groups PC14_2.00 and PC20_2.00 respectively. This is outside the range for the groups that did undergo block failure (52 to 69 °). Interestingly, it is strongly believed that both these groups showed signs of central soil depression and 'block effect' failure, indicating this failure angle is on the cusp of block failure. For the remaining three groups no sensible β value could be calculated, which means that the failure must have taken place along only a clay-pile interface. In other words, the groups must have failed as individual piles, which is supported by the evidence from the centrifuge tests. Two of these groups are PC10_2.00 and PC12_3.00, which is as expected. The third group was PC16_2.00, which does not make sense at first glance (particularly since it is 'mid-way' between PC14_2.00 and PC20_2.00 that have just been discussed), however, this group was installed in test 3b, where the soil was

particularly firm and the s_u range was 0 kPa, leading to various unexpected results, which may affect this method of analysis.

The two PC12_1.25 groups, which were tested as part of test 4a and 4b showed β angles of 67 and 55 ° respectively, which is a more significant difference than may be expected for two identical groups. However, the average s_u in test 4a was 65 kPa and in test 4b this value was 54 kPa and so the failure path through the clay was shorter in the clay of higher strength. On closer inspection, the failure path through the stronger clay is in fact only 3 mm shorter around the entire group. Also, the difference in clay strength is only 11 kPa and what's more, there is in fact very little difference between the αs_u values. A second similar observation is the comparison between the two block failures in test 5d and the two in test 5e. The average s_u in test 5d was 53 kPa and the calculated β angles for the two groups were 69 and 64 °; whereas the average s_u in test 5e was 47 kPa and the β values were 52 and 57 °. So yet again, the higher strength clay appears to force a shorter failure path.

In the analysis above, the base capacity is the sum of the base capacities of the individual piles. For the groups that failed as blocks, an alternative was to calculate the base capacity assuming that the pile group behaved as a single block, and therefore the base area became significantly greater. The angles of β that result are larger than the β angles in the previous analysis. A larger β angle is congruent to a reduction in shaft capacity since the shaft perimeter becomes smaller (see Figure 6.26). In order for the total capacity to have the same calculated magnitude, a reduction in shaft capacity allows a larger contribution of capacity to come from the base. The β angles were found to be in the range of 74 to 93 °, with the exception of PC12_1.25 (test 4b) where β equals 59 ° (see "block base" column, Table 6.09). Referring back to Tables 6.07 and 6.08, the principle difference between these two spreadsheets is that the possibility of a 'block base' capacity can be calculated for one of them (Table 6.08, group PC12_1.50) and cannot for the other (Table 6.07, group PC14_1.75). However, it is thought improbable that the base capacity of the single block can be mobilised when there is no true basal surface, and it is likely that movements and stresses would dissipate horizontally outwards as the pile group is loaded. In addition, it can be seen

from the photographs of the shear surfaces that the β angles were not in the range of 74 to 93 ° (Figures 6.27 and 6.28). It is unknown whether some small portion of capacity may come from the base of the group block, but to determine this was beyond the scope of the research.

With reference to Table 6.09, columns "$Q_{clay\text{-}pile}$" and "$Q_{clay\text{-}clay}$" separate the total capacity into the portions generated from clay-pile friction and clay-clay friction. The final column shows the portion of load that is generated form clay-clay friction, as a fraction of the total group capacity (which includes the capacity of the individual pile bases). An average is calculated for each pile spacing and the findings are summarised as follows:

- Pile spacing, 1.25 d $Q_{clay\text{-}clay}$ = 16 %
- Pile spacing, 1.5 d $Q_{clay\text{-}clay}$ = 25 %
- Pile spacing, 1.75 d $Q_{clay\text{-}clay}$ = 33 %
- Pile spacing, 2.0 d $Q_{clay\text{-}clay}$ = 45 %

In summary, this β analysis gives a consistent indication of block failure that reliably ties in with centrifuge observations and shows sensible correlation between groups.

6.6 Target groups

6.6.1 Arrangement

In total, 12 target groups were tested successfully. The distribution of tests was as follows: 4b (1), 4c (3), 4e (3), 5a (1), 5b (2) and 5c (2). Eight tests had piles spaced at 2.0 d centres, with alternative pile spacing as follows: 1.5 (1), 1.75 (2) and 2.25 (1). Four groups were in square arrangements and eight in circular arrangements. The number of piles in each group was as follows: 12 (3), 14 (2), 16 (5), 18 (1) and 20 (1). A summary of the target groups tested is presented in Table 6.10. It was not necessary to omit any data (although two target groups made up the failed test 4d) and so all 12 groups were analysed, totalling nine different arrangements, since one group was tested three times and another group was repeated a second time.

6.6.2 Capacity determination

Load vs settlement curves of the target groups are shown in Figure 6.29. The same graph is shown in Figure 6.30, but over just the first 1 mm of settlement. It should be noted that the curves of TC16_1.75 and TC18_1.50 have been slightly modified to create a clearer graph, but the overall pattern has not been affected. The two groups with the lowest capacity per pile were the two from test 5b, with the softer soil, so this is as expected. In Figure 6.30, the groups with the next lowest capacities are TC14_1.75 followed by TC18_1.50, two of the three groups where the piles are spaced at less than 2.0 d. The next two groups with relatively low capacity are the two groups with 13 piles (TC12_2.00 and TC12_2.25, both from test 4e) and TC16_1.75. The remaining five groups have similar capacities per pile and all have between 15 and 21 piles per group; the group with the highest capacity per pile is TC14_2.00. The data described in this section and in the following sections are summarised in Table 6.11.

6.6.3 Failure mechanism

Of the 12 groups under analysis, six failed via the block mechanism and six did not. This can be summarised as follows:

- Block: TS16_2.00, TC14_1.75, TC12_2.00 [x2], TC18_1.50, TC16_1.75
- Individual: TC16_2.00, TS16_2.00 [x2], TS20_2.00, TC12_2.25, TC14_2.00

It was unusual to observe that the group TS16_2.00, which was tested three times, failed twice as individuals and once as a block. This variable behaviour is an indication of the sensitivity of the conditions and that very slight changes can be the difference between one type of failure mechanism and the other. The block failure occurred in soil with an average s_u of 54 kPa and the s_u range (the difference between the s_u at the top of the pile and the toe of the pile) was 20 kPa. The first individual failure occurred in soil with an average s_u of 61 kPa and s_u range of 6 kPa, the other individual failure occurred in soil with an average s_u of 33 kPa and an s_u range of 9 kPa. It would appear that this group is on the very cusp of failure mechanism behaviour and that a small change is s_u range can be the defining factor between the different types of behaviour.

Clearly, the behaviour is broadly dependent on the spacing and the number of piles, and thus, the diameter of the group. There is a point, a critical spacing, where the spacing is too large and no matter how small the diameter of the group, it will never fail as a block. At the same time, there will be a critical group diameter, and when exceeded, no matter how close the spacing, it will never fail as a block. Of course, these two critical factors are inter-related and therefore do not each have a specific single value, because both properties are dependent on the other, over a particular range. For example, the circular group of 12 piles fails individually at 2.25 d, but as a block at 2.0 d; the groups of 14 and 16 piles fail individually at 2.0 d, but as blocks at 1.75 d. By the same reasoning, a group of 20 piles may fail individually at 1.75 d, but as a block at 1.5 d, although there will come a point when the group diameter will be too big to fail as a block at a spacing of 1.25 d, or even 1.0 d.

6.6.4 Efficiency

The efficiencies will be described in the same way as the perimeter groups; low, normal, favourable and high (high/abnormal) efficiencies. Of the 12 groups under analysis, three had a low efficiency, two groups had a normal efficiency, three groups had a favourable efficiency, and four groups had high efficiencies of between 1.10 and 1.18. Unlike the perimeter groups, there is a less clear distinction between the properties of the groups that share similar efficiencies. It is true that the groups with favourable and high efficiencies are comprised entirely of groups with a pile spacing of 2.0 d (with the exception of one group at 2.25 d), but two of the five groups with normal and low efficiencies also have a spacing of 2.0 d. In addition, there is no apparent pattern regarding the size of the group, or indeed the geometry of the group. All that can be concluded at this stage is that the target groups generally have favourable or high efficiencies where they fail individually (five out of seven cases) and they generally have low or normal efficiencies where they fail as a block (four out of five cases). It is true that the central pile seems to complicate any previously observed patterns associated with the perimeter groups. However, when revisiting the R_{cs} values, a pattern does emerge. Groups with low or normal efficiencies have R_{cs} values between 3.9 and 4.8 and groups with favourable or high efficiencies have R_{cs} values between 4.8 and 6.1 (with the exception of TC12_2.00, which has an R_{cs} value of 4.5).

As for the perimeter groups, there was only one occurrence where a circular target group could be compared with a square target group. It was calculated that group TC16_2.00 had an efficiency of 1.12; TS16_2.00 was tested three times and was found to have a wide range of efficiencies, 0.99, 1.06 and 1.17. The average of these square group efficiencies is 1.07, which is lower than the circular group efficiency; this would tend to support the findings from the perimeter groups, although this evidence is not strong.

6.6.5 Central soil monitoring

Central soil monitoring was first discussed in Section 6.5.6 for the monitoring of perimeter groups. This method was also used to monitor the target groups, although it excludes the central measurement because of the presence of the central pile. As previously shown, this monitoring was useful for measuring movements that were not easy to see, for example, in test 5a the group TC14_2.00 did not show any visible settlement, but the results in Figure 6.31 clearly show that the central soil had settled relative to the soil outside the group and the recorded measurement was 0.68 mm. In Section 6.5.6, the subject of group interaction was touched upon; and it can now be seen that when comparing PC20_2.00 (Figure 6.20) to TC14_2.00 (Figure 6.31), group interaction appears not to affect the target group. Group TC14_2.00 appears to be equally unaffected from either side (outside left and outside right), and the neighbouring groups were a minimum of 68 mm away. Equating both these results suggests that group interaction becomes active when the groups are between about 11 and 14 pile diameters apart. This only became an issue in test 5e.

6.6.6 Analysis

As for the perimeter groups, this analysis is explained with the aid of Figures 6.23 to 6.26. There were eight circular target groups available for analysis. The calculations were carried out in the same way as for the perimeter groups (described in Section 6.5.7) and the results are displayed in the same format in Table 6.12. Five of the groups had failed as blocks and four of these groups had a calculated β angle of 73 to 75 °. The fifth group, TC18_1.50 had a calculated β angle of 52 °. The situation

regarding the calculation of base capacity was the same for the perimeter groups, and it can be seen from column "block base" (Table 6.12) that only one angle of β could be calculated. Interestingly, this was for group TC18_1.50 where the β angle was 74 °, which is within the range of the β angles of the four other 'block failure' groups.

Three groups did not fail as blocks, although two of them, TC16_2.00 and TC14_2.00, yielded sensible β angles of 74 and 58 ° respectively. Interestingly, as for the perimeter groups, it is strongly believed that both these groups showed signs of central soil depression and 'block effect' failure. This cannot be proven for TC16_2.00, but it has been shown clearly that this occurred for group TC14_2.00. Table 6.12 also shows that as the spacing increases, the proportion of capacity generated from clay-clay shear increases, as would be expected. The value of $Q_{clay\text{-}clay}$ / Q_{total} for TC18_1.50 is 25 %, this increases to 47 % for group TC12_2.25.

In summary, this simple analysis gives a consistent indication of block failure that reliably ties in with centrifuge observations.

6.6.7 Target group and perimeter group comparison

In one observed case, the addition of the central pile to a perimeter group (therefore making it a target group), was the difference between the group failing individually, and failing as a block. This occurred for a group of 16 piles at 2.0 d spacing in a square arrangement; the perimeter group failed as individual piles and the target group failed as a block.

However, as previously mentioned, the piles in group TS16_2.00 also failed as individuals. It was tested three times in total and on two of those occasions (one as part of test 5b) the piles failed individually. What is more, when the group did fail as a block (in test 4b) the capacity was unusually high compared to all other groups, and since this was not observed in any other group, the overall observation is deemed inconclusive. A number of other groups with the same number of perimeter piles and the same spacing were also tested as both perimeter and target groups and the results are summarised as follows:

- PC14_2.00(2e) and TC14_2.00(5a) individual failure
- PC14_1.75(5d) and TC14_1.75(4e) block failure
- PC16_2.00(3b) and TC16_2.00(4c) individual failure
- PC16_1.75(5e) and TC16_1.75(5c) block failure
- PC18_1.50(5e) and TC18_1.50(5c) block failure

The load vs settlement curves can be seen in Figures 6.32 and 6.33. If considering the capacities at 0.02 d, the two perimeter groups spaced at 1.75 d have higher efficiencies than their equivalent target groups. At a pile spacing of 2.0 d the target groups have higher efficiencies.

Whilst there was only one, slightly dubious, circumstance where the addition of the central pile visibly changed the behaviour and failure mechanism of the group, it is believed that the central pile does indeed have an influence, which is just more subtle than initially expected. It appears that the central pile has a positive effect in terms of efficiency, on most of the groups, to differing extents. There is an apparent correlation between R_{cs} value and the extent of effect that the central pile has. For the three groups where the effect was relatively large (and increase in efficiency of between 11 and 15 %), the R_{cs} values of the perimeter groups were between 5.0 and 6.5. For the two groups where the effect was minimal, the R_{cs} values were 4.1 and 4.3.

The β analysis is useful and shows that the range of β angles where pile-pile shear transitions to clay-pile shear is between 52 and 78 $^{\circ}$ for both perimeter and target groups where block or block effect failure occurs.

6.7 Grid groups

6.7.1 Arrangement

Three grid groups were tested and they can be summarised as follows: test 4a, GS25_2.00; test 5a, GS16_2.00 and test 5b, GS25_2.00. The group of 16 piles was arranged as a 4x4 grid and the groups of 25 piles were arranged as 5x5 grids. One of the principal reasons for including grid groups was to try and correlate the experiments with work conducted by previous Authors. If agreement existed between

the grid groups in this research and in previous research, then there would be increased confidence in the findings for the new perimeter and target groups.

6.7.2 Capacity determination

Load vs settlement curves are shown in Figures 6.34 and 6.35. As expected, the group in test 5b (softer soil) has the lowest capacity per pile. The other two groups show a higher capacity, but more importantly, the group with fewer piles shows a stiffer response than either of the groups of 25 piles. As with previous group types, the peak capacities were ascertained for each grid group, along with the capacities at 0.02, 0.05, 0.10 and 0.20 d settlement. A calculation was then made to determine the percentage of the peak capacity that had been attained at each of the three stages of settlement. It was found that at 0.02 d settlement, 45 % of the peak capacity had been reached; at 0.05 d settlement 69 % of the peak capacity had been reached; at 0.10 d settlement 84 % had been reached; and at 0.20 d settlement the capacity was 97 % of the peak capacity. These percentages compare similarly to those calculated for other groups, and can be summarised as follows:

	0.02 d	0.05 d	0.10 d	0.20 d
• Linear*	52 %	78 %	95 %	99 %
• Perimeter	58 %	79 %	93 %	98 %
• Target	49 %	72 %	87 %	96 %
• Grid	45 %	69 %	84 %	97 %

[*These percentages exclude LL05_1.00, as discussed in Section 6.4.1 along with two other anomalous results from LL05_2.00 (test 3a) and LL05_2.75]

It is clear from this that the linear and perimeter groups respond most quickly and thereby achieve their peak capacity at smaller settlements, although the target and grid groups are not far behind. By a settlement of 0.20 d, all groups have attained at least 96 % of their peak capacity. Having said that, at more practical limits of settlement, such as 0.10 d, the grid groups have achieved only 84 % of their peak capacity, compared to the linear and perimeter groups, which have attained about 10 % more. However, in practical terms, it is unlikely that a pile group would be

designed such that these kind of settlements would be tolerated. More realistically, in terms of design, for a grid group at a settlement of 0.02 d, it has achieved 45 % of its peak capacity, whereas a perimeter group has, on average, achieved 58 % of its peak capacity. The grid group data described in this section and in the following sections are summarised in Table 6.13.

6.7.3 Failure mechanism

Two of the three groups failed as a block; the group where the piles failed individually was GS25_2.00, in test 4a. It is believed that this group would have failed as a block, had it not been for the following conditions: the test had a high average s_u of 65 kPa, the s_u range was just 13 kPa. As previously discussed (most notably for target groups, Section 6.6.3) it is believed that a narrow s_u range can have an influence on failure mechanism. This matter is returned to in Chapter 9. In addition, there were problems with the loading beam tilting, as discussed in Section 5.6.

The results reported by Whitaker (refer back to Figure 2.05) show that the bigger the group, the more likely it is to observe block failure. For example, the widest pile spacing where block failure was observed in the 5x5 group was at spacing of 1.5 d; for the 7x7 group, the widest spacing was 2.0 d; and for the 9x9 group, the widest spacing was 2.25 d. Barden and Monckton note that block failure was only observed in the soft clay sample, at a pile spacing of 1.5 d.

6.7.4 Efficiency

The calculated efficiencies of the three groups are as follows:

- GS16_2.00 (test 5a): $\eta = 0.97$
- GS25_2.00 (test 4a): $\eta = 0.84$
- GS25_2.00 (test 5b): $\eta = 0.81$

The efficiency of the GS25_2.00 (or 5x5) group arrangement, tested by other Authors are as follows:

- Whitaker (1957) = 0.66 (soft clay)

- Barden and Monckton (1970) = 0.7 (soft clay), 0.9 (stiff clay)

The results reported for the soft clay correspond well with each other, and the results reported by Barden and Monckton correspond reasonably well with these model tests. It would be a reasonable argument to assume that had Barden and Monckton tested a firm clay, they may well have observed an efficiency of about 0.8, which would fit very well with the results in firm clay from these model tests. Whitakers results showed that the bigger the group, the lower the efficiency, between pile spacings of 1.5 and 2.25 d. At pile spacings of greater than 2.25 all groups show similar efficiencies.

6.7.5 Comparison with perimeter and target groups

It is clear from the observations thus far, that perimeter groups and target groups are more efficient than grid groups. However, what has not been established is whether, for a given area of ground, a higher capacity could be achieved by installing a greater number of less efficient piles, or a lesser number of more efficient piles. To investigate this matter, the following groups have been compared, all of which occupy the same footprint: GS25_2.00, PS16_2.00 and TS16_2.00. The results are shown in Table 6.14. Unfortunately, the group PS16_2.00 has been guesstimated from three other groups since the result from the actual test was discarded. Where a group was tested more than once in the centrifuge, the average has been calculated and the bottom three rows in the table contain the data for comparison.

The findings presented in the table suggest the greatest capacity can be achieved from group GS25_2.00, which is only true at higher levels of settlement, but this does not necessarily make it a better group. The four columns entitled "efficient pile equivalent" have been calculated from the group efficiencies (at the relevant degrees of settlement) multiplied by the total number of piles in the group to give a theoretical number of fully efficient piles. In this example, if group TS16_2.00 was chosen over GS25_2.00, eight fewer piles would need to be installed (17 from 25) but there would only be a loss of capacity equivalent to that of three piles (21 to 18) at a settlement of 0.20 d. This revelation is even more pronounced at lower settlements; at a settlement of 0.02 d and 0.05 d, the capacity of each of these groups is exactly the same (equivalent to 9 or 14 fully efficient piles, respectively), but again, group TS16_2.00 is

comprised of eight fewer piles than GS25_2.00. The perimeter group shows similar results to the target group, although to a lesser degree.

6.8 Composite pile tests

Much of the equipment is made from aluminium, which is a common material for centrifuge apparatus for a number of reasons: it is easily workable, lightweight and it has a unit weight similar to that of concrete.

Model piles have been made from aluminium in a number of previous centrifuge research projects, and this has been done with success. However, it was decided to try and replicate more realistically a reinforced concrete pile, which would be significantly less stiff than the aluminium pile.

A number of materials were considered for their different properties. An injected resin pile was considered, which is another common method used in centrifuge testing, but rejected because the construction process would be very awkward and the 5 mm diameter pile would be likely to suffer from the formation of air bubbles.

The final solution comprised an aluminium tube injected with resin, with a brass rod inserted through the centre. The aluminium tube had an outside diameter of 5 mm and a wall thickness of 0.45 mm; the pile length was kept at 270 mm. The brass rod had a diameter of 1.2 mm. This composite pile would have the same soil interface properties as used in the main centrifuge tests but would have a longitudinal stiffness comparable to reinforced concrete. The resin was made by mixing casting resin (Biresin G27) with hardener and powder (trihydrated alumina) at a weight proportion of 1:1:2 (resin:hardener:powder).

The stiffness of a concrete pile multiplied by its area was calculated as follows:

- $E_cA_c = 30\ N/mm^2 \times 19.6\ mm^2 = 588\ N$

Where E_c is the concrete stiffness (assuming a high strength concrete) and A_c is the concrete area. The stiffness of a section of the new composite pile, multiplied by its area, was also calculated:

- $(E_aA_a) + (E_rA_r) + (E_bA_b) = (70\ N/mm^2 \times 6.4\ mm^2) + (1.3\ N/mm^2 \times 12.1\ mm^2) + (110\ N/mm^2 \times 1.1\ mm^2) = 585\ N$

Where subscript 'a' is aluminium, subscript 'r' is resin and subscript 'b' is brass. [NB, the best available approximate values of material stiffness were used].

The composite piles were included in test 3c, as a single pile test and group LL05_2.25, also in test 3d as LL05_2.75. Results showed very little difference in response and ultimate pile capacity over these three tests, as compared to identical groups with aluminium piles. Whilst the scope of testing was not particularly thorough, it gave a good indication to the behaviour of a pile with a longitudinal stiffness similar to that of concrete. Composite piles were not used in any further tests.

6.9 Summary

- Single pile

The single pile tests were an essential part of the experiments and without them it would have been virtually impossible to provide reasonable comparison between the separate tests. There were a number of unsuccessful tests, but the majority of later tests yielded good results. From these results it was possible to formulate a convincing relationship between α and s_u, which could then be applied to all tests and allow each group to be normalised by a common factor. This method has assumed that the capacity of the pile base was negligible and can be considered equal to zero.

- Linear groups

The linear pile tests were a good starting point from where to continue the research. Unfortunately a high proportion of the tests were unsuccessful because almost all of the linear groups were in the initial tests, which were largely problematic. The problems were generally caused by the loading mechanism and faults within the various components, which took a number of tests to fully realise and remedy. However, the successful tests provided a good range of data and some limited conclusions could be made. There appeared to be a slight peak in the efficiency

between pile spacings of 1.25 and 1.75 d, allowing the first hypothesis that there is some 'engagement' of the central soil. This idea was pursued in later group tests.

- Perimeter groups

The perimeter pile groups were the main focus of the work and were akin to the comparable prototype, Cannon Place. Despite only half of the groups tested yielding good results and workable data, some interesting observations were made and new findings emerged. It was noted that the three groups with favourable efficiencies, although different in geometry, number of piles, pile spacing and failure mechanism, all had exactly the same group diameter (within 1 mm), which resulted in almost the same efficiency. These groups also fell within a very similar range of R_{cs} values.

- Target groups

The target pile groups were an interesting diversion from the mainstay perimeter groups and on the whole they proved to be the most efficient type of group. However, over the range of tests conducted the addition of the central pile seemed to have little influence over the failure mechanism of the group. The patterns of behaviour were more difficult to characterise because of the increased complexity of the shape and soil-pile interaction mechanisms.

- Grid groups

The grid groups provided an extremely valuable data set. Not only did this allow comparison with the traditional pile group formation, but also helped validate the new research against existing data. The results from this research correlate well with the work published by Barden and Monckton, which in turn correlate well with the widely referred work of Whitaker. As expected, the grid groups are the least efficient type of group, with the group of 25 piles being less efficient than the smaller group of 16 piles.

- Overall

The 46 successful single piles and pile groups that were tested provided a wide range of data from which to make an array of new observations, as well as correlating the

tests both within the research and with existing work. The number of variables has made the analysis quite arduous and the compilation of observations and results has been a complex process. However, there is good reliability and consistency in the data and on the whole the experimental work is considered successful.

7 Numerical Modelling

7.1 Introduction

The performance of the pile groups have been evaluated numerically using the method of non-linear finite element (FE) analysis. The results from the numerical modelling exercise are being used to assist in interpreting and extending the understanding of pile group behaviour, which was observed during the experimental centrifuge work.

A range of pile group models were analysed numerically using the FE programme, Abaqus (Hibbitt et al, 2008), many of which were similar to those tested in the centrifuge. A relatively simple constitutive soil model has been used, and the 3D capability along with the sophistication of this software allows accurate relative comparison between all the numerical models. The numerical modelling also allowed the consideration of different pile group configurations and spacing, enabling comparison with the findings of other Authors, as well as additional groups that could not be tested in the centrifuge because of time constraints. A summary of the pile groups investigated is shown in Table 7.01.

FE modelling is becoming increasingly popular both in industry and academia and it was felt important to combine this numerical work to support the centrifuge experiments and see if the findings concurred with other Authors' data. This would potentially attach further confidence to these experimental findings, which could then be appreciated by the more extensive community of numerical modellers, in addition to centrifuge modellers.

The numerical modelling work was carried out in two phases at the University of Western Ontario, Canada, in collaboration with their Geotechnical Research Centre. The initial phase took place from October 2010 to March 2011 and at this stage 18 of the 23 centrifuge experiments were complete. However, these 18 centrifuge experiments had yielded just 26 of the 46 successful single/group tests. A secondary phase of numerical modelling took place in October 2011 once all 23 centrifuge tests

were complete. Whilst the initial phase was considerably longer, it allowed for the numerical model to be carefully constructed and the programme to be better understood; all the models were in fact run in the second phase of numerical modelling work.

7.2 Model formation

7.2.1 Introduction

A number of techniques were trialled with this software to try and determine the best way of getting realistic, reliable and comparable data. Also, since this aspect of work was only to support the main component of experimental work, the method and models would need to be relatively easy to formulate and with no unnecessary time consuming complications. With this in mind it was decided to analyse the equivalent prototype rather than the centrifuge model, because modelling a centrifuge test introduced several additional complexities. Therefore, all numerical models will be at a 60:1 scale of the centrifuge tests and so all quoted dimensions (stress, force etc.) will also be at equivalent prototype (numerical model) scale. One important difference is that the numerical mesh boundaries will be more remote than the boundaries of the centrifuge strongbox and it is not known what effect this difference may have. The material constituents in the analysis were intended to represent the centrifuge experiments and so parameters for kaolin clay and aluminium were selected. This philosophy resulted in a relatively simple model, with as few complications as possible, but yet gave believable results and provided an interesting and useful comparison to other data.

7.2.2 Soil model

Since only the undrained behaviour of the soil was being considered, it was deemed sufficient to use a total stress model for the soil. The soil has been simulated using eight-node hexahedron elements, whose behaviour is given by the Tresca failure criterion. This failure criterion is implemented in Abaqus as a modification of the Mohr-Coulomb failure criterion and therefore, from this point onwards, the soil model will be referred as 'Mohr-Coulomb'. The following five parameters are required: unit

weight (γ), cohesion (c), friction angle (ϕ), Young's modulus (E) and Poisson's ratio (ν). The analysis assumed undrained conditions and therefore the undrained shear strength (s_u) and associated total stress values were used:

$\gamma = 1800\ kg/m^3$

s_u = various (see Section 8.1.1)

$\phi = 0$

E = 50 MPa

$\nu = 0.5$

The Mohr-Coulomb criterion assumes that failure occurs when the shear stress at any point in a material reaches a maximum value that is given by the normal stress in the same plane. The Mohr-Coulomb model is based on plotting Mohr's circles for states of stress at failure in the plane of the maximum and minimum principal stresses. The failure line is the best straight line that touches these circles. Therefore, the Mohr-Coulomb model is defined by:

$$\tau = c + \sigma\tan\phi \qquad \text{(Equation 7.1)}$$

The friction angle, ϕ, controls the shape of the yield surface in the deviatoric plane (σ_1, σ_2, σ_3). The friction angle in each of these analyses has been taken as zero; and where this is assumed, the Mohr-Coulomb reduces to the pressure-independent Tresca model with a perfectly hexagonal deviatoric section.

Since the conditions are assumed to be undrained and the load is considered to be applied relatively quickly; pore pressures, and the change thereof, have not been accounted for. The Mohr-Coulomb model is often considered too basic to model real in-situ soils with enough accuracy; but in this instance it was considered acceptable, especially since its primary purpose was to allow a comparison, rather than generate absolute values required for design.

7.2.3 Soil profile

The shear strength of the clay in the numerical model increased with depth in a similar way to the true shear strength values measured from the centrifuge tests. The soil was divided into three 5 m sections over the length of the pile, with a further single section extending from the toe of the pile to the base of the model. This technique of course created an imperfect staggered s_u profile, but a sensitivity analysis was carried out by further dividing the soil into five 3 m sections over the length of the pile and very little difference was observed. The soil profiles tested are discussed in Section 8.1.1.

7.2.4 Piles and pile caps

The numerical analyses used equivalent prototype pile dimensions of the centrifuge tests, i.e. 300 mm diameter and 15 m length. The piles were modelled as aluminium and given appropriate corresponding parameters. In reality, the material should not make a significant difference if it is appreciably stiff compared to the soil, and where the l/d ratio is not significantly high. The pile cap was modelled with discrete rigid elements. A constraint was established whereby the underside of the pile cap was tied to the tops of the piles.

7.2.5 Soil-pile interface

Abaqus assumes by default that the interaction between contacting bodies is frictionless and it was necessary to set-up an alternative for the pile-soil interface. The basic concept of the Coulomb friction model is to relate the maximum allowable shear stress (friction) across an interface to the contact pressure between the contacting bodies. Thus, two contacting surfaces can carry a shear stress up to a certain magnitude across their interface before they start sliding relative to one another; this is the state of sticking. The critical shear stress, τ_{crit} (the point at which sliding starts) is defined as a fraction of the contact pressure P_c between the surfaces, which is governed by μ, the coefficient of friction;

$$\tau_{crit} = \mu P_c \qquad \text{(Equation 7.2)}$$

A maximum shear stress, τ_{max}, was also set in each of the analyses and was equal to a proportion of the shear strength of the soil. This was chosen to be similar to the centrifuge value of αs_u. Setting a value for τ_{max} automatically makes it the controlling factor regardless of the magnitude of the contact pressure stress. The piles were divided into three sections, which corresponded with the soil sections to enable appropriate interface values to be applied and therefore the value of τ_{max} varied with depth.

7.2.6 The mesh

The soil-pile system is simulated using a 3D FE model that is comprised of solid eight-node hexahedron elements to represent the soil and the piles. Reduced integration elements were chosen as opposed to fully integrated elements, to overcome the volumetric locking effect of the fully integrated elements when the model material is almost incompressible. The dimensions of the mesh were such that it extended 2L in height (z-axis), where L is the pile length, and a distance L in both the x and y axes.

A staged mesh refinement was carried out to reach an optimum solution. In order to accurately capture the geometry of piles, the average aspect ratio of elements was kept below 1:4. In high stress concentration regions, the aspect ratio was kept as close to unity as possible. The models were seeded by hand and on the whole the same numbers of seeds were placed in the same locations in each model. There was inevitable variation where the soil surrounded the piles, which depended on the number of piles in the group and the spacing. However, every attempt was made to ensure that the models had about the same number of elements, which was kept at approximately 25,000.

In order to reduce the computational time and effort but keep good accuracy, the soil-pile system is simplified to quarter symmetric rectangular models as shown in Figure 7.01. This figure also shows the division of the mesh into sub-sections and highlights the top third of the soil-pile interface. Consequently, symmetry boundary conditions were employed on faces A and B. A fully fixed boundary condition was applied to the base of the model and the faces diametrically opposite A and B were

fully fixed in the x and y directions. The boundary conditions and effects of the far field were rather different in the numerical tests to those in the centrifuge experiments. In the numerical tests, each group is modelled separately and so there is no possibility of neighbouring groups impacting on each other. Also, in the numerical tests, the far field is at a distance of 50 d, whereas in the centrifuge experiments, this distance is down to as low as 10 d. These differing aspects between methods of modelling have not been investigated.

7.2.7 Geostatic stress

Geostatic stresses are used to verify that the initial geostatic stress field is in equilibrium with the applied loads and boundary conditions at negligible strain. This procedure also allows for pore pressure degrees of freedom. However, since pore pressures are not accounted for in this undrained analysis, the function was not required. The geostatic stresses assume a gravitational acceleration of 10 m/s^2 and were applied in the first step, prior to pile installation. The affect of this step is to generate increasing stress with depth (Figure 7.02) with only minute strains and in doing so replicate prototype stress conditions.

The horizontal stresses were directly proportional to the vertical stresses in all models, therefore, $\sigma_h = \sigma_v$ and K = 1.

7.2.8 Loading

The loading was displacement controlled, and this displacement was applied over the surface of the pile cap, with zero allowance of pile cap rotation. To stabilise the model during the onset of deformation, the displacement was applied with an amplitude curve, which meant it was applied very gradually to begin with and getting faster as the displacement continued. This was done to help keep the model stable and avoid element distortions from forming too early on in the solution.

7.2.9 Model test summary

A range of models were tested, many of which corresponded to the centrifuge tests carried out. Square and circular groups were tested, with pile numbers ranging from

12 to 25 piles and spacing ranging from 1.5 to 3.0 d. Occasional numerical instabilities were encountered, although on the whole the tests worked well and problems with convergence rarely occurred.

8 Numerical Analysis and Comparison

8.1 Introduction

8.1.1 Soil strength

A range of soil profiles were tested with a single pile to ensure the numerical analysis was behaving in an expected manner and that it would generate results that give an accurate representation of the centrifuge tests. Naturally, the soil profile chosen for the numerical models would need to reflect the true s_u profile obtained from the hand vane tests taken from the model after centrifuge testing. The value of τ_{max} was adjusted accordingly, as explained in Section 7.2.5, using the equation from the findings of the centrifuge experiments to calculate the appropriate proportion of the soil shear strength:

$$\alpha = 1.1 - 0.008 s_u \qquad \text{(Equation 6.1, from Section 6.3.4)}$$

The first stage of numerical modelling was done before the centrifuge tests were complete and used an approximate soil profile. The principle soil profile that was used in the second stage of modelling was soil profile A (sp_A), which was chosen because it most accurately represented the average soil profile of all centrifuge tests under analysis. All soil profiles used in the numerical analyses are shown in Figure 8.01, along with the associated αs_u paths and the Nuñez correlation profile (discussed in Section 6.2). The s_u values were calculated over three equal staged depths of 0 – 83 mm, 83 – 167 mm and 167 – 250 mm. These depths correspond to prototype depths of 0 – 5 m, 5 – 10 m and 10 – 15 m respectively. The corresponding α values were calculated and the resulting soil profile A was as follows:

- Section 1: 0 – 5 m; s_u = 30 kPa; α = 0.84
- Section 2: 5 – 10 m; s_u = 50 kPa; α = 0.68
- Section 3: 10 – 15 m; s_u = 60 kPa; α = 0.60

Since it was found that the strength of the soil beneath the piles had little effect on the overall results, it was decided that the soil from 15 – 30 m would have the same profile as the soil in section 3, listed above.

8.1.2 Single pile

In the centrifuge tests, the reported capacity of a single pile was equal to the peak capacity. In the numerical model, the load vs settlement curve for sp_A is shown in Figure 8.02 and it can be observed that the peak capacity is equal to the ultimate capacity. The single pile centrifuge tests were only used for comparison, and it was the calculated values that were used for all normalisations, although the actual test results showed very good correlation with the calculated values. A different approach to normalisation will be used for the numerical analysis.

The single piles from the numerical modelling will be used to normalise all group numerical models and this was trialled in three ways. Firstly, (1) the capacity of the single pile was determined at the same stages of settlement as the groups, at 0.02, 0.05, 0.10 and 0.20 d. This approach was not possible in the centrifuge tests since testing problems had resulted in there being only one value for the capacity of a single pile whereas for the numerical modelling there is an equivalent single pile capacity at each stage of settlement. Secondly, (2) the peak capacity of the single pile was compared with the group capacities at the various stages of settlement, which allows a direct comparison of group efficiencies in the same way as was done for the centrifuge tests. Finally, (3) the staged group capacities (0.02, 0.05, 0.10 and 0.20 d) were compared with a specific stage of single pile settlement (0.02, 0.05, 0.10 or 0.20 d), which was chosen as a result of the outcome of the first two methods of analysis. It turned out that for this third method of analysis, comparison with a single pile settlement of 0.10 d gave the most analogous outcome between numerical and centrifuge results. It is not surprising that the centrifuge experiments do not compare well with the numerical tests that are normalised against a single pile at small settlements. This is because the simple numerical soil model is not capable of accurately predicting the non-linear small strain stiffness behaviour of soil, but can predict well at moderate strains. The numerical soil model tends to over predict at

high strains, which is thought to be caused by the difficulty in forming a clay-clay failure surface.

The peak capacity of the single pile in the numerical analysis (refer back to Figure 8.02) is comparable to its ultimate capacity and is reached after a settlement of 90 mm, or 0.30 d. The capacity does not significantly increase any further and the analysis was terminated at 100 mm settlement. A capacity calculation using Skempton's equation (Equation 2.1), gives a single pile capacity of 487 N, a difference of about 10 % compared with the numerical results. The average capacity of a single pile obtained from the centrifuge tests was 148 N. The centrifuge scaling law for force is $1:1/N_g^2$ (where N_g is the dimensional scale factor); so at prototype scale the model capacity equates to 533 kN. The actual single pile peak capacity calculated by the numerical model for sp_A was 538 kN, which is a difference of only 1 %. A more thorough analysis is possible with the numerical modelling than for the centrifuge tests since there are not the same problems with test errors and inevitable differences between tests.

8.2 Perimeter groups

8.2.1 Introduction

Seven perimeter groups were tested and were selected for testing on the basis of results from the centrifuge tests. The intention was to investigate the transition between the two types of failure mechanism and the higher efficiency groups; as a result only a relatively narrow range of groups were tested. Five groups were circular groups and five groups were arranged at a pile spacing of 1.75 d. Unfortunately, three of the groups did not reach a settlement of 60 mm (0.20 d) before the soil elements at the base of the piles over-distorted and the model could no longer converge. Four of the seven groups had been tested in the centrifuge, and a further numerical square group, PS16_2.00, was compared with its circular equivalent, PC16_2.00, which had been tested in the centrifuge. These five group comparisons allowed a good evaluation between the two modelling methods. A summary of the data is shown in Table 8.01. The first part of the table shows the results of the seven groups that were analysed and displays the data as the group capacity divided by the number of piles (assuming

all piles carry equal load) at increasing stages of settlement. The following three parts of the table show efficiency results only for the five groups that were tested experimentally and numerically. The first shows a numerical comparison of different stages of single pile settlement, which could not be done with the centrifuge results, for reasons already given. The second shows the results of both modelling methods compared with a single pile peak capacity, which was how the centrifuge results were analysed. The final part shows results from the centrifuge (as above) compared with numerical results where the efficiencies were calculated against a single pile at 0.10 d settlement. These different comparison methods were introduced in Section 8.1.2. This analysis includes the comparison of PS16_2.00 (numerical) with PC16_2.00 (centrifuge). As stated, the most successful comparison was with a single pile capacity at 0.10 d settlement. This, the final part of Table 8.01, is what will be discussed in the following efficiency comparison.

8.2.2 Efficiency comparison

- Numerical only

The efficiencies of the groups at a settlement of 0.02 d were all very similar at approximately 0.38, with the exception of PS16_2.00, where the efficiency was only 0.32. At a settlement of 0.05 d, these values had increased to 0.74 and 0.66 respectively, with the exception of PC12_1.50, which had only increased to 0.68. The efficiencies at 0.10 d further increased to approximately 0.92 for all groups, with the exception of PS16_2.00, where the efficiency was 0.88, and PC12_1.50, where the efficiency was 0.79. At a settlement of 0.20 d the efficiencies had increased to between 1.00 and 1.02 for three of the groups, except for PC12_1.50, which was only 0.84 and PC16_1.75 which failed to converge to this point.

- Numerical / centrifuge comparison

With the exception of the efficiencies at a settlement of 0.02 d (an average efficiency difference of 0.16, where the centrifuge tests had significantly higher values), each of the other stages of settlement are very comparable. At 0.05 d, the average variation is 0.08, with the centrifuge tests generally showing higher efficiencies; the comparison at

0.10 d shows a discrepancy of just 0.05 between efficiencies. The average difference at 0.20 d is even less, just 0.03 separates the efficiency measured in the centrifuge tests from that obtained by this method of numerical analysis.

8.2.3 Central soil settlement

Of the four groups that reached 100 mm of pile settlement, the degree of central soil settlement is shown below. Also shown are the group efficiencies from the third method of analysis at a group settlement of 0.20 d (with centrifuge data preceding numerical data):

- PS16_2.00 central soil = 0 mm efficiency = 1.00 / 1.00
- PC14_1.75 central soil = 50 mm efficiency = 1.00 / 1.02
- PS20_1.75 central soil = 70 mm efficiency = 1.09 / 1.01
- PC12_1.50 central soil = 80 mm efficiency = 0.90 / 0.84

These results suggest that moderate settlement of the central soil (greater than 0 mm, but less than 80 mm), which indicates a block type failure mechanism, is associated with pile groups displaying higher efficiencies, although there is not enough evidence to substantiate the proposal at this stage. It also suggests that if the depression of the central soil is too great then this has a detrimental effect on the group efficiency, although this may only be the case for groups with pile spacing less than 1.75 d. The group PS16_2.00 displays no movement of the central soil, indicating that the piles behave independently, and this is supported by the result of an efficiency of 1.00, as shown in both the centrifuge and the numerical modelling. It should be noted that in the centrifuge group PS20_1.75 shows a very high 'favourable' efficiency, and it is possible this is caused by experimental error, rather than showing a trend. The load vs settlement curves for these groups are shown in Figures 8.03 to 8.06; plotted as Q_{test}/Q_{calc} [per pile] vs settlement, where Q_{test} is the capacity per pile obtained in the centrifuge/numerical analysis, and Q_{calc} is the calculated capacity of a single pile based on Skempton's equation (Equation 2.1). The intention was to strip away the differences between test methods and allow pure comparison. This method of

presenting the results takes into account the differences in the s_u and α profiles of the two methods of modelling.

The load vs settlement curves for PS20_1.75 and PC12_1.50 show generally good agreement and similar form, although the centrifuge shows a higher peak beyond a settlement of 0.10 d. The curves for PS16_2.00/PC16_2.00 show a similar end shape but a different initial stiffness, which may be a direct result of the difference in group shape and indicating that a circular arrangement is stiffer. The curve for PC14_1.75 shows excellent agreement between the two methods of modelling.

Each of the three groups that showed settlement of the central soil in the numerical modelling failed as a block in the centrifuge. A further worthwhile comparison is that the numerical group PS16_2.00 showed no central soil depression, and the circular arrangement of this group (PC16_2.00) that was tested in the centrifuge showed no signs of block failure either.

8.3 Target groups

8.3.1 Introduction

Five target groups were analysed and were selected on the basis of results from the centrifuge tests. As a result, the range of group size was relatively narrow. Three groups were circular groups and four groups were arranged at a pile spacing of 2.0 d. One group did not reach a settlement of 0.20 d before the soil elements at the base of the piles over-distorted and the model could not converge. Capacities and efficiencies are summarised in Table 8.02, and presented as they were for the perimeter groups.

8.3.2 Efficiency comparison

All five target groups had been tested in the centrifuge, allowing a good comparison between the two modelling methods. However, slightly anomalous centrifuge results were obtained for group TC14_1.75 relative to the others and it has been excluded from the following efficiency analysis. In addition, TS16_2.00 was tested three times in the centrifuge, but one result (from test 5b, softer soil) was noticeably different from

the other two at higher settlements and is also excluded with an average of the other two tests used in the analysis.

The following paragraph compares the results from the group analyses, normalised against the capacity of a single pile at a settlement of 0.10 d. When compared at a settlement of 0.02 d, the resulting efficiencies are rather different, as was the case for the perimeter groups, and the average discrepancy is very similar, approximately 0.17, with the centrifuge results always higher than the numerical results. The discrepancy reduces to about 0.09 by a settlement of 0.05 d. At a settlement of 0.10 d the two modelling methods give more similar results, with an average difference of just 0.07. At a settlement of 0.20 d the difference further reduces to 0.04.

8.3.3 Central soil settlement

Of the four groups that reached 100 mm of pile settlement, the degree of central soil settlement is shown below. Also shown are the group efficiencies from the third method of analysis at a group settlement of 0.20 d (with centrifuge data preceding numerical data):

- TC14_1.75 central soil = 80 mm efficiency = 0.94 / 0.95
- TC16_2.00 central soil = 50 mm efficiency = 1.12 / 1.09
- TS16_2.00 central soil = 60 mm efficiency = 1.08 / 1.06
- TS20_2.00 central soil = 20 mm efficiency = 1.10 / 1.02

As was the case for the perimeter groups, these results suggest that groups that develop a moderate settlement of the central soil (which can now be refined to about 20 to 70 mm) often have the highest efficiencies. The load vs settlement curves for the target groups are shown in Figures 8.07 to 8.10, which are plotted in the same way as the perimeter group graphs. Groups TC16_2.00, TC14_1.75 and TS20_2.00 all show good correlation between test methods. Group TS16_2.00 also shows good correlation with test 4c, but only moderate correlation with test 4b and 5b.

Group TC14_1.75 failed as a block in the centrifuge. Groups TC16_2.00 and TS20_2.00 failed as individual piles, although it is possible that some settlement of the central soil

may have taken place within these groups, especially TC16_2.00, without a visible shear plane forming. Group TS16_2.00 was tested three times and failed once as a block and twice as individual piles. Group TC16_2.00 and TS20_2.00 were both part of test 4c, where the average s_u was 61 kPa and the s_u range was just 6 kPa; one of the TS16_2.00 groups that failed as individual piles was also in this test. Had the soil been softer or the s_u range been greater it is likely that block failure would have occurred. On a basic level, both modelling methods show that the smaller the area of the group, the more the central soil settles, which is logical. This point will be expanded upon in Section 8.5 with the introduction of alternative soil profiles.

8.3.4 Perimeter and target group comparison

Two groups were analysed as perimeter and target groups and can be summarised as follows (as per previous formats):

- PC14_1.75 central soil = 50 mm efficiency = 1.00 / 1.02
- TC14_1.75 central soil = 80 mm efficiency = 0.94 / 0.95
- PS16_2.00 central soil = 0 mm efficiency = 1.00 / 1.00
- TS16_2.00 central soil = 60 mm efficiency = 1.08 / 1.06

For the group of fourteen piles spaced at 1.75 d, the addition of the central pile gradually leads to a reduction in efficiency, which increases with larger settlements (see Table 8.03), although there is little difference up until 0.20 d. The central pile also increases the extent to which the central soil settles with the piles. For the group of sixteen piles spaced at 2.0 d, the addition of the central pile leads to an increase in efficiency, which is pronounced at all stages of settlement, but reduces slightly with increasing settlement. The central pile causes the central soil to settle with the piles, whereas the soil had not moved at all in the equivalent perimeter group. In summary, the central pile causes different effects depending on the group geometry. Results indicate that target groups can have higher efficiencies at bigger spacings (2.0 d) than in perimeter groups, but lower efficiencies at smaller spacings (1.75 d). The numerical modelling reveals how the central pile can have an effect on dragging down the central

soil for a square group of 16 piles and 2.0 d spacing. The results are shown in Figures 8.11 and 8.12.

As discussed previously, one significant difference between modelling techniques is the way the numerical analyses model the shear surface. Figure 8.12 (inset) shows TS16_2.00, which illustrates the effect of the central pile in dragging down the central soil and the lack of sliding between soil element interfaces. This consequence may have been less pronounced if modelled with a finer mesh, but its effect on mobilisation of shear stress is thought to be minimal. [NB: the displayed scale does not apply to the inset, which is shown for illustrative purposes only. The vertical scale of the inset is exaggerated by a factor of five].

8.4 Grid groups

8.4.1 Introduction

Four grid groups were analysed and the main intention was to allow a good comparison, not only with centrifuge results, but also with results published by other Authors. Three groups consisted of 25 piles, at a pile spacing of 1.5, 2.0 and 3.0 d; the fourth group was a grid of 16 piles spaced at 2.0 d. Group GS25_3.00 did not fully converge and therefore no data are available at a settlement of 0.20 d. A summary of the comparison is given in Table 8.04 (in the same way as for perimeter and target groups) and load vs settlement curves are shown in Figures 8.13 and 8.14.

8.4.2 Efficiency comparison

As for perimeter and target groups, this method of comparison, whereby the groups are normalised by the capacity of a single pile at a settlement of 0.10 d, provided the best similarity between modelling methods. The results were slightly different at 0.02 d, with a disparity of 0.08. The strongest similarities were at settlements of 0.05 d and 0.10 d, where the difference was just 0.02 and so the modelling methods show a very good likeness.

8.4.3 Central soil settlement

All three groups that reached 100 mm of pile settlement showed that the central soil also settled by 100 mm. Group GS25_3.00 appeared as if the central soil was settling by less than the piles and would not have settled the full 100 mm had the model fully converged.

The two groups with piles spaced at 2.0 d had been tested in the centrifuge and GS25_2.00 was tested twice. Group GS16_2.00 failed as a block; group GS25_2.00 failed once as a block and once as individual piles. The occasion where block failure did not occur, the group was in an unusually strong clay sample, with average s_u of 65 kPa, compared to the global group average of 53 kPa. This is an important point that is investigated in more detail in the following section.

8.5 Varying soil strength

Soil profile B (sp_B), soil profile C (sp_C) and soil profile C2 (sp_{C2}) were tested for comparison against sp_A, to make further use of the numerical modelling; not just to affirm centrifuge results but to make predictions beyond. In general terms, sp_B is double the strength of sp_A and sp_C is half the strength of sp_A (refer back to Figure 8.01). Soil profile sp_{C2} is similar to sp_C, but also has reduced soil stiffness, to the same proportion of the reduced soil strength. The soil profiles are summarised as follows:

- sp_A 0 – 5 m: $s_u = 30$ kPa, $\alpha = 0.84$, $s_u\alpha = 25$
  5 – 10 m: $s_u = 50$ kPa, $\alpha = 0.68$, $s_u\alpha = 34$
  10 – 30 m: $s_u = 60$ kPa, $\alpha = 0.60$, $s_u\alpha = 36$
- sp_B 0 – 5 m: $s_u = 60$ kPa, $\alpha = 0.60$, $s_u\alpha = 36$
  5 – 10 m: $s_u = 100$ kPa, $\alpha = 0.49$, $s_u\alpha = 49$
  10 – 30 m: $s_u = 120$ kPa, $\alpha = 0.43$, $s_u\alpha = 52$
- sp_C 0 – 5 m: $s_u = 15$ kPa, $\alpha = 1.13$, $s_u\alpha = 17$
  5 – 10 m: $s_u = 25$ kPa, $\alpha = 0.96$, $s_u\alpha = 24$
  10 – 30 m: $s_u = 30$ kPa, $\alpha = 0.84$, $s_u\alpha = 25$

The values of s_u were simply calculated as either double (sp_B) or half (sp_C) the s_u values from sp_A. This meant that the top section of sp_B had the same s_u as the bottom section of sp_A, thus the same α value. The $s_u\alpha$ value was also 36 therefore. The $s_u\alpha$ value for the top section of sp_A was 25, and 36 is a 1.44 proportion of this value. A 1.44 multiplication factor was used to calculate the remaining $s_u\alpha$ values, and thus, the α values. It is important to note that the α values could not be calculated from the same equation as previously done, and it was stated in Section 6.3.4 that it was only considered appropriate to apply the linear equation over the original narrow range of clay representing a firm consistency. The calculation of sp_C was done in much the same way, only this time the bottom section of sp_C was the same as the top section of sp_A and the multiplication factor of 1.44 became a reduction factor. In the case of sp_{C2}, the soil stiffness was reduced from 50 to 25 MPa in all three soil sections.

Four groups were tested in soil profile sp_B, which can be compared directly with sp_A, these are: PS20_1.75, TC14_1.75, TS16_2.00 and GS25_2.00. The latter two groups listed were done to help make sense of the different behaviour and failure modes that were witnessed in the centrifuge tests. The other two groups were tested because they had shown considerable central soil settlement in soil profile sp_A (without having fully settled with the piles) and there was interest in what effect the stronger soil would have on such groups.

Efficiency comparisons were carried out at the customary stages of settlement, using the single pile capacity of 0.10 d, as it was shown to be successful in previous comparisons. The data discussed in this paragraph is shown in Table 8.05. At lower levels of settlement (0.02 d and 0.05 d) there is little difference between the two soil profiles; this is also true at 0.10 d, with the exception of GS25_2.00, where the efficiency climbs to 0.98, compared to 0.71 in sp_A. This indicates that for GS25_2.00, at a settlement of 0.10 d, an efficiency increase of 0.27 is obtained in a soil of double strength. There are moderately higher differences in all four groups at a settlement of 0.20 d, where the pile groups in soil profile sp_B show higher efficiencies than sp_A. The least difference is 0.13, for PS20_1.75, followed by 0.16 for TS16_2.00 and 0.21 for TC14_1.75. The most notable difference is group GS25_2.00, where the efficiency is 1.17, an increase of 0.39 from the efficiency found for sp_A.

The stronger soil causes a reduction in central soil settlement for all groups, summarised as follows (where pile settlement was 100 mm):

- GS25_2.00 sp_A = 100 mm sp_B = 80 mm
- TC14_1.75 sp_A = 80 mm sp_B = 0 mm
- PS20_1.75 sp_A = 70 mm sp_B = 0 mm
- TS16_2.00 sp_A = 50 mm sp_B = 0 mm

Only group GS25_2.00 was tested with soil profile sp_C and sp_{C2}. The impact was quite pronounced at a settlement of 0.02 d, where the difference in efficiency was 0.13; an efficiency of 0.37 for sp_C, falling to 0.25 for sp_{C2}. The difference is negligible for all other stages of settlement. The result is what might be expected since, as previously discussed, the simple Mohr-Coulomb model does not predict well at small strains. The outcome also suggests that the stiffer soil does cause groups to have a higher efficiency at lower levels of settlement, which is likely to be because strength is mobilised more rapidly as the loads are transferred through the soil at smaller shear strains.

8.6 Varying l/d ratio

To further advance the centrifuge work, it was decided it would be of value to test pile groups with a different l/d ratio. The standard l/d ratio was 50, and the modified l/d ratio would be 100; this was chosen partly for the ease of assessment, but also to allow a comparison with Cannon Place, where the l/d is approximately 100. The piles were kept the same length (15 m) but were reduced in diameter from 300 mm to 150 mm. The data discussed in the following paragraph is given in Table 8.06.

Efficiency comparisons were carried out in the same way to previous numerical analyses and emphasis is placed on the results of the method that uses the single pile capacity of 0.10 d. Three groups were tested: PS20_1.75, TS16_2.00 and GS25_2.00, but unfortunately only PS20_1.75 fully converged to provide a total solution. In each case, the result was compared to the standard groups, where the piles have an l/d ratio of 50. For all groups, the efficiency is lower for the slender piles at settlements of 0.02 and 0.05 d. At 0.10 d, the slender piles have a higher efficiency for groups

PS20_1.75 and GS25_2.00, but lower for TS16_2.00. At 0.20 d, the efficiency of the slender piles is higher for every group. The efficiency exceeds 1.00 quite significantly; for PS20_1.75 the value increases to 1.19 (from 1.01 for standard piles) and for TS16_2.00 the value increases to 1.12 (from 1.06 for standard piles), whilst the efficiency of the grid group increases from 0.78 to 0.88. Also, in each case, the slender piles cause less central soil settlement; the reduction is by approximately half. In previous comparison, the efficiency at 0.10 d single pile settlement, compared with 0.10 and 0.20 d group settlement provided the best similarities. In summary, the slender piles have lower efficiencies at lower levels of settlement and they have higher efficiencies at higher levels of settlement, although this is not universally true, as it is partially dependent on group geometry.

8.7 Soil stresses and movements

8.7.1 Introduction

In order to make comparisons regarding the soil stresses and movements in the most effective way possible, two models have been considered. Group PS20_1.75 has been analysed both in soil profile A (sp_A) and soil profile B (sp_B). The reasons for this were that, not only was the group tested in the centrifuge as well, but the differing soil profiles caused different failure mechanisms, which was likely to lead to an interesting comparison. Group PS20_1.75 fails as a block in sp_A and fails as individual piles in sp_B.

The variables under analysis are the vertical stress (S33), the horizontal stress (S22), the vertical displacement (U3) and the horizontal displacement (U2). The horizontal variables (S22 and U2) are analysed along three vertical paths on the y-axis; one path is inside the group and two are outside, as shown by the green lines in Figure 8.15. The diagram is a sketch of the y-plane of the mesh and shows an approximate location of the pile. The vertical variables (S33 and U3) are analysed along the following three horizontal paths; 2 m (near pile top), 8 m (near pile middle) and 16 m (beneath pile toe), as shown by the purple lines in Figure 8.15. The data are taken from the following stages of pile settlement: 0.01, 0.02, 0.05, 0.10 and 0.20 d.

8.7.2 Soil stresses

To calculate and assess the changes in vertical stress, the magnitude of stress at the defined stages of settlement has been recorded and was then plotted as a proportion of the initial geostatic stress. All lines plotted in Figure 8.16 are taken from the results at a settlement of 0.20 d only. The x-axis is the distance from the centre of the group, out towards the model boundary; the right-hand y-axis is the depth of the path through the model; and the left-hand y-axis is the measured stress divided by the initial stress, with three individual axes for each depth considered within the model. As a consequence, values that plot higher than 1 on the y-axis represent an increase in stress (relative to the initial in-situ stress) as displacement proceeds, and values that plot lower than 1 represent a decrease in stress. The location of the nearest pile is also marked on the graphs.

The three sets of lines show the results of PS20_1.75 at the three specified depths within the model and where the lines represent a path from the centre of the group along a line of x = 0, y = 0 to 15 (15 m is the width of the model) and z = constant. The results from sp_A are shown in blue and results from sp_B are shown in red. At z = 2 m, there is a reduction in stress in both sp_A and sp_B, although the reduction in sp_A is more pronounced close to the pile. At z = 8 m, there is an increase in stress in sp_A and no changes in stress in sp_B. Finally, at z = 16 m, there is an increase in stress in both soil profiles, but the increase is distributed more evenly in sp_A, whereas the increase is more highly concentrated beneath the pile toe in sp_B. Figures 8.17 and 8.18 show how these lines change as pile settlement progresses, from 0.01 d to 0.20 d for sp_A and sp_B respectively. It is interesting to observe that the patterns appear to be a reflection of one another; the 'peak' reduction in stress shown at z = 2 m in sp_A, is mirrored by the 'peak' increase in stress shown at z = 16 m in sp_B. The main difference in this pattern, as noted previously, is at z = 8 m where there is an increase in stress in sp_A and no increase in sp_B.

A similar illustration of results for the horizontal stresses is shown in Figure 8.19. The y-axis shows the depth of the model; the top x-axis is the distance from the centre of the group, with paths at 0.5 m, 1.5 m and 2.5 m; the bottom x-axis shows the recorded

stress as a proportion of the initial stress, with each path having a separate axis. Stresses within the top 5 m are markedly different between soil profiles and the stress in sp_B is significantly higher. However, it should be noted that results are exaggerated since they are displayed as a proportion of the initial stress, which is very low near the surface of the soil and so a stress several times higher is not necessarily a high stress in absolute terms. The path at a distance of 1.5 m outwards from the centre of the group (i.e. just on the outside of the pile group) shows that the stresses at a depth of approximately 2 m decrease in sp_A, whereas in sp_B stresses at this level have increased and this is the principle difference between the soil profiles. As may be expected, just below the horizon of the pile toe, horizontal stresses have increased. However, for sp_B, there is a region just above the toe of the piles where the stresses appear to have decreased, particularly just on the outside of the group. Figure 8.20 shows how the horizontal stresses in sp_A develop and show a general increase with time for each of the three vertical paths, below about 5 m depth. This is least pronounced for the path furthest from the piles. In sp_B, the stresses between 5 and 10 m go almost unchanged (Figure 8.21).

8.7.3 Soil movements

The vertical soil movements from the numerical modelling are shown in Figure 8.22. The path profiles are the same as those in the measurement of the vertical stresses, at depths of 2 m, 8 m and 16 m from the soil surface. The results are clear; in sp_A, the vertical settlement is significant, in the order of 40 mm, and hence the group has failed as a block. In sp_B, the vertical settlement is much less, only a few millimetres difference between the soil level on the inside and outside of the group, and so the group failed as individual piles. Beneath the piles the vertical settlement is much less for sp_A, 10 to 15 mm, but has a similar magnitude from sp_B as was observed within the pile group. The development of central soil settlement for sp_A is shown in Figure 8.23, where the soil settlement is plotted at increasing stages of pile settlement. It can be seen that it is somewhere between 0.02 and 0.05 d where the block mechanism begins to develop.

The horizontal soil movements from the numerical modelling are shown in Figure 8.24. The path profiles are the same as those in the measurements of the horizontal

stresses, at distances of 0.5 m, 1.5 m and 2.5 m from the centre of the group. The main observable pattern is that the horizontal movements are greater in sp_A and the soil moves outwards, away from the pile group, except from at the top of the piles, where the soil can be seen to be moving inwards. The path at 1.5 m in sp_A is thought to have suffered numerical instabilities, which has given it a pronounced wavy shape.

From observations made during the centrifuge testing, it appeared that groups which failed via the block mechanism suffered significant displacement of soil. For example, with reference back to Figure 5.21, it is clear that approximately 8 mm of soil has 'disappeared' from the centre of the group (scaled from the 5 mm pile). The test is a quick undrained test and therefore no volume change can occur, and the only logical explanation is that the soil which has been pushed down in the centre redistributes other soil resulting in an increase in the overall soil level outside the groups. This can be observed, to some extent, in Figure 8.22. This clay level change is not clearly observable in the centrifuge tests since the redistribution is over a large area and would only raise the overall height of the clay surface by a fraction of a millimetre. A diagram of these hypothesised mechanisms of movement and associated stresses are shown in Figure 8.25.

8.8 Design considerations

In order to make the research more relevant for practical design purposes, it would be preferable to define failure conditions of capacity and settlement for each of the groups. However, design criteria will differ from project to project and since the research has not incorporated full scale site tests, the allocation of specific values will not be attempted. In addition, each design will have differences regarding settlement tolerances and design parameters so specific guidance would not prove productive.

Efficiency vs settlement curves from centrifuge and numerical modelling are shown in Figures 8.26 and 8.27. The non-linear zone has been highlighted and the mid-point of this zone is suggested as a reasonable value for Q_{ult}. The non-linear zone is wider for the centrifuge modelling and this is likely to be a more realistic response (since the numerical modelling is known to represent this section of the curve with less realism).

Interestingly, the mid-point of the non-linear zone is at almost exactly the same place for both sets of results, at 0.10 d, and this was the point where results showed best correlation, as demonstrated in earlier sections. It can also be observed that the curves have a similar order for both modelling methods. For example, GS25_2.00 has the lowest efficiency and groups TS16_2.00 and TC16_2.00 have the highest efficiencies.

In summary, if a simple single pile design is completed, using the traditional Skempton equation, then once this capacity has been multiplied by the number of piles in the group, these curves can be used to determine the approximate efficiency of the group and what reduction factor, if any, needs to be applied. Of course, this is in addition to the factor of safety that needs to be applied.

8.9 Comparison with Cannon Place

As stated in the initial introduction to this research, any extrapolation and comparison between the centrifuge tests and Cannon Place is done for interest and illustrative purposes only. This is because the relationship between the centrifuge models and the full scale 'prototype' at Cannon Place is not directly comparable.

As discussed in Section 6.7.2, a traditional 5x5 grid group has achieved 69 % of its peak capacity at a settlement of 0.05 d, but at 0.02 d this reduces to just 45 %. Similarly, a perimeter group has achieved 79 % of its peak capacity at 0.05 d and only 58 % of its peak capacity at 0.02 d settlement. On completion and handover of Cannon Place in September 2011, the monitoring showed a maximum settlement of approximately 4 mm, which corresponds to about 1.3 % of the 305 mm pile diameter. Therefore, it may be said that the pile groups at Cannon Place, under full load, are below 58 % of their peak capacity, which would fit well inside the required factors of safety. It could also be said that a traditional grid group, at this same stage, would be below 45 % of its peak capacity and it could therefore be argued that such a pile arrangement would be less efficient, since larger settlements are required to mobilise a given percentage of the peak capacity and the inclusion of central piles in a grid arrangement are, in effect, wasted.

The numerical modelling enabled testing of higher soil strengths and higher l/d ratios, akin to those at Cannon Place, allowing an extended and more enlightened comparison to be made. The following analyses refer to Tables 8.05 and 8.06. Since the settlements at Cannon Place were very small, the 'staged single pile capacity' comparison gives the most representative efficiencies.

Group PS20_1.75 was tested as part of the numerical modelling, and can be considered very similar to a number of the groups at Cannon Place, which have 18 or 22 piles and are spaced at 1.64 d. At low settlements of 0.02 and 0.05 d, the results show that the stronger soil has a slightly lower efficiency. It is only from a settlement of 0.10 d onwards that the efficiency increases and exceeds that of the softer soil. For the staged single pile capacity comparison (top section of Table 8.05) the efficiencies at a settlement of 0.02 d are 0.88 and 0.83 for the softer and stronger soils respectively; these values increase to 0.91 and 0.94 respectively, at settlements of 0.10 d.

The effect of a higher l/d ratio is similar to the effect of a stronger soil. At a low settlement of 0.02 d, the efficiency of the high l/d group is lower than the low l/d group. At settlements of 0.10 d and beyond the efficiency of the high l/d group is higher. For the staged single pile capacity comparison the efficiencies at a settlement of 0.02 d are 0.88 and 0.86 for the low and high l/d groups respectively; these values increase to 0.92 and 0.97 respectively, at settlements of 0.10 d.

The coupled effect of a high l/d ratio and a stronger soil indicate that the pile groups at Cannon Place, which have seen very low measured settlements, may have fractionally lower efficiencies than postulated from the results of the centrifuge tests.

9 Discussion

9.1 Capacity and efficiency

The grid groups proved to be the most inefficient type of the group, and the group of 25 piles was less efficient than the group of 16 piles. This is perhaps not surprising when it is considered that in the group of 25 piles, nine of the piles are 'central piles' and 16 are 'outside piles'. For the group of 16 piles, four are 'central piles' and 12 are 'outside piles'. Put another way, the group of 25 piles is less efficient because 36 % of the piles are central, whereas only 25 % of the piles are central in the group of 16 piles.

Findings from the centrifuge and numerical modelling show a combination of agreement and deviation. Importantly, the peak capacity of a single pile was calculated to be very similar for both methods of analysis. Unfortunately it had not been possible in the centrifuge tests to measure in reliable detail the full load vs settlement response of a single pile, whereas a full response did come out of the numerical analysis. Hence, it was necessary to find the best capacity to use to normalise the data, to calculate efficiencies, and in doing so provide comparison between groups. It was found that using the capacity of a single pile at a settlement of 0.10 d in the numerical results gave a good comparison between the centrifuge and the numerical results. Comparison with the peak capacity of a single pile from the numerical modelling, as was done for the centrifuge results, was less successful.

The three methods of comparison showed similar outcomes for perimeter, target and grid groups, with the efficiencies well compared when correlated with the capacity of a single pile at a settlement of 0.10 d. Target groups generally showed higher efficiencies than perimeter groups. The highest efficiencies were for target groups with piles spaced at 2.0 d. For perimeter groups, the lowest efficiencies were seen at a pile spacing of 1.5 d and the highest efficiencies were at a pile spacing of 1.75 d; these highest efficiencies were accompanied by moderate settlement of the central soil (50 to 70 mm). However, it should be remembered than these observations are partly a function of the groups that were tested.

9.2 Failure mechanism and central soil settlement

Approximately fifty percent of the pile groups tested in the centrifuge failed via the block mechanism. Groups that failed via the block mechanism generally, but not always, had lower efficiencies. Measurements of the central soil were particularly useful for movements that were not easy to see, and in a number of examples this methodology showed that the central soil had settled relative to the soil outside the group, which would have otherwise gone undetected.

It is suggested that limitations of numerical modelling prevent the prediction of group efficiencies of significantly greater than unity, since a true shear surface cannot develop even when there is substantial settlement of the central soil. The soil model will not allow development of a shear surface and full shear stress mobilisation because the soil elements will not slide relative to each other. The load vs settlement curves show good agreement between methods. Some groups (PS20_1.75 and PC12_1.50) are capable of mobilising additional load in the centrifuge (compared with numerical results) beyond pile settlements of 20 mm (prototype scale), which is likely to be attributable to the beneficial development of clay-clay shear.

Perimeter groups with pile spacing greater than 2.0 d did not show block failure, but the addition of a central pile can lead to failure mechanism change. However, where pile spacing is less than 2.0 d, the central pile causes a reduction in efficiency. Both methods show a transition from individual failure to block failure can occur for both perimeter and target groups.

The settlement of the central soil shows correlation between test methods, but accurate measurements within the centrifuge tests have not always been possible. It is probable that there is a point in the settlement of the central soil, as shown for the numerical modelling, which corresponds to a change in failure mechanism in the centrifuge modelling. For these standard test groups this is equivalent to about 0.20 d (60 mm at equivalent prototype scale), although the value is dependent on soil strength and l/d ratio, as well as the s_u range. It is believed that these characteristics govern the ability of the soil to develop block failure. If the soil strength is high, the soil

will shear less easily, and if the l/d ratio is high the group will less easily mobilise as a unit. This occurs because the longer the pile, the lower the development of shear strains towards the base of the pile, resulting in reduced mobilisation of shear stress and a greater contrast in shear stress mobilisation over the length of the pile. A high s_u range allows the softer central core of soil at the top to 'stretch', then to shear with relatively high displacements, and 'react' against the stiffer soil below, as displayed in Figure 8.25. At lower settlements there is little difference between pile groups tested in different soil profiles. At higher settlements, the stronger soil generates higher efficiencies accompanied by reduced central soil settlement. The effect is the same for slender piles, also generating higher efficiencies.

The R_{cs} value was shown to be significant in earlier chapters and is considered important in determining the failure mechanism of a pile group. Table 9.01 shows R_{cs} values for the groups that were tested successfully (for groups of 12 or more piles and up to a spacing of 3.0 d) and suggests that for the perimeter and target groups there is a division between mechanisms of failure at an R_{cs} value of between 5.0 and 5.3. In other words, each unit area of pile can 'support' approximately five unit areas of soil in failing via the block mechanism. Where the unit area of soil exceeds about five times that of the unit area of a pile, then the piles are much more likely to fail individually.

9.3 Soil stresses and soil movements

Near the top of the pile, there is a reduction in vertical stress in both sp_A and sp_B. Close to the middle of the pile, there is an increase in stress in sp_A and no change in stress in sp_B, and below the pile, there is an increase in stress in both soil profiles. The patterns appear to be a reflection of one another; the 'peak' reduction in stress at the top of the pile in sp_A, is mirrored by the 'peak' increase in stress at the base of the pile in sp_B. This decreased stress in sp_A is compensated by the increase in stress over the mid section of the pile.

Horizontal stresses over the top section of the piles are markedly different between soil profiles. The principal difference is that just outside the pile group, the stresses at about 2 m depth decrease in sp_A, whereas in sp_B stresses at this level have increased

significantly. At the pile toe the horizontal stresses have increased. Horizontal stresses in sp_A develop and increase as the pile load (and settlement) increases over most of the mid section of the pile, whereas in sp_B, the stresses over this range go almost unchanged.

The soil movements confirm what was already observed concerning the failure mechanism. In sp_A, the vertical central soil settlement is significant and the group failed as a block; in sp_B, the vertical soil settlement is much less and the group failed as individual piles. The horizontal movements were greater in sp_A and the soil moved outwards, away from the pile group, except at the top of the piles, where the soil was calculated to move inwards.

10 Conclusions and Further Work

10.1 Conclusions

10.1.1 Failure mechanism

Of the 16 perimeter groups under analysis, eight failed via the block mechanism and these groups generally, but not always, had lower efficiencies. It was unusual to observe that the group TS16_2.00, which was tested three times, failed twice as individual piles and once as a block. Group GS25_2.00 was also tested twice and showed contrasting mechanisms of failure. This variable behaviour is an indication of the sensitivity of the conditions and that very slight changes can be the difference between one type of failure mechanism and the other.

The behaviour is broadly dependent on the spacing and the number of piles, and thus, the diameter of the group. There is a point, a critical spacing, where the spacing is too large for the group to fail as a block, no matter how small the diameter of the group. At the same time, there is a critical group diameter, and when exceeded, no matter how close the spacing, it will not fail as a block. Of course, these two critical factors are inter-related and therefore they do not each have a specific single value, because both properties are dependent on the other, over a particular range. They also vary for different soil strength profiles, l/d ratios, and whether or not a central pile has been installed. General changes in behavioural trends are summarised in Figure 10.01, which also indicates that pile spacing has a greater sensitivity than the number of piles in a group. The trends are from broad observations of perimeter (and target) groups.

The central soil monitoring was particularly useful for measuring movements that were not easy to see and assessing groups that showed 'block effect' failure. For example, groups PC20_2.00 and TC14_2.00 did not show any visible central soil settlement, but careful measurements showed that the central soil had settled relative to the soil outside the group.

10.1.2 Failure path

The β analysis (first discussed in Section 6.5.7) revealed that all 11 of the circular perimeter groups that failed as blocks showed a range of calculated β values between 52 and 69 °. Of the five groups that did not fail as blocks, two groups suggested that for the calculated capacity to correspond with the centrifuge capacity, the β value would have to equal 77 and 78 °, for groups PC14_2.00 and PC20_2.00 respectively. It is strongly believed that both these groups showed signs of central soil settlement and 'block effect' failure, indicating these failure angles are on the cusp of block failure. For the remaining three groups no β value could be calculated, which verifies that the groups must have failed purely as individual piles.

10.1.3 Efficiency

Eight perimeter groups had a low efficiency and six of these have a pile spacing of less than 2.0 d. The three groups with favourable efficiencies have very similar cross sectional ratios and efficiencies, yet the number of piles is different as is the pile spacing, and more crucially, the failure mechanism.

Of the 12 target groups under analysis, three groups had a favourable efficiency, and four groups had high efficiencies. Unlike the perimeter groups, there is a less clear distinction between the properties of the target groups that share similar efficiencies. All that can be concluded is that the target groups generally have favourable or high efficiencies where they fail individually (five out of seven cases) and they generally have low or normal efficiencies where they fail as a block (four out of five cases).

The results reported by other Authors' testing grid groups within soft clay correspond well with each other, and Barden and Monckton (1970) also report results for stiff clay. It would be reasonable to argue that had Barden and Monckton tested a firm clay, they probably would have observed an efficiency of about 0.8, which would fit very well with the results in firm clay from these model tests for group GS25_2.00, but only at higher settlements.

With these points in mind, general trends of η vs s have been plotted in Figure 10.02, for perimeter, target and grid groups. All group types converge towards an efficiency of unity beyond a pile spacing of approximately 3.0 d. For grid groups; as the spacing decreases, so does the efficiency. Results from perimeter and target groups have shown that the efficiency can be greater than unity, for certain arrangements, which peaks between at pile spacing of approximately 1.75 and 2.0 d.

10.1.4 Central pile

In one observed case, PS16_2.00/TS16_2.00, the addition of the central pile was the difference between the group failing individually and failing as a block. However, in a repeat test, TS16_2.00 also failed individually and so the observation is deemed inconclusive. Five other groups with the same number of perimeter piles and the same spacing were also tested as both perimeter and target groups and showed no difference in failure mechanism. It appears that the central pile has a positive effect on groups where piles are spaced at 2.0 d, which may be caused by the central pile 'binding' the group together engaging the central soil, thus inducing a higher capacity. The same effect causes a reduction in capacity at a spacing of 1.75 d, where the central pile is no longer beneficial.

10.1.5 Capacity

As an average of all perimeter groups, it was found that at 0.02 d settlement, 58 % of the peak capacity had been reached; at 0.05 d settlement, 79 % of the peak capacity had been reached; at 0.10 d settlement 93 % had been reached; and at 0.20 d settlement the capacity was 98 % of the peak capacity. At practical limits of settlement, such as 0.10 d, the grid groups have achieved only 84 % of their peak capacity, compared to the perimeter groups, which have attained about 10 % more. However, in practical terms, it is unlikely that a pile group would be designed such that these levels of settlement would be tolerated.

10.1.6 Stiffness

The circular perimeter groups exhibiting the least stiff responses and therefore the slowest rate of build up of load are generally those where the piles are most closely

spaced (PC18_1.50, PC12_1.50 and PC12_1.25). This effect is more prominent in bigger groups. Group GS16_2.00 showed a stiffer response than either of the grid groups of 25 piles. In the case of the square perimeter groups, the pattern of load vs settlement is less clear. Groups that undergo block failure, which is often coincident with closely spaced piles, show less stiff responses. This is because the increased clay-clay component requires higher displacement for shear stress mobilisation.

10.1.7 Shear strength

From multiple tests it was observed that groups TS16_2.00 and GS25_2.00 failed both as a block and as individual piles, and so it would appear that these groups are on the very cusp of possible failure mechanisms. It is believed that a narrow s_u range can be the defining factor between the very different types of behaviour. Block failure mechanisms are more likely where there is a broad s_u range over the length of the pile. A significant change in soil consistency means the softer section at the top experiences comparatively higher strains than the soil further down, and this contrast makes the top section more susceptible to shearing. A high overall s_u also appears to make block failure less likely.

10.1.8 Group shape

There is only one perimeter group and one target group arrangement where it is possible to compare directly the influence of group shape and both results indicate it is more efficient to utilise circular groups. It would be expected that a circular group is favourable in comparison to square groups where the load distribution is likely to be unequal, particularly for the corner piles. Also, the area of soil encompassed by the piles is greater for circular groups, than the comparative square groups.

10.1.9 Final comparison

Three groups have been compared, all of which occupy the same outer area: GS25_2.00, PS16_2.00 and TS16_2.00. The findings suggest the greatest capacity can be achieved from the GS25_2.00, but this is only true at higher levels of settlement and so does not necessarily make it a 'better' group. The calculated "efficient pile equivalent" shows that if group TS16_2.00 was chosen over GS25_2.00, eight fewer

piles would need to be installed (17 from 25) but there would only be a loss of capacity equivalent to that of three piles at a settlement of 20 % d. This revelation is even more pronounced at lower settlements; at a settlement of 0.02 d, the capacity of each of these groups is exactly the same (equivalent to 9 fully efficient piles) and the capacity is also exactly the same at a settlement of 0.05 d, but again, TS16_2.00 is comprised of eight fewer piles than GS25_2.00. The perimeter group shows similar results to the target group, although to a lesser degree, perhaps indicating that the central pile is worth installing.

10.1.10 Summary of main findings

- Block failure mechanism usually leads to low efficiency and a low group stiffness
- Block failure is very likely where pile spacing is less than 2.0 d
- The same group can show different failure mechanisms, dependent on s_u range
- A central pile has little effect on failure mechanism but can generate higher group efficiency at a pile spacing of 2.0 d
- Circular groups are generally more efficient than square groups
- Perimeter groups with favourable efficiencies have similar R_{cs} values
- Perimeter and target groups are stiffer than grid groups:
    - At lower settlements (0.02 and 0.05 d), perimeter groups achieve a notably higher proportion of their peak capacity than grid groups
    - At lower settlements, a target group of 17 piles has the same capacity as a grid group of 25 piles

10.2 Further Work

The research has been successful in solving a number of issues, but there are several questions that still require answers. Some of these questions were always there, but outside the scope of the research, and some have been raised as a result of the work undertaken. Within the research that was carried out several variables were not tested, creating a number of uncertainties, outlined in the following sections.

10.2.1 Group dimensions

Having not done any experiments with shorter piles, it is not known whether the phenomena associated with progressive debonding and increased efficiency is linked to perimeter groups of a particular l/d ratio. It is hypothesised that shorter piles, where l/d may only be ≤ 25, that the same patterns of behaviour would not be observed. It is possible that the pile diameter may affect the behaviour and the response, which would be interesting to understand. However, in terms of the practical 'prototype' implications, these pile groups would generally be intended for small diameter piles / minipiles / micropiles and so, to a certain extent, the variation with pile diameter is made somewhat redundant. Only circular and square groups were fully tested as part of this research. It would be interesting to learn if different shaped groups behave in a similar way. However, it is likely that for the majority of practical applications, the pile groups will be of circular or square geometry, thus making this variable more pertaining to curious interest rather than practical applications.

10.2.2 Soil properties

Generally speaking, the undrained shear strength of the clay was kept consistent, with the exception of test 5b, which it was intentionally reduced to approximately two thirds of the normal strength. This single variation, along with all the individual measurements of s_u in each of the tests, gave an idea as to how this factor affects the results. However, it was not tested with enough rigour to enable convincing conclusions to be drawn. All that can really be said is that the strength of the clay has an influence over the mechanism, but less impact on the efficiency. It would be interesting to discover the behaviour of a similar range of pile groups in sand. It is well documented that traditional grid pile groups installed in loose sand can gain efficiency greater than unity; similarly, that pile groups in dense sand will suffer an efficiency lower than unity, but it is not known what may happen in the case of perimeter and target groups. Additionally, it would be of interest to discover any behavioural differences if the pile groups were installed in London Clay, to allow better comparison with Cannon Place.

10.2.3 Modelling

There is a small amount of uncertainty concerning the effect of the wall and base boundaries of the strongbox. It is known that the boundaries are at sufficient distance that the effect would be minimal, but even so, it has not been quantified as part of this work. In addition, the effect of interaction between pile groups is another issue, which has not been solved. It would be necessary to run a series of tests with the pile groups at various distances and pile spacing to try and quantify this effect. A range of other factors will have influenced the results, and the way in which they are affected is, to some extent, unknown since the factors were kept the same in every test. Firstly, the installation technique aimed to mimic a bored pile, but there are two implications with this (1) the clay recovery was usually about 60 %, implying the pile was to some extent a displacement pile; (2) it is not known what would have happened if the piles were driven. Secondly, it was decided to load the pile groups at a particular rate of displacement, but of course it is unknown what would have resulted had a different rate been chosen. As commented upon in Section 6.3.2, it may have proved beneficial to have commissioned loading apparatus capable of loading the groups completely independently.

In short, because this is brand new type of pile group, it was not possible to test every variable, so there are still several unknowns that require further research for a more complete understanding.

10.2.4 Other investigations

- Pile strain gauges

It would have been desirable to have instrumented the piles with strain gauges to gain an understanding into the loads carried by each pile and how this varies with depth. This addition would have possibly culminated in the confirmation of the 'progressive debonding' phenomenon and its contribution to the efficiencies of greater than unity. This is considered to be one of the most important aspects of future work.

- Base capacity

The potential contribution of the 'whole group' base capacity remains unknown. In cases where block failure or block effect failure occurred, it is possible that there may be some additional base capacity beyond that of the individual piles. For this to be discovered, a device would have to be installed at the base of the groups to monitor changes in the stress or strain of the soil.

- Load distribution

It can be assumed that the load distribution is equally shared amongst all piles in a circular group, but the same cannot be said for piles within a square group. A supplementary study would be necessary to investigate the distribution of load within square perimeter and target groups. Some work has already been completed in this area, but a comparison would be required for perimeter groups.

- Field tests

It is of great benefit to have comparison between the centrifuge modelling and numerical modelling, however, there is no replacement for real field testing. Of course, the prototype, Cannon Place is a useful source of additional data, but unfortunately the groups were not monitored in a way in which would allow much valuable comparison. This is principally because the modelling considered the failure condition, and of course Cannon Place did not.

References

Al-Mhaidib, A. I. (2005). Loading rate effects on pile groups in clay. Electronic Journal Geotech. Engng, No. 05-83.

Al-Tabbaa, A. (1987). Permeability and Stress-strain Response of Speswhite Kaolin, PhD Thesis, University of Cambridge.

Atkinson, J. H., Richardson, D. and Stallebrass, S. E. (1990). Effects of recent stress history on the stiffness of overconsolidated soil. Geotechnique, Vol. 40, No. 4, pp 531-540.

Atkinson, J. H. (1993). An Introduction to the Mechanics of Soils and Foundations. McGraw Hill, London.

Azizi, F. (2000). Applied Analyses in Geotechnics. E & FN Spon. London.

Banerjee, P.K. and Butterfield, R. (1981). Boundary Element Methods in Engineering Science, McGraw-Hill, London.

Barden, L. and Monckton, M. F. (1970). Tests on model pile groups in soft and stiff clay. Geotechnique, Vol. 20, No. 1, pp 94-96.

Begaj-Qerimi, L. (2009). Re-use of Pile Foundations in Urban Environments, PhD Thesis, City University.

Bolin, H. W. (1941). The Pile Efficiency Formula of the Uniform Building Code. Building Standards Monthly, Vol. 10, No.1, pp 4-5.

Brinch Hansen, J. (1963). Discussion: hyperbolic stress-strain response in cohesive soils. ASCE, J. Soil Mech. and Found. Div. 89(SM4), pp 241-242.

British Standard BS 1377-9:1990. Methods for test for soils for civil engineering purposes. In-situ tests.

British Standard BS EN 14199:2005. Execution of special geotechnical works. Micropiles.

Burland, J. B. (1973). Shaft friction of piles in clay – a simple fundamental approach. Ground Engng. Vol. 6, No. 6, pp 30-42.

Burland, J. B. and Cooke, R. W. (1974). The design of bored piles in stiff clays. Ground Engng, Vol. 7, No. 4, pp 28-35.

Burland, J. B. and Twine, D. (1988). The shaft friction of bored piles in terms of effective strength. Proc. 1st Geotech. Sem. on Deep Found. On Bored and Auger Piles, Ghent, pp 411-420.

Butterfield, R. & Banerjee, P. K. (1971). The elastic analysis of compressible piles and pile groups. Geotechnique, vol. 21, pp 43-60.

Chandler, R. J. (1966). The measurement of residual strength in triaxial compression. Geotechnique, Vol. 16, No. 3, pp 181-186.

Chandler, R. J. (1968). The shaft friction of piles in cohesive soils in terms of effective stresses. Civ. Engng. Publ. Wks Rev. 63, pp 48-51.

Chandler, R. J. and Martins, J. P. (1982). An experimental study of skin friction around piles in clay. Geotechnique, Vol. 32, No. 2, pp 119-132.

Chin, F. K. (1970). Estimation of the ultimate load of piles not carried to failure. Proc. 2nd SE Asian Conf. Soil Engng, pp 81-90.

Chin, F. K. (1972). The inverse slope as a prediction of ultimate bearing capacity of piles. Proc. 3rd SE Asian Conf. Soil Engng, pp 83-91.

Cooke, R. W. and Price, G. (1973). Strains and displacements around friction piles. Proc. of 8th Int. Conf. on Soil Mech. and Found. Engng, Moscow, Vol. 2.1, pp 53-60.

Cooke, R. W. (1974). Piled foundations: A survey of research at the building research station. Building Research Establishment.

Coyle, H. M. and Reese, L. C. (1966). Load transfer for axially loaded piles in clay. J. of Soil Mech. and Found. Engng. Div, 92/2, pp 1-26.

Craig, W. H. (1984). Installation studies for model piles. Proc. Application of Centrifuge Modeling to Geotechnical Design, pp 441-448.

Craig, W. H. (1995). Geotechnical centrifuges: past, present and future. Geotechnical Centrifuge Technology, Taylor, R. N. (Ed) Blackie Academic and Professional, Glasgow.

Davis, E. H. and Poulos, H. G. (1968). The use of elastic theory for settlement prediction under three-dimensional conditions. Geotechnique, Vol. 18, No. 1, pp 67-91.

De Mello, V. F. B. (1969). Foundations of buildings on clay. State of the art report. Proc. 7th Int. Conf. Soil Mech. & Found. Engng. Mexico City, pp 49-136.

Federal Highway Administration. (2000). Micropile Design and Construction Guidelines. FWHA-SA-97-070. US Dept. Trans.

Feld, J. (1943). Discussion on friction pile foundations. Trans. Amer. Soc. Civ. Engrs. 108, pp 143-144.

Fleming, W. G. K. (1992). A new method for single pile settlement prediction and analysis. Geotechnique, Vol. 42, No. 3, pp 411-425.

Fleming, W. G. K., Weltman, A. J., Randolph, M. F. and Elson, W. K. (1992). 2nd Ed. Piling Engineering. Blackie and Son Ltd, London.

Fleming, W. G. K., Weltman, A. J., Randolph, M. F. and Elson, W. K. (2009). 3rd Ed. Piling Engineering. Taylor and Francis, Abingdon.

Gibson, R. E. (1950). Discussion on paper: The bearing capacity of screw piles and screwcrete cylinders. J. Instn. Civ. Engrs. 34, p 382.

Grant, R. J. (1998). Movements around a tunnel in two-layer ground. PhD Thesis, City University London.

Hayward, D. (2009). Cannon Street Cunning. New Civil Engineer publ. Emap, pp 30-31.

Hibbitt, D., Karlsson, B. and Sorensen, P. (2008). ABAQUS 6.8: A computer software for finite element analysis. Hibbitt, Karlsson and Sorensen Inc., Rhode Island, USA.

Kerisel, J. L. (1967). Vertical and horizontal bearing capacity of deep foundation in clay. Proc. Symp. Bearing Capacity and Sett. Of Deep Found. Duke University, Durham, p 45.

Klotz, U. E. (2000). The influence of state on the capacity of driven piles in sands. PhD Thesis, City University.

Lambe, T. W. and Whitman, R. V. (1969). Soil Mechanics. John Wiley and Sons.

Lo, M. B. (1967). Discussion to paper by Y.O. Beredugo. Canadian Geotechnical Journal, Vol. 4, pp 353-354.

Martin, J., St John, H., Fraser, J., Taylor, T. and Smith, M. (2010). Cannon Station Redevelopment, London. Proc. 11th DFI & EFFC Int. Conf. on Geotechnical Challenges in Urban Regeneration, London.

McNamara, A. M. (2001). Influence of heave reducing piles on ground movements around excavations. PhD Thesis, City University.

Meyerhof, G. G. (1951). The ultimate bearing capacity of foundations. Geotechnique, 2: pp 301-332.

Meyerhof, G. G. (1976). Bearing capacity and settlement of pile foundations. J. of Geotech. Engng. Div, Vol. 102, No. 3, pp 197-228.

Motta, E. (1994). Approximate elastic-plastic solution for axially loaded piles. J. of Geotech. Engng Div, Vol. 120, No. 9, pp 1616-1624.

Nuñez, I. L. (1989). Centrifuge model tension piles in clay. PhD Thesis, University of Cambridge.

O'Neill, M. W., Hawkins, R. A. and Mahar, L. J. (1982). Load transfer mechanisms in piles and pile groups. J. Geotech. Eng. ASCE, Vol. 108, No. 12, pp 1605-1623.

O' Neill, M. W. (1983). Group action in offshore piles. Proc. Conf. on Geotech. Engng. In offshore practice, ASCE, Houston, TX, pp 25-64.

Patel, D. C. (1992). Interpretation of results of pile tests in London clay. Piling: European Practice and Worldwide Trends. Thomas Telford, London.

Phillips, R. (1989). Centrifuge lateral pile tests in clay (exhibit A-PR-10592). Task 1 – final report. A report to Exxon Product Research Corporation by Lynxvale Ltd. Cambridge University.

Phillips, R. (1995). Geotechnical Centrifuge Technology, Blackie Academic & Professional, Taylor, R. N. (Ed) Glasgow, pp 34-59.

Poulos, H. G. (1989). Pile behaviour – theory and application. Geotechnique, Vol. 39, pp 365-415.

Poulos, H. G. and Davis, E. H. (1968). The settlement behaviour of single axially loaded incompressible piles and piers. Géotechnique, Vol. 18(3), pp 351-371.

Poulos, H. G. and Davis, E. H. (1980). Pile foundation analysis and design. John Wiley and Sons, New York.

Randolph, M. F., Carter, J. P. and Wroth, C. P. (1979). Driven piles in clay – the effect of installation and subsequent consolidation. Geotechnique, Vol. 29, No.4, pp 361-393.

Randolph, M. F. (1994). Design methods for pile groups and piled rafts. Proc. 13th Int. Conf. Soil Mech. and Found. Engng, New Delhi. Vol. 4, pp 718-742.

Saffery, M. and Tate, A. P. K. (1961). Model tests on pile groups in clay soil. Proc. 5th Int. Conf. Soil Mech, Paris, Vol. 2, 129.

Schofield, A. N. and Taylor, R. N. (1988). Development of standard geotechnical centrifuge operations. Centrifuge 1988, Ed Corte, Balkema, Rotterdam, pp 29-32.

Skempton, A.W. (1951). The Bearing Capacity of Clays. Proc. Building Research Congress, Vol. 1, pp 180-189.

Skempton, A. W. (1959). Cast in-situ bored piles in London Clay, Geotechnique, No. 9, pp 153 – 173.

Skempton, A. W. (1961). Horizontal stresses in an over-consolidated Eocene clay. In Proc. 5th Int. Conf. Soil Mech., Paris, Vol. 1, pp 351–357.

Springman, S. M. (1989). Lateral loading on piles due to simulated embankment construction. PhD Thesis, Cambridge University.

Stallebrass, S. E. (1990). Modelling the effect of recent stress history on the behaviour of overconsolidated soils. PhD Thesis, City University, London.

Stewart, D. I. (1989). Groundwater effects on in-situ walls in stiff clay. PhD Thesis, Cambridge University.

Synthesis and recommendations of the French national project on micropiles: FOREVER (1993-2001). RGCU and IREX, ENPC Press, Paris. (in French, English translation by FHWA to be published by ADSC, Dallas, TX).

Taylor, R. N (1995). Centrifuges in modelling: principles and scale effects. Geotechnical Centrifuge Technology, Blackie Academic & Professional, Taylor, R. N. (Ed) Glasgow, pp 19-33.

Terzaghi, K. and Peck, R. B. (1948). Soil Mechanics in Engineering Practice, John Wiley and Sons, New York.

Terzaghi, K. and Peck, R. B. (1967). Soil Mechanics in Engineering Practice. 2nd Ed. John Wiley and Sons, New York.

Tomlinson, M. J. (1963). Foundation design and construction. John Wiley and Sons, New York.

Tomlinson, M. J. (1971). Some effects of pile driving on skin friction. Proc. Conf. Behaviour of Piles, ICE, London, pp. 107-114.

Tomlinson, M. J. and Woodward, J. (2008). Pile design and construction practice. 5th Ed. Taylor and Francis, Abingdon.

Vesic, A. S. (1969). Experiments with instrumented pile groups in sand. ASTM special tech. publ. no. 444, performance of deep found., pp 177-222.

Whitaker, T. (1957). Experiments with model piles in groups. Geotechnique, Vol. 7, No. 4, pp 147-167.

Whitaker, T. and Cooke, R. W. (1966). An investigation of the shaft and base resistance of large bored piles in London Clay. Proc. Conf. Large Bored Piles, Institute of Civil Engineers, London, pp 7-49.

Wroth, C. P., Carter, J. P. and Randolph, M. F. (1980). Stress changes around a pile driven into cohesive soil. In recent developments in design and construction of piles, pp 345-354. London: Institution of Civil Engineers.

Xu, X., Lehane, B. M., Gaudin, C., Zhang, T. and Liu, H. (2006). Centrifuge studies of single and group displacement piles in clay. Int. Conf. on Phys. Mod. in Geotech, Hong Kong, pp 895-900.

Yetginer, A. G., White, D. J. and Bolton, M. D. (2006). Field measurements of the stiffness of jacked piles and pile groups. Geotechnique, Vol. 56, No. 5, pp 349-354.

Tables

parameter	range	centrifuge	numerical
geometry	single	✓	✓
	line	✓	
	perimeter	✓	✓
	target (with central pile)	✓	✓
	grid	✓	✓
shape	circle	✓	✓
	square	✓	✓
	triangle	✓	
number of piles	1 - 25	✓	✓
pile spacing	1.00 - 4.00 d (approx.)	✓	✓
soil strength	soft	✓	✓
	firm	✓	✓
	stiff		✓
l/d ratio	50	✓	✓
	100		✓

Table 1.01 Properties under investigation

parameter	range	centrifuge	numerical
geometry	single	✓	✓
	line	✓	
	perimeter	✓	✓
	target (with central pile)	✓	✓
	grid	✓	✓
shape	circle	✓	✓
	square	✓	✓
	triangle	✓	
number of piles	1 - 25	✓	✓
pile spacing	1.00 - 4.00 d (approx.)	✓	✓
soil strength	soft	✓	✓
	firm	✓	✓
	stiff		✓
l/d ratio	50	✓	✓
	100		✓

Table 3.01 Cannon Place perimeter group summary

property	equivalent prototype	scaling factor	model
unit weight of pile*	25 kN/m^3 (concrete)	1:1	27 kN/m^3 (aluminium)
unit weight of soil	18 kN/m^3	1:1	18 kN/m^3
pile length (in soil)	15 m	1:Ng	0.25 m
pile diameter	300 mm	1:Ng	5 mm
single pile capacity (approx.)	540 kN	1:1/Ng^2	0.15 kN
time to displace pile 0.10 d	5 days (120 hrs)	1:1/Ng^2	120 s
time to displace pile 0.02 d	1 day (24 hrs)	1:1/Ng^2	24 s
stress at pile toe	2700 kN/m^2	1:1	2700 kN/m^2

*there is a difference between these properties, although it is so small it can be considered negligible

Table 4.01 Scaling relationships for test dimensions

day	activity
1	pour clay slurry, increase pressure to 25 kPa
2	
3	
4	morning: increase pressure to 50 kPa afternoon: increase pressure to 100 kPa
5	increase pressure to 250 kPa
6	increase pressure to 500 kPa
7	(500 kPa)
8	(500 kPa)
9	
10	
11	morning: reduce pressure to 250 kPa afternoon: insert PPTs (x4)
12	remove sample from press, make model, place in centrifuge and accelerate
13	(wait for pore pressure equilibrium)
14	**centrifuge test**

Table 5.01 Two-week testing cycle

	test no.		1	2	3	4*
	date		07-Aug-09	20-Aug-09	03-Sep-09	05-Nov-09
	test		**test 1a**	**test 1b**	**test 1c**	**test 1d**
phase 1	load cell no.	29	LL05_2.00	LL05_1.75	LL05_2.00	Sx1
		30	LL05_2.50	LL05_2.25	LL05_2.50	LL05_2.25
		31	LL05_3.00	LL05_2.75	LL05_3.00	Sx3
		32	LL05_1.50	LL05_1.25	LL05_1.50	Sx1

	test no.		5*	6*	7*	8	9
	date		24-Sep-09	08-Oct-09	22-Oct-09	03-Dec-09	17-Dec-09
	test		**test 2a**	**test 2b**	**test 2c**	**test 2d**	**test 2e**
phase 2	load cell no.	29	PS12_2.00	PC16_2.00	PC10_2.00	PS16_2.00	PC14_2.00
		30	PT12_2.00	PC18_2.00	PS20_2.00	PC08_2.00	PT18_2.00
		31	~	~	~	~	~
		32	PC12_2.00	PS08_2.00	PT09_2.00	PS18_2.00	PS10_2.00

	test no.		10	11	12	13
	date		18-Mar-10	29-Apr-10	13-May-10	10-Jun-10
	test		**test 3a**	**test 3b**	**test 3c**	**test 3d**
phase 3	load cell no.	29	LL05_1.25	PS20_2.00	LL05_2.50	LL05_2.75(A)
		30	LL05_2.00	PC10_2.00	Sx2	LL05_1.00
		31	LL05_2.75	~	Sx2(A)	LL05_1.75
		32	Sx2	PC16_2.00	LL05_2.25(A)	LL05_2.25

	test no.		14	15	16	17	18
	date		24-Jun-10	15-Jul-10	29-Jul-10	12-Aug-10	26-Aug-10
	test		**test 4a**	**test 4b**	**test 4c**	**test 4d**	**test 4e**
phase 4	load cell no.	29	PS14_2.00	TS16_2.00	TC16_2.00	TR16_2.00	TC14_1.75
		30	GS25_2.00	PC12_1.25	TS16_2.00	Sx2	LL05_2.00
		31	~	~	Sx2	LL05_2.00	TC12_2.00
		32	PC12_1.25	GO13_2.00	TS20_2.00	TC12_2.00	TC12_2.25

	test no.		19	20	21	22	23
	date		21-Apr-11	06-May-11	16-Jun-11	01-Jul-11	04-Aug-11
	test		**test 5a**	**test 5b**	**test 5c**	**test 5d**	**test 5e**
phase 5	load cell no.	29	PS08_4.00	GS25_2.00	TC18_1.50	Sx2	PC16_1.75
		30	TC14_2.00	Sx2	TC16_1.75	PS20_1.75	PC18_1.50
		31	GS16_2.00	TC12_2.00	Sx2	PC14_1.75	PC20_2.00
		32	Sx2	TS16_2.00	PS20_1.50	PC12_1.50	PC12_3.00

Table 6.01 Centrifuge testing programme

	test	test 1d
phase 1	29	**Sx1**
	30	
	31	**Sx3**
	32	**Sx1**
	s_u average (kPa)	50
	s_u top (kPa)	48
	s_u toe (kPa)	54
	s_u range (kPa)	6
	Q_{test} [single pile] (kN)	0.146
	Q_{calc} [single pile] (kN)	0.143

	test	test 3a	test 3c
phase 3	29		
	30		**Sx2**
	31		**Sx2(A)**
	32	**Sx2**	
	s_u average (kPa)	47	49
	s_u top (kPa)	36	40
	s_u toe (kPa)	58	61
	s_u range (kPa)	22	21
	Q_{test} [single pile] (kN)	0.157	0.140
	Q_{calc} [single pile] (kN)	0.141	0.144

	test	test 4c
phase 4	29	
	30	
	31	**Sx2**
	32	
	s_u average (kPa)	61
	s_u top (kPa)	56
	s_u toe (kPa)	62
	s_u range (kPa)	6
	Q_{test} [single pile] (kN)	0.151
	Q_{calc} [single pile] (kN)	0.152

	test	test 5a	test 5b	test 5c	test 5d
phase 5	29				**Sx2**
	30		**Sx2**		
	31			**Sx2**	
	32	**Sx2**			
	s_u average (kPa)	53	33	50	53
	s_u top (kPa)	40	27	38	40
	s_u toe (kPa)	63	36	52	63
	s_u range (kPa)	23	9	14	23
	Q_{test} [single pile] (kN)	0.152	0.113	0.142	0.151
	Q_{calc} [single pile] (kN)	0.148	0.113	0.143	0.148

Table 6.02 Single pile test summary

number	test	group
1	2b	PS08_2.00
2	2e	PC14_2.00
3	2e	PS10_2.00
4	3a	LL05_1.25
5	3a	LL05_2.00
6	3a	LL05_2.75
7	3b	PC10_2.00
8	3b	PC16_2.00
9	3c	LL05_2.50
10	3d	LL05_1.00
11	3d	LL05_1.75
12	4a	GS25_2.00
13	4a	PC12_1.25
14	4b	TS16_2.00
15	4b	PC12_1.25
16	4c	TC16_2.00
17	4c	TS16_2.00
18	4c	TS20_2.00
19	4e	TC14_1.75

number	test	group
20	4e	LL05_2.00
21	4e	TC12_2.00
22	4e	TC12_2.25
23	5a	PS08_4.00
24	5a	TC14_2.00
25	5a	GS16_2.00
26	5b	GS25_2.00
27	5b	TC12_2.00
28	5b	TS16_2.00
29	5c	TC18_1.50
30	5c	TC16_1.75
31	5c	PS20_1.50
32	5d	PS20_1.75
33	5d	PC14_1.75
34	5d	PC12_1.50
35	5e	PC16_1.75
36	5e	PC18_1.50
37	5e	PC20_2.00
38	5e	PC12_3.00

linear
7

perimeter
16

target
12

grid
3

Table 6.03 Successful group test summary

	test	test 3a	test 3c	test 3d
phase 3	29	**LL05_1.25**	**LL05_2.50**	
	30	**LL05_2.00**		**(LL05_1.00)**
	31	**LL05_2.75**		**LL05_1.75**
	32			
	s_u average (kPa)	47	49	49
	s_u top (kPa)	36	40	42
	s_u toe (kPa)	58	61	61
	s_u range (kPa)	22	21	19
	Q_{calc} [single pile] (kN)	0.141	0.144	0.144

	test	test 4e
phase 4	29	
	30	**LL05_2.00**
	31	
	32	
	s_u average (kPa)	50
	s_u top (kPa)	36
	s_u toe (kPa)	62
	s_u range (kPa)	26
	Q_{calc} [single pile] (kN)	0.144

Table 6.04 Linear group test summary

	test	test 2b	test 2e
phase 2	29		PC14_2.00
	30		
	31		
	32	PS08_2.00	PS10_2.00
	s_u average (kPa)	53	58
	s_u top (kPa)	39	52
	s_u toe (kPa)	62	65
	s_u range (kPa)	23	13
	Q_{calc} [single pile] (kN)	0.148	0.153

	test	test 3b
phase 3	29	
	30	PC10_2.00
	31	
	32	PC16_2.00
	s_u average (kPa)	63
	s_u top (kPa)	67
	s_u toe (kPa)	67
	s_u range (kPa)	0
	Q_{calc} [single pile] (kN)	0.153

	test	test 4a	test 4b
phase 4	29		
	30		PC12_1.25
	31		
	32	PC12_1.25	
	s_u average (kPa)	65	54
	s_u top (kPa)	61	43
	s_u toe (kPa)	74	63
	s_u range (kPa)	13	20
	Q_{calc} [single pile] (kN)	0.156	0.149

	test	test 5a	test 5c	test 5d	test 5e
phase 5	29	PS08_4.00			PC16_1.75
	30			PS20_1.75	PC18_1.50
	31			PC14_1.75	PC20_2.00
	32		PS20_1.50	PC12_1.50	PC12_3.00
	s_u average (kPa)	53	50	53	47
	s_u top (kPa)	40	38	40	34
	s_u toe (kPa)	63	52	63	59
	s_u range (kPa)	23	14	23	25
	Q_{calc} [single pile] (kN)	0.148	0.143	0.148	0.141

circle
square

Table 6.05 Perimeter group test summary

group	number	type	shape	piles	spacing	test	s_u average (kPa)	s_u toe (kPa)	s_u range (kPa)	Q_u single pile (N)	block failure?	soil area (mm^2)	R_{cs}	equiv. pile (0.20 d)
PS08_2.00	1	P	S	8	2	2b	53	62	23	148	N	400	2.5	8.1
PC14_2.00	2	P	C	14	2	2e	58	65	13	153	N	1560	5.7	15.0
PS10_2.00	3	P	S	10	2	2e	58	65	13	153	N	600	3.1	8.4
PC10_2.00	7	P	C	10	2	3b	63	67	0	153	N	796	4.1	9.3
PC16_2.00	8	P	C	16	2	3b	63	67	0	153	N	2037	6.5	16.0
PC12_1.25	13	P	C	12	1.25	4a	65	74	13	156	Y	448	1.9	9.5
PC12_1.25	15	P	C	12	1.25	4b	54	63	20	149	Y	448	1.9	10.2
PS08_4.00	23	P	S	8	4	5a	53	63	23	148	N	1600	10.2	8.1
PS20_1.50	31	P	S	20	1.5	5c	50	52	14	143	Y	1406	3.6	17.2
PS20_1.75	32	P	S	20	1.75	5d	53	63	23	148	Y	1914	4.9	21.9
PC14_1.75	33	P	C	14	1.75	5d	53	63	23	148	Y	1194	4.3	13.7
PC12_1.50	34	P	C	12	1.5	5d	53	63	23	148	Y	645	2.7	10.8
PC16_1.75	35	P	C	16	1.75	5e	47	59	25	141	Y	1560	5.0	17.4
PC18_1.50	36	P	C	18	1.5	5e	47	59	25	141	Y	1450	4.1	17.1
PC20_2.00	37	P	C	20	2	5e	47	59	25	141	N	3183	8.1	20.3
PC12_3.00	38	P	C	12	3	5e	47	59	25	141	N	2578	10.9	13.7

group	Q 0.02 d	Q 0.05 d	Q 0.10 d	Q 0.20 d	Q peak	0.02 d efficiency	0.05 d efficiency	0.10 d efficiency	0.20 d efficiency	peak efficiency	Q 0.02 d / Q peak	Q 0.05 d / Q peak	Q 0.10 d / Q peak	Q 0.20 d / Q peak
PS08_2.00	656	888	1088	1192	1200	0.55	0.75	0.92	1.01	1.01	55%	74%	91%	99%
PC14_2.00	1470	2142	2240	2296	2324	0.69	1.00	1.05	1.07	1.08	63%	92%	96%	99%
PS10_2.00	1000	1200	1250	1280	1370	0.65	0.78	0.82	0.84	0.90	73%	88%	91%	93%
PC10_2.00	1040	1330	1420	1420	1420	0.68	0.87	0.93	0.93	0.93	73%	94%	100%	100%
PC16_2.00	1440	2096	2320	2448	2448	0.59	0.86	0.95	1.00	1.00	59%	86%	95%	100%
PC12_1.25	888	1284	1500	1476	1500	0.47	0.69	0.80	0.79	0.80	59%	86%	100%	98%
PC12_1.25	936	1248	1476	1524	1524	0.52	0.70	0.83	0.85	0.85	61%	82%	97%	100%
PS08_4.00	968	944	1144	1192	1200	0.82	0.80	0.97	1.01	1.01	81%	79%	95%	99%
PS20_1.50	1060	1760	2320	2460	2740	0.37	0.62	0.81	0.86	0.96	39%	64%	85%	90%
PS20_1.75	1500	2220	2780	3240	3260	0.51	0.75	0.94	1.09	1.10	46%	68%	85%	99%
PC14_1.75	1078	1526	1862	2030	2058	0.52	0.74	0.90	0.98	0.99	52%	74%	90%	99%
PC12_1.50	816	1176	1476	1596	1596	0.46	0.66	0.83	0.90	0.90	51%	74%	92%	100%
PC16_1.75	1296	1856	2272	2448	2464	0.57	0.82	1.01	1.09	1.09	53%	75%	92%	99%
PC18_1.50	954	1548	2034	2412	2430	0.38	0.61	0.80	0.95	0.96	39%	64%	84%	99%
PC20_2.00	1560	2300	2620	2860	2860	0.55	0.82	0.93	1.01	1.01	55%	80%	92%	100%
PC12_3.00	1224	1752	1944	1932	1944	0.72	1.04	1.15	1.14	1.15	63%	90%	100%	99%
											58%	79%	93%	98%
											averages			

Table 6.06 Perimeter group data

d	5	mm	L	250	mm	s_u average	53	kPa	$Q_{cent\ 0.20\ d}$	2030	N	
piles	14	no.	r	19.496	mm	s_u toe	63	kPa	indiv. calc.	2079	N	
target?	14	no.	nP	219.911	mm	$\alpha_{clay\text{-}clay}$	1		Q_{cent}/indiv.	0.98		
spacing	1.75	d	ng	907.544	mm^2	$\alpha_{clay\text{-}pile}$	0.66		β	69	°	block shaft
π	3.14159		nf	274.889	mm^2	N	9		β	~		block base

angle		perimeter					area			capacity		
		clay-pile	clay-clay				clay base				block shaft	block base
degrees	radians	mm	mm	degrees	degrees	mm	mm	mm^2	mm^2		N	N
β		total (n2t)	r'	ϕ	θ	total (nc)	k	h	(ng+nh)	nPα	Q_{calc}	Q_{calc}
0	0.000	0.000	16.996	0.000	25.714	106.792	0.000	0.000	907.544	251.934	3494	3853
10	0.175	12.217	17.040	1.460	22.795	94.909	0.044	0.313	911.933	231.987	3230	3591
20	0.349	24.435	17.169	2.855	20.005	83.922	0.172	1.172	923.953	212.937	2977	3345
30	0.524	36.652	17.376	4.125	17.464	74.149	0.380	2.455	941.919	195.100	2741	3119
40	0.698	48.869	17.655	5.222	15.269	65.870	0.658	4.059	964.365	178.758	2524	2915
50	0.873	61.087	17.992	6.110	13.494	59.320	0.995	5.904	990.206	164.145	2331	2736
60	1.047	73.304	18.374	6.767	12.181	54.687	1.378	7.947	1018.804	151.448	2163	2584
69	1.204	84.299	18.746	7.152	11.410	52.267	1.750	9.941	1046.716	141.771	2034	2472
70	1.222	85.521	18.789	7.183	11.349	52.103	1.792	10.172	1049.946	140.801	2021	2461
80	1.396	97.738	19.221	7.359	10.996	51.641	2.224	12.585	1083.739	132.275	1909	2367
90	1.571	109.956	19.656	7.307	11.100	53.313	2.660	15.208	1120.454	125.884	1824	2303
100	1.745	122.173	20.082	7.042	11.630	57.069	3.086	18.058	1160.350	121.576	1767	2269

Table 6.07 Perimeter group β analysis for PC14_1.75

d	5	mm	L	250	mm	s_u average	53	kPa	$Q_{cent\ 0.20\ d}$	1596	N	
piles	12	no.	r	14.324	mm	s_u toe	63	kPa	indiv. calc.	1782	N	
target?	12	no.	nP	188.496	mm	$\alpha_{clay\text{-}clay}$	1		Q_{cent}/indiv.	0.90		
spacing	1.5	d	ng	439.212	mm^2	$\alpha_{clay\text{-}pile}$	0.66		β	64	°	block shaft
π	3.14159		nf	235.619	mm^2	N	9		β	84	°	block base

angle		perimeter					area			capacity		
		clay-pile	clay-clay				clay base				block shaft	block base
degrees	radians	mm	mm	degrees	degrees	mm	mm	mm^2	mm^2		N	N
β		total (n2t)	r'	ϕ	θ	total (nc)	k	h	total (ng+nh)	nPα	Q_{calc}	Q_{calc}
0	0.000	0.000	11.824	0.000	30.000	74.292	0.000	0.000	439.212	198.699	2766	2882
10	0.175	10.472	11.870	2.096	25.808	64.159	0.046	0.265	442.391	181.655	2541	2658
20	0.349	20.944	12.005	4.084	21.831	54.892	0.181	0.976	450.920	165.476	2326	2448
30	0.524	31.416	12.223	5.870	18.261	46.747	0.399	2.012	463.361	150.419	2127	2256
40	0.698	41.888	12.512	7.379	15.242	39.944	0.689	3.277	478.539	136.705	1945	2083
50	0.873	52.360	12.860	8.564	12.872	34.670	1.036	4.705	495.678	124.519	1783	1931
60	1.047	62.832	13.252	9.403	11.194	31.069	1.428	6.269	514.443	114.007	1644	1802
64	1.117	67.021	13.418	9.641	10.719	30.122	1.594	6.933	522.407	110.295	1595	1758
70	1.222	73.304	13.672	9.894	10.212	29.242	1.848	7.973	534.893	105.269	1528	1698
80	1.396	83.776	14.106	10.051	9.897	29.240	2.282	9.846	557.363	98.355	1437	1619
84	1.466	87.965	14.281	10.026	9.947	29.751	2.457	10.651	567.018	96.102	1407	1595
90	1.571	94.248	14.540	9.900	10.199	31.061	2.717	11.925	582.310	93.264	1369	1566
100	1.745	104.720	14.962	9.471	11.058	34.651	3.138	14.245	610.148	89.943	1325	1538

Table 6.08 Perimeter group β analysis for PC12_1.50

group	block failure?	test	$Q_{cent\ 0.20\ d}$ / indiv. calc.	block shaft β (°)	block base β (°)	s_u ave. (kPa)	s_u toe (kPa)	indiv. pile area (mm^2)	α (clay-pile)	$P_{clay\text{-}pile}$ (mm)	$P_{clay\text{-}clay}$ (mm)	$Q_{clay\text{-}pile}$ (N)	$Q_{clay\text{-}clay}$ (N)	Q_{base} indiv. pile (N)	$Q_{clay\text{-}clay}$ / Q_{total}
PC14_2.00	N	2e	1.07	77		58	65	275	0.62	125.84	68.97	1131	1000	161	0.44
PC10_2.00	N	3b	0.93												
PC16_2.00	N	3b	1.00												
PC12_1.25	**Y**	4a	0.79	67	74	65	74	236	0.56	118.33	14.74	1077	239	157	0.16
PC12_1.25	**Y**	4b	0.85	55	59	54	63	236	0.65	130.90	17.78	1149	240	134	0.16
PC14_1.75	**Y**	5d	0.98	69		53	63	275	0.66	135.61	52.27	1186	693	156	0.34
PC12_1.50	**Y**	5d	0.90	64	84	53	63	236	0.66	121.48	30.12	1062	399	134	0.25
PC16_1.75	**Y**	5e	1.08	52		47	59	314	0.71	178.72	67.78	1491	796	167	0.32
PC18_1.50	**Y**	5e	0.95	57	93	47	59	353	0.71	193.21	51.51	1612	605	188	0.25
PC20_2.00	N	5e	1.01	78		47	59	393	0.71	136.14	99.42	1136	1168	209	0.46
PC12_3.00	N	5e	1.14												

Table 6.09 Perimeter group β analysis results

	test	test 4b	test 4c	test 4e
phase 4	29	TS16_2.00	TC16_2.00	TC14_1.75
	30		TS16_2.00	
	31			TC12_2.00
	32		TS20_2.00	TC12_2.25
	s_u average (kPa)	54	61	50
	s_u top (kPa)	43	56	36
	s_u toe (kPa)	63	62	62
	s_u range (kPa)	20	6	26
	Q_{calc} [single pile] (kN)	0.149	0.152	0.144

	test	test 5a	test 5b	test 5c
phase 5	29			TC18_1.50
	30	TC14_2.00		TC16_1.75
	31		TC12_2.00	
	32		TS16_2.00	
	s_u average (kPa)	53	33	50
	s_u top (kPa)	40	27	38
	s_u toe (kPa)	63	36	52
	s_u range (kPa)	23	9	14
	Q_{calc} [single pile] (kN)	0.148	0.113	0.143

circle
square

Table 6.10 Target group test summary

group	number	type	shape	piles	spacing	test	s_u average (kPa)	s_u toe (kPa)	s_u range (kPa)	Q_u single pile (N)	block failure?	soil area (mm^2)	R_{cs}	equiv. pile (0.20 d)
TS16_2.00	14	T	S	17	2	4b	54	63	20	149	(Y)	1600	4.8	18.7
TC16_2.00	16	T	C	17	2	4c	61	62	6	152	N	2037	6.1	19.0
TS16_2.00	17	T	S	17	2	4c	61	62	6	152	(N)	1600	4.8	18.0
TS20_2.00	18	T	S	21	2	4c	61	62	6	152	N	2500	6.1	23.1
TC14_1.75	19	T	C	15	1.75	4e	50	62	26	144	Y	1194	4.1	14.2
TC12_2.00	21	T	C	13	2	4e	50	62	26	144	Y	1146	4.5	13.6
TC12_2.25	22	T	C	13	2.25	4e	50	62	26	144	N	1450	5.7	14.0
TC14_2.00	24	T	C	15	2	5a	53	63	23	148	N	1560	5.3	17.7
TC12_2.00	27	T	C	13	2	5b	34	36	9	113	Y	1146	4.5	12.7
TS16_2.00	28	T	S	17	2	5b	34	36	9	113	(N)	1600	4.8	16.8
TC18_1.50	29	T	C	19	1.5	5c	50	52	14	143	Y	1450	3.9	18.9
TC16_1.75	30	T	C	17	1.75	5c	50	52	14	143	Y	1560	4.7	15.9

group	Q 0.02 d	Q 0.05 d	Q 0.10 d	Q 0.20 d	Q peak	0.02 d efficiency	0.05 d efficiency	0.10 d efficiency	0.20 d efficiency	peak efficiency	Q 0.02 d / Q peak	Q 0.05 d / Q peak	Q 0.10 d / Q peak	Q 0.20 d / Q peak
TS16_2.00	1615	2244	2550	2788	3196	0.64	0.89	1.01	1.10	1.26	51%	70%	80%	87%
TC16_2.00	1547	2295	2737	2890	2924	0.60	0.89	1.06	1.12	1.13	53%	78%	94%	99%
TS16_2.00	1037	2074	2635	2737	2737	0.40	0.80	1.02	1.06	1.06	38%	76%	96%	100%
TS20_2.00	1722	2520	3045	3507	3507	0.54	0.79	0.95	1.10	1.10	49%	72%	87%	100%
TC14_1.75	870	1350	1740	2040	2085	0.40	0.63	0.81	0.94	0.97	42%	65%	83%	98%
TC12_2.00	1014	1378	1703	1963	1989	0.54	0.74	0.91	1.05	1.06	51%	69%	86%	99%
TC12_2.25	1001	1417	1768	2015	2054	0.53	0.76	0.94	1.08	1.10	49%	69%	86%	98%
TC14_2.00	1230	1965	2430	2625	2685	0.55	0.89	1.09	1.18	1.21	46%	73%	91%	98%
TC12_2.00	988	1196	1339	1430	1482	0.67	0.81	0.91	0.97	1.01	67%	81%	90%	96%
TS16_2.00	1139	1479	1751	1904	1904	0.59	0.77	0.91	0.99	0.99	60%	78%	92%	100%
TC18_1.50	1064	1805	2261	2698	2698	0.39	0.66	0.83	0.99	0.99	39%	67%	84%	100%
TC16_1.75	1343	1921	2244	2278	2720	0.55	0.79	0.92	0.94	1.12	49%	71%	83%	84%
											49%	73%	88%	97%
											averages			

Table 6.11 Target group data

group	block failure?	test	$Q_{cent\ 0.20\ d}$ / indiv. calc.	block shaft β (°)	block base β (°)	s_u ave. (kPa)	s_u toe (kPa)	indiv. pile area (mm^2)	α (clay-pile)	$P_{clay\text{-}pile}$ (mm)	$P_{clay\text{-}clay}$ (mm)	$Q_{clay\text{-}pile}$ (N)	$Q_{clay\text{-}clay}$ (N)	Q_{base} indiv. pile (N)	$Q_{clay\text{-}clay}$ / Q_{total}
TC16_2.00	N	4c	1.12	73		61	62	334	0.59	165.11	79.51	1486	1213	186	0.42
TC14_1.75	**Y**	4e	0.94	74		50	62	295	0.68	145.21	51.66	1234	646	164	0.32
TC12_2.00	**Y**	4e	1.05	73		50	62	255	0.68	127.76	58.84	1086	736	142	0.37
TC12_2.25	N	4e	1.07	92		50	62	255	0.68	107.86	76.36	917	954	142	0.47
TC14_2.00	N	5a	1.18	55		53	63	295	0.66	168.42	74.19	1473	983	167	0.37
TC12_2.00	**Y**	5b	0.98	73		33	36	255	0.82	127.76	58.84	864	485	83	0.34
TC18_1.50	**Y**	5c	1.00	52	74	50	52	373	0.68	216.77	54.90	1843	686	175	0.25
TC16_1.75	**Y**	5c	0.94	75		50	52	334	0.68	162.32	59.35	1380	742	156	0.33

Table 6.12 Target group β analysis results

group	number	type	shape	piles	spacing	test	s_u average (kPa)	s_u toe (kPa)	s_u range (kPa)	Q_u single pile (N)	block failure?	soil area (mm^2)	R_{cs}	equiv. pile (0.20 d)
GS25_2.00	12	G	S	25	2	4a	65	74	13	156	(N)	1600	3.3	21.0
GS16_2.00	25	G	S	16	2	5a	53	63	23	148	Y	900	2.9	15.6
GS25_2.00	26	G	S	25	2	5b	34	36	9	113	Y	1600	3.3	20.4

group	Q 0.02 d	Q 0.05 d	Q 0.10 d	Q 0.20 d	Q peak	0.02 d efficiency	0.05 d efficiency	0.10 d efficiency	0.20 d efficiency	peak efficiency	Q 0.02 d / Q peak	Q 0.05 d / Q peak	Q 0.10 d / Q peak	Q 0.20 d / Q peak
GS25_2.00	1150	2000	2700	3275	3525	0.29	0.51	0.69	0.84	0.90	33%	57%	77%	93%
GS16_2.00	1296	1824	2128	2304	2320	0.55	0.77	0.90	0.97	0.98	56%	79%	92%	99%
GS25_2.00	1125	1700	2000	2300	2350	0.40	0.60	0.71	0.81	0.83	48%	72%	85%	98%
											45%	69%	84%	97%
											averages			

Table 6.13 Grid group data

group	test	piles	soil area (mm^2)	capacity (N)			
				settlement			
				0.02 d	0.05 d	0.10 d	0.20 d
PS08_2.00	2b	8	400	656	888	1088	1192
PS08_4.00	5a	8	1600	968	944	1144	1192
PS20_1.75	5d	20	1914	1500	2220	2780	3240
TS16_2.00	4b	17	1600	1615	2244	2550	2788
TS16_2.00	4c	17	1600	1037	2074	2635	2737
TS16_2.00	5b	17	1600	1139	1479	1751	1904
GS25_2.00	4a	25	1600	1150	2000	2700	3275
GS25_2.00	5b	25	1600	1125	1700	2000	2300
PS16_2.00	~	16	1600				
TS16_2.00	~	**17**	**1600**				
GS25_2.00	~	**25**	**1600**				

group	efficiency				efficient pile equivalent (no.)			
					settlement			
	Q 0.02 d / Q peak	Q 0.05 d / Q peak	Q 0.10 d / Q peak	Q 0.20 d / Q peak	0.02 d	0.05 d	0.10 d	0.20 d
PS08_2.00	0.55	0.75	0.92	1.01	4	6	7	8
PS08_4.00	0.82	0.80	0.97	1.01	7	6	8	8
PS20_1.75	0.51	0.75	0.94	1.09	10	15	19	22
TS16_2.00	0.64	0.89	1.01	1.10	11	15	17	19
TS16_2.00	0.40	0.80	1.02	1.06	7	14	17	18
TS16_2.00	0.59	0.77	0.91	0.99	10	13	15	17
GS25_2.00	0.29	0.51	0.69	0.84	7	13	17	21
GS25_2.00	0.40	0.60	0.71	0.81	10	15	18	20
averages								
PS16_2.00	0.63	0.77	0.94	1.04	10	12	15	17
TS16_2.00	0.54	0.82	0.98	1.05	**9**	**14**	**17**	**18**
GS25_2.00	0.35	0.56	0.70	0.83	**9**	**14**	**18**	**21**

Table 6.14 Comparison group data

group	standard soil profile (sp_A)	l/d ratio = 100 (sp_A_100)	higher soil strength (sp_B)	lower soil strength (sp_C)	low strength & stiffness (sp_{C2})	tested in centrifuge?
single	✓	✓	✓	✓	✓	✓
GS25_1.50	✓					
GS25_2.00	✓	✓	✓	✓	✓	✓
GS25_3.00	✓					
GS16_2.00	✓					✓
PC14_1.75	✓					✓
PC16_1.75	✓					✓
PC18_1.75	✓					
PC20_1.75	✓					
PS16_2.00	✓					
PC12_1.50	✓					✓
PS20_1.75	✓	✓	✓			✓
TC14_1.75	✓		✓			✓
TC14_2.00	✓					✓
TC16_2.00	✓					✓
TS16_2.00	✓	✓	✓			✓
TS20_2.00	✓					

Table 7.01 Numerical testing summary

group reference	modelling method	capacity at stages of settlement (N)			
		0.02 d	0.05 d	0.10 d	0.20 d
single_spA	numerical	197	363	464	518
PC14_175d_spA	numerical	175	345	426	474
PC16_175d_spA	numerical	176	342	424	dnf
PC18_175d_spA	numerical	175	341	426	dnf
PC20_175d_spA	numerical	175	342	428	dnf
PS16_200d_spA	numerical	148	305	408	462
PC12_150d_spA	numerical	175	316	368	389
PS20_175d_spA	numerical	174	343	425	469

group reference	modelling method	efficiency			
		0.02 d	0.05 d	0.10 d	0.20 d
PC14_175d_spA	numerical	0.89	0.95	0.92	0.92
PC16_175d_spA	numerical	0.89	0.94	0.91	dnf
PS20_175d_spA	numerical	0.88	0.94	0.92	0.91
PC12_150d_spA	numerical	0.89	0.87	0.79	0.75
PS16_200d_spA	numerical	0.75	0.84	0.88	0.89
		staged single pile capacity			

group reference	modelling method	efficiency			
		0.02 d	0.05 d	0.10 d	0.20 d
PC14_175d_spA	numerical	0.33	0.64	0.79	0.88
PC14_1.75	centrifuge	0.59	0.86	0.95	1.00
PC16_175d_spA	numerical	0.33	0.64	0.79	dnf
PC16_1.75	centrifuge	0.57	0.82	1.01	1.09
PS20_175d_spA	numerical	0.32	0.64	0.79	0.87
PS20_1.75	centrifuge	0.51	0.75	0.94	1.09
PC12_150d_spA	numerical	0.33	0.59	0.68	0.72
PC12_1.50	centrifuge	0.46	0.66	0.83	0.90
PS16_200d_spA	numerical	0.28	0.57	0.76	0.86
PC16_2.00	centrifuge	0.59	0.86	0.95	1.00
		peak single pile capacity			

group reference	modelling method	efficiency			
		0.02 d	0.05 d	0.10 d	0.20 d
PC14_175d_spA	numerical	0.38	0.74	0.92	1.02
PC14_1.75	centrifuge	0.59	0.86	0.95	1.00
PC16_175d_spA	numerical	0.38	0.74	0.91	dnf
PC16_1.75	centrifuge	0.57	0.82	1.01	1.09
PS20_175d_spA	numerical	0.38	0.74	0.92	1.01
PS20_1.75	centrifuge	0.51	0.75	0.94	1.09
PC12_150d_spA	numerical	0.38	0.68	0.79	0.84
PC12_1.50	centrifuge	0.46	0.66	0.83	0.90
PS16_200d_spA	numerical	0.32	0.66	0.88	1.00
PC16_2.00	centrifuge	0.59	0.86	0.95	1.00
		0.10 d single pile capacity (numerical)			

*dnf = did not finish

Table 8.01 Perimeter group efficiency comparison

group reference	modelling method	capacity at stages of settlement (N)			
		0.02 d	0.05 d	0.10 d	0.20 d
single_spA	numerical	197	363	464	518
TC14_175d_spA	numerical	175	343	416	443
TC14_200d_spA	numerical	177	350	439	dnf
TC16_200d_spA	numerical	178	355	458	508
TS16_200d_spA	numerical	176	356	446	490
TS20_200d_spA	numerical	171	340	427	475

group reference	modelling method	efficiency			
		0.02 d	0.05 d	0.10 d	0.20 d
TC14_175d_spA	numerical	0.89	0.94	0.90	0.86
TC14_200d_spA	numerical	0.90	0.96	0.95	dnf
TC16_200d_spA	numerical	0.90	0.98	0.99	0.98
TS20_200d_spA	numerical	0.87	0.94	0.92	0.92
TS16_200d_spA	numerical	0.89	0.98	0.96	0.95
		staged single pile capacity			

group reference	modelling method	efficiency			
		0.02 d	0.05 d	0.10 d	0.20 d
TC14_175d_spA	numerical	0.33	0.64	0.77	0.82
TC14_1.75	centrifuge	0.40	0.63	0.81	0.94
TC14_200d_spA	numerical	0.33	0.65	0.82	dnf
TC14_2.00	centrifuge	0.55	0.89	1.09	1.18
TC16_200d_spA	numerical	0.33	0.66	0.85	0.94
TC16_2.00	centrifuge	0.60	0.89	1.06	1.12
TS20_200d_spA	numerical	0.32	0.63	0.79	0.88
TS20_2.00	centrifuge	0.54	0.79	0.95	1.10
TS16_200d_spA	numerical	0.33	0.66	0.83	0.91
TS16_2.00 (4b)	centrifuge	0.64	0.89	1.01	1.10
TS16_2.00 (4c)	centrifuge	0.40	0.80	1.02	1.06
TS16_2.00 (5b)	centrifuge	0.59	0.77	0.91	0.99
		peak single pile capacity			

group reference	modelling method	efficiency			
		0.02 d	0.05 d	0.10 d	0.20 d
TC14_175d_spA	numerical	0.38	0.74	0.90	0.95
TC14_1.75	centrifuge	0.40	0.63	0.81	0.94
TC14_200d_spA	numerical	0.38	0.75	0.95	dnf
TC14_2.00	centrifuge	0.55	0.89	1.09	1.18
TC16_200d_spA	numerical	0.38	0.77	0.99	1.09
TC16_2.00	centrifuge	0.60	0.89	1.06	1.12
TS20_200d_spA	numerical	0.37	0.73	0.92	1.02
TS20_2.00	centrifuge	0.54	0.79	0.95	1.10
TS16_200d_spA	numerical	0.38	0.77	0.96	1.06
TS16_2.00 (4b)	centrifuge	0.64	0.89	1.01	1.10
TS16_2.00 (4c)	centrifuge	0.40	0.80	1.02	1.06
TS16_2.00 (5b)	centrifuge	0.59	0.77	0.91	0.99
		0.10 d single pile capacity (numerical)			

*dnf = did not finish

Table 8.02 Target group efficiency comparison

group reference	modelling method	efficiency			
		0.02 d	0.05 d	0.10 d	0.20 d
PC14_175d_spA	numerical	0.89	0.95	0.92	0.92
TC14_175d_spA	numerical	0.89	0.94	0.90	0.86
PS16_200d_spA	numerical	0.75	0.84	0.88	0.89
TS16_200d_spA	numerical	0.89	0.98	0.96	0.95
		staged single pile capacity			

Table 8.03 Perimeter/target efficiency comparison

group reference	modelling method	capacity at stages of settlement (N)			
		0.02 d	0.05 d	0.10 d	0.20 d
single_spA	numerical	197	363	464	518
GS25_150d_spA	numerical	128	211	250	275
GS25_200d_spA	numerical	150	285	330	363
GS25_300d_spA	numerical	159	307	384	dnf
GS16_200d_spA	numerical	169	333	381	412

group reference	modelling method	efficiency			
		0.02 d	0.05 d	0.10 d	0.20 d
GS25_200d_spA	numerical	0.76	0.79	0.71	0.70
GS16_200d_spA	numerical	0.86	0.92	0.82	0.80
		staged single pile capacity			

group reference	modelling method	efficiency			
		0.02 d	0.05 d	0.10 d	0.20 d
GS25_200d_spA	numerical	0.28	0.53	0.61	0.67
GS25_2.00	centrifuge	0.29	0.51	0.69	0.84
GS25_2.00	centrifuge	0.40	0.60	0.71	0.81
GS16_200d_spA	numerical	0.31	0.62	0.71	0.77
GS16_2.00	centrifuge	0.55	0.77	0.90	0.97
		peak single pile capacity			

group reference	modelling method	efficiency			
		0.02 d	0.05 d	0.10 d	0.20 d
GS25_200d_spA	numerical	0.32	0.61	0.71	0.78
GS25_2.00	centrifuge	0.29	0.51	0.69	0.84
GS25_2.00	centrifuge	0.40	0.60	0.71	0.81
GS16_200d_spA	numerical	0.36	0.72	0.82	0.89
GS16_2.00	centrifuge	0.55	0.77	0.90	0.97
		0.10 d single pile capacity (numerical)			

Table 8.04 Grid group efficiency comparison

group reference	efficiency				settlement (mm)	
	0.02 d	0.05 d	0.10 d	0.20 d	pile	central soil
GS25_200d_spA	0.76	0.79	0.71	0.70	100	100
GS25_200d_spB	0.77	0.91	0.98	0.97	100	80
spB-spA	*0.01*	*0.12*	*0.27*	*0.27*		
PS20_175d_spA	0.88	0.94	0.92	0.91	100	70
PS20_175d_spB	0.83	0.93	0.95	0.94	100	0
spB-spA	*-0.05*	*-0.01*	*0.03*	*0.03*		
TC14_175d_spA	0.89	0.94	0.90	0.86	100	80
TC14_175d_spB	0.85	0.95	0.97	0.96	100	0
spB-spA	*-0.04*	*0.01*	*0.07*	*0.11*		
TS16_200d_spA	0.89	0.98	0.96	0.95	100	50
TS16_200d_spB	0.85	0.97	1.00	1.00	100	0
spB-spA	*-0.04*	*-0.01*	*0.04*	*0.06*		
	staged single pile capacity					

group reference	efficiency				settlement (mm)	
	0.02 d	0.05 d	0.10 d	0.20 d	pile	central soil
GS25_200d_spA	0.32	0.61	0.71	0.78	100	100
GS25_200d_spB	0.31	0.68	0.98	1.17	100	80
spB-spA	*-0.01*	*0.07*	*0.27*	*0.39*		
PS20_175d_spA	0.38	0.74	0.92	1.01	100	70
PS20_175d_spB	0.34	0.70	0.95	1.14	100	0
spB-spA	*-0.04*	*-0.04*	*0.03*	*0.13*		
TC14_175d_spA	0.38	0.74	0.90	0.95	100	80
TC14_175d_spB	0.34	0.72	0.97	1.17	100	0
spB-spA	*-0.03*	*-0.02*	*0.07*	*0.21*		
TS16_200d_spA	0.38	0.77	0.96	1.06	100	50
TS16_200d_spB	0.34	0.73	1.00	1.22	100	0
spB-spA	*-0.03*	*-0.04*	*0.04*	*0.16*		
	0.10 d single pile capacity					

group reference	efficiency				settlement (mm)	
	0.02 d	0.05 d	0.10 d	0.20 d	pile	central soil
GS25_200d_spA	0.32	0.61	0.71	0.78	100	100
GS25_200d_spB	0.31	0.68	0.98	1.17	100	80
GS25_200d_spC	0.37	0.49	0.54	0.59	100	100
GS25_200d_spC$_2$	0.25	0.47	0.52	0.57	100	100
	0.10 d single pile capacity					

Table 8.05 Soil profile comparison

group reference	efficiency			
	0.02 d	0.05 d	0.10 d	0.20 d
PS20_175d_spA	0.88	0.94	0.92	0.91
PS20_175d_100_spA	0.86	0.95	0.97	0.95
TS16_200d_spA	0.89	0.98	0.96	0.95
TS16_200d_100_spA	0.82	0.88	0.90	0.89
GS25_200d_spA	0.76	0.79	0.71	0.70
GS25_200d_100_spA	0.76	0.86	0.80	0.70
	staged single pile capacity			

group reference	efficiency			
	0.02 d	0.05 d	0.10 d	0.20 d
PS20_175d_spA	0.32	0.64	0.79	0.87
PS20_175d_100_spA	0.18	0.43	0.67	0.83
TS16_200d_spA	0.33	0.66	0.83	0.91
TS16_200d_100_spA	0.17	0.40	0.63	0.78
GS25_200d_spA	0.28	0.53	0.61	0.67
GS25_200d_100_spA	0.16	0.39	0.56	0.61
	peak single pile capacity			

group reference	efficiency			
	0.02 d	0.05 d	0.10 d	0.20 d
PS20_175d_spA	0.38	0.74	0.92	1.01
PS20_175d_100_spA	0.25	0.62	0.97	1.19
TS16_200d_spA	0.38	0.77	0.96	1.06
TS16_200d_100_spA	0.24	0.57	0.90	1.12
GS25_200d_spA	0.32	0.61	0.71	0.78
GS25_200d_100_spA	0.22	0.56	0.80	0.88
	0.10 d single pile capacity			

group reference	settlement (mm)	
	pile	central soil
PS20_175d_spA	100	70
PS20_175d_100_spA	100	40
TS16_200d_spA	100	50
TS16_200d_100_spA	50	0
GS25_200d_spA	100	100
GS25_200d_100_spA	50	40

Table 8.06 l/d ratio comparison

no. of piles (excl. central)	group	spacing							
		1.25	**1.5**	**1.75**	**2**	**2.25**	**2.5**	**2.75**	**3**
12	**PS12**	1.5	2.1	2.9	**3.8**	4.8	6.0	7.2	8.6
16	**PS16**	2.0	2.9	3.9	**5.1**	6.4	8.0	9.6	11.5
20	**PS20**	2.5	**3.6**	**4.9**	**6.4**	8.1	9.9	12.0	14.3
12	**TS12**	1.3	1.9	2.6	3.4	4.4	5.4	6.6	7.9
16	**TS16**	1.8	2.6	3.6	**4.7***	6.0	7.4	9.0	10.7
20	**TS20**	2.3	3.4	4.6	**6.0**	7.6	9.4	11.4	13.6
16	**GS16**	0.9	1.4	1.9	**2.6**	3.4	4.2	5.2	6.2
25	**GS25**	1.1	1.7	2.3	**3.1^**	4.0	4.9	6.0	7.2
12	**PC12**	**1.9**	**2.7**	3.7	**4.9**	6.2	7.6	9.2	**10.9**
14	**PC14**	2.2	3.2	**4.3**	**5.7**	7.2	8.9	10.7	12.8
16	**PC16**	2.5	3.6	**5.0**	**6.5**	8.2	10.1	12.3	14.6
18	**PC18**	2.8	**4.1**	5.6	**7.3**	9.2	11.4	13.8	16.4
20	**PC20**	3.2	4.6	6.2	**8.1**	10.3	12.7	15.3	18.2
12	**TC12**	1.7	2.4	3.4	**4.4**	**5.6**	6.9	8.4	10.0
14	**TC14**	2.0	2.9	**4.0**	**5.2**	6.6	8.2	9.9	11.8
16	**TC16**	2.3	3.4	**4.6**	**6.0**	7.7	9.5	11.5	13.7
18	**TC18**	2.6	**3.8**	5.2	6.9	8.7	10.7	13.0	15.5
20	**TC20**	3.0	4.3	5.9	7.7	9.7	12.0	14.5	17.3

block
individual
Both

* block: s_u = 54 kPa; individual: s_u = 34 and 61 kPa

^ block: s_u = 33 kPa; individual: s_u = 65 kPa

Table 9.01 Relationship between R_{cs} value and failure mechanism

Figures

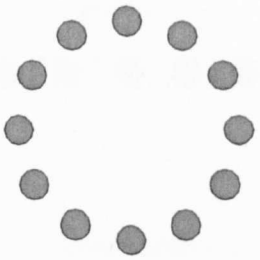

Figure 1.01 Perimeter pile group plan view

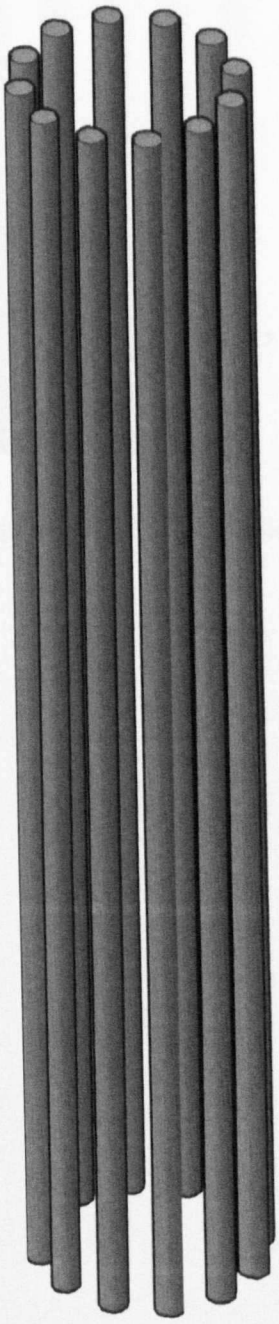

Figure 1.02 Perimeter pile group 3D view

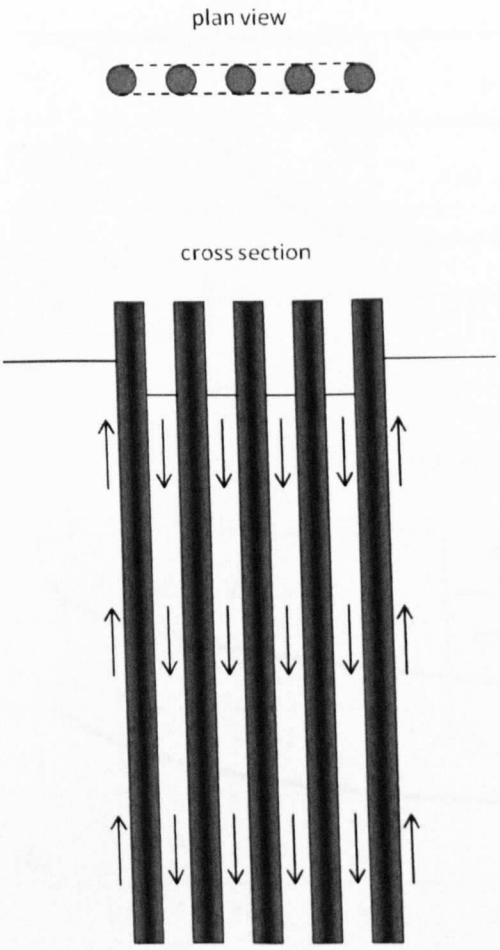

Figure 1.03 Failure planes in a bored pile wall (linear group)

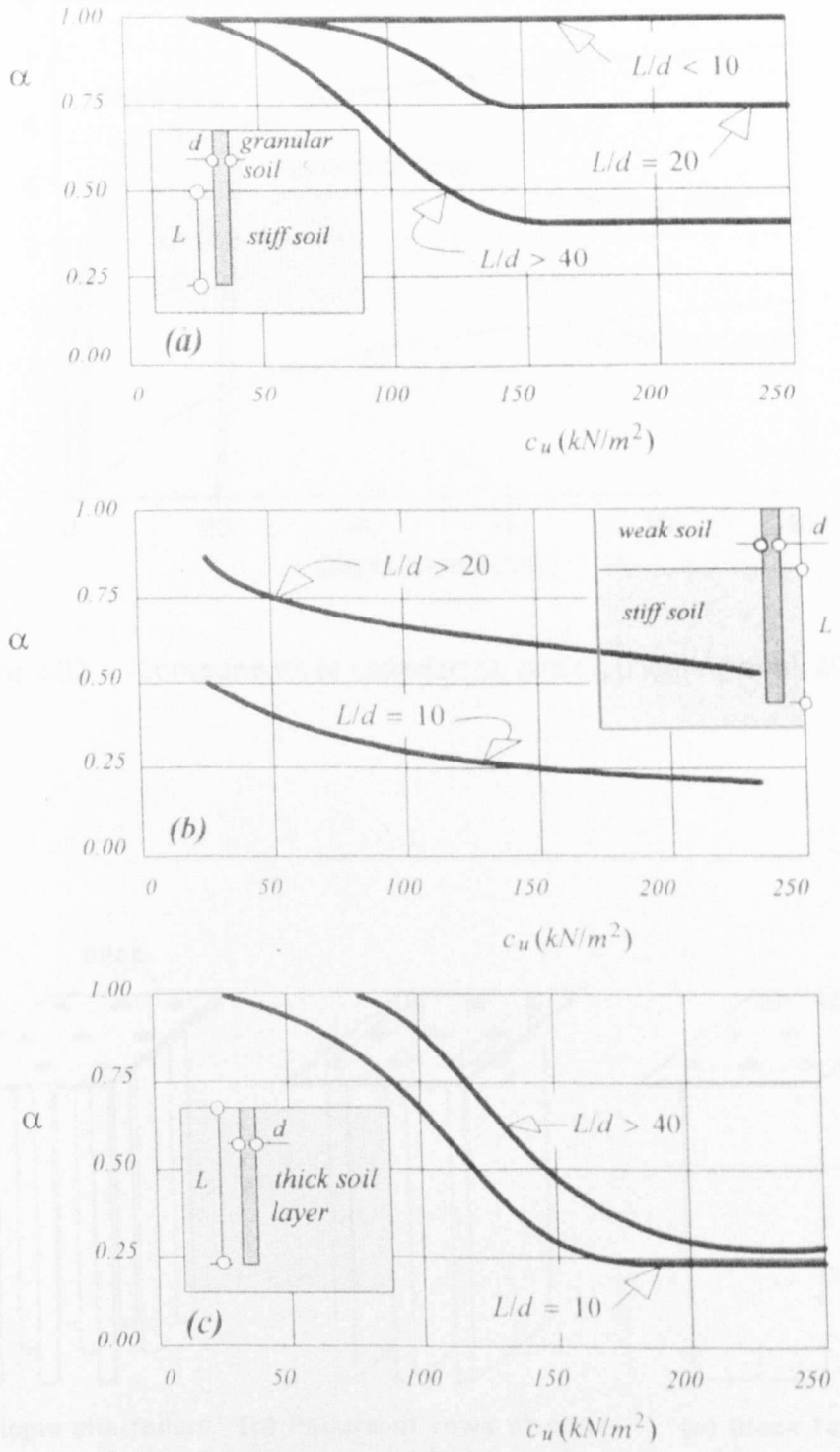

Figure 2.01 The adhesion factor profile for different soil strata (Azizi, 2000)

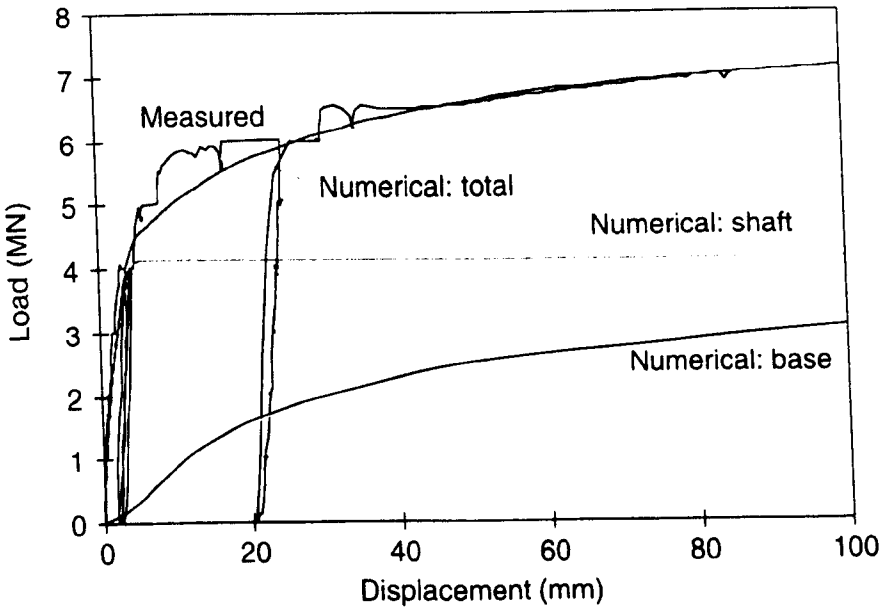

Figure 2.02 Components of capacity: Q_s and Q_b (Fleming et al, 2009)

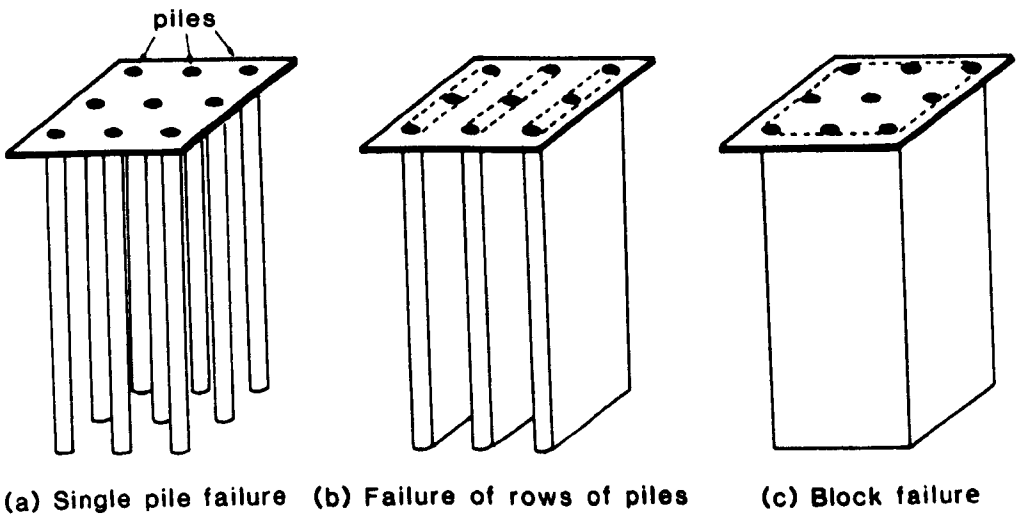

Figure 2.03 Idealised group failure planes (Fleming et al, 2009)

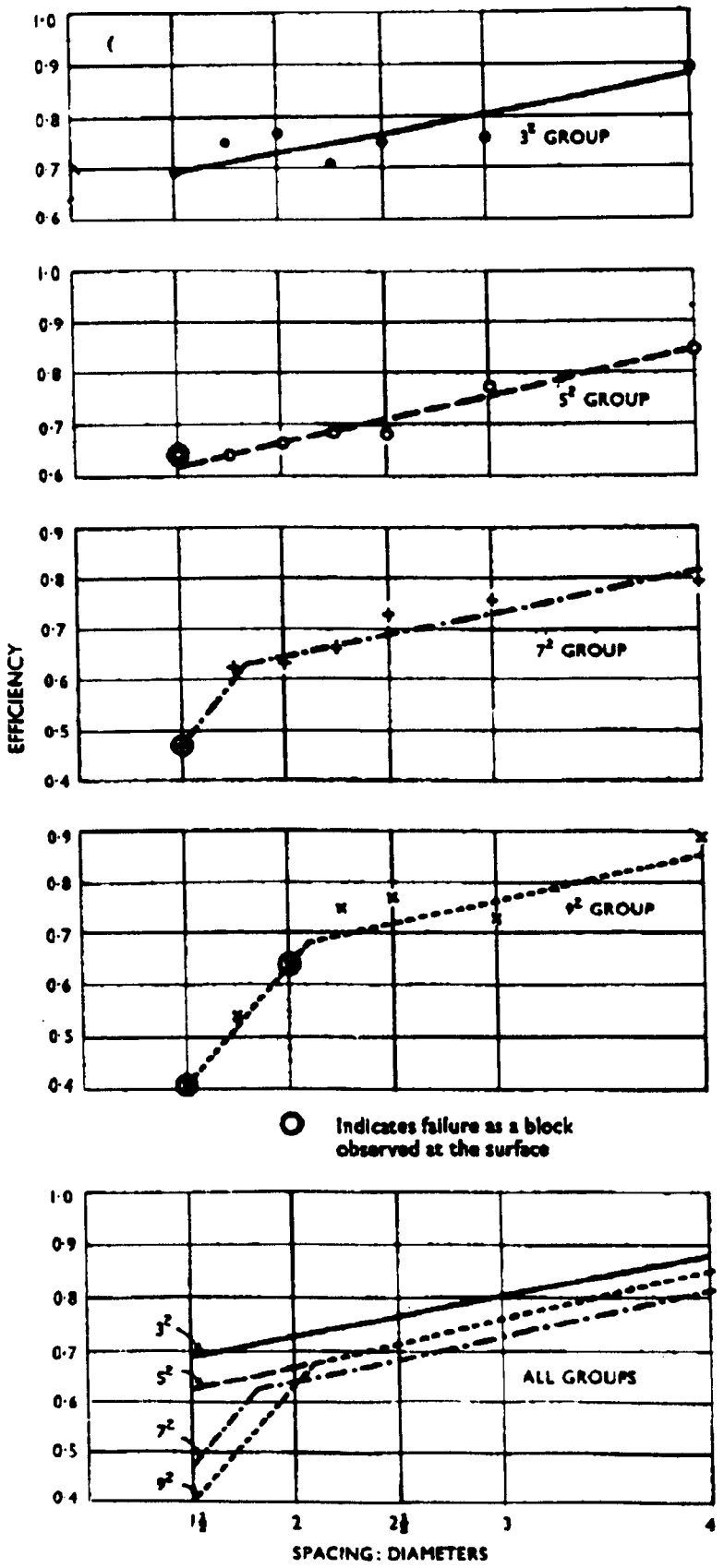

Figure 2.04 Spacing vs efficiency: grid groups with l/d = 24 (Whitaker, 1957)

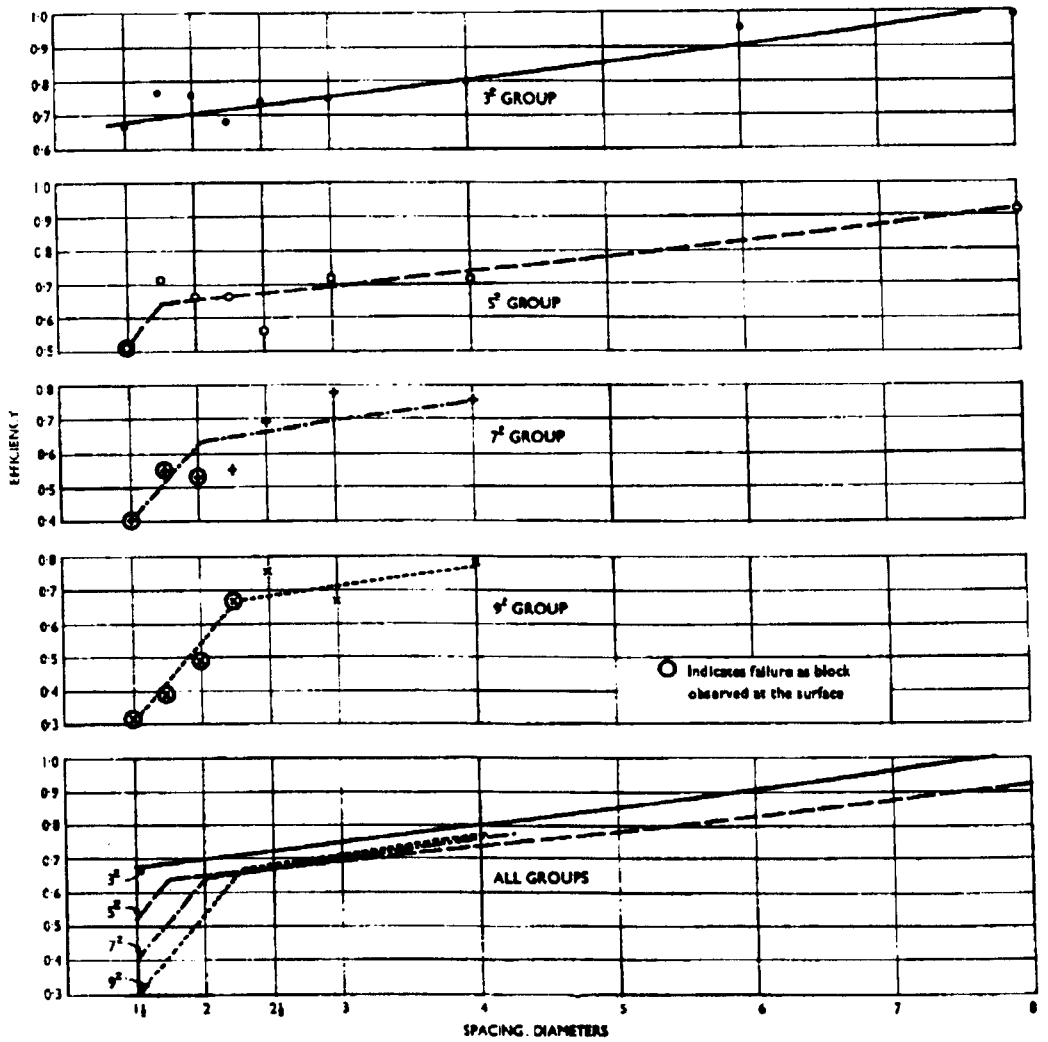

Figure 2.05 Spacing vs efficiency: grid groups with l/d = 48 (Whitaker, 1957)

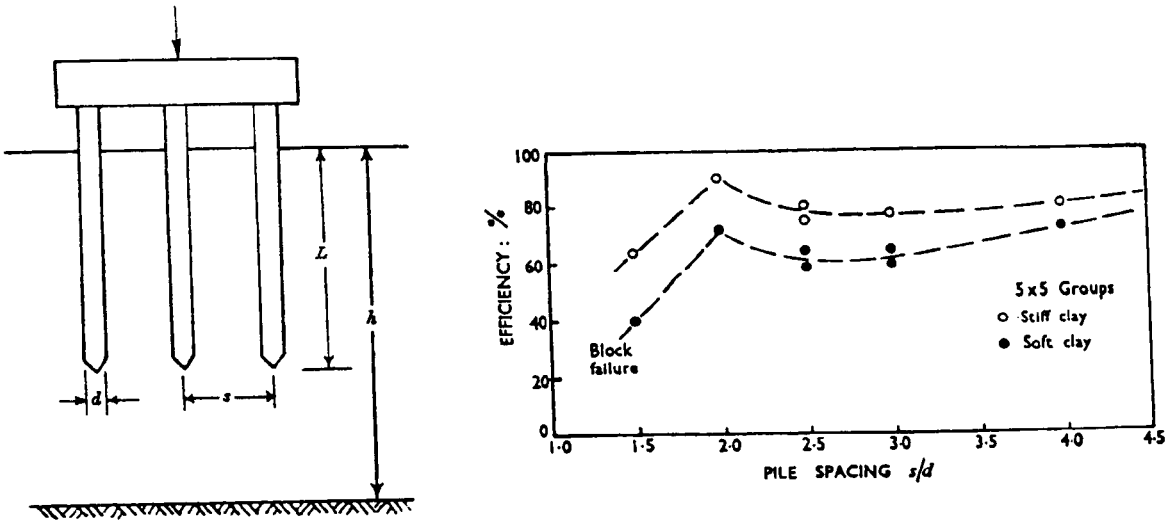

Figure 2.06 Spacing vs efficiency: Barden and Monckton's test results (1970)

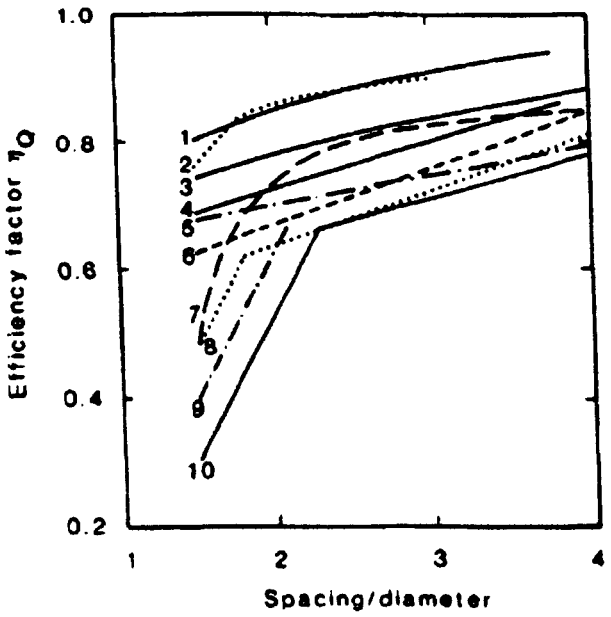

1 = 3^2 (ST); 2 = 2^2 x 12d (SF); 3 = 3^2 x 30d (ST); 4 = 3^2 x 24d (W); 5 = 3^2 x 48d (W); 6 = 5^2 x 24d (W); 7 = 3^2 x 24d (SF); 8 = 7^2 x 24d (W); 9 = 9^2 x 24d (W); 10 = 9^2 x 48d (W).

W = Whitaker (1957); ST = Saffery-Tate (1961); SF = Sowers-Fausold (1961) (De Mello, 1969)

Figure 2.07 Pile group efficiencies in clay (Fleming et al, 1992)

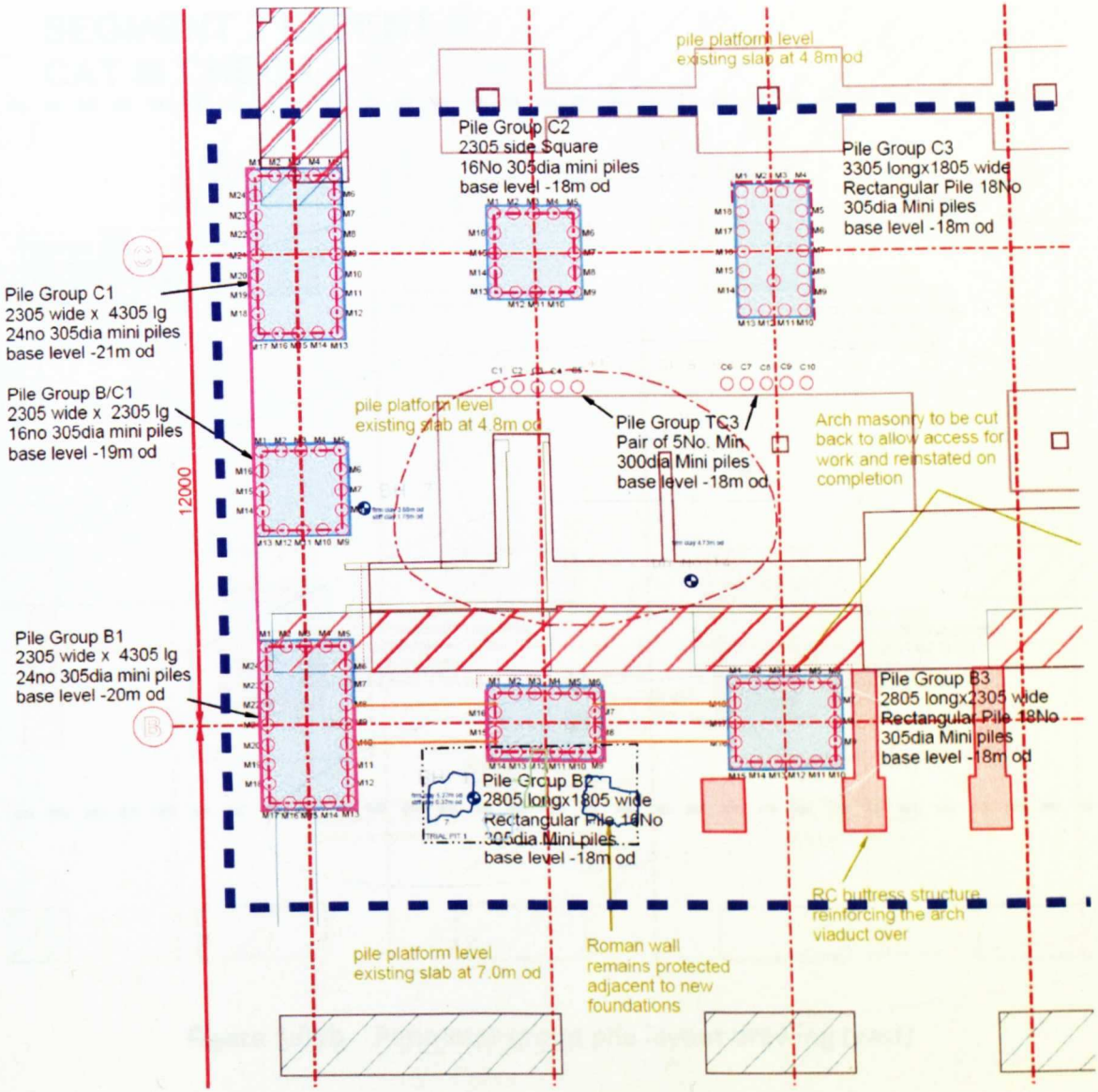

Figure 3.01a Perimeter group pile layout drawing (west)

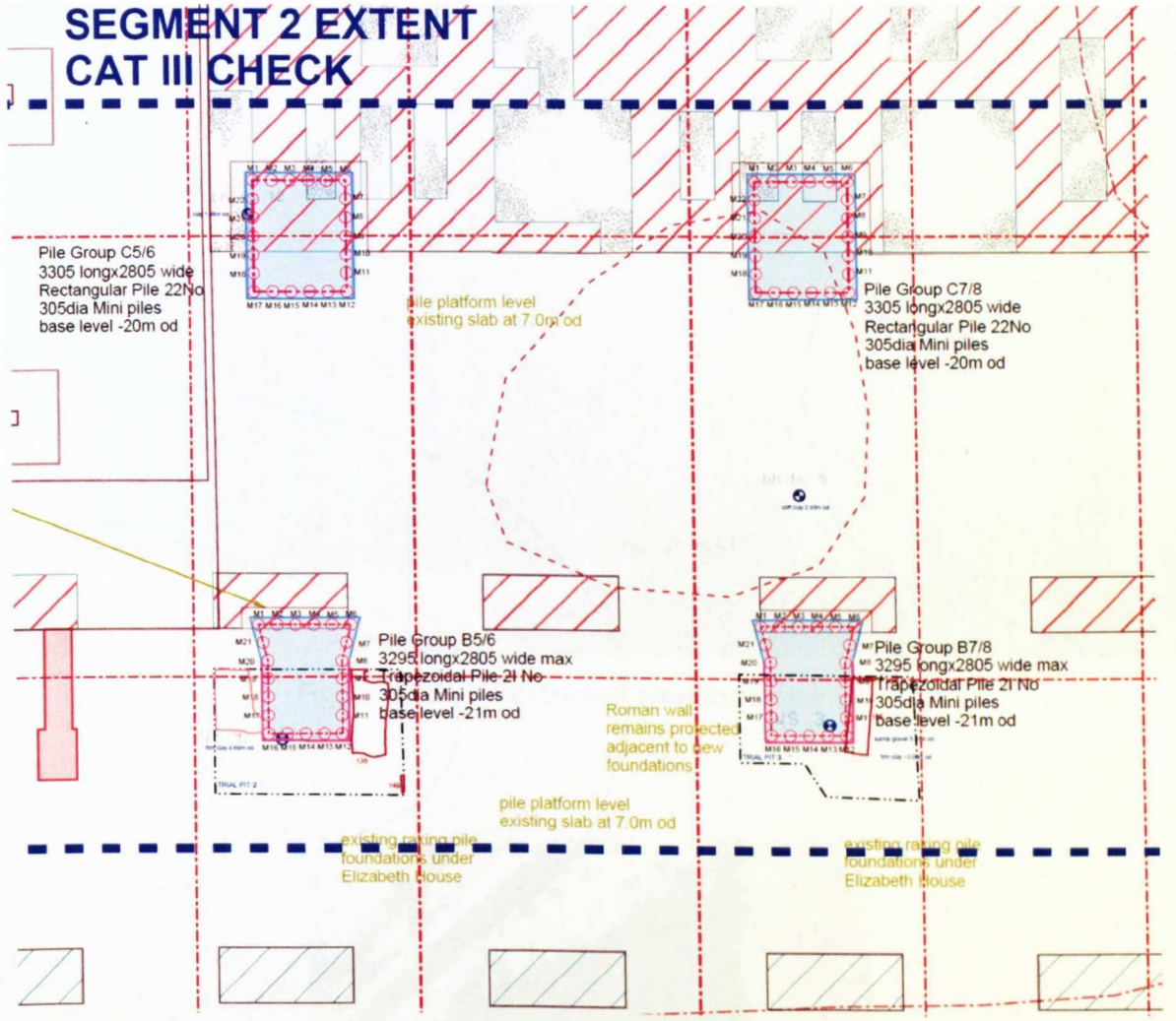

Figure 3.01b Perimeter group pile layout drawing (east)

Figure 3.02 Restricted working space [1]

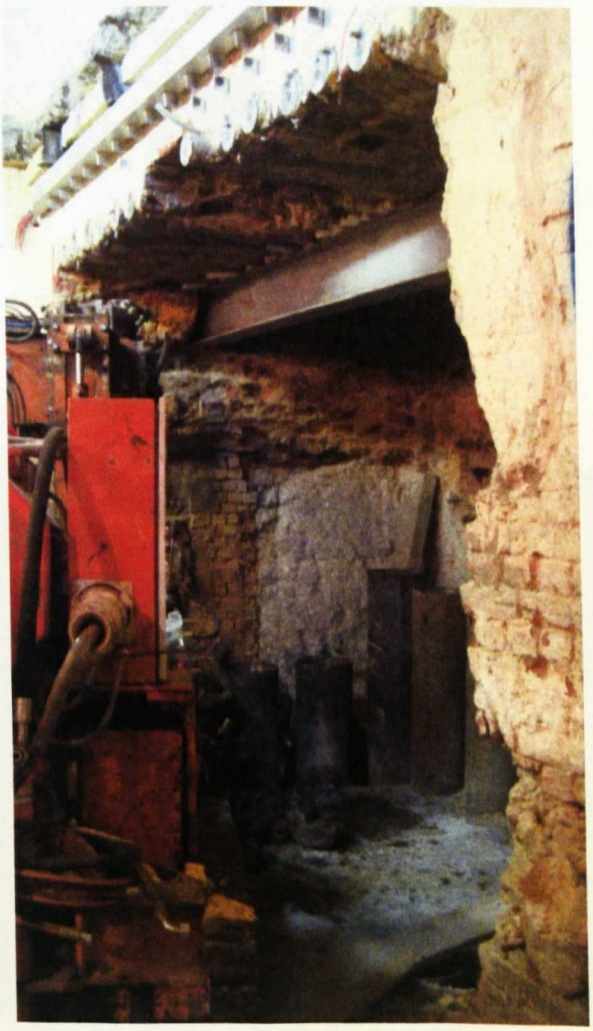

Figure 3.03 Restricted working space [2]

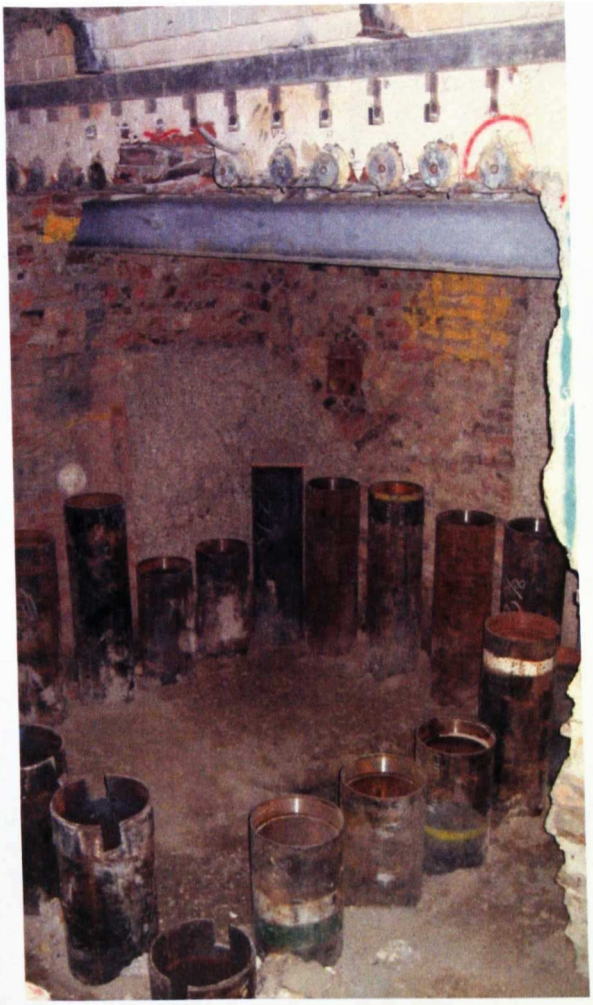

Figure 3.04 Piles installed through casing

Figure 3.05 Excavation to pile cap formation level

Figure 3.06 Cutting down pile heads to formation level

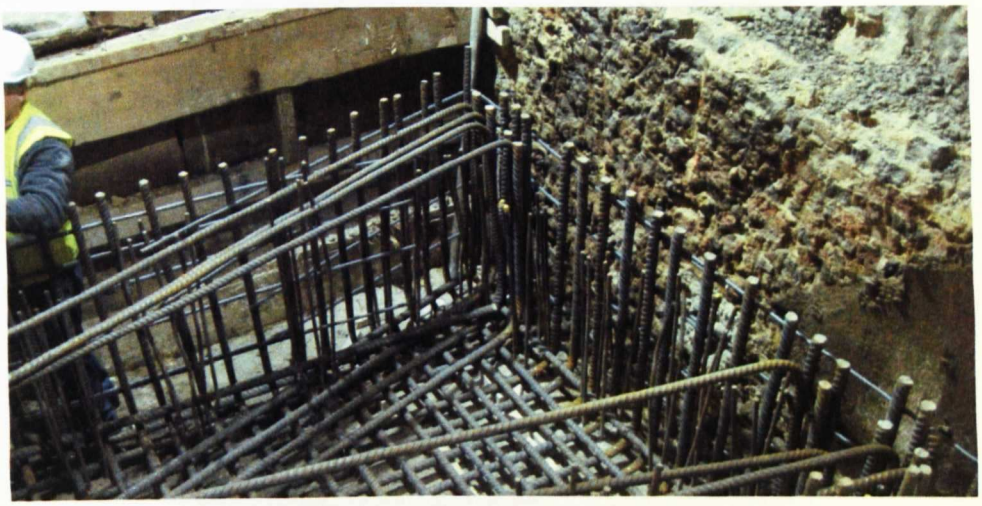

Figure 3.07 Installation of pile cap reinforcement

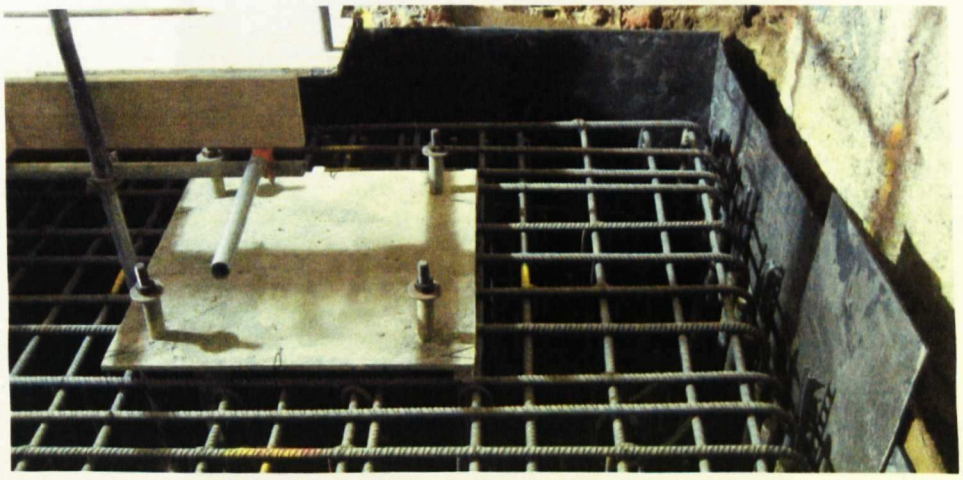

Figure 3.08 Installation of structural column connection plate

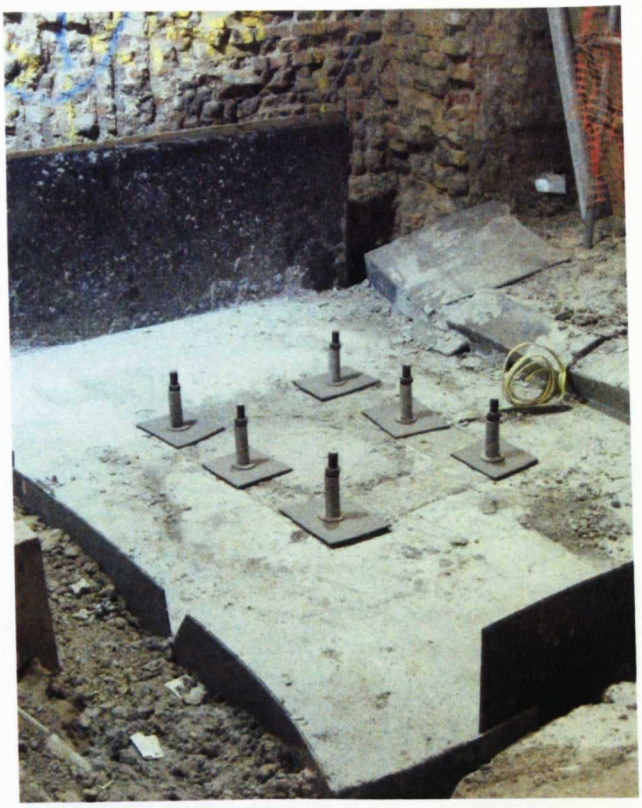

Figure 3.09 Concrete pile cap poured

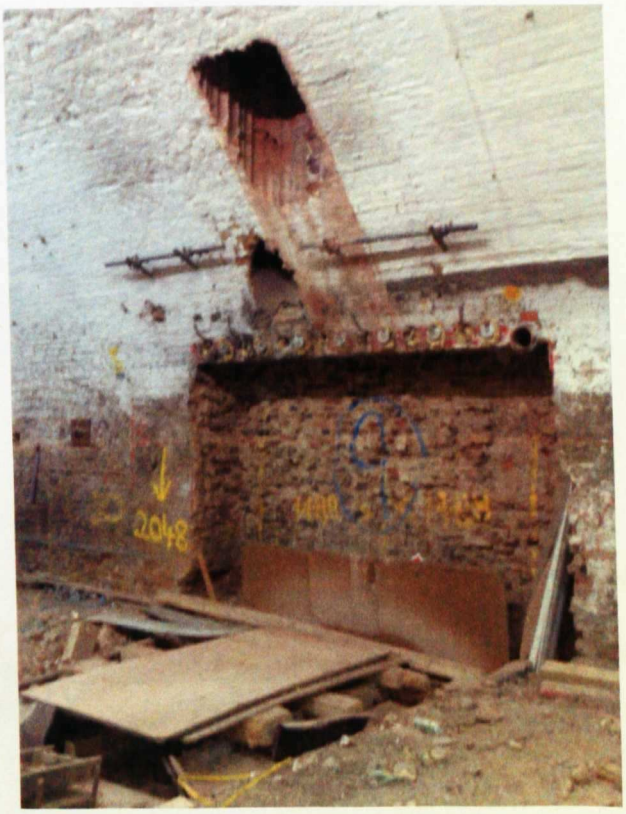

Figure 3.10 Hole cut through arch to allow placement of column

Figure 3.11 Structural column installed

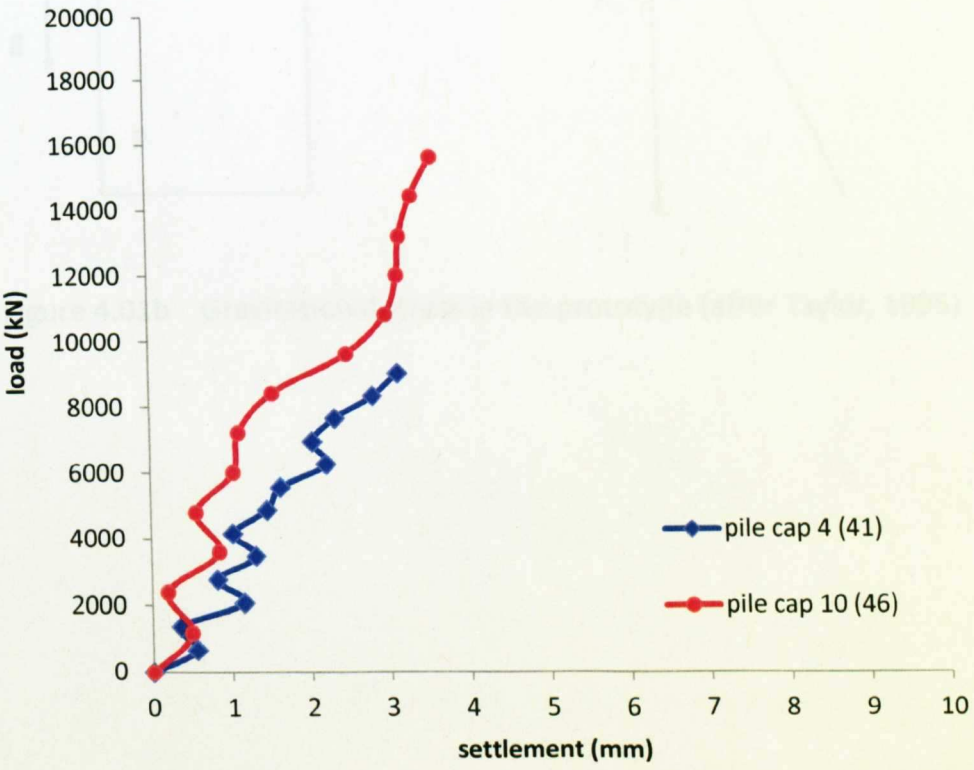

Figure 3.12 Load vs settlement: perimeter group monitoring

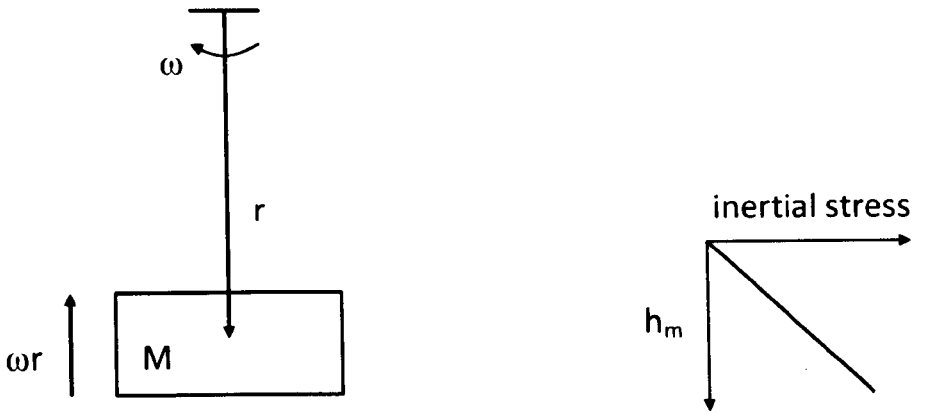

Figure 4.01a Inertial stress in the model (after Taylor, 1995)

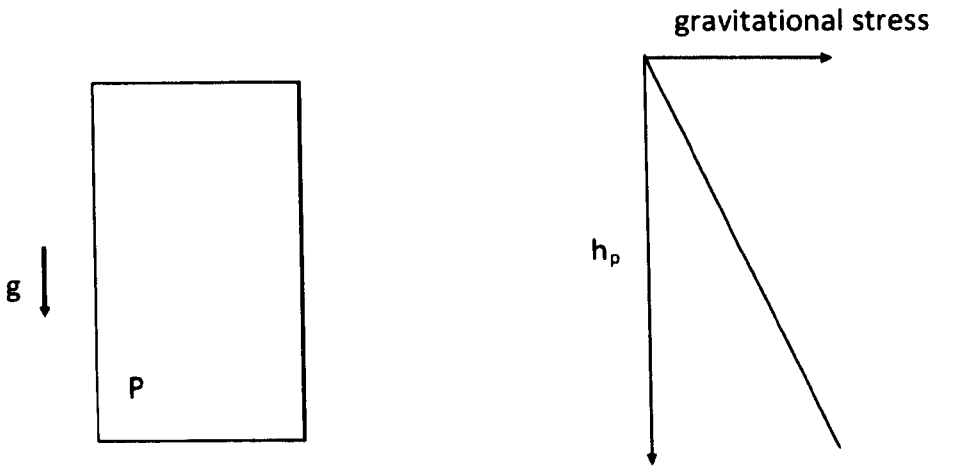

Figure 4.01b Gravitational stress in the prototype (after Taylor, 1995)

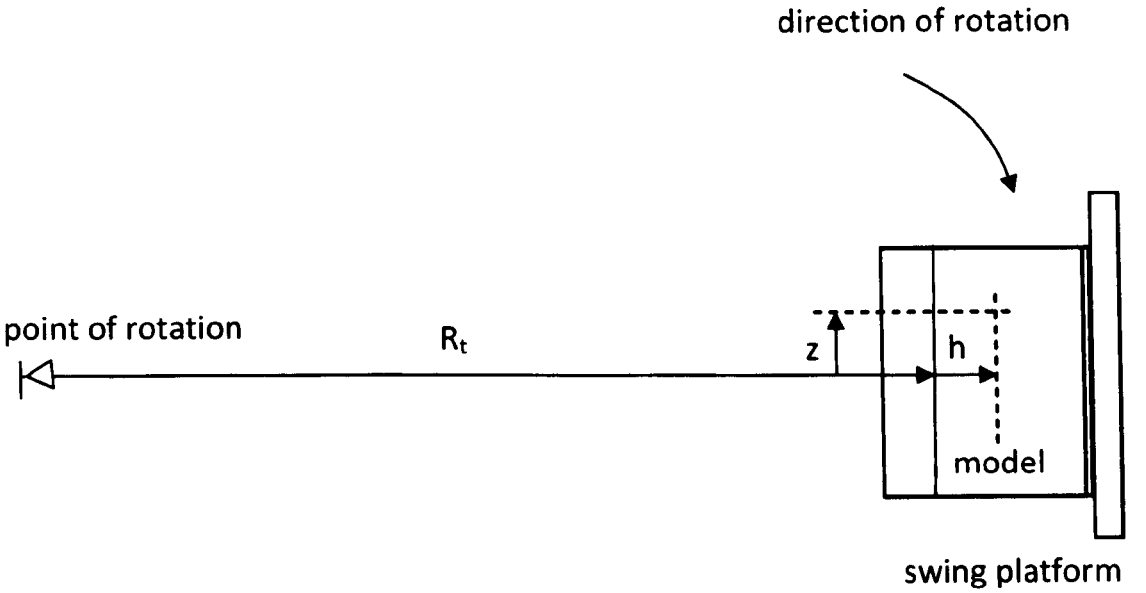

Figure 4.02 Variation in model height and acceleration (plan view)

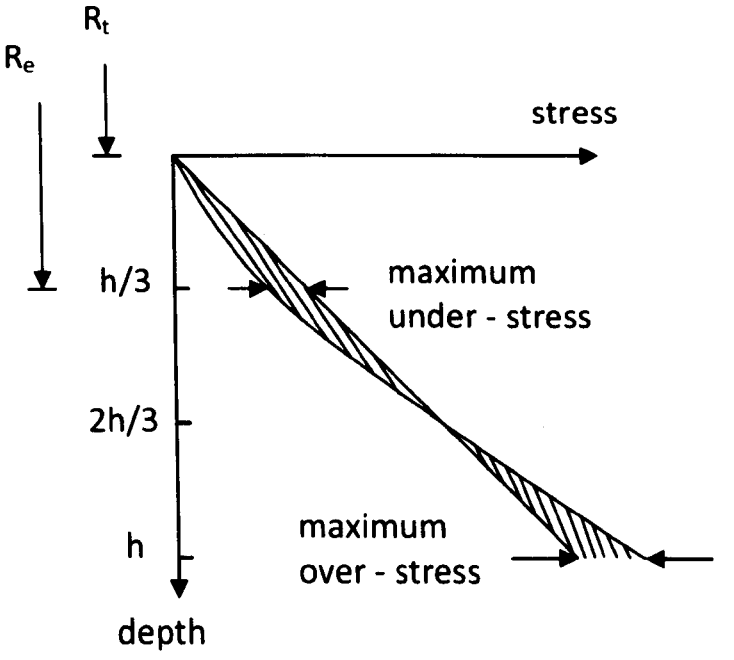

Figure 4.03 Calculation of acceleration errors (Taylor, 1995)

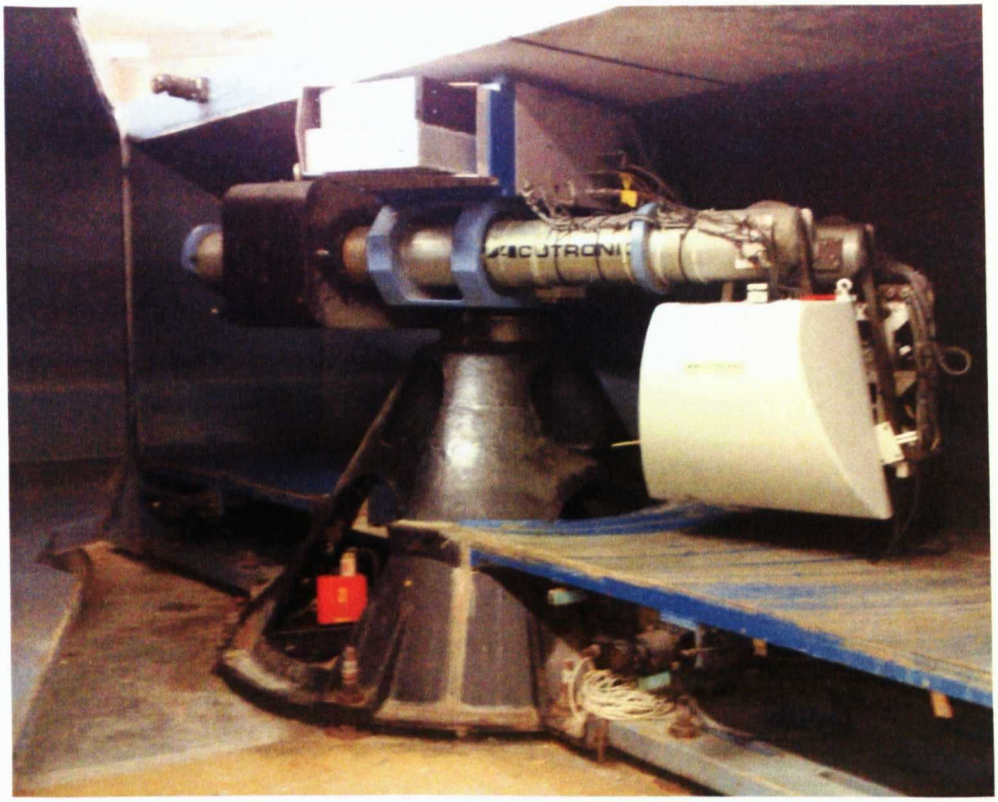

Figure 4.04 City University London centrifuge

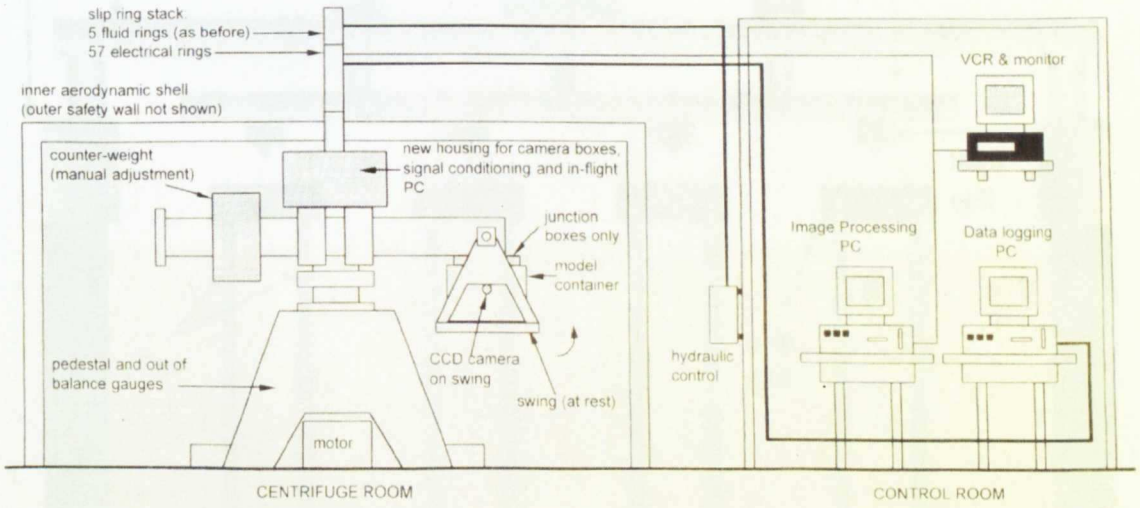

Figure 4.05 Schematic diagram of the centrifuge (Grant, 1998)

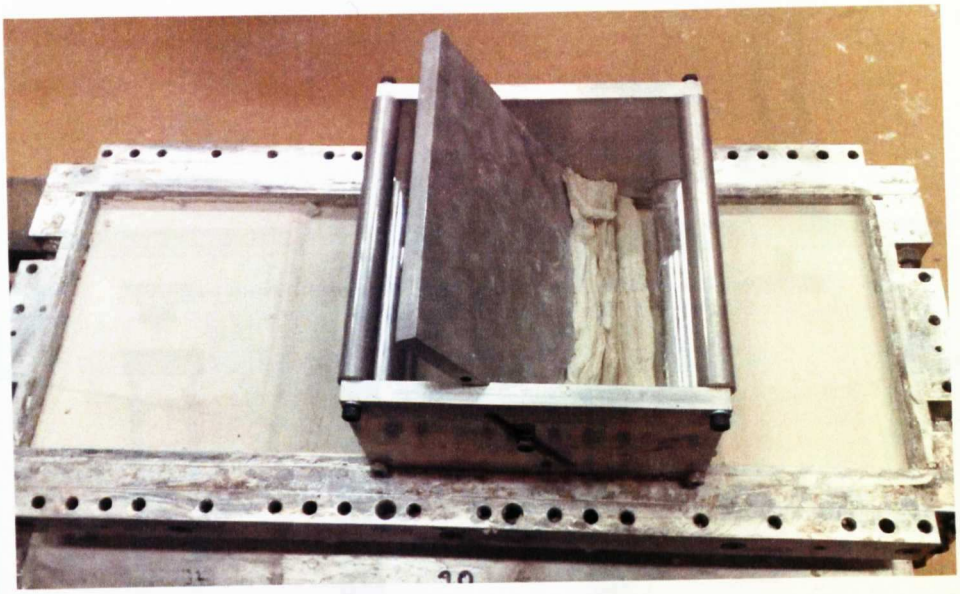

Figure 5.01 Cutting the clay surface to the correct height

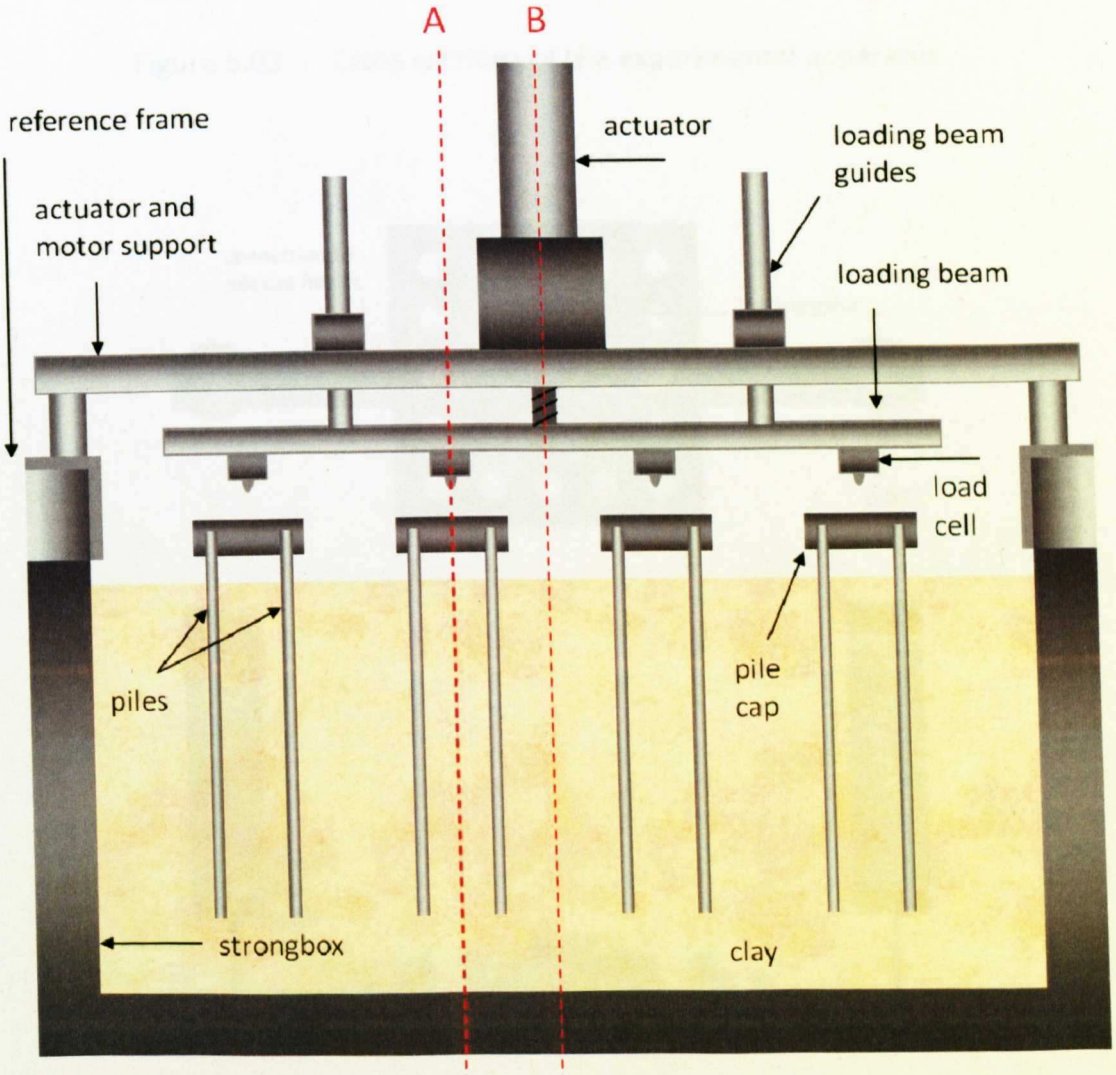

Figure 5.02 Long section of the experimental apparatus

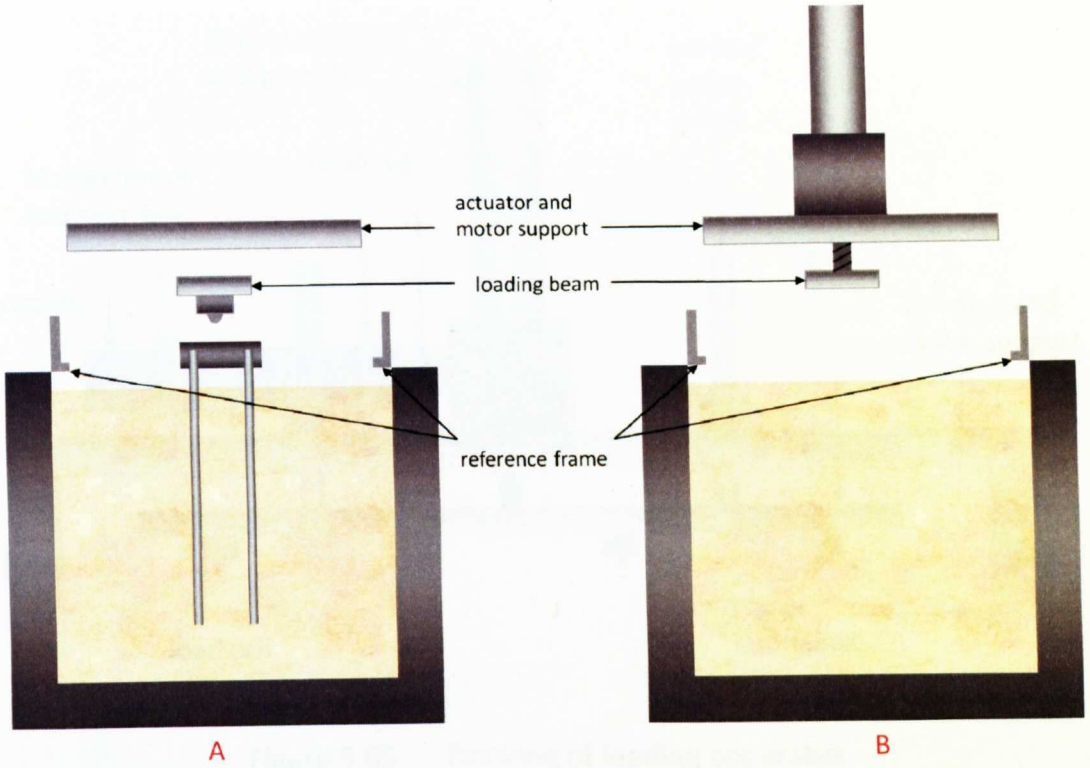

Figure 5.03 Cross sections of the experimental apparatus

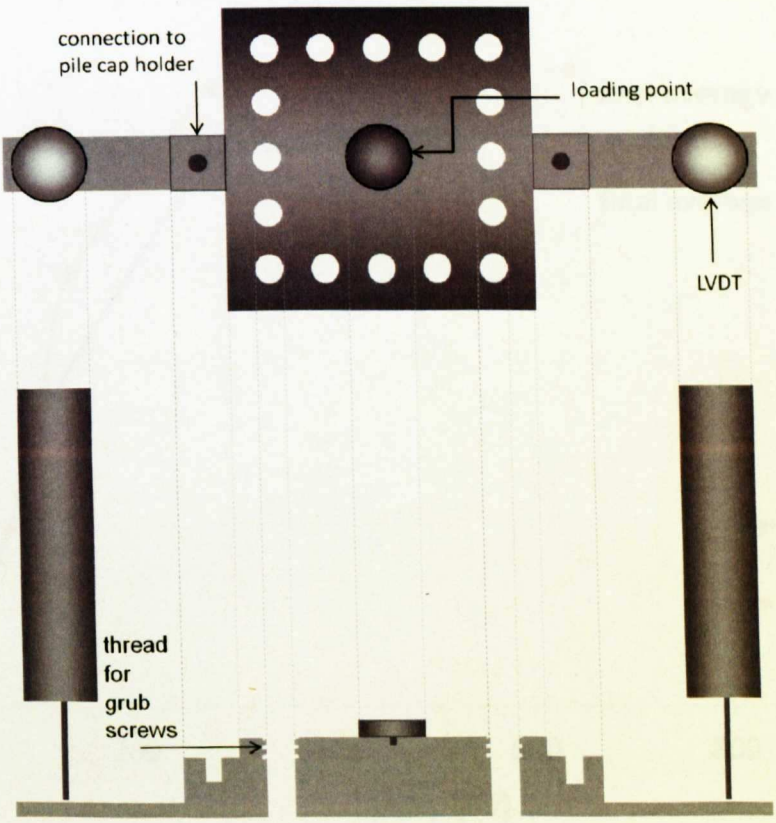

Figure 5.04 Plan view and cross section of the pile cap showing location of the LVDTs and loading point

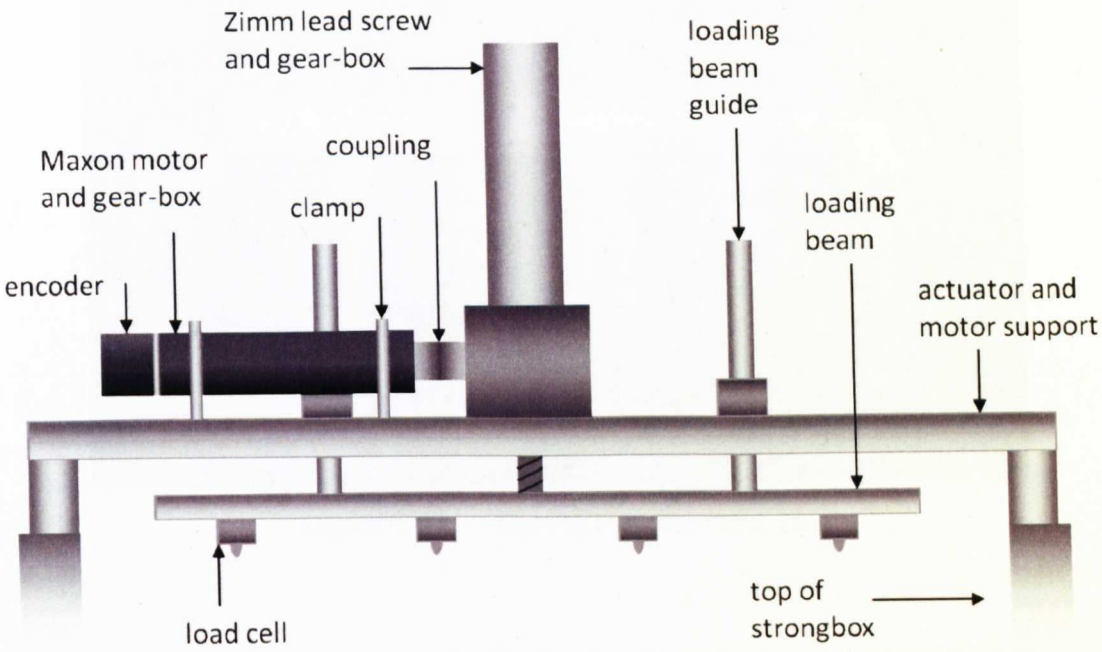

Figure 5.05 Drawing of loading apparatus

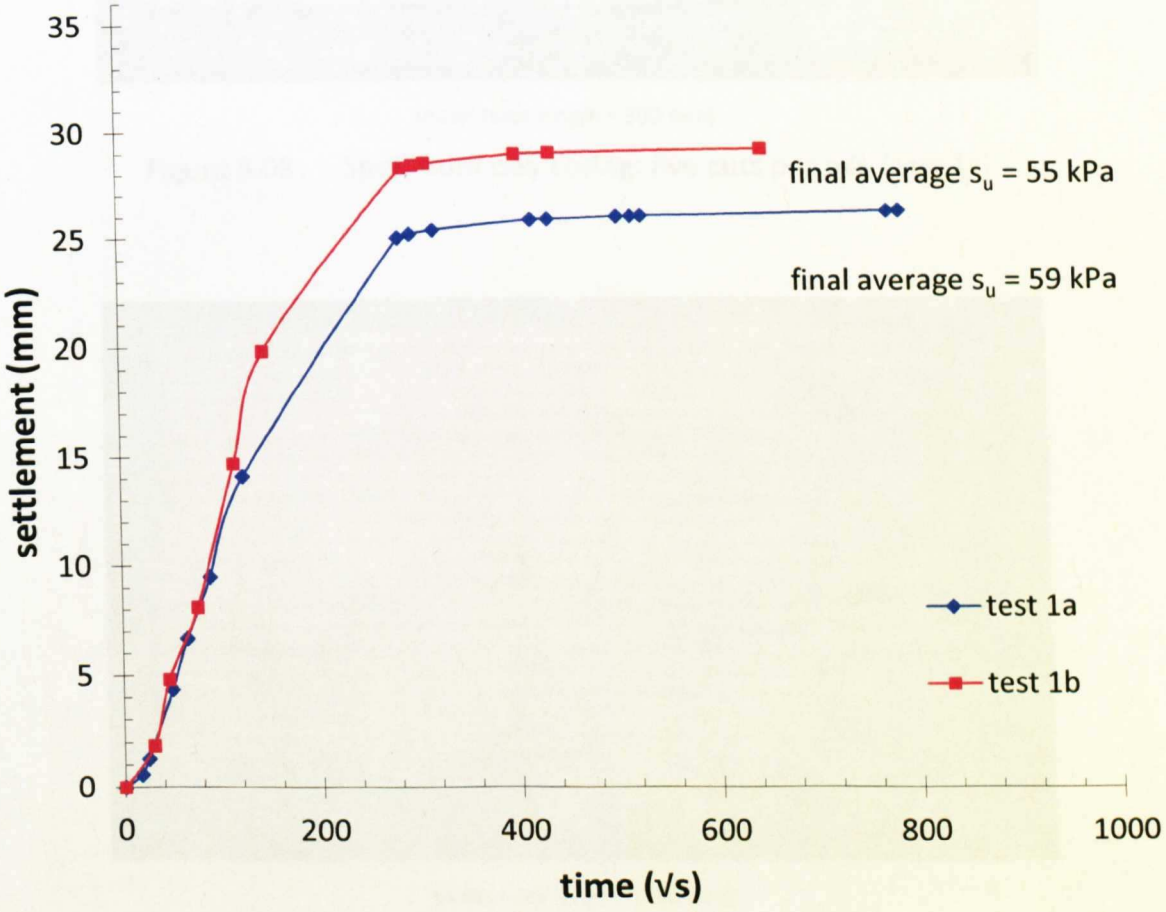

Figure 5.06 Consolidation to 500 kPa: settlement vs time

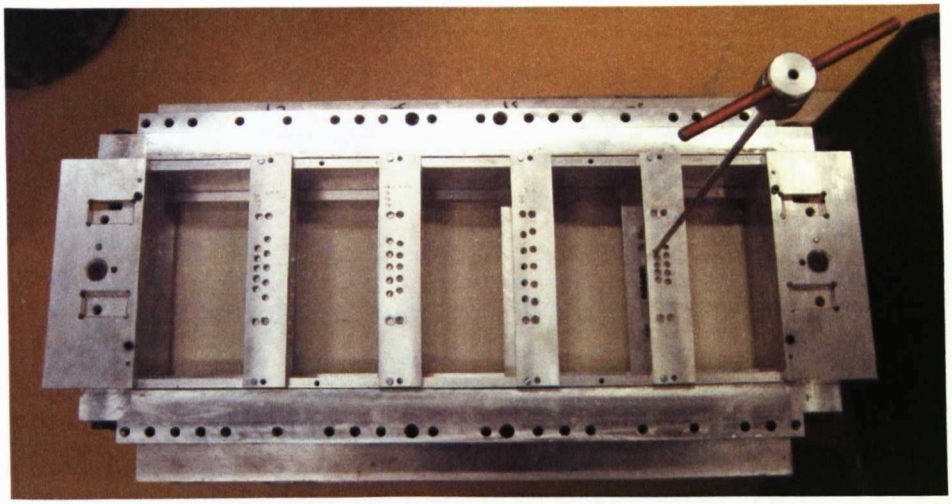

Figure 5.07 Coring the clay (test 1b)

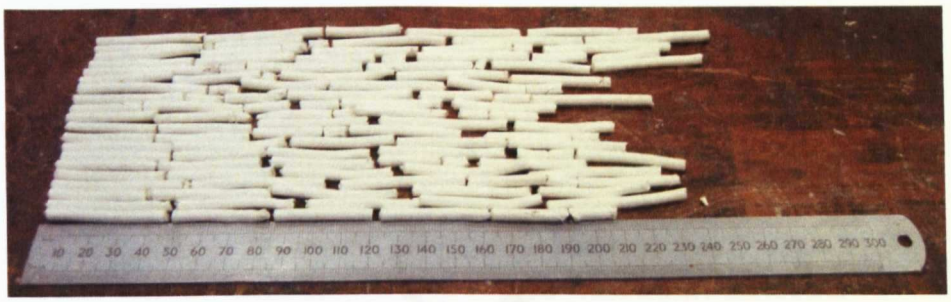

[note: ruler length = 300 mm]

Figure 5.08 Spoil from clay coring: five cuts per pile (test 1c)

[note: ruler length = 150 mm]

Figure 5.09 Spoil from clay coring: three cuts per pile (test 3b)

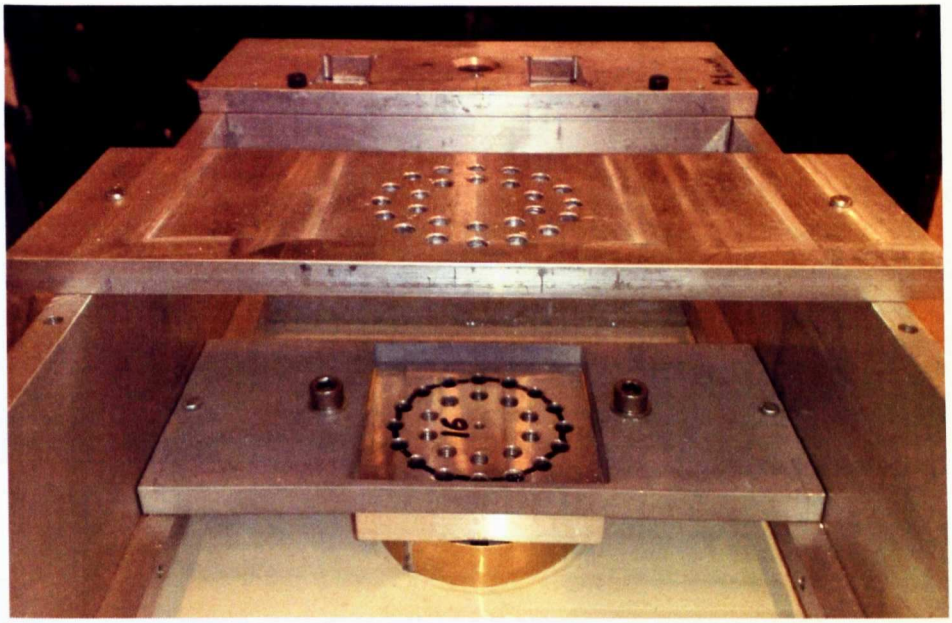

Figure 5.10 Pile installation set-up (test 3b)

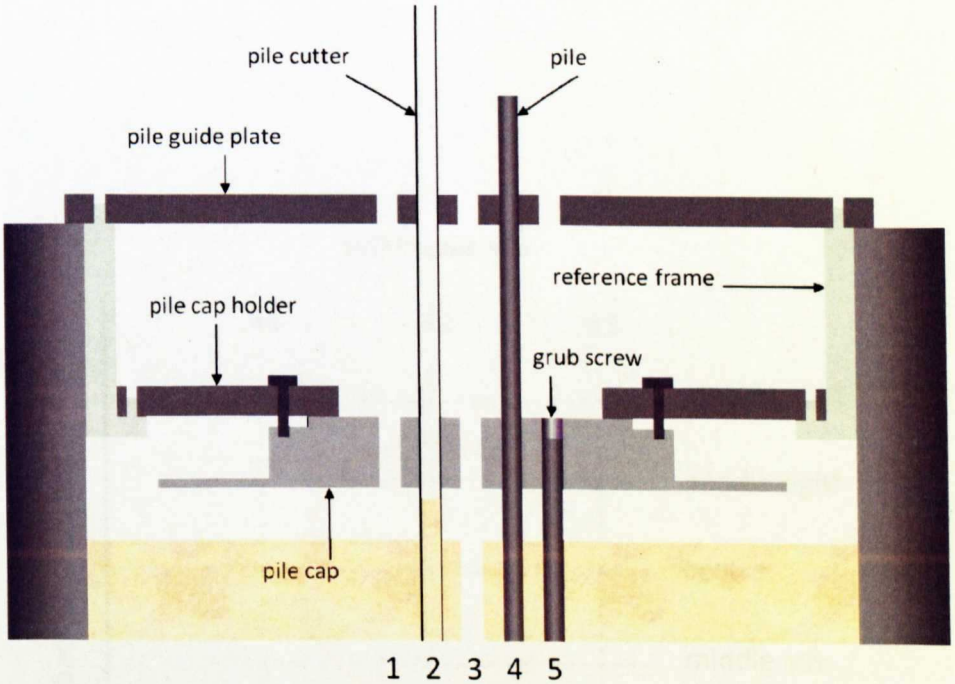

1. Apparatus in place pre pile installation
2. Cutting tube inserted, clay sheared and extracted [NB: this process is completed in stages, so initially the cutter is only pushed into the top section of clay]
3. Pile bore created
4. Pile inserted
5. Grub screw threaded into the top of the pile cap to provide reaction to the pile during loading

Figure 5.11 Pile installation process

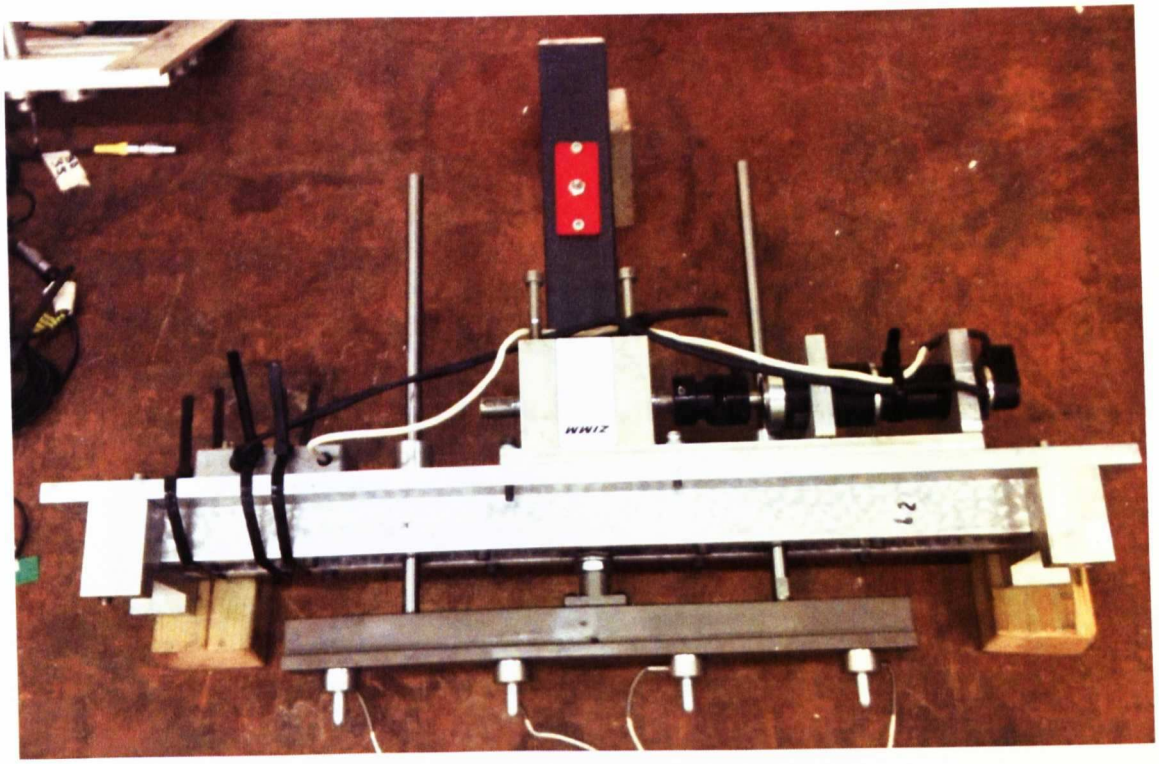

Figure 5.12 Photograph of loading apparatus

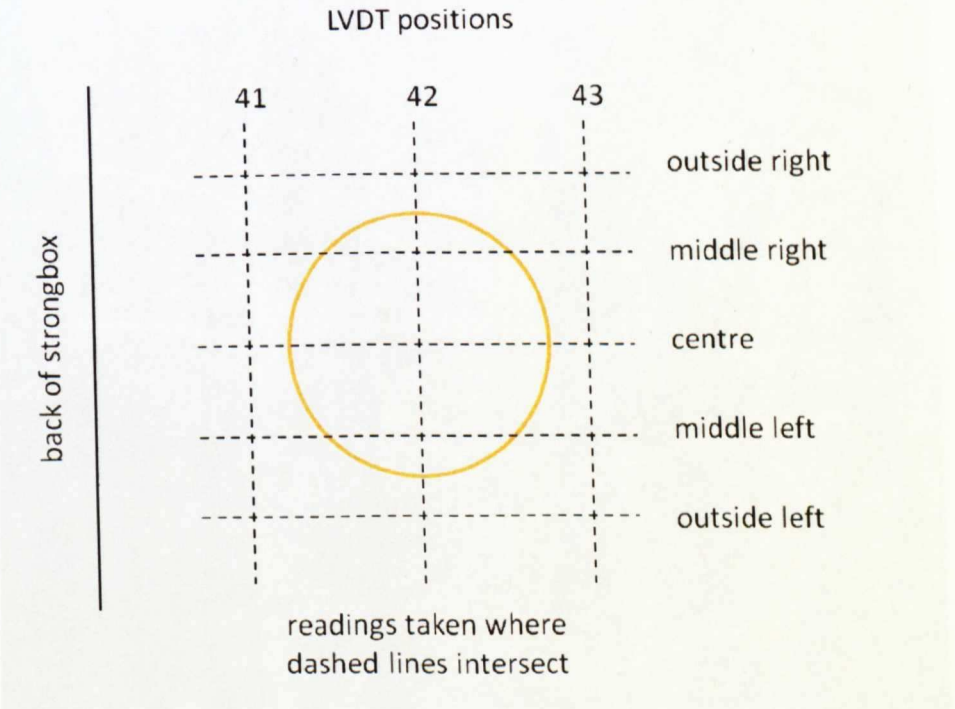

Figure 5.13 Central soil settlement data recording points

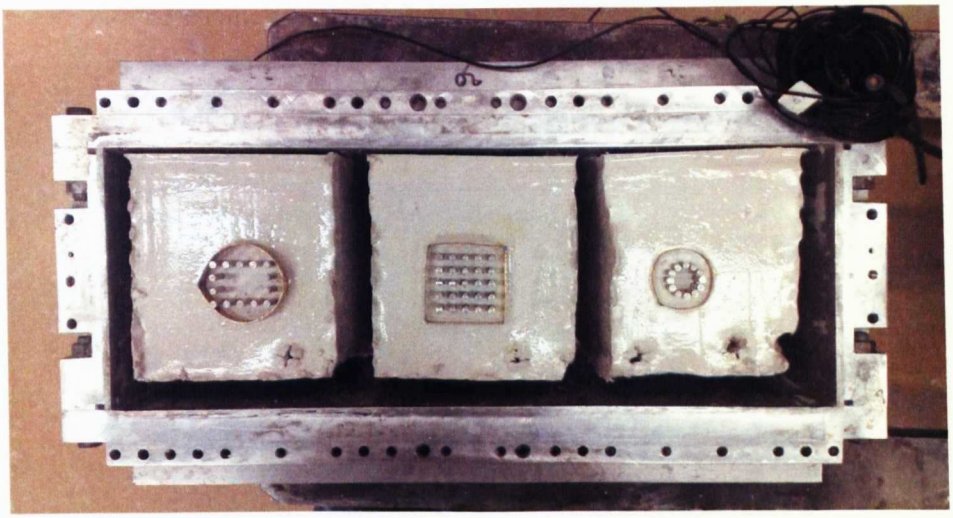

Figure 5.14 Model excavation [1] (test 4a)

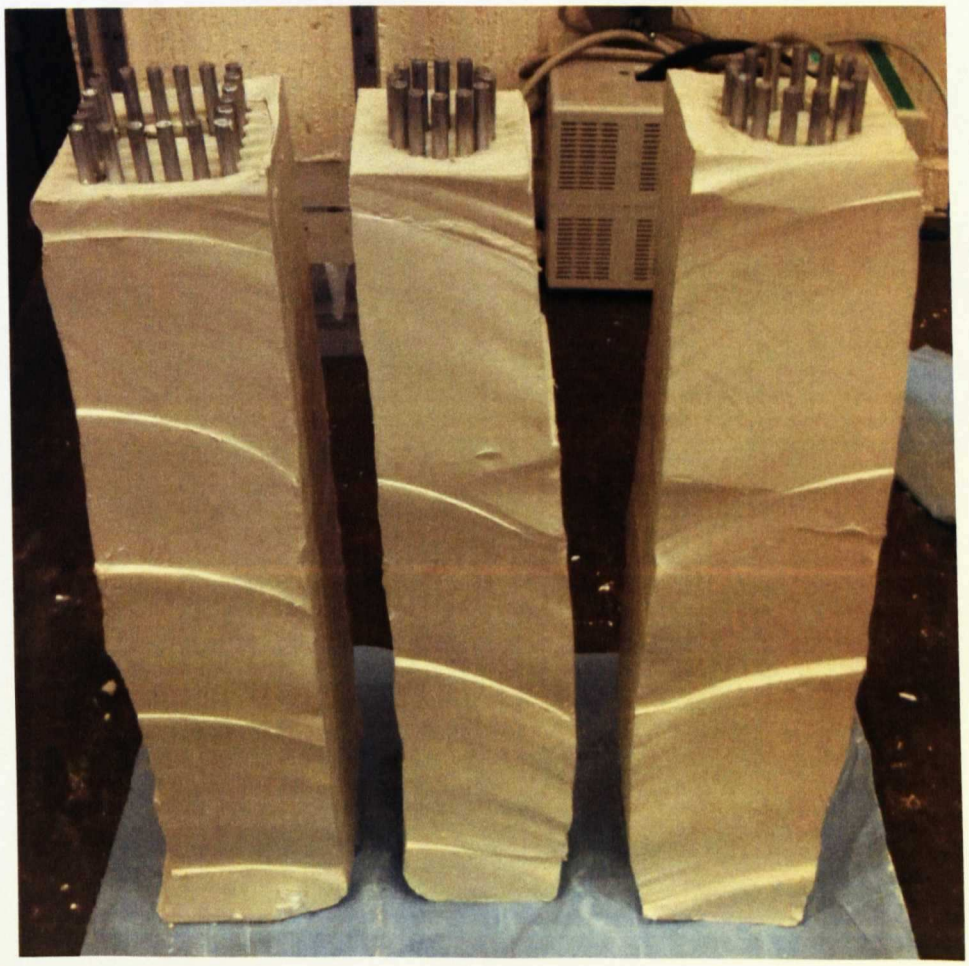

Figure 5.15 Model excavation [2] (test 5d)

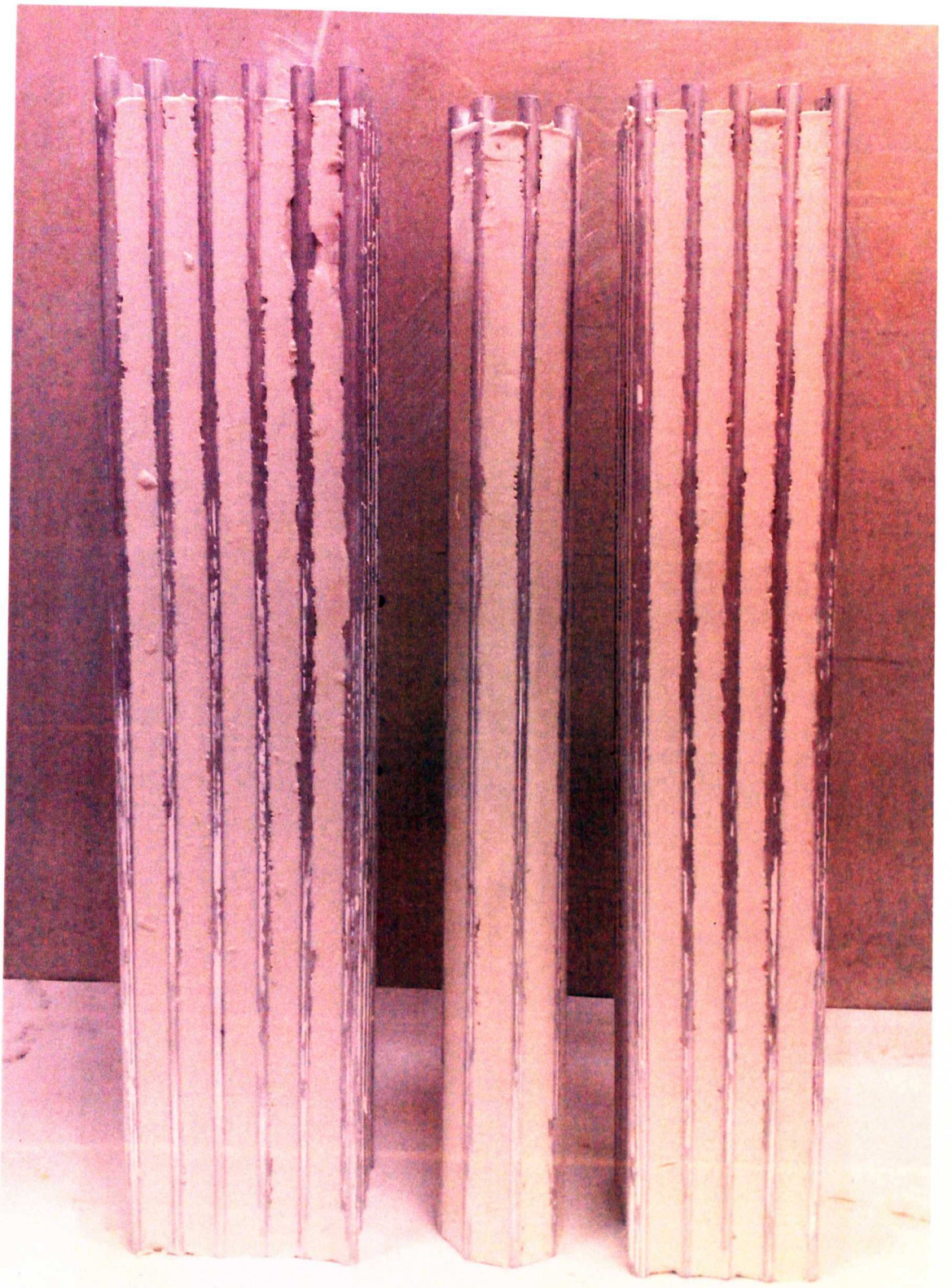

Figure 5.16 Pile verticality (test 2d)

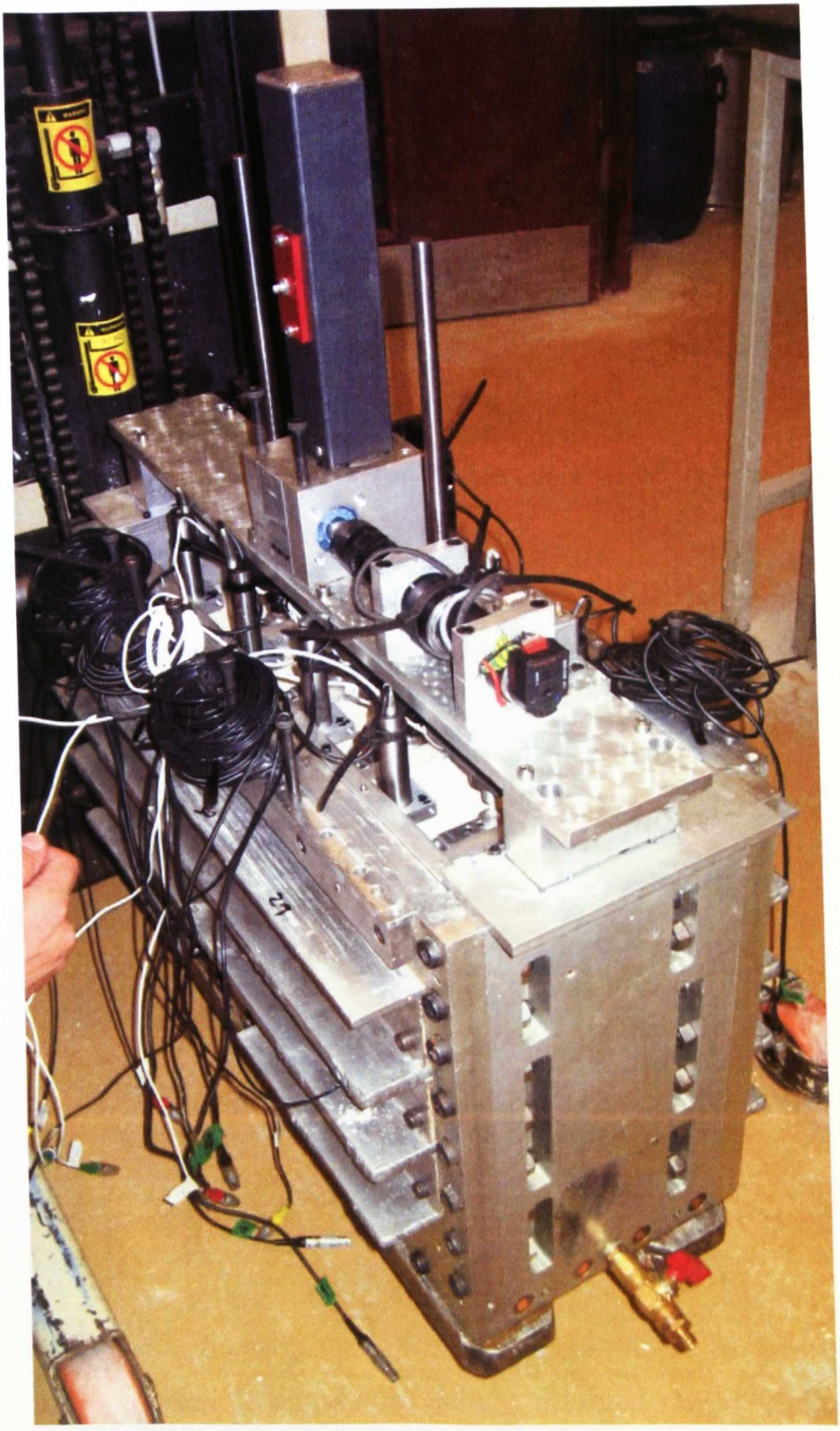

Figure 5.17 Completed model prior to testing (test 1c)

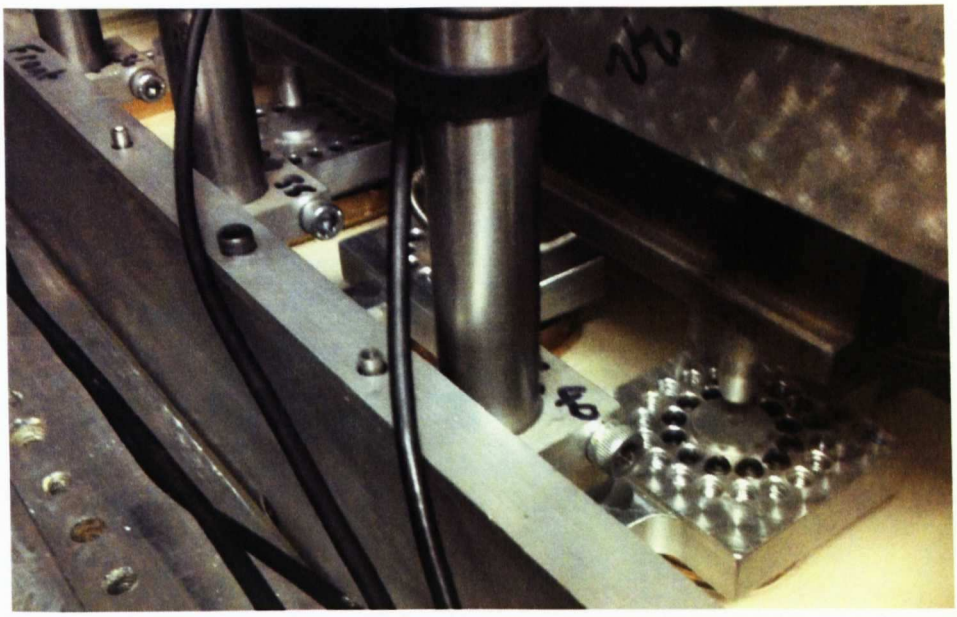

Figure 5.18 Loading beam and load cell in place above loading point and pile cap (test 5d)

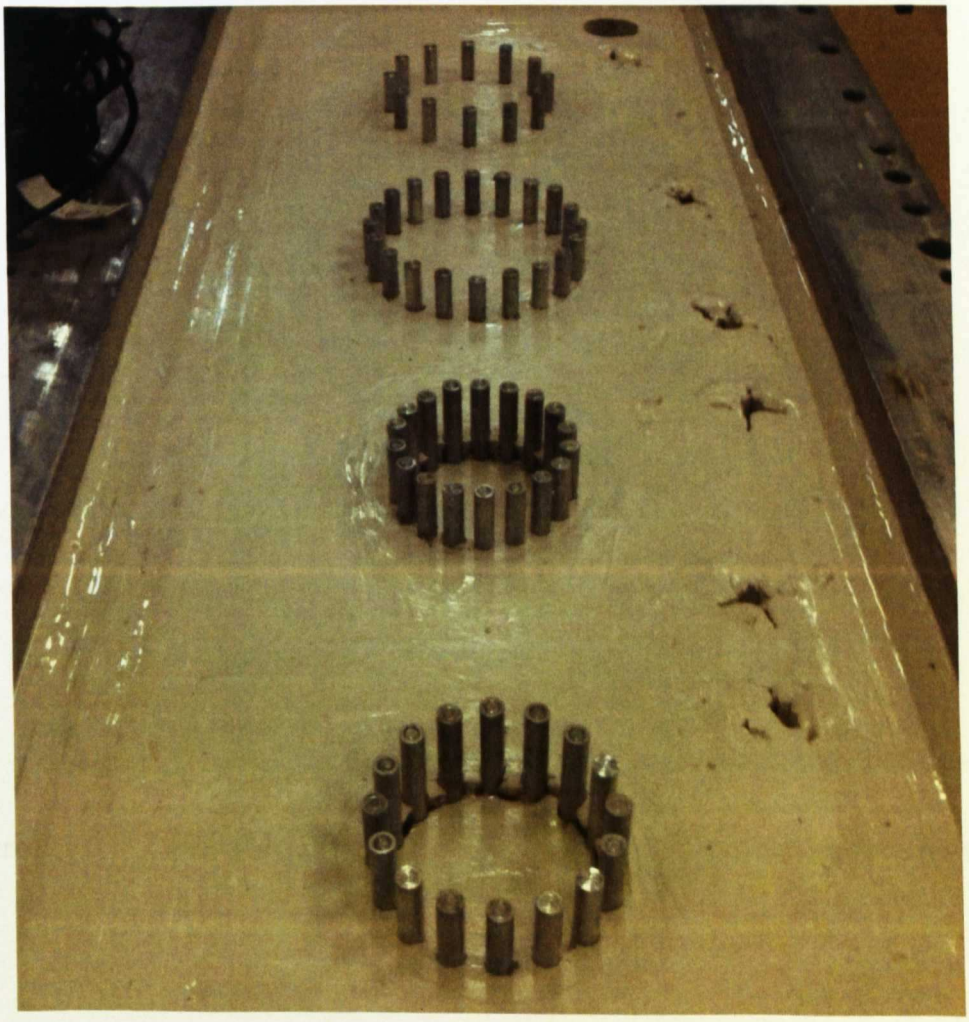

Figure 5.19 Pile groups in strongbox post test (test 5e)

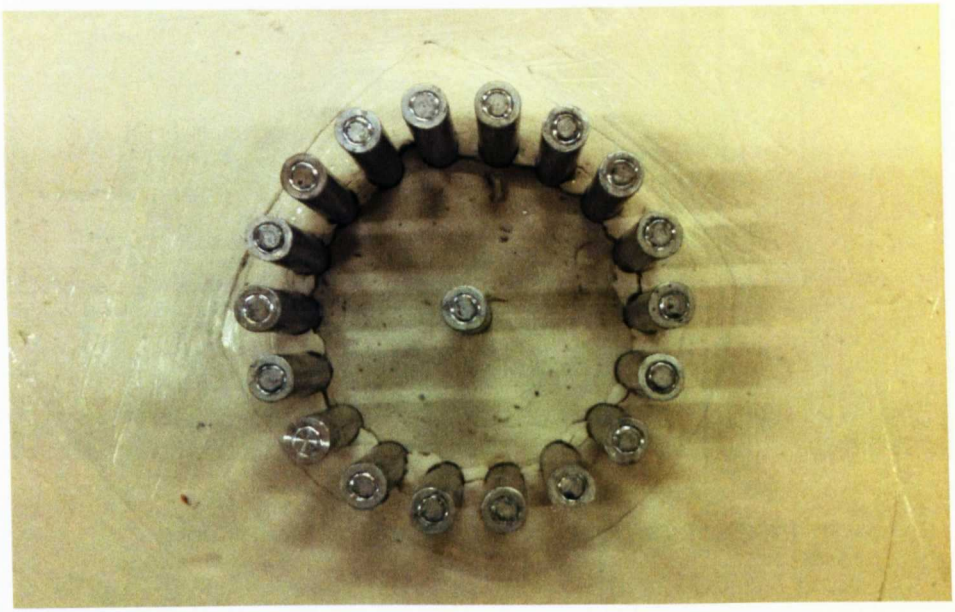

Figure 5.20 Plan view of TC18_1.50 showing shear surface (test 5c)

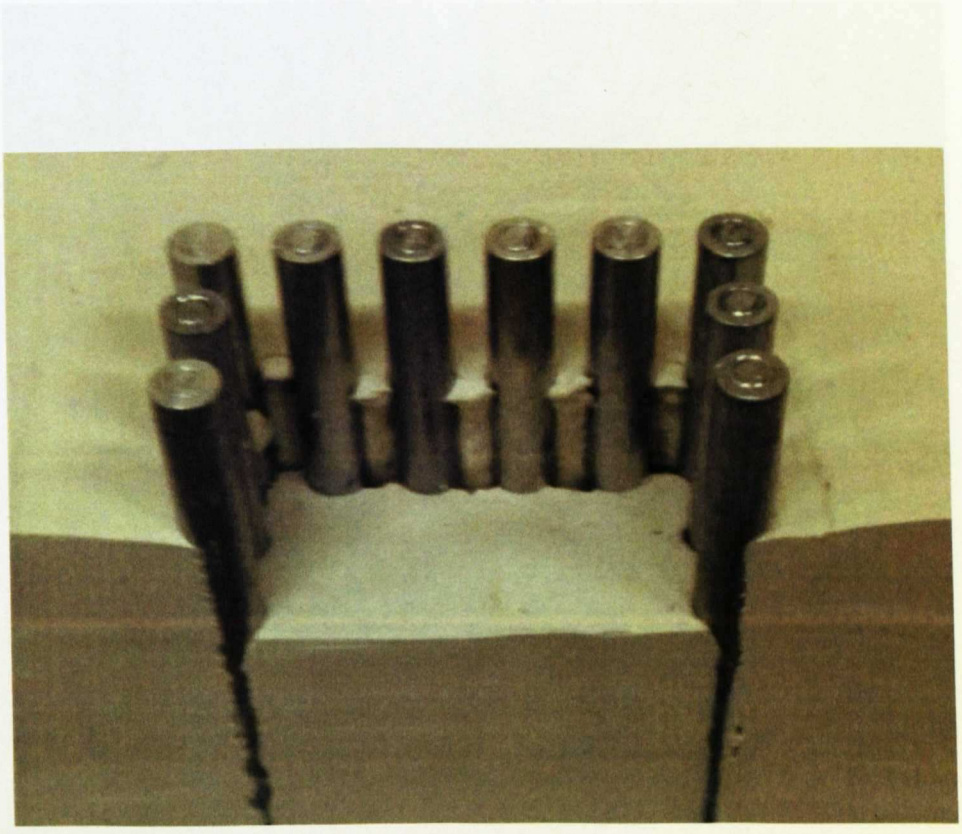

Figure 5.21 Cross sectional view of PS20_1.50 showing shear surface (test 5c)

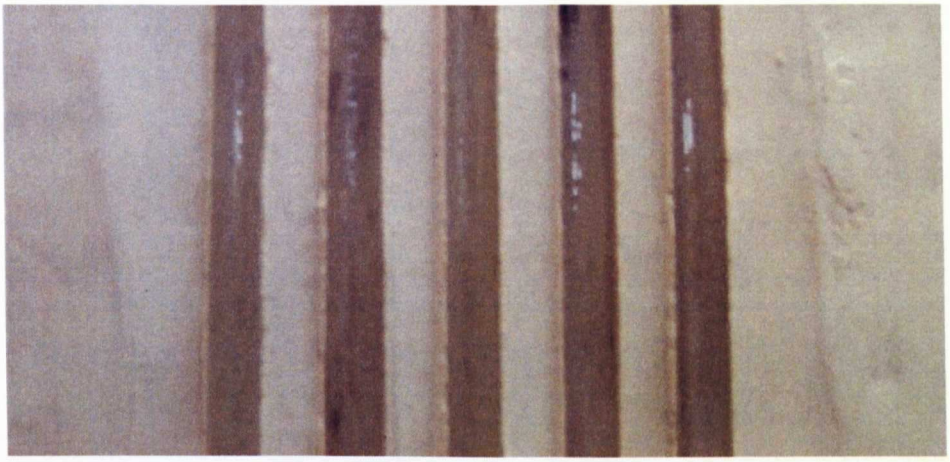

Figure 5.22 Silicone oil on clay bore (test 1c)

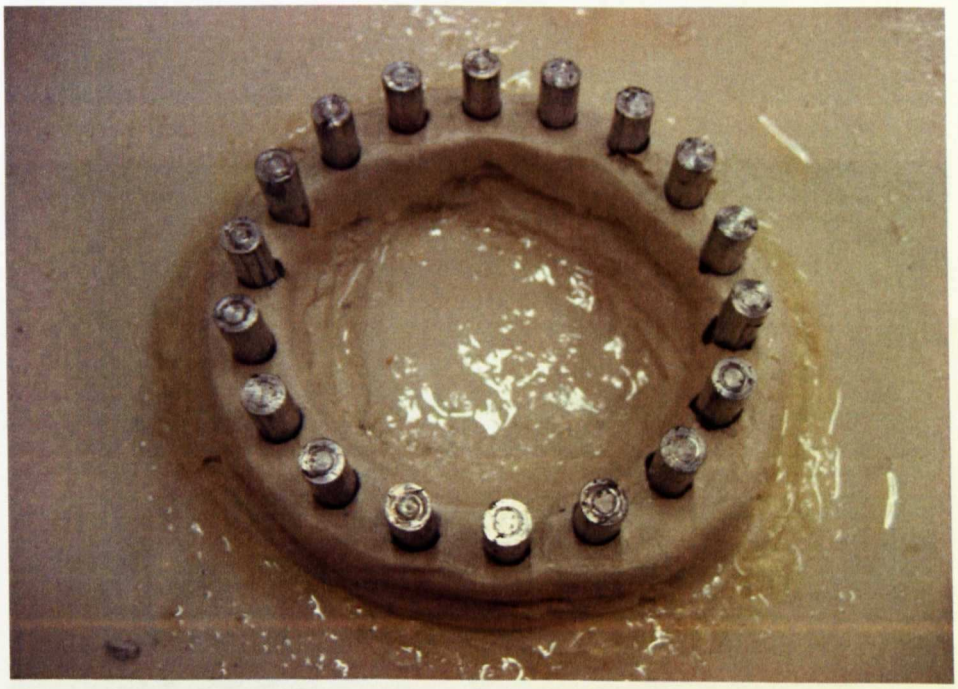

Figure 5.23 Oil prevention techniques: clay bund (test 2b)

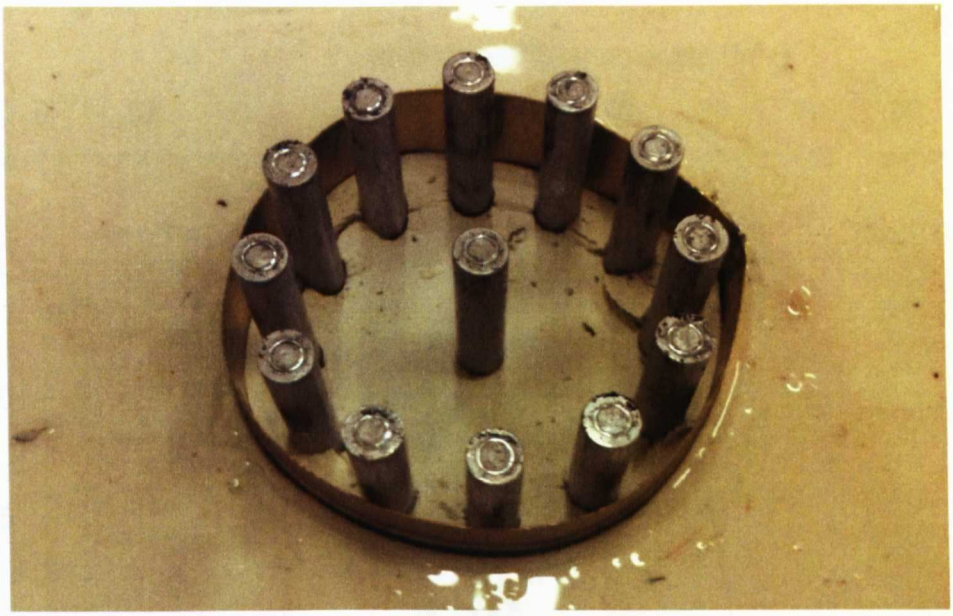

Figure 5.24 Oil prevention techniques: brass ring (test 4e)

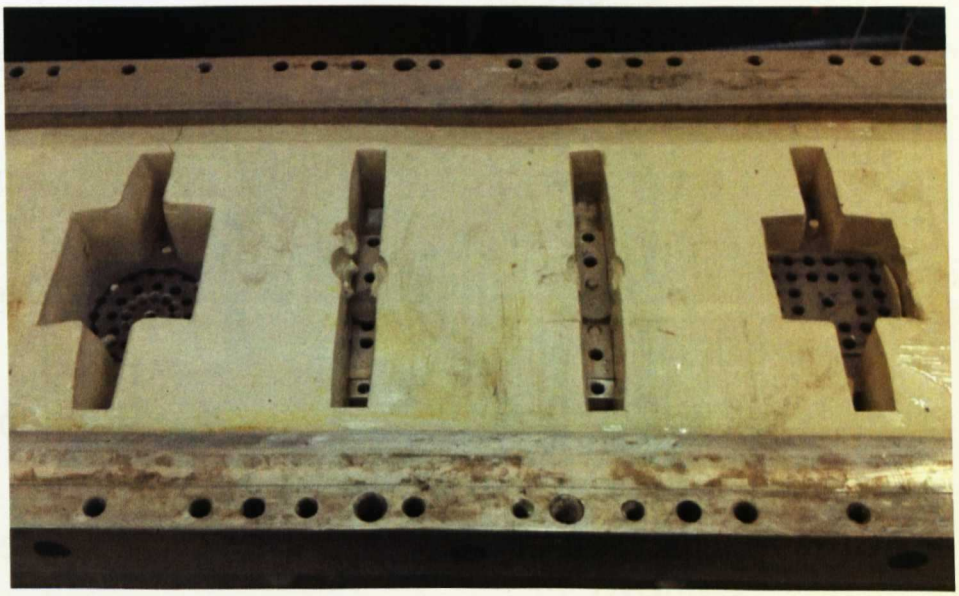

Figure 5.25 Actuator malfunction: pile caps forced into clay (test 4d)

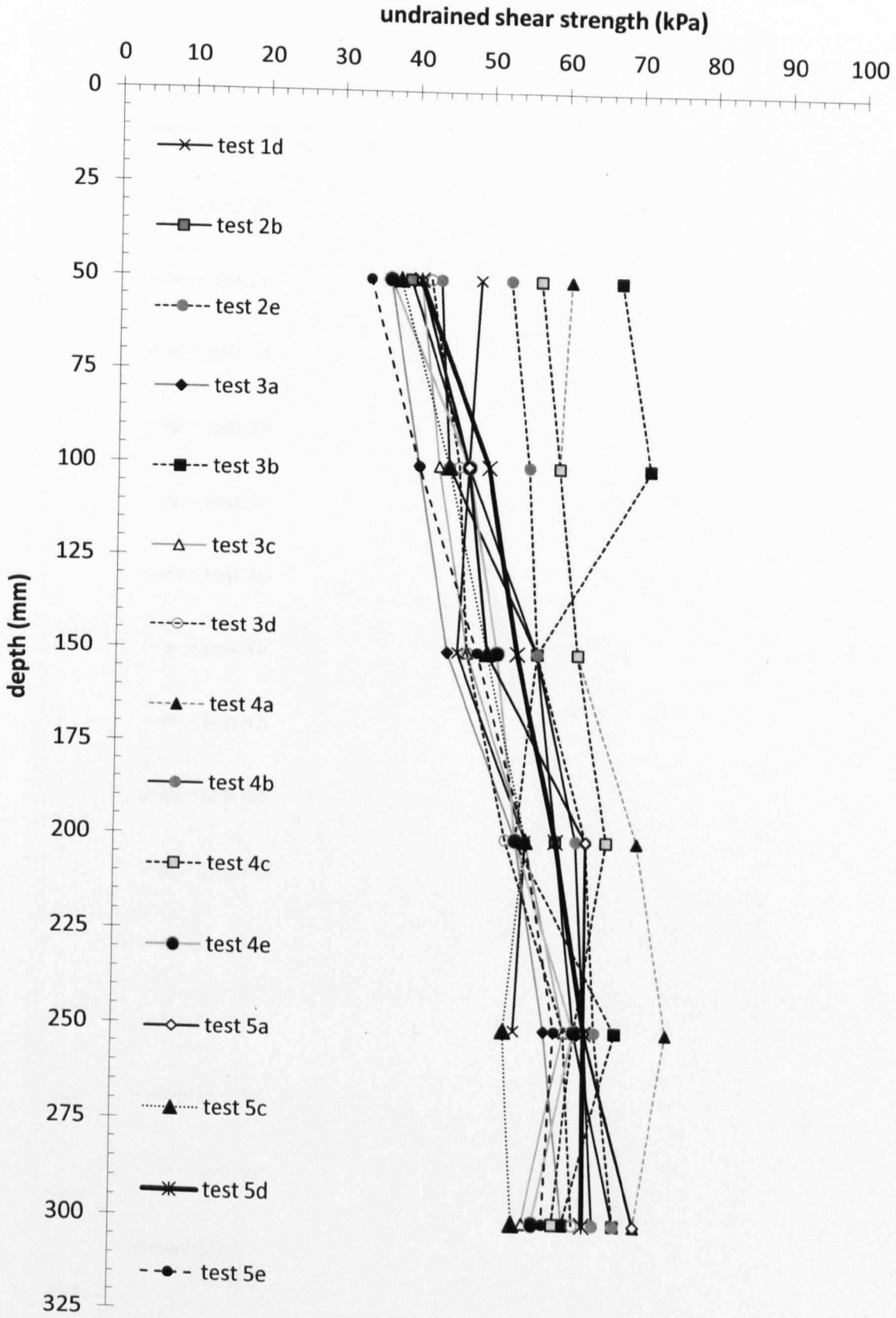

Figure 6.01 Undrained shear strength profile from hand vane tests

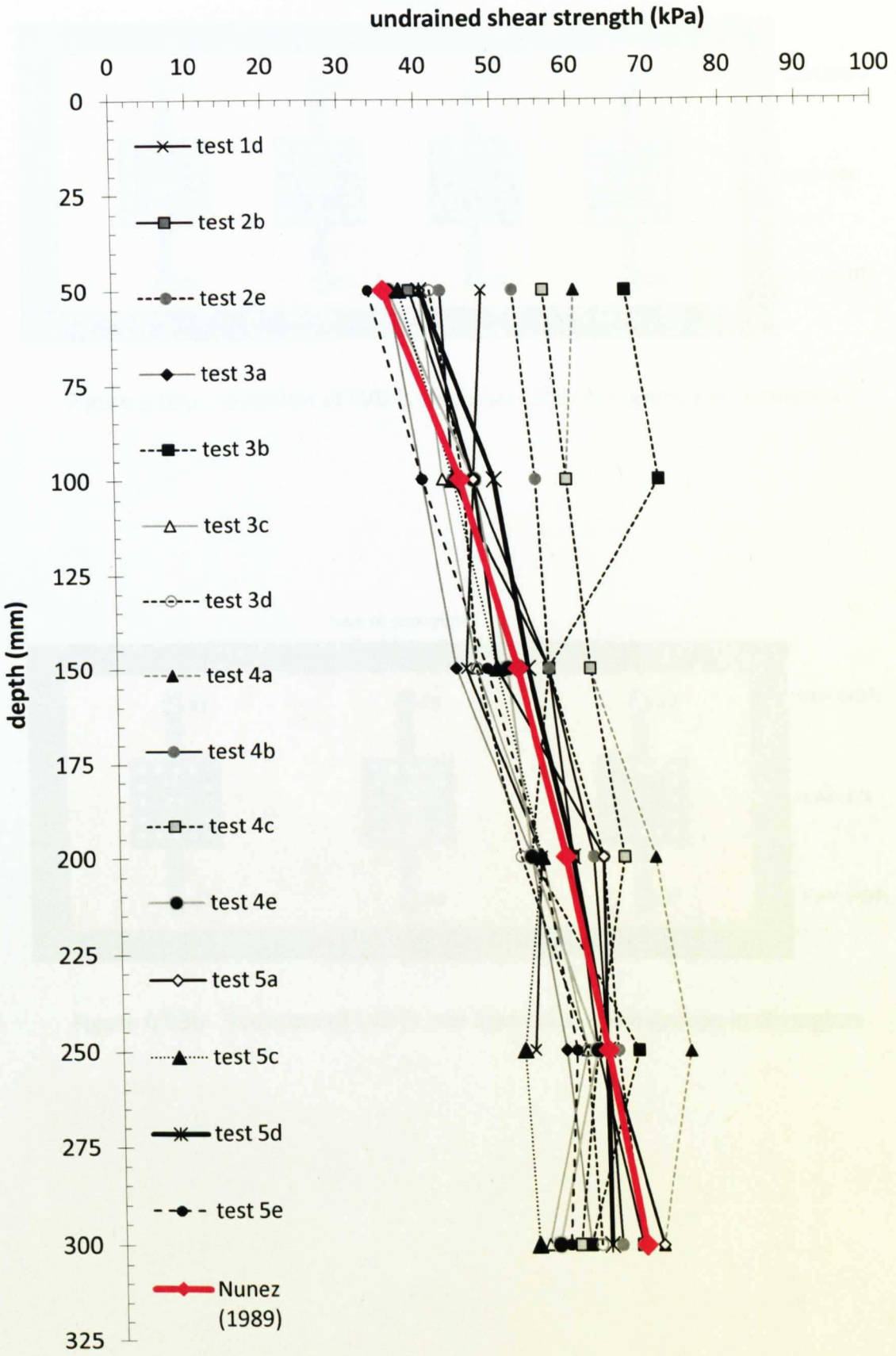

Figure 6.02 Correlation between s_u and the relationship established by Nuñez (1989)

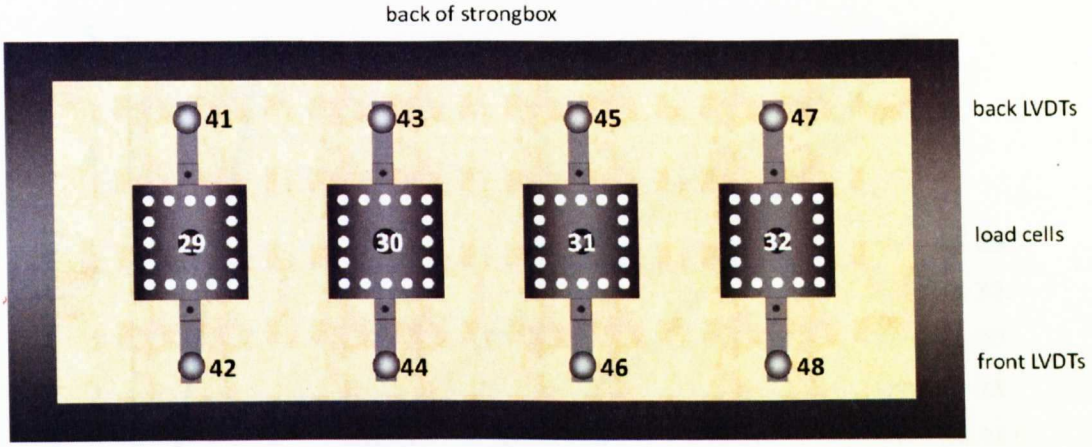

Figure 6.03a Location of LVDTs and load cells: four groups in strongbox

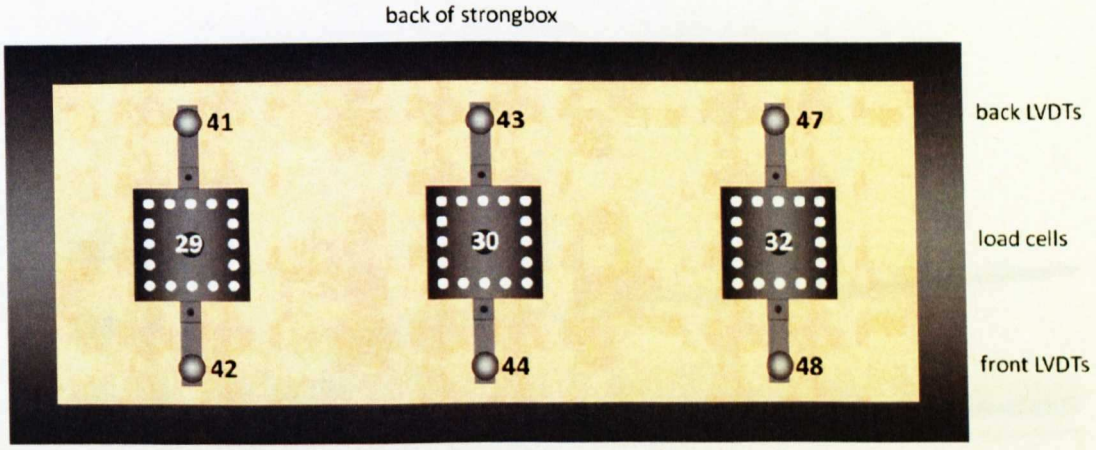

Figure 6.03b Location of LVDTs and load cells: three groups in strongbox

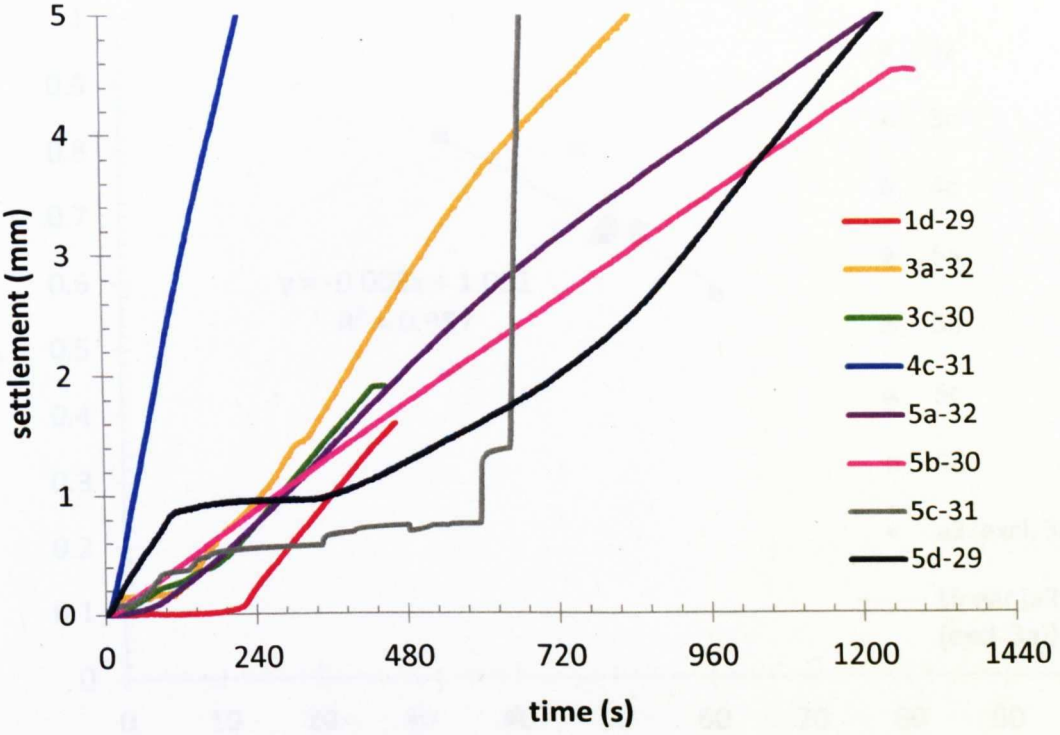

Figure 6.04 Settlement vs time: single piles

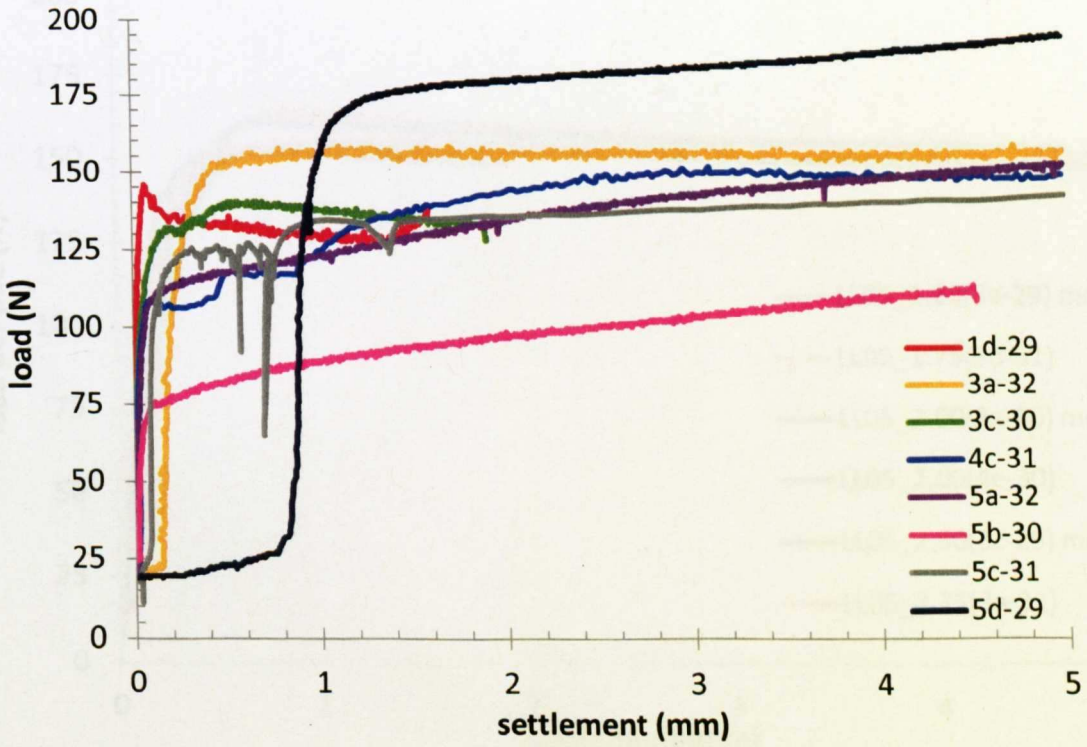

Figure 6.05 Load vs settlement: single piles

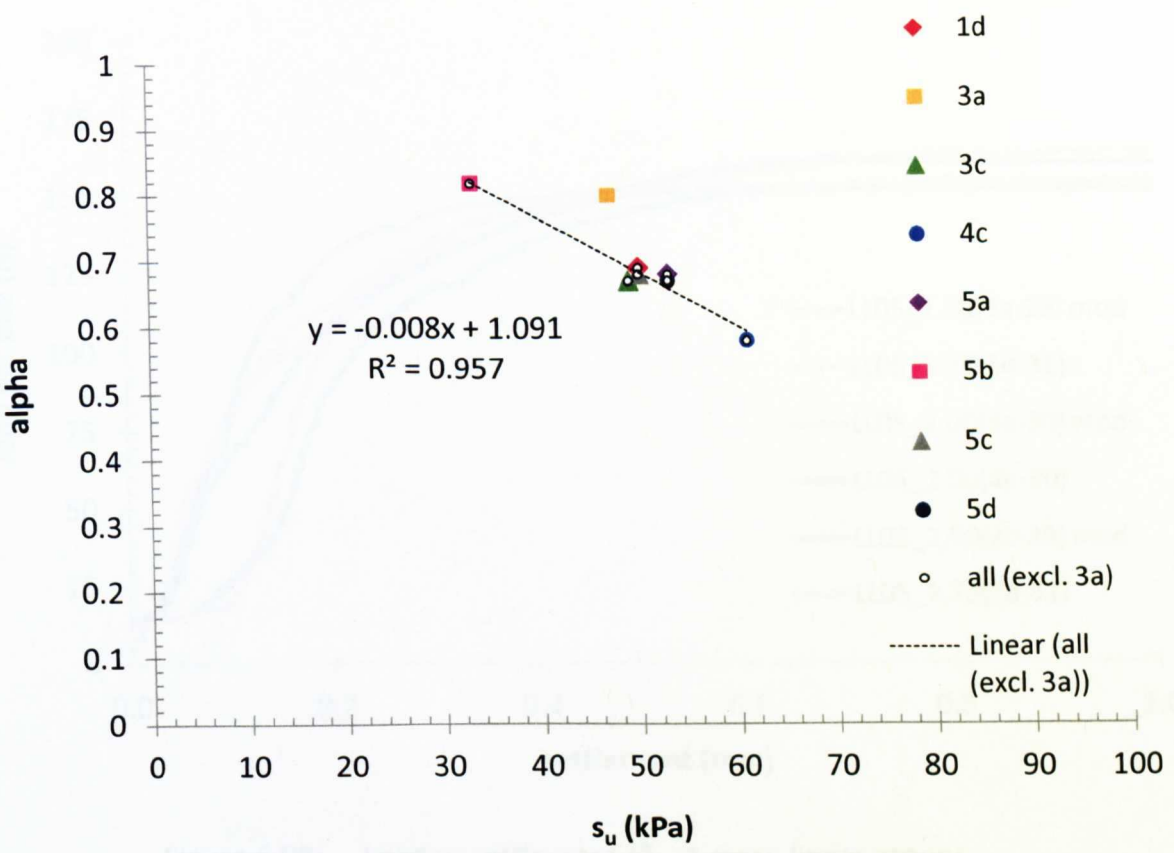

Figure 6.06 α vs s_u: from hand vane tests and back calculations

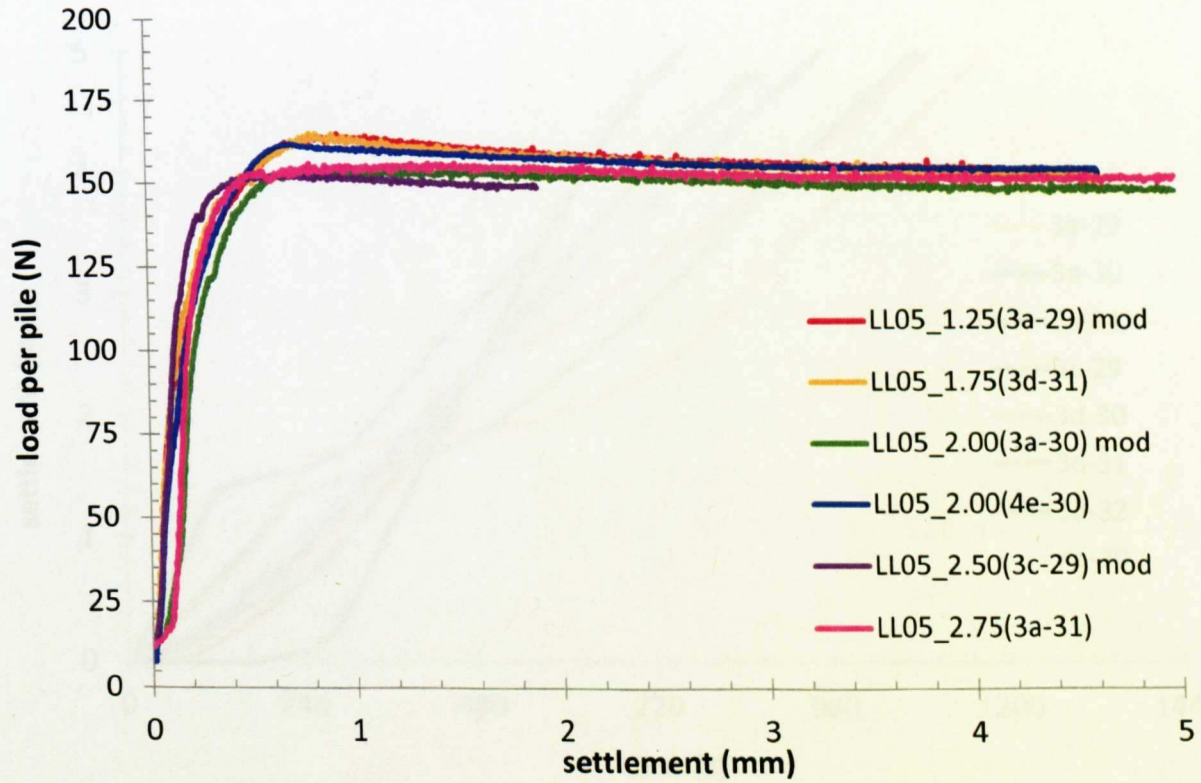

Figure 6.07 Load vs settlement (0 – 5 mm): linear groups

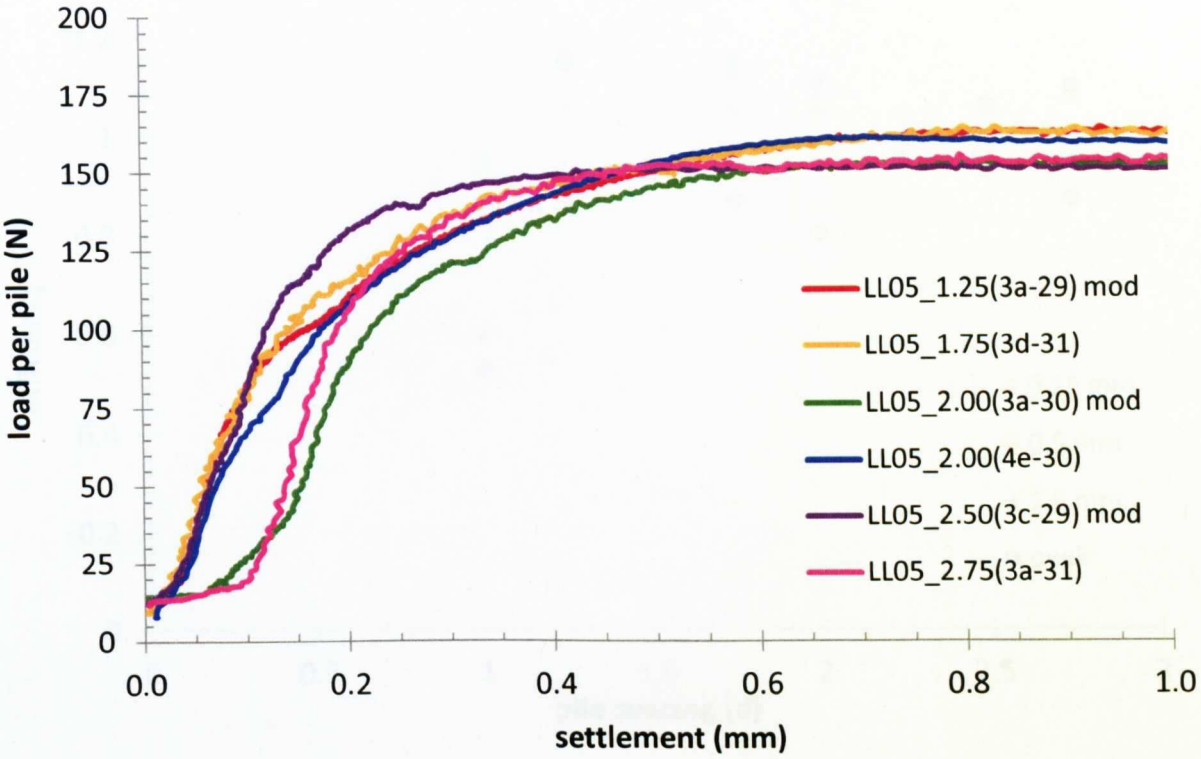

Figure 6.08 Load vs settlement (0 – 1 mm): linear groups

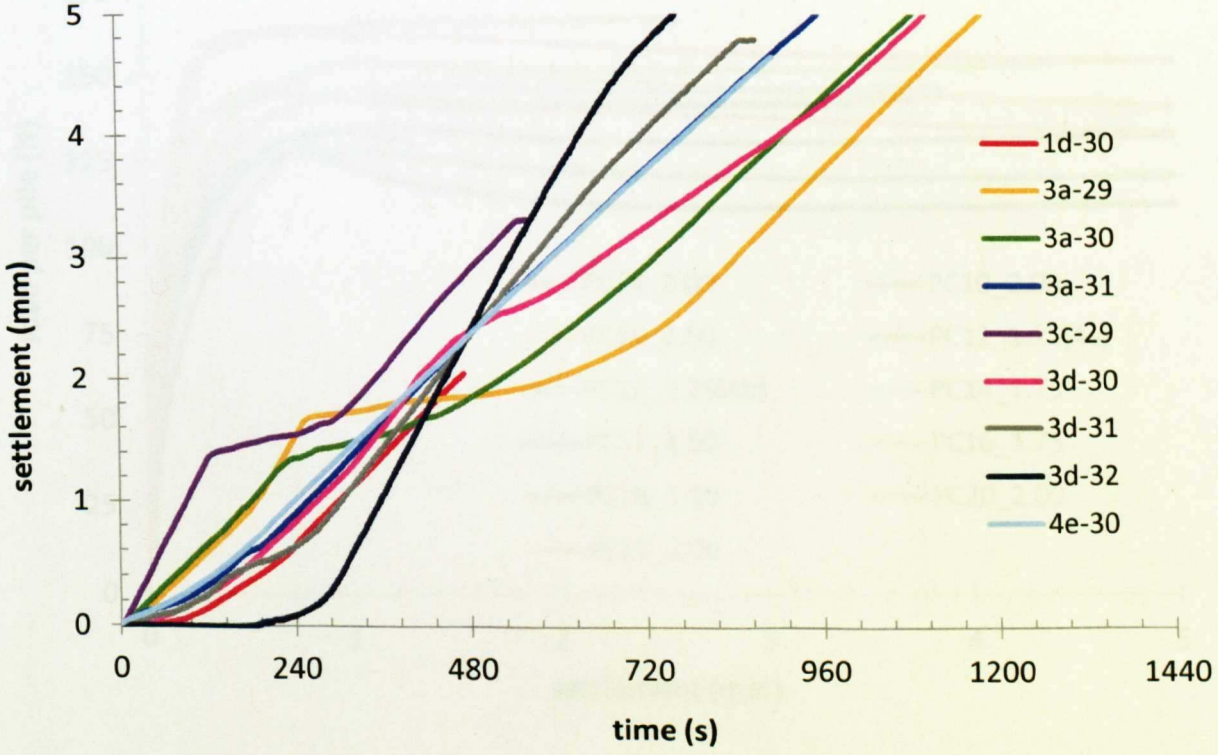

Figure 6.09 Settlement vs time: linear groups

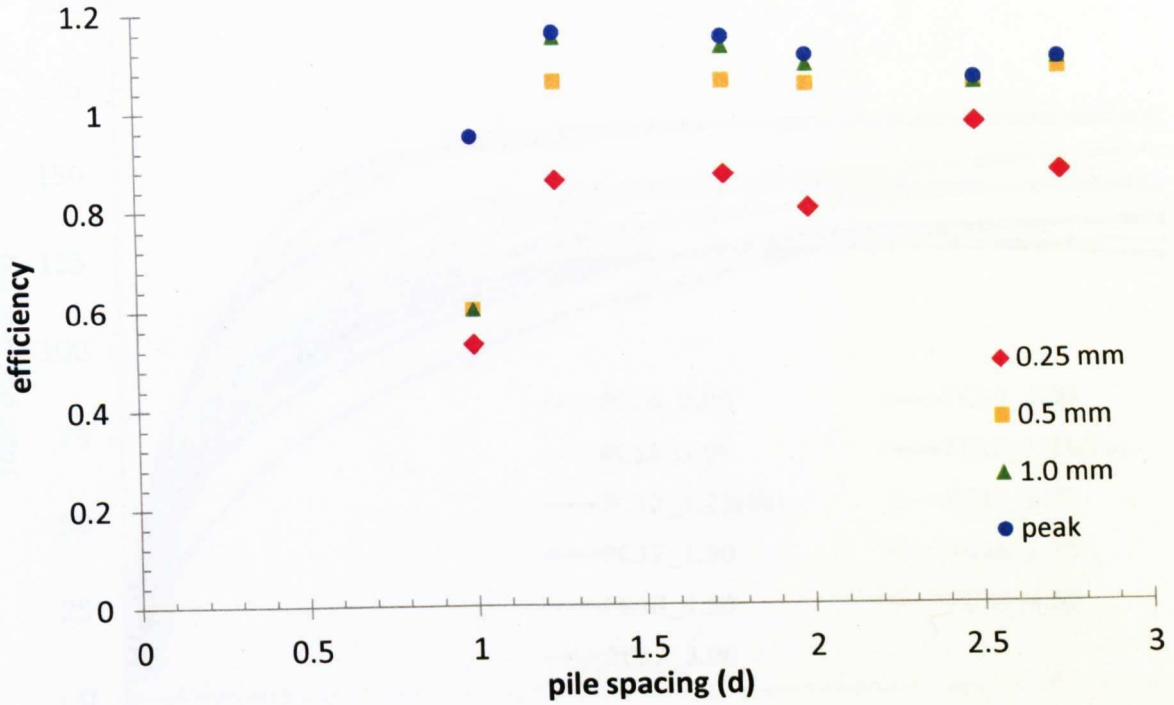

Figure 6.10 Efficiency vs pile spacing: linear groups

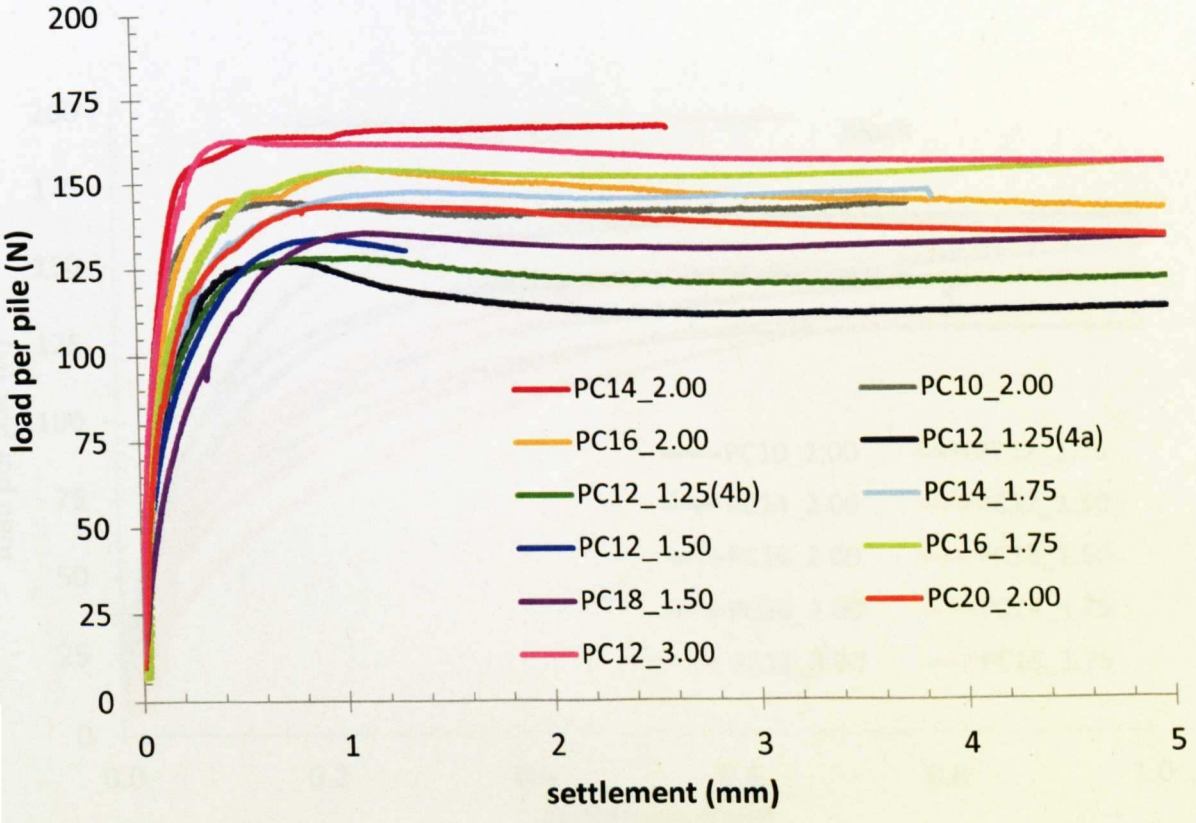

Figure 6.11 Load vs settlement (0 – 5 mm): perimeter groups (circular)

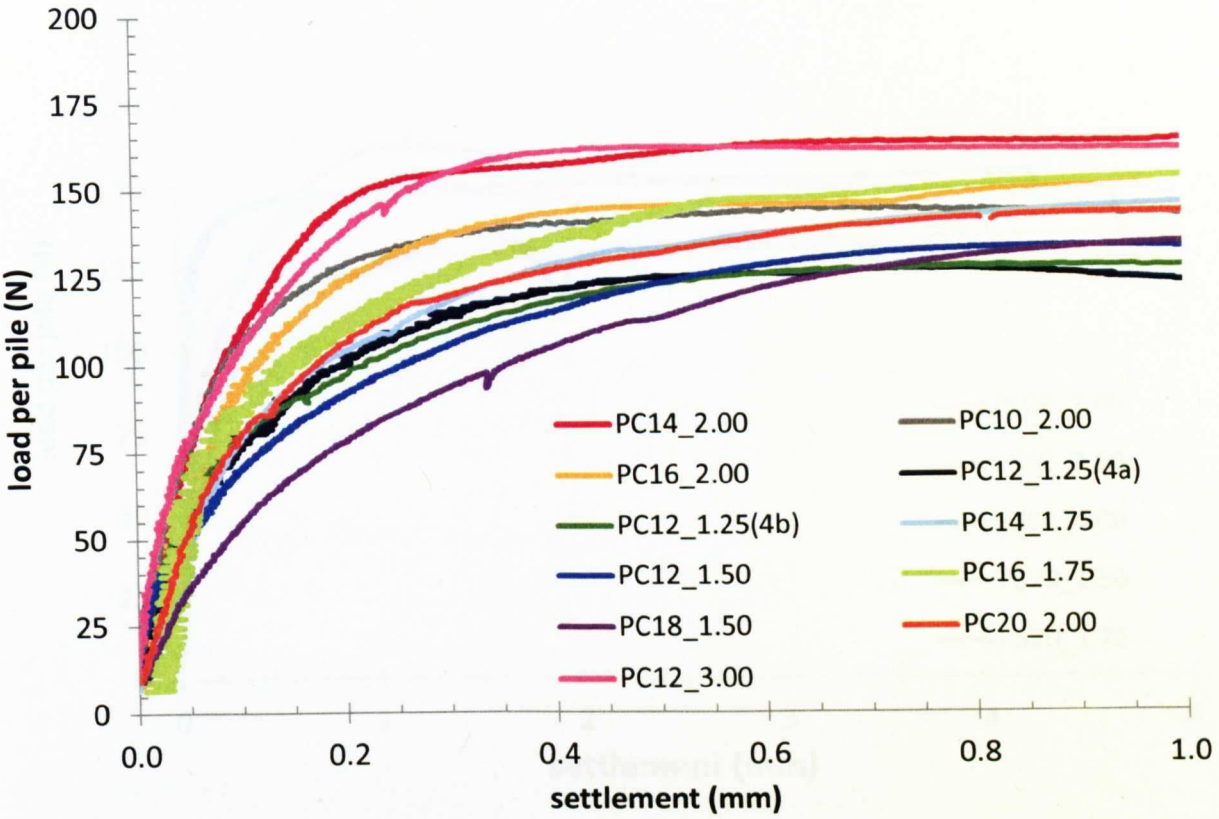

Figure 6.12 Load vs settlement (0 – 1 mm): perimeter groups (circular)

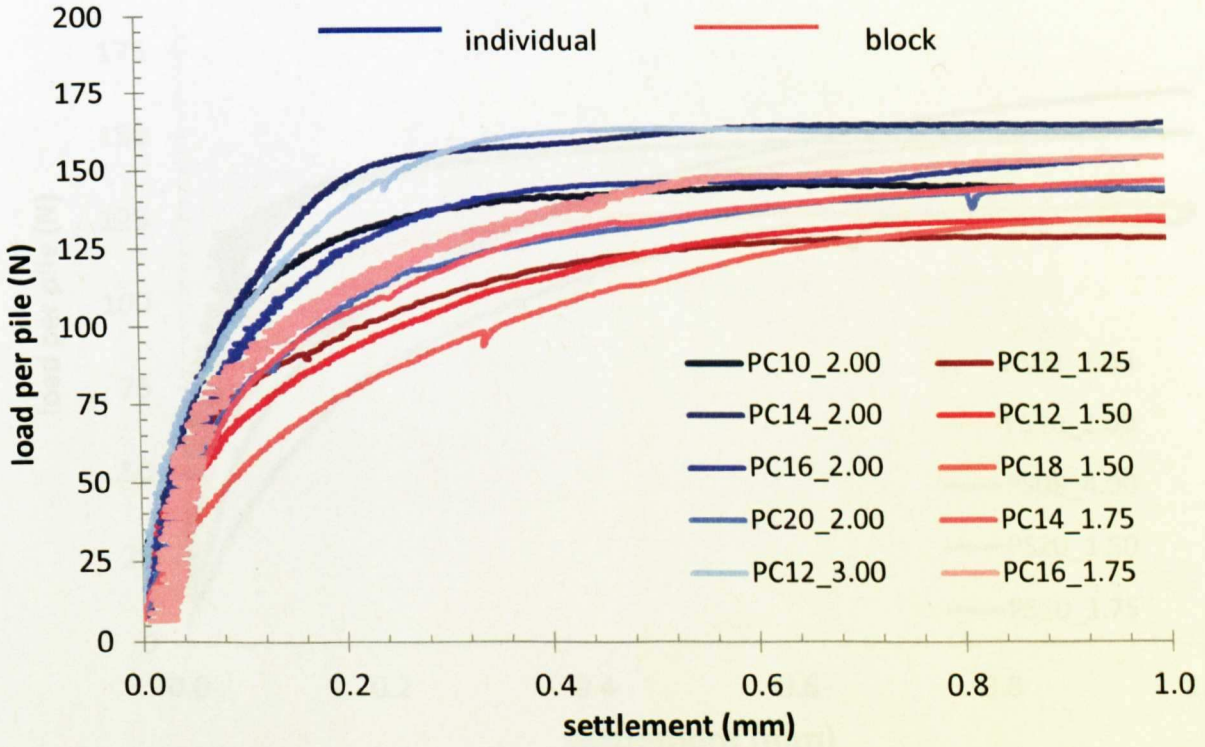

Figure 6.13 Load vs settlement: individual/block comparison - perimeter groups (circular)

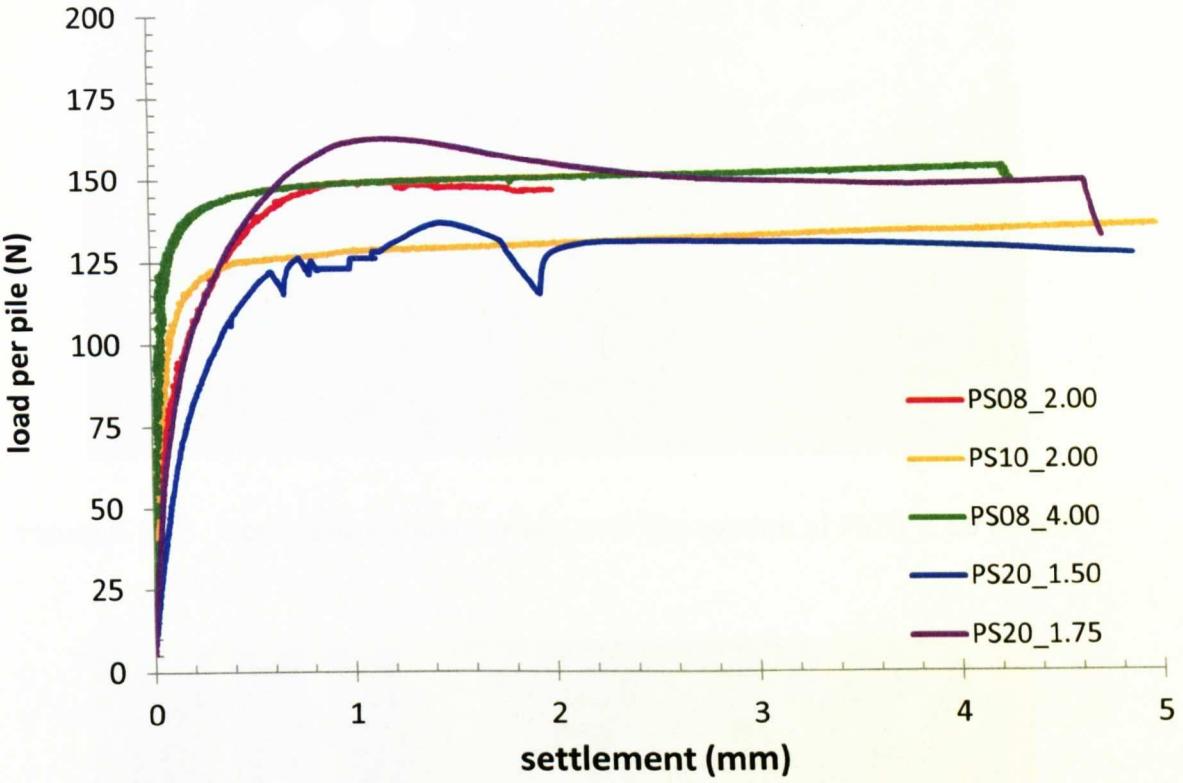

Figure 6.14 Load vs settlement (0 – 5 mm): perimeter groups (square)

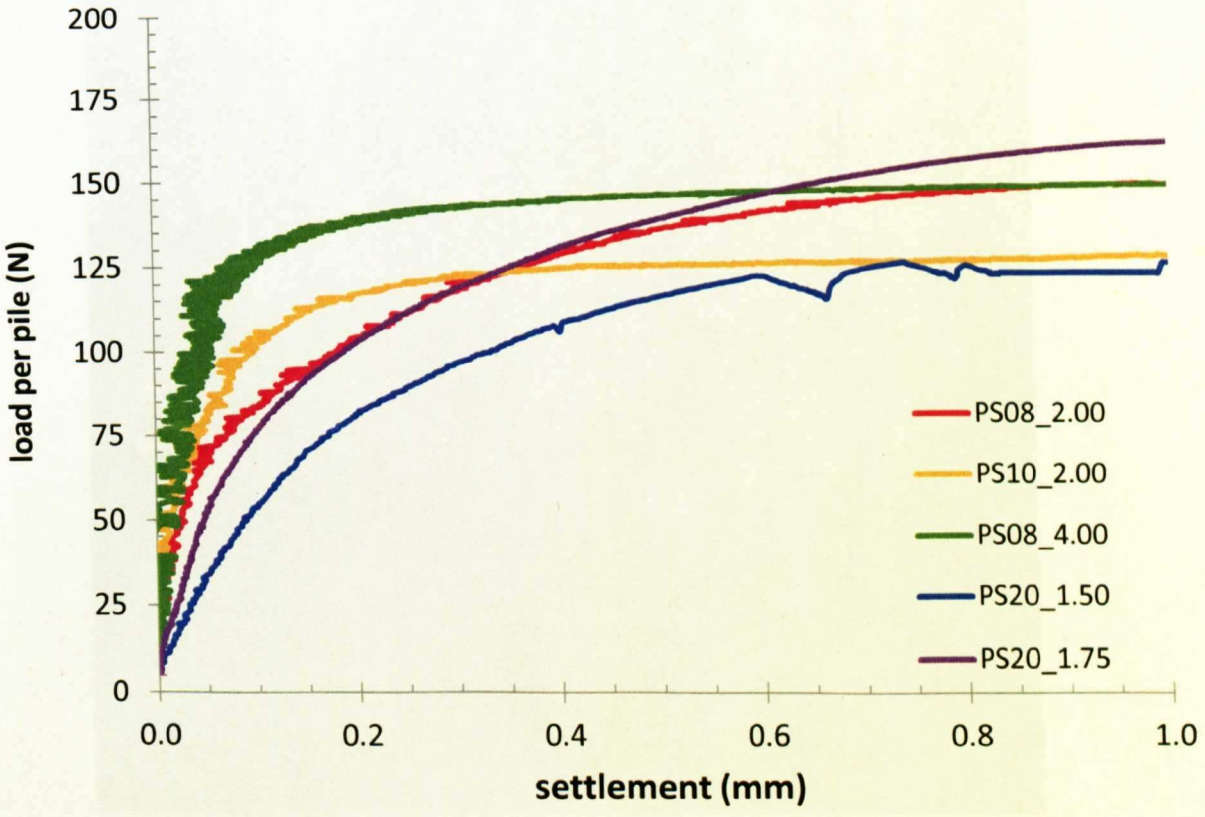

Figure 6.15 Load vs settlement (0 – 1 mm): perimeter groups (square)

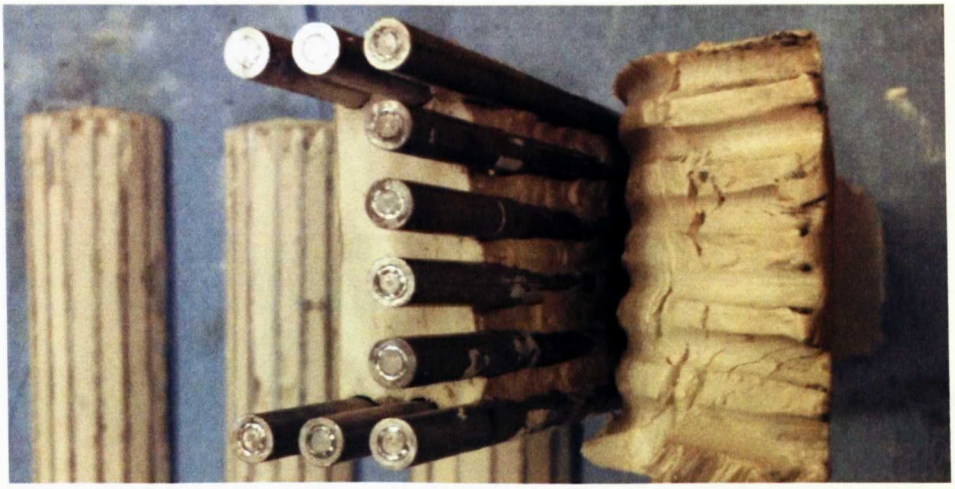

Figure 6.16 Block failure shear surface over top section of PS20_1.50 (test 5c)

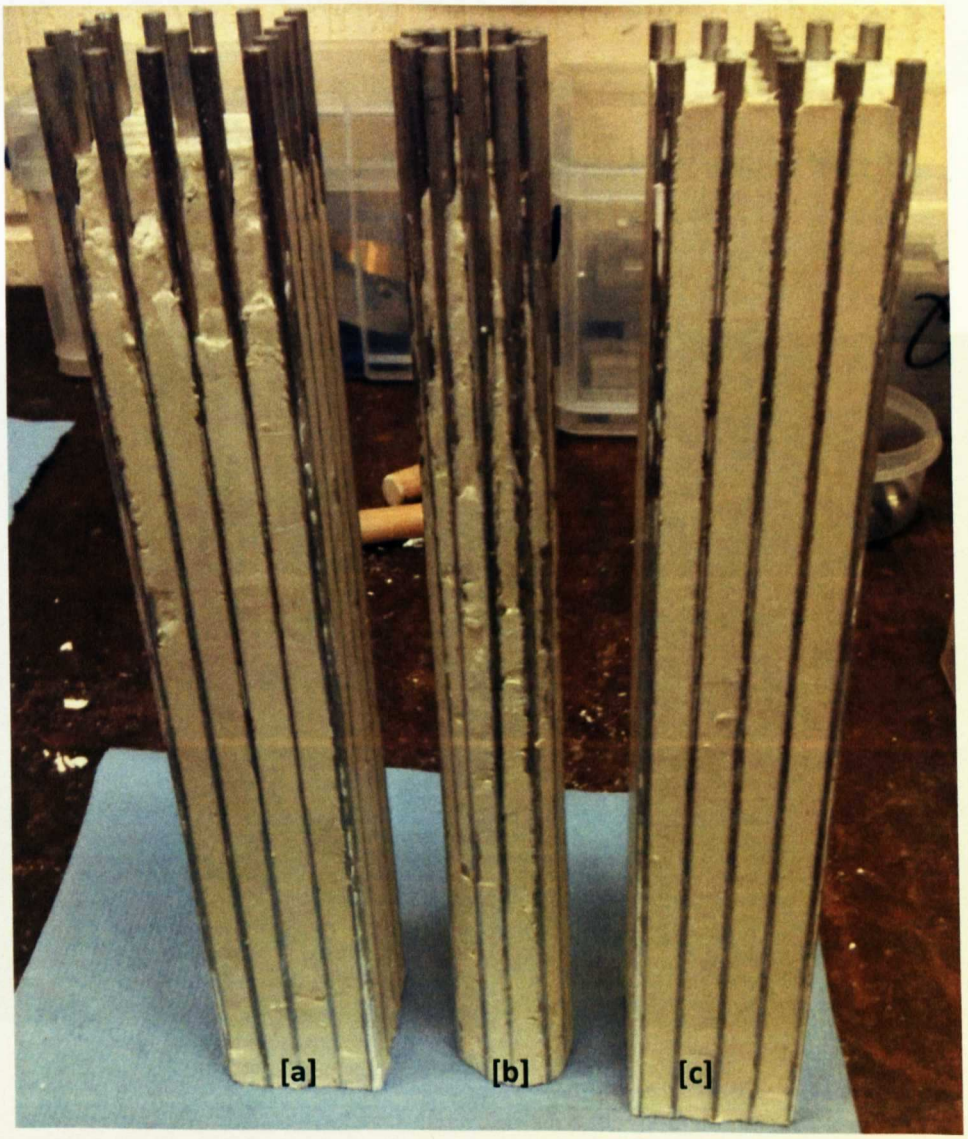

Figure 6.17 Excavated pile groups showing varying degrees of block failure: [a] shallow, [b] deep, [c] none (test 4b)

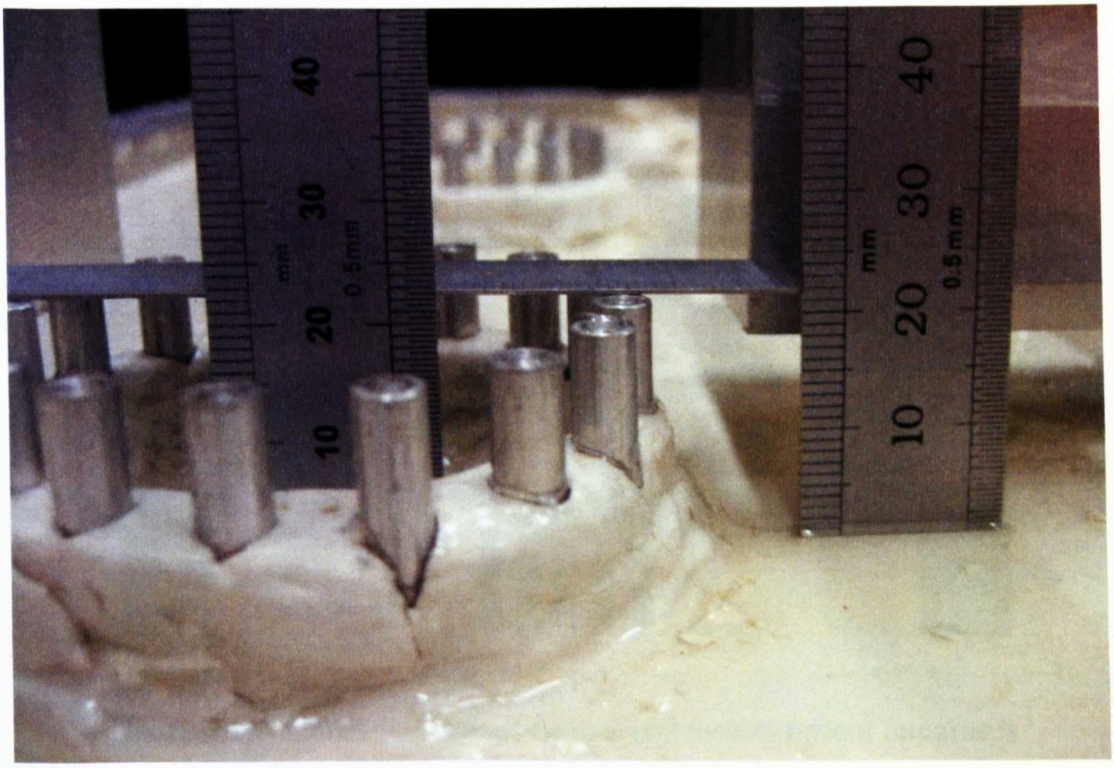

Figure 6.18a Early measurement of 'block effect' failure (test 2b)

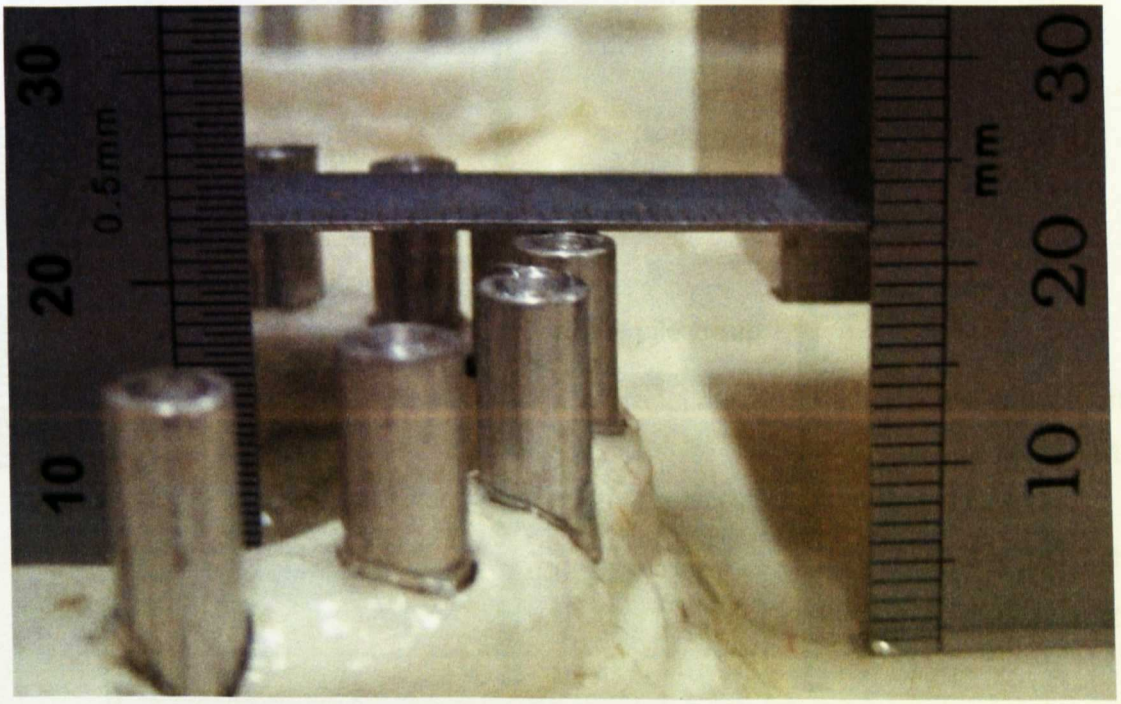

Figure 6.18b Close up of Figure 6.18a

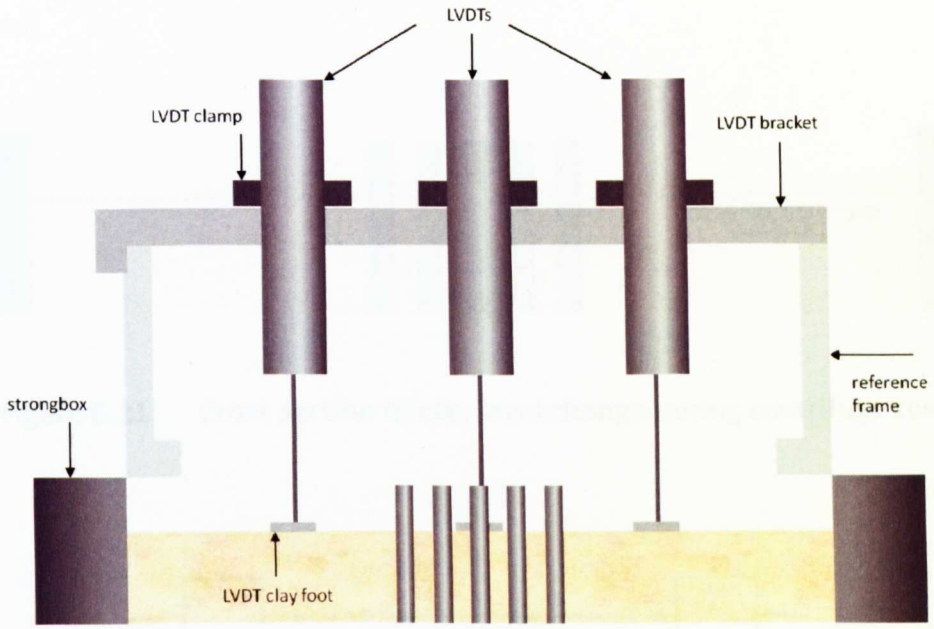

Figure 6.19 Cross section of central soil measurement apparatus

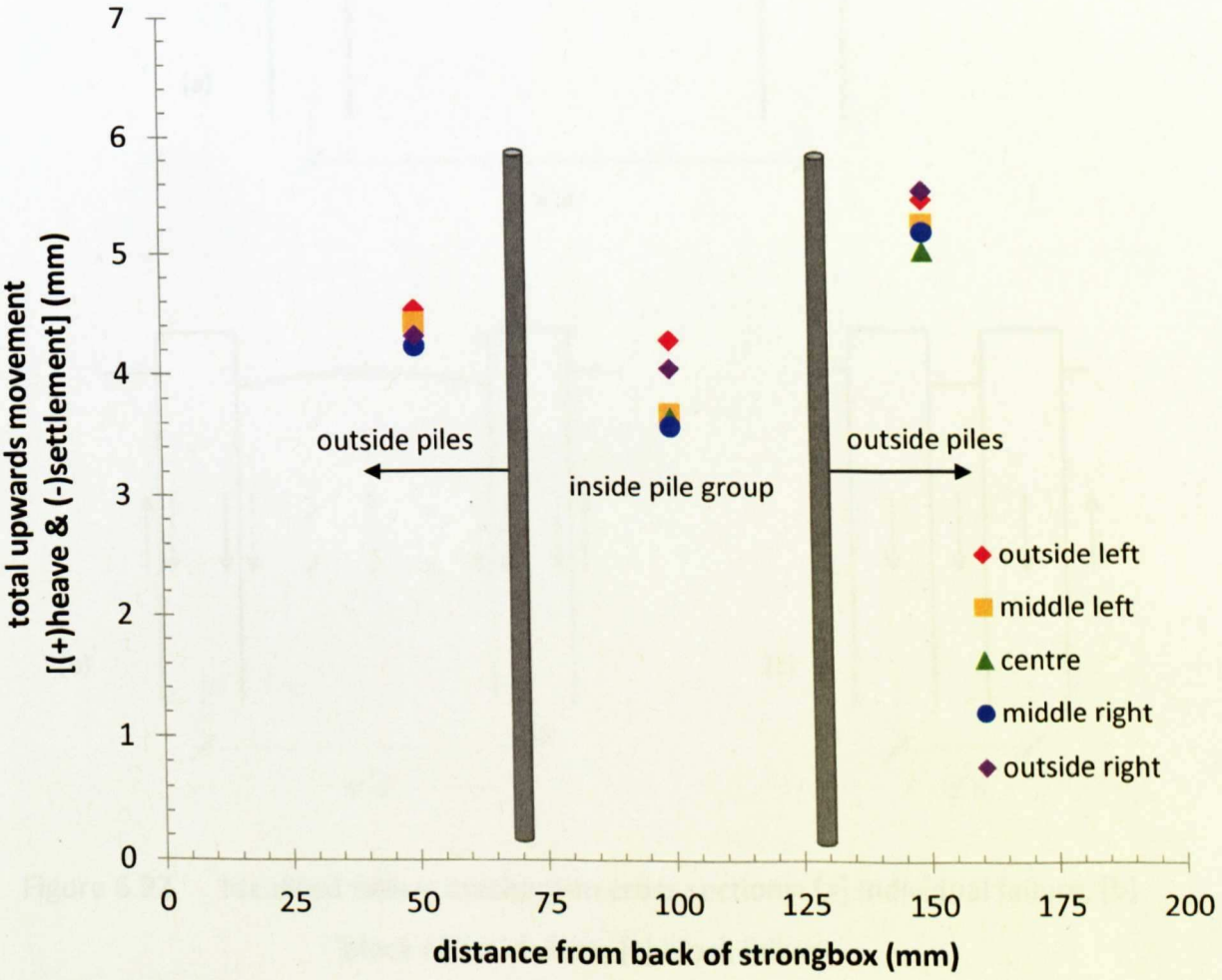

Figure 6.20 Central soil settlement measurements of PC20_2.00

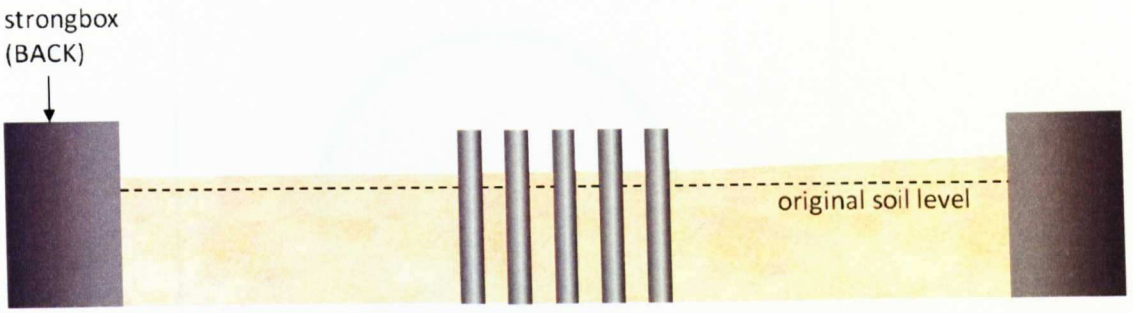

Figure 6.21 Cross section of clay level change during centrifuge test

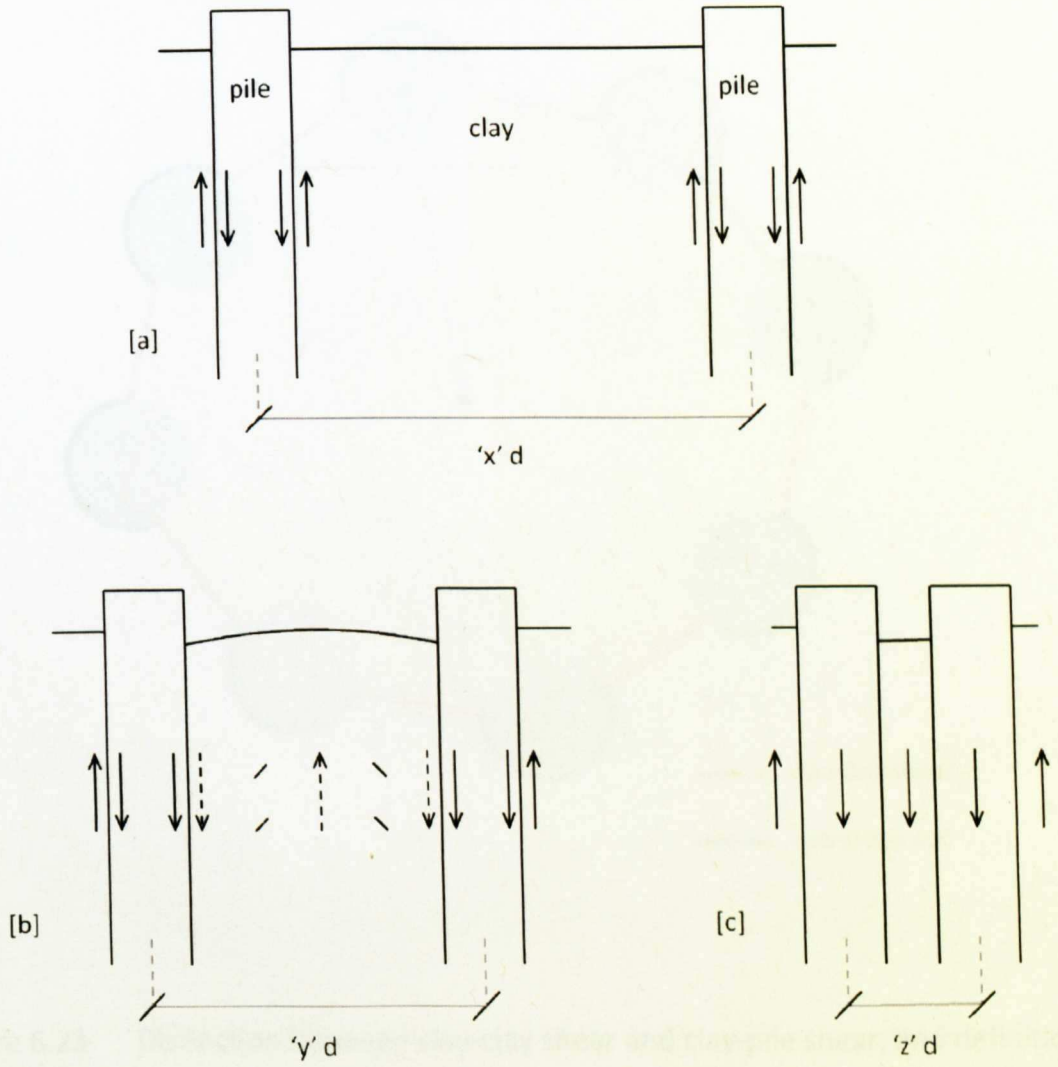

Figure 6.22 Idealised failure mechanism cross sections: [a] individual failure, [b] 'block effect' failure, [c] block failure

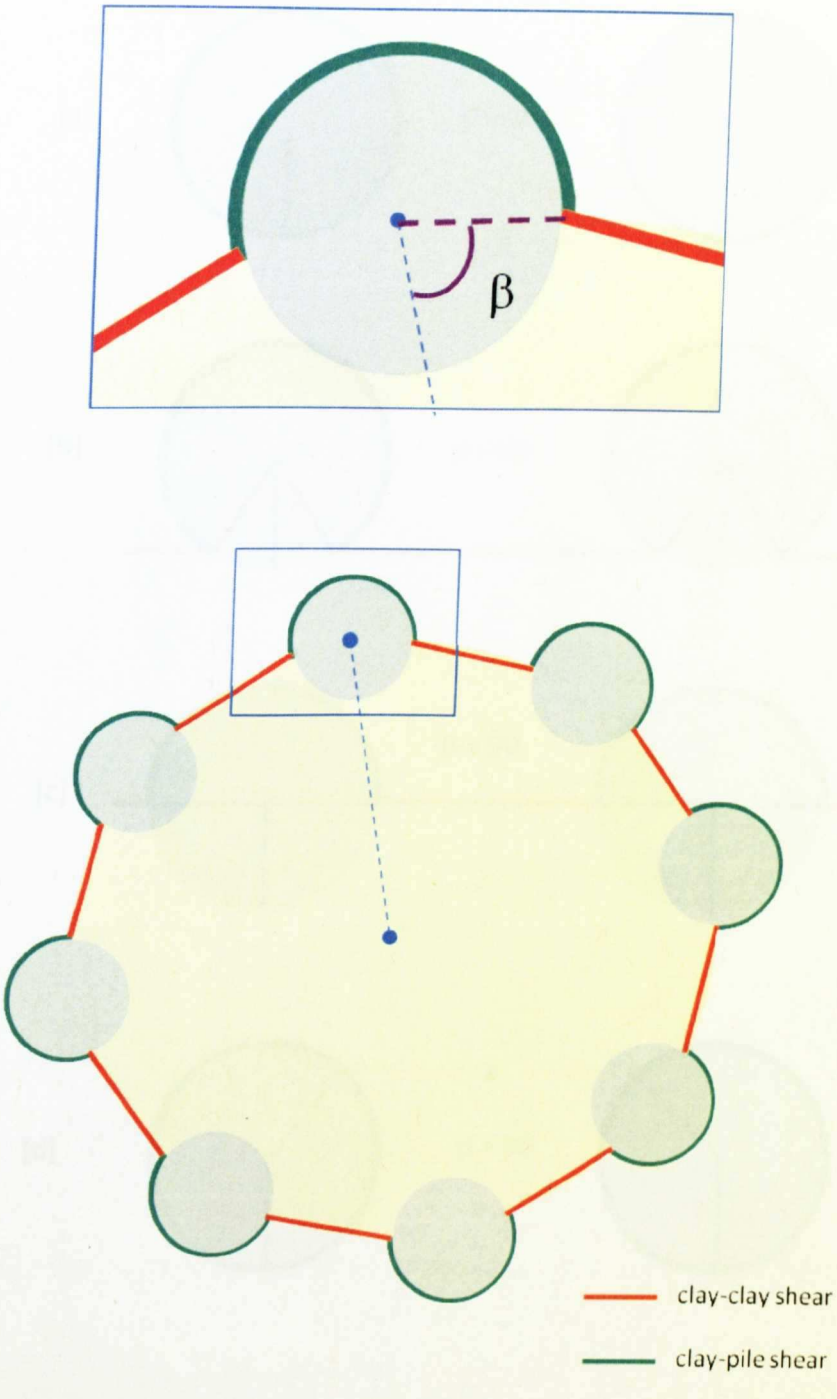

Figure 6.23 Distinction between clay-clay shear and clay-pile shear; and definition of β

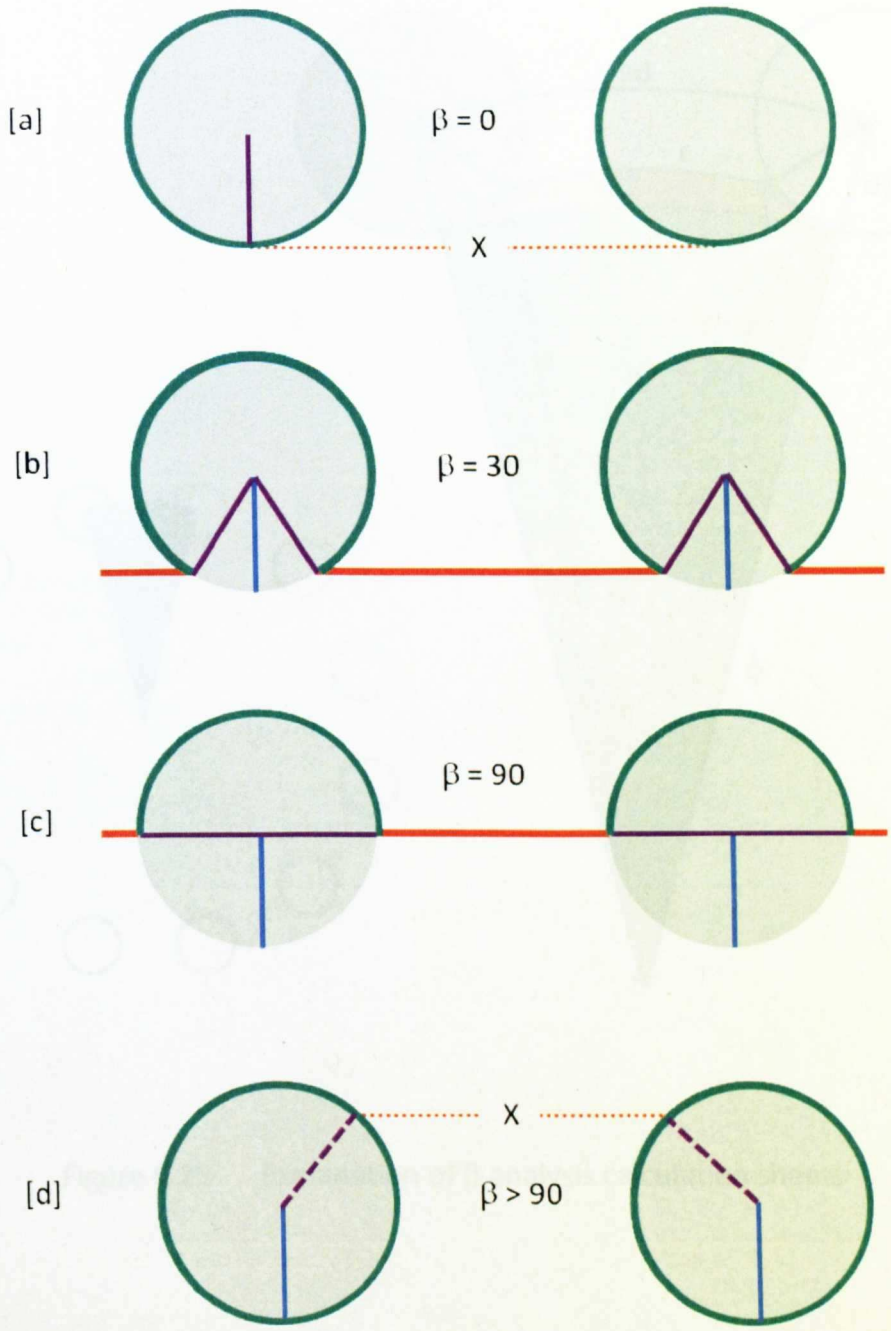

Figure 6.24 Variation of β: [a] 0°, [b] 30°, [c] 90°, [d] >90°

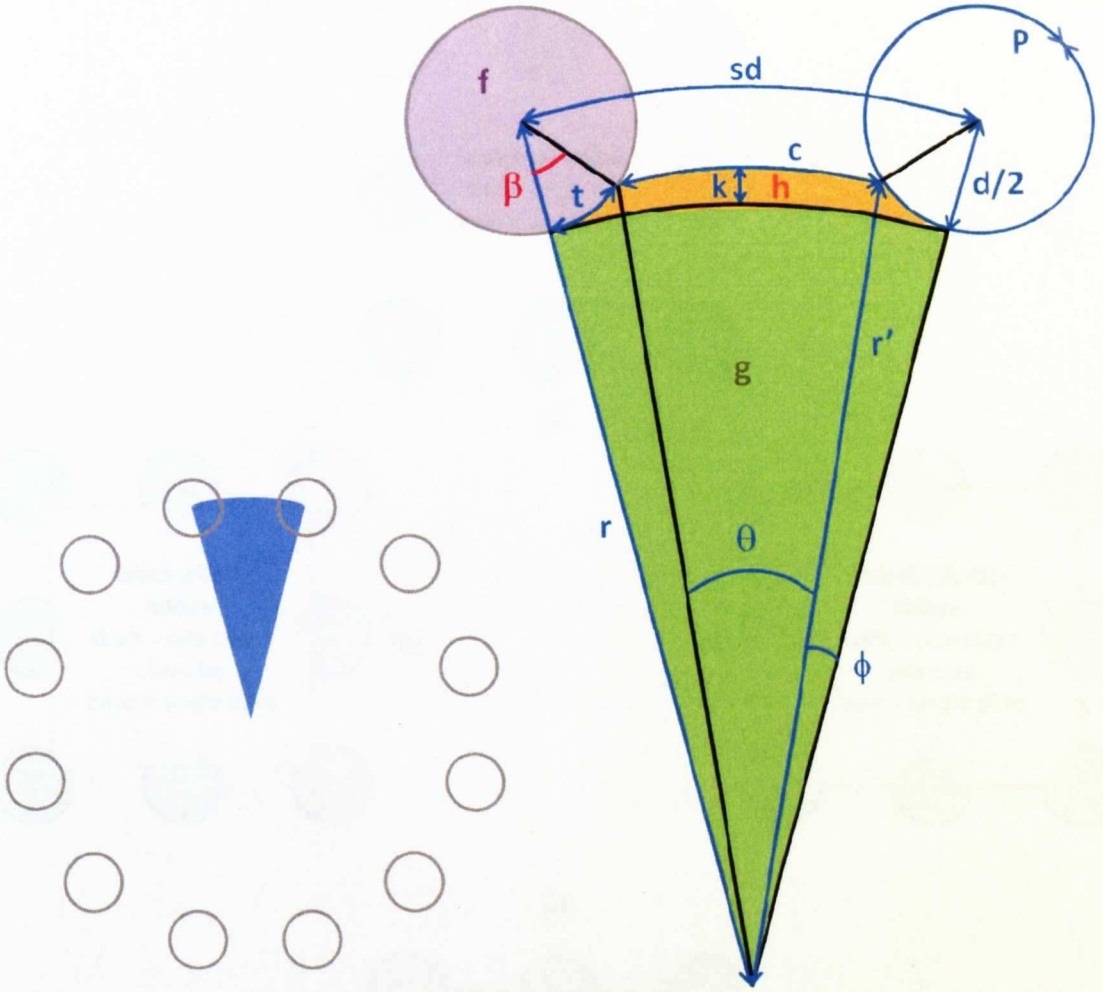

Figure 6.25 Explanation of β analysis calculation sheets

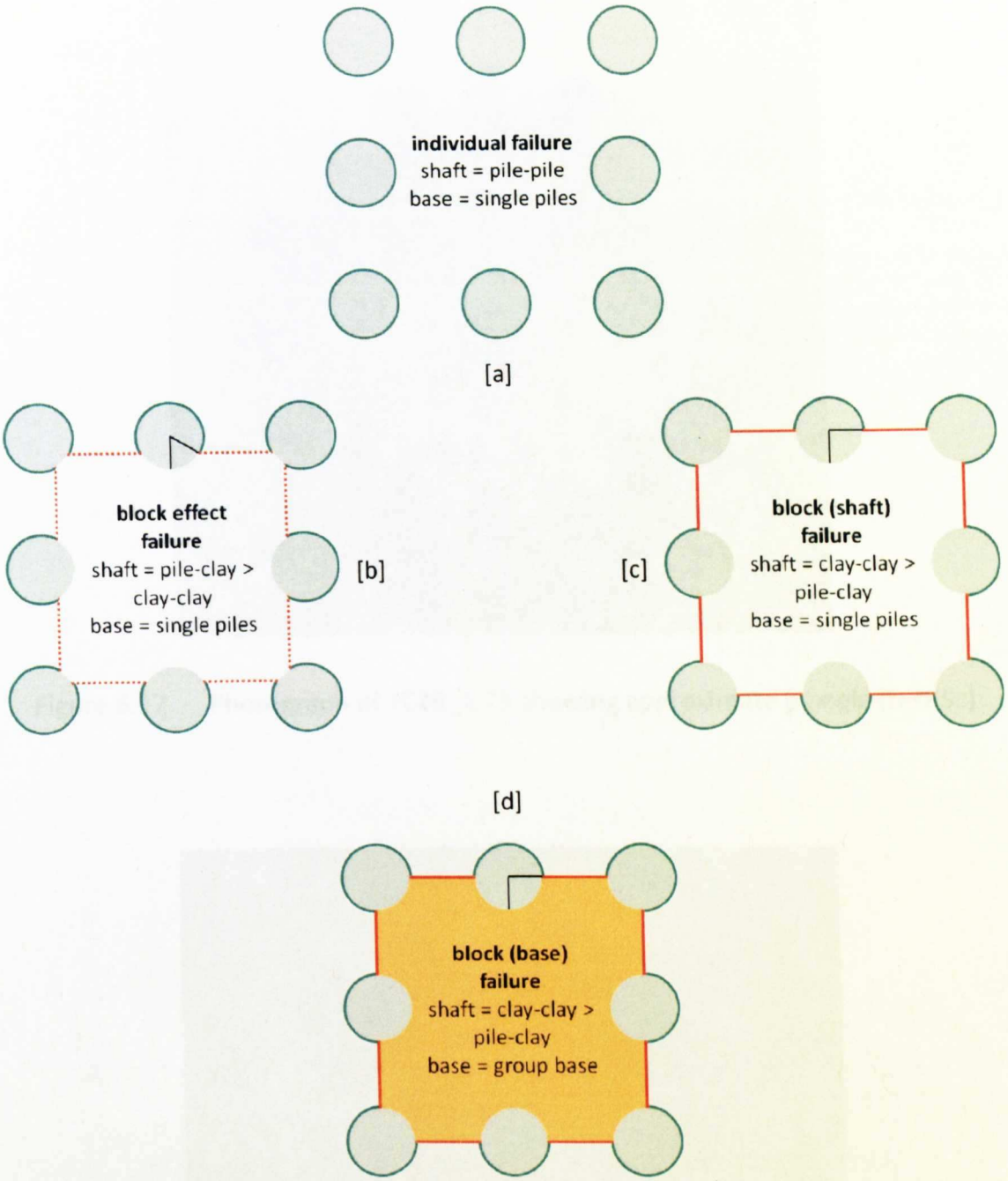

Figure 6.26 Change in Q_s and Q_b and the contribution to total capacity: [a] individual failure, [b] 'block effect' failure, [c] and [d] block failure

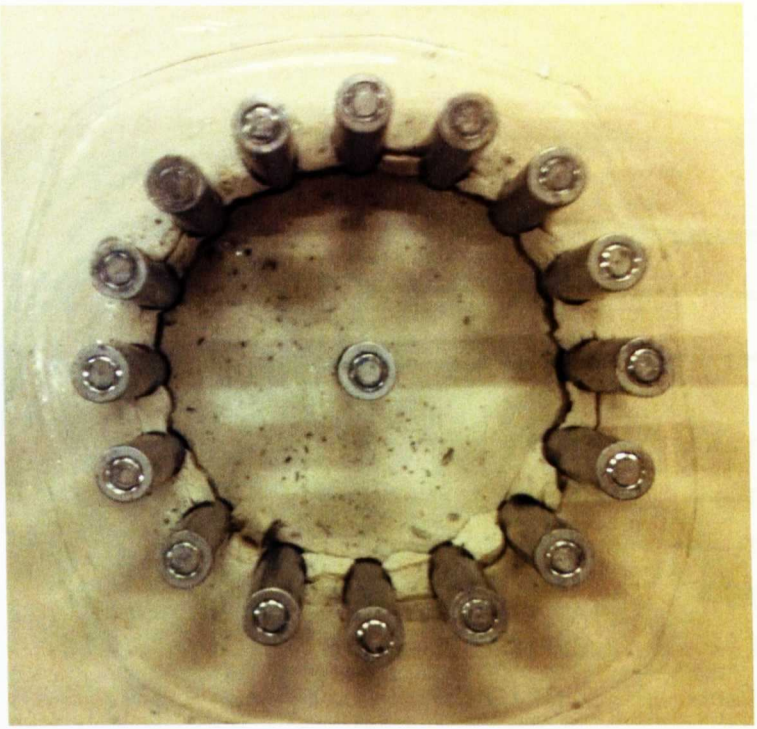

Figure 6.27 Photograph of TC16_1.75 showing approximate β angle (test 5c)

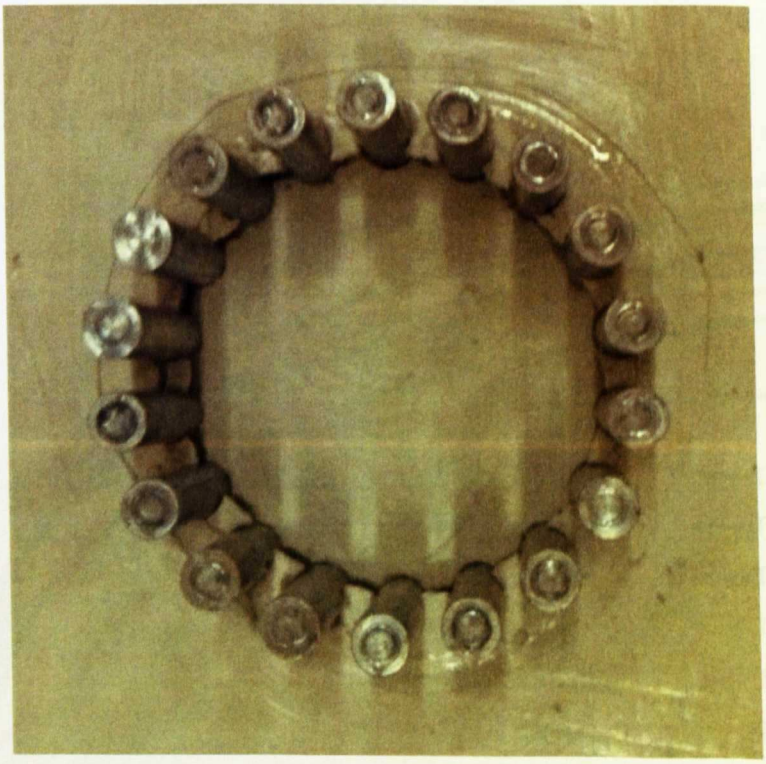

Figure 6.28 Photograph of PC18_1.50 showing approximate β angle (test 5e)

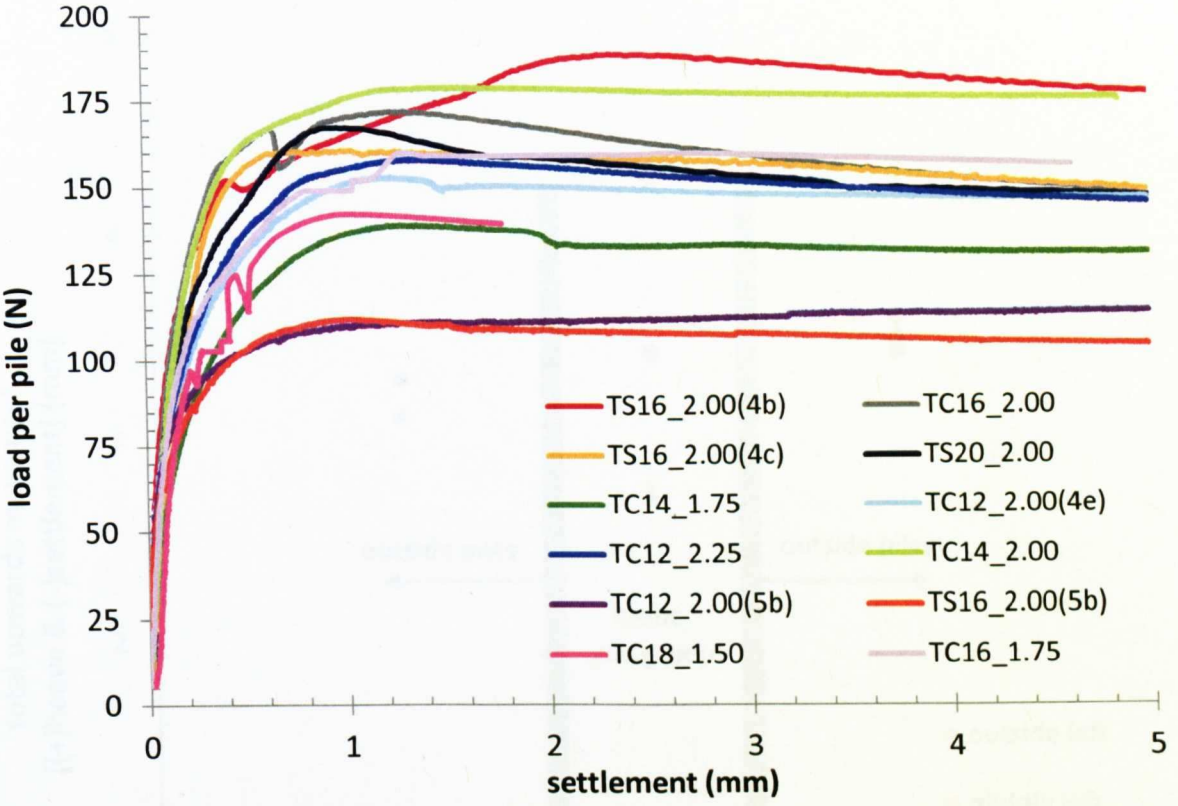

Figure 6.29 Load vs settlement (0 – 5 mm): target groups

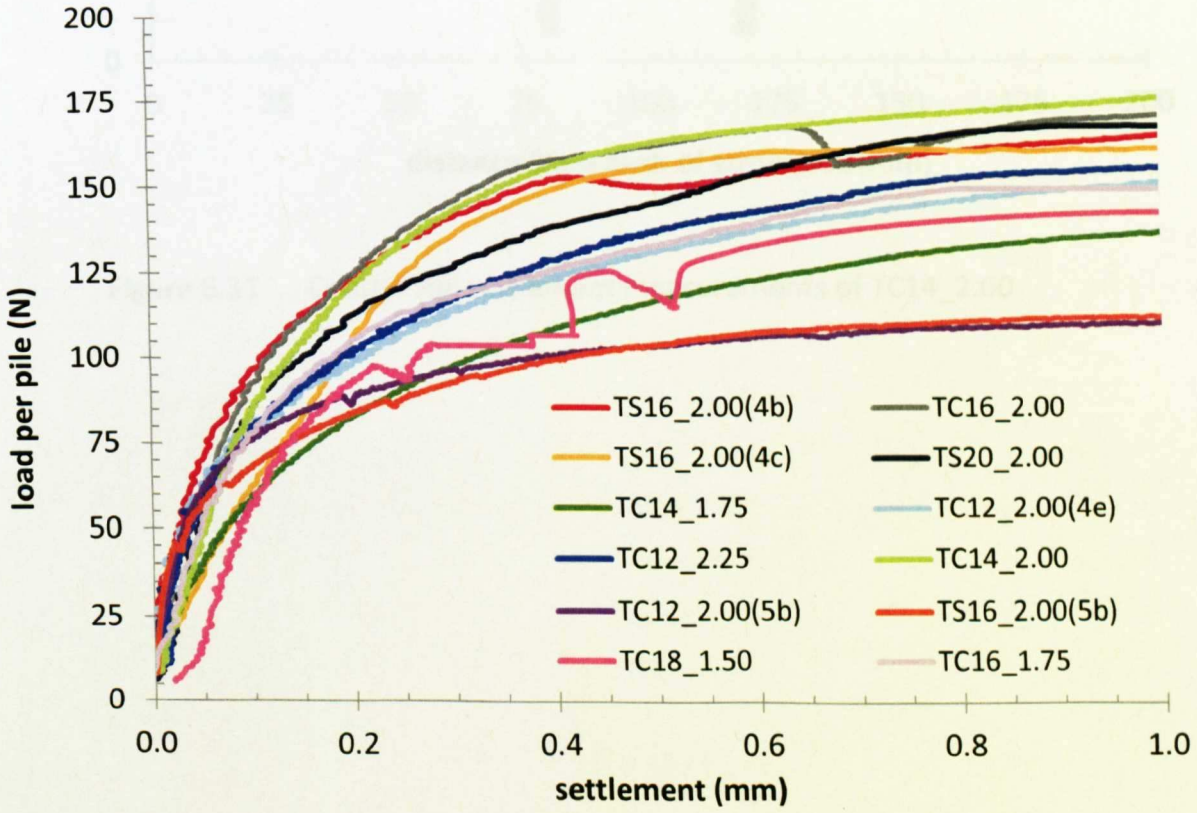

Figure 6.30 Load vs settlement (0 – 1 mm): target groups

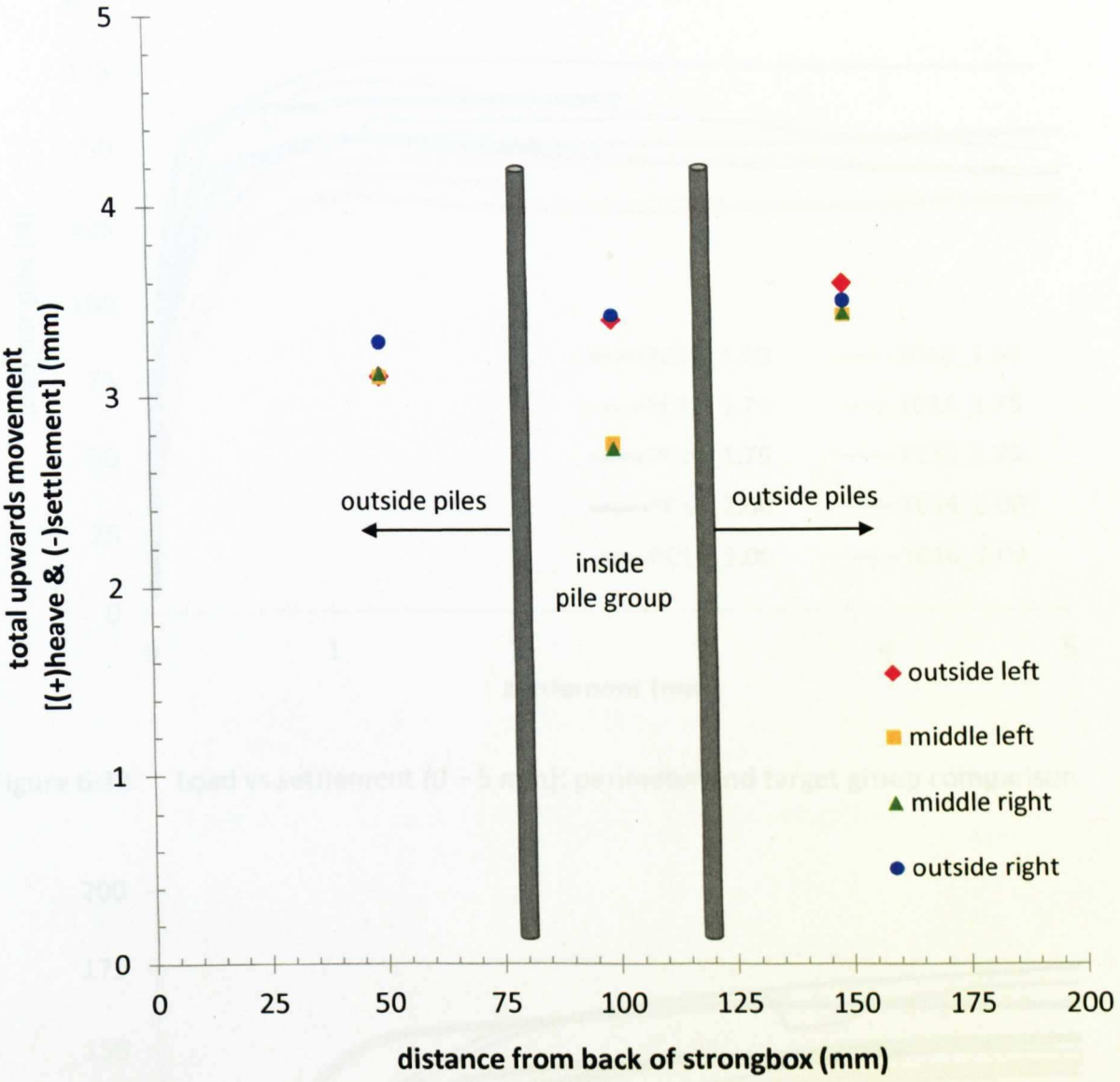

Figure 6.31 Central soil settlement measurements of TC14_2.00

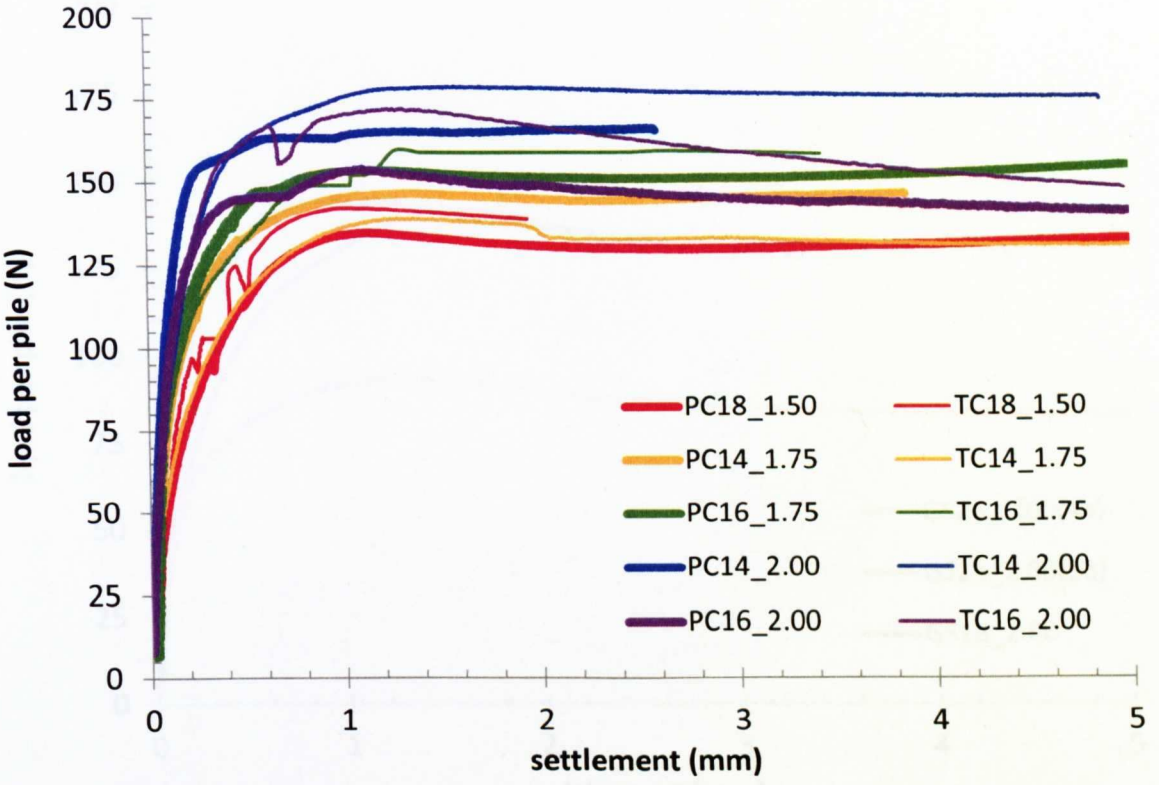

Figure 6.32 Load vs settlement (0 – 5 mm): perimeter and target group comparison

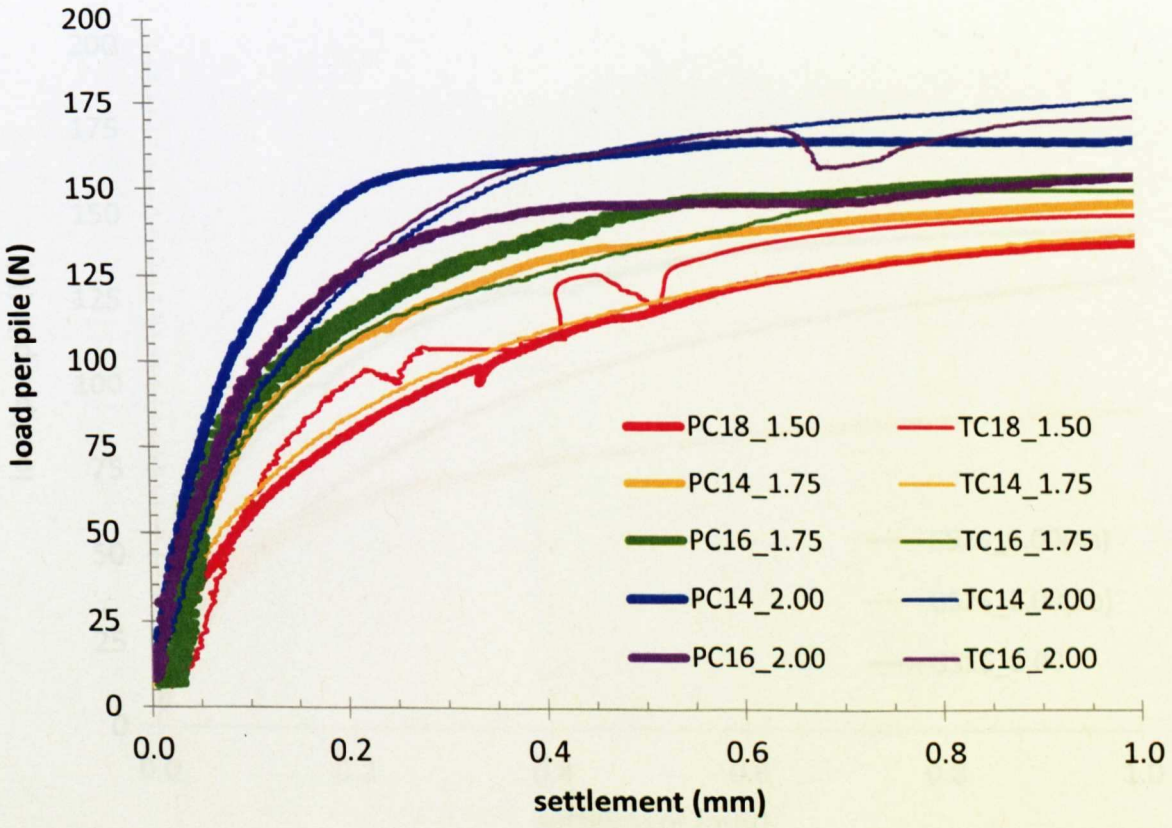

Figure 6.33 Load vs settlement (0 – 1 mm): perimeter and target group comparison

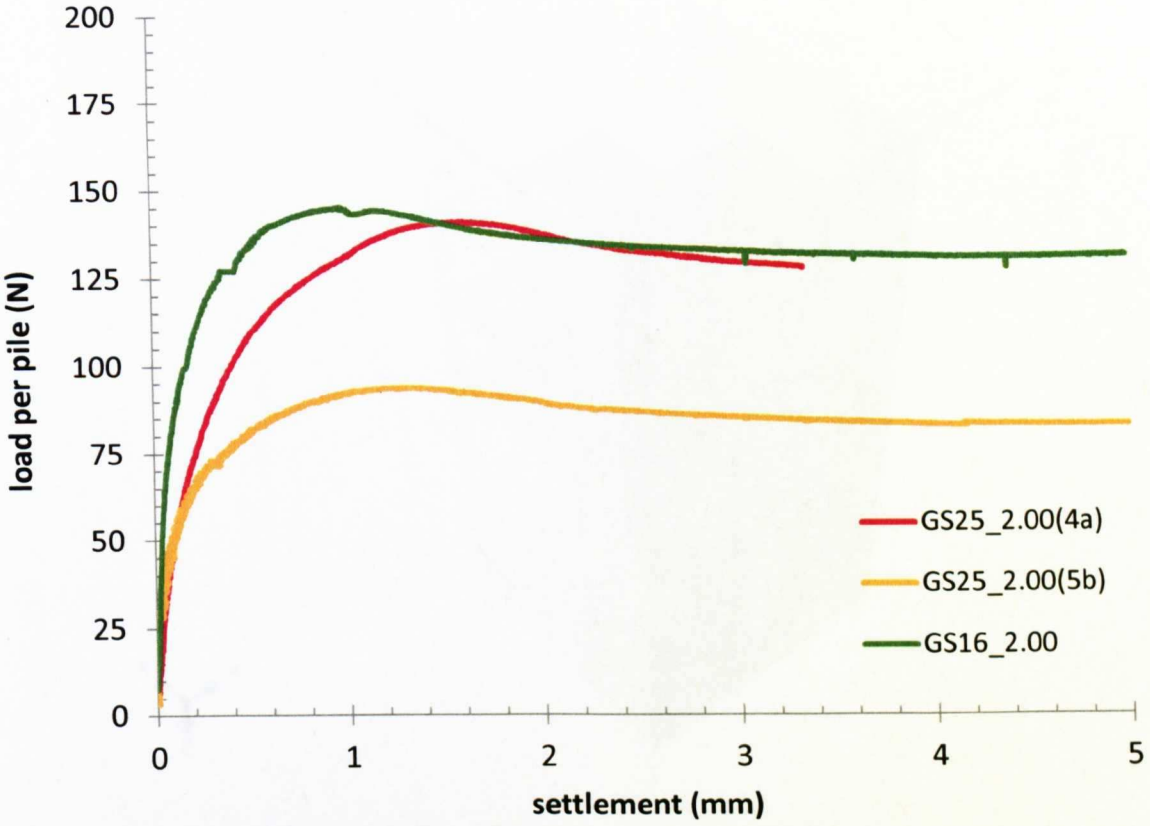

Figure 6.34 Load vs settlement (0 – 5 mm): grid groups

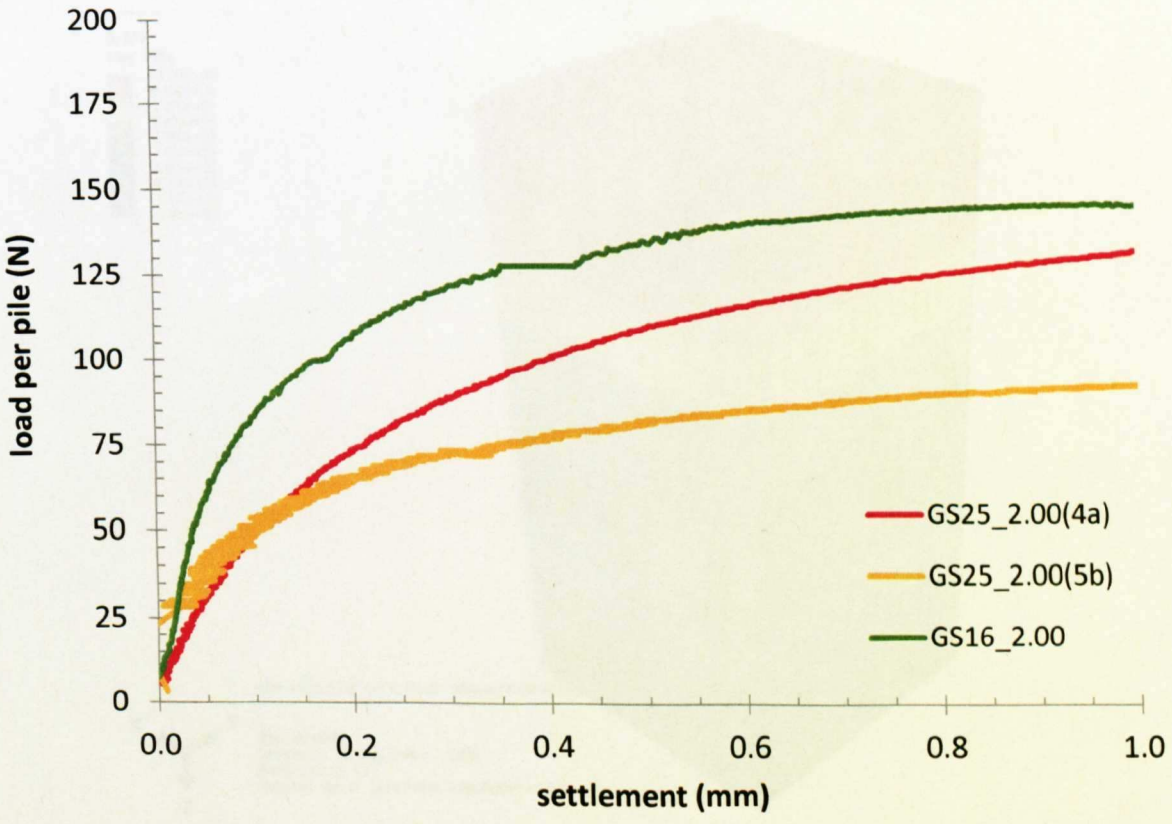

Figure 6.35 Load vs settlement (0 – 1 mm): grid groups

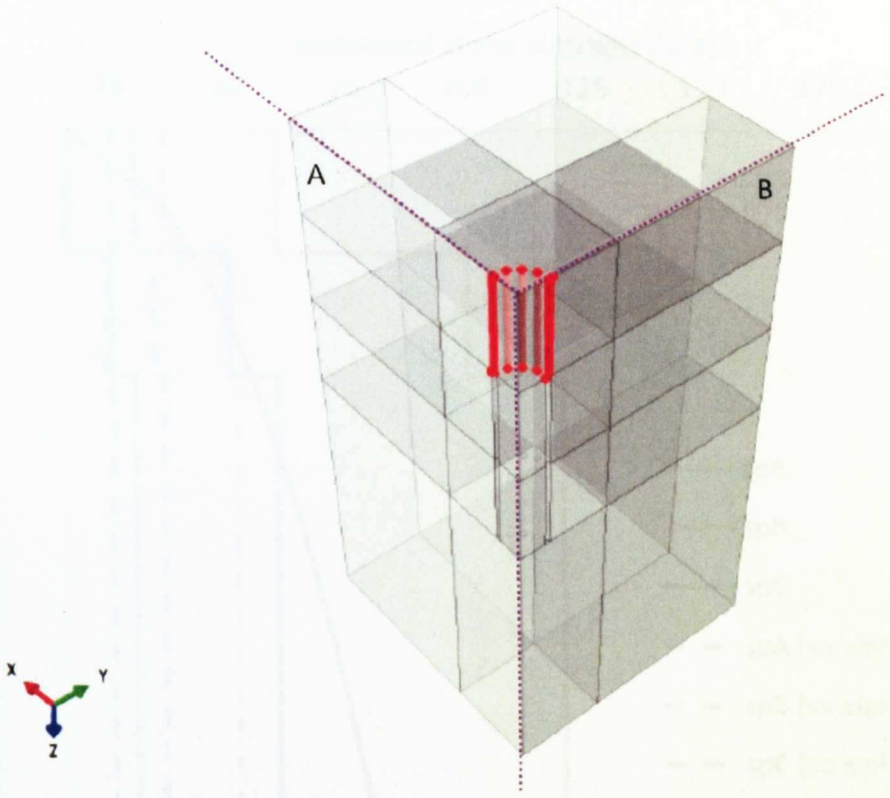

Figure 7.01 Quarter symmetric model

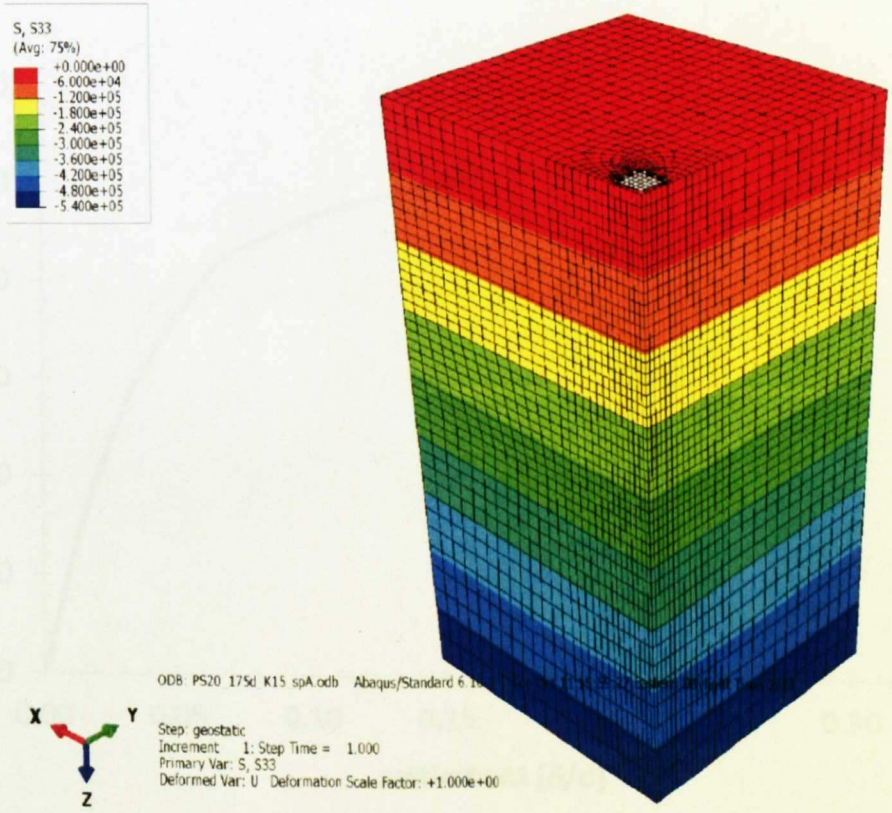

Figure 7.02 Geostatic stress distribution

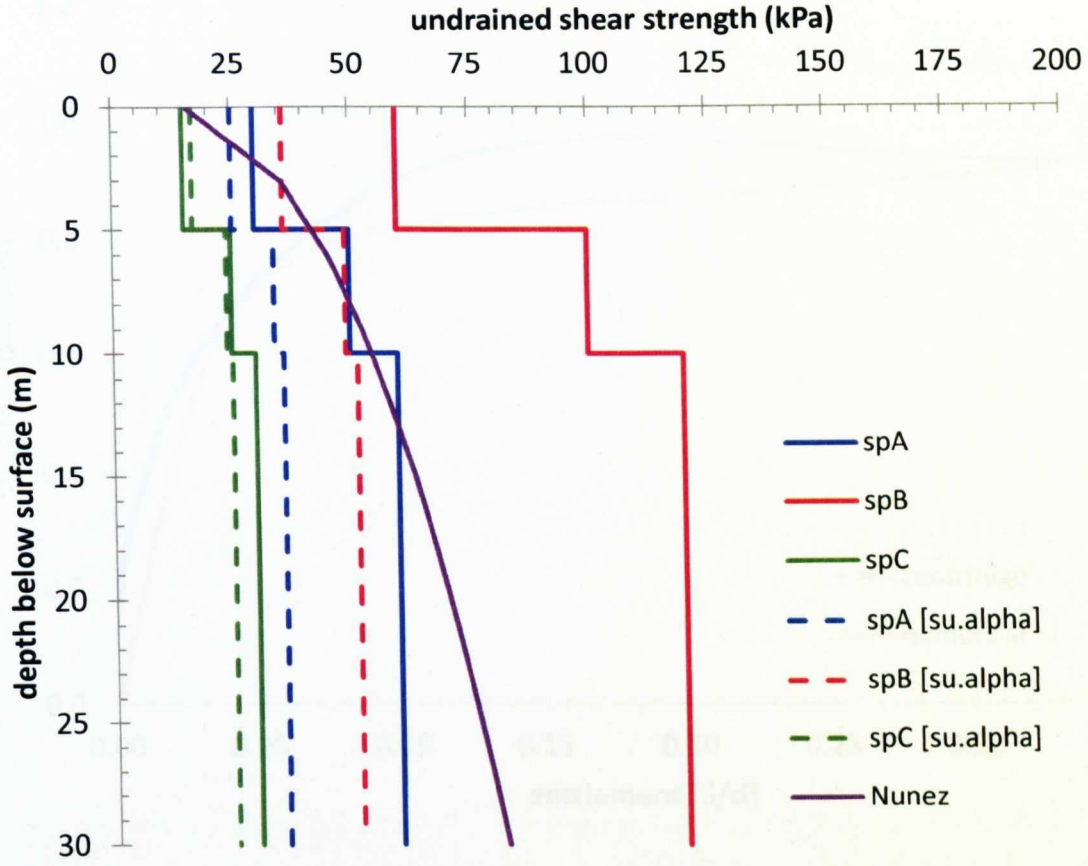

Figure 8.01 Soil profiles sp_A, sp_B and sp_C (inc. $s_u\alpha$ and Nuñez profiles)

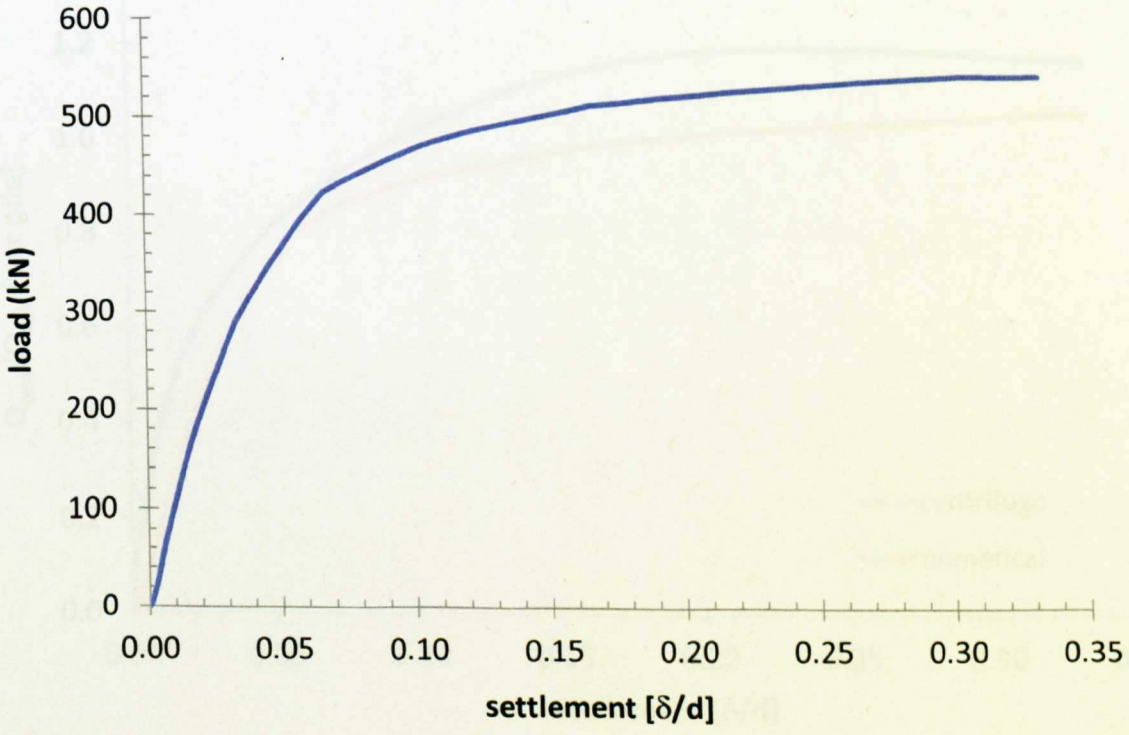

Figure 8.02 Load vs settlement: single pile

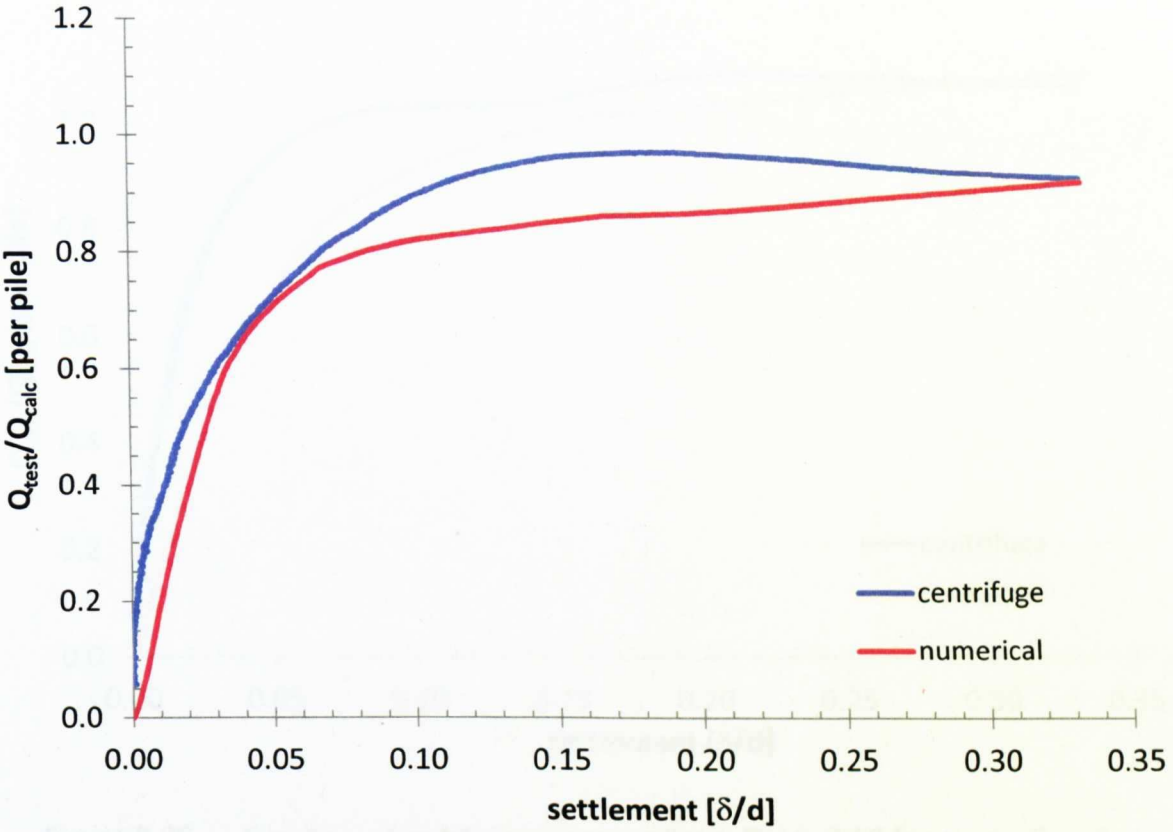

Figure 8.03 Q_{test}/Q_{calc} vs settlement comparison: PC12_1.50

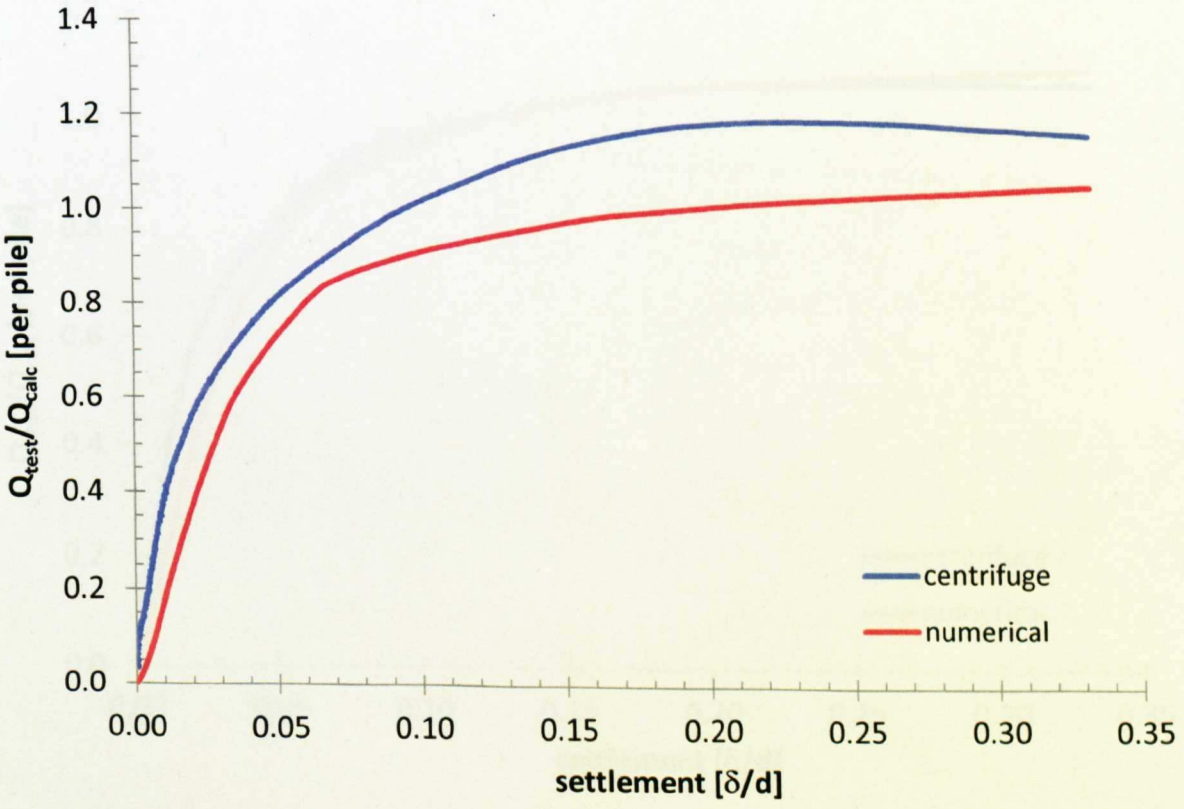

Figure 8.04 Q_{test}/Q_{calc} vs settlement comparison: PS20_1.75

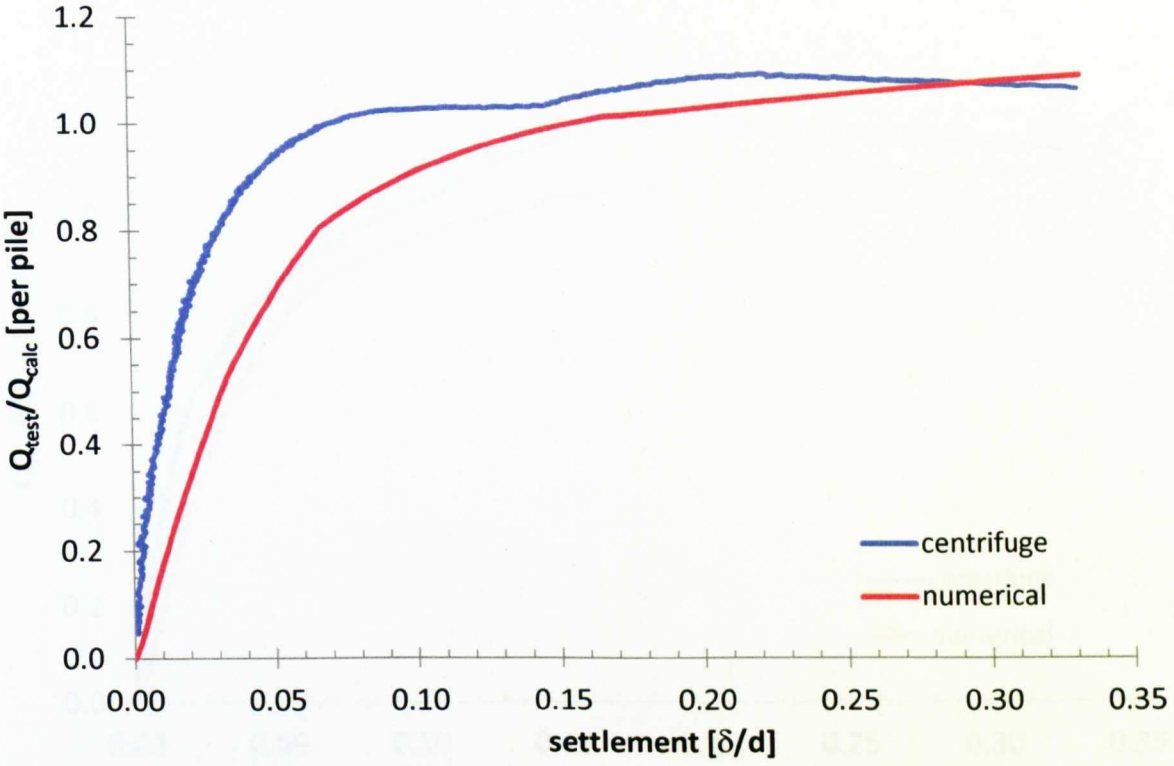

Figure 8.05 Q_{test}/Q_{calc} vs settlement comparison: PS16_2.00 (numerical) and PC16_2.00 (centrifuge)

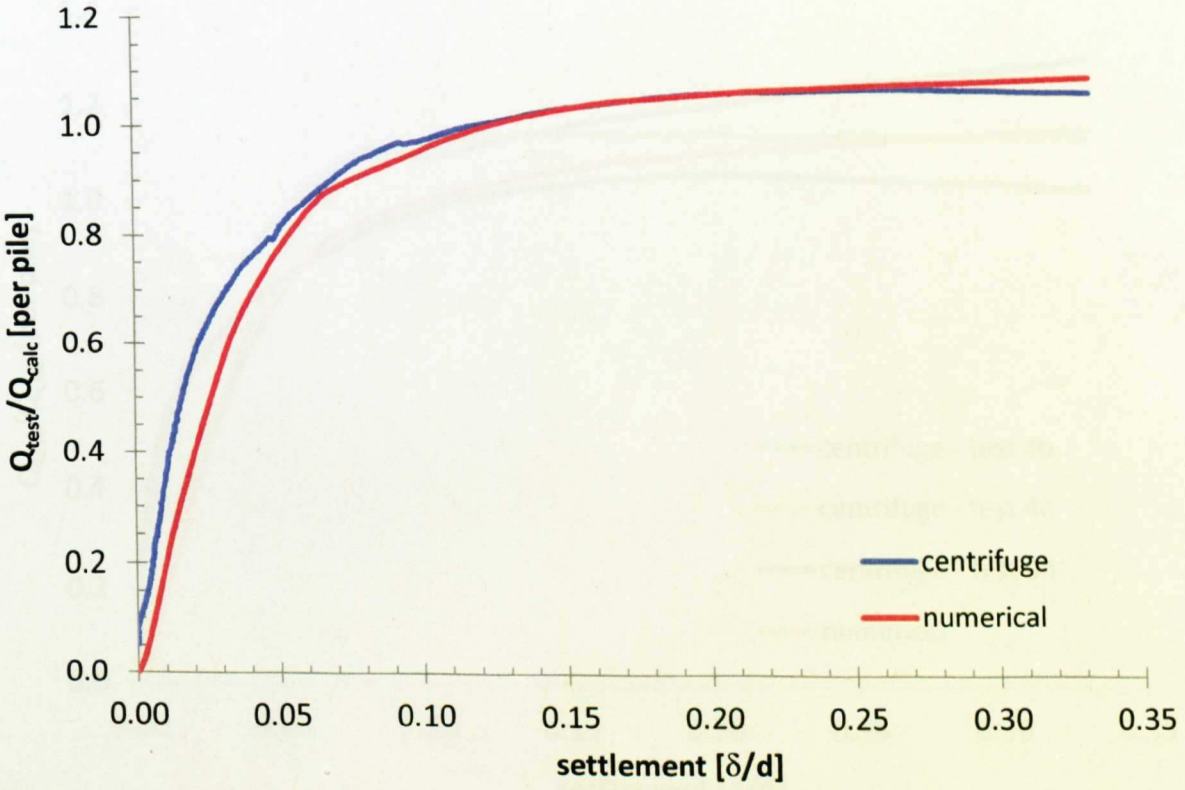

Figure 8.06 Q_{test}/Q_{calc} vs settlement comparison: PC14_1.75

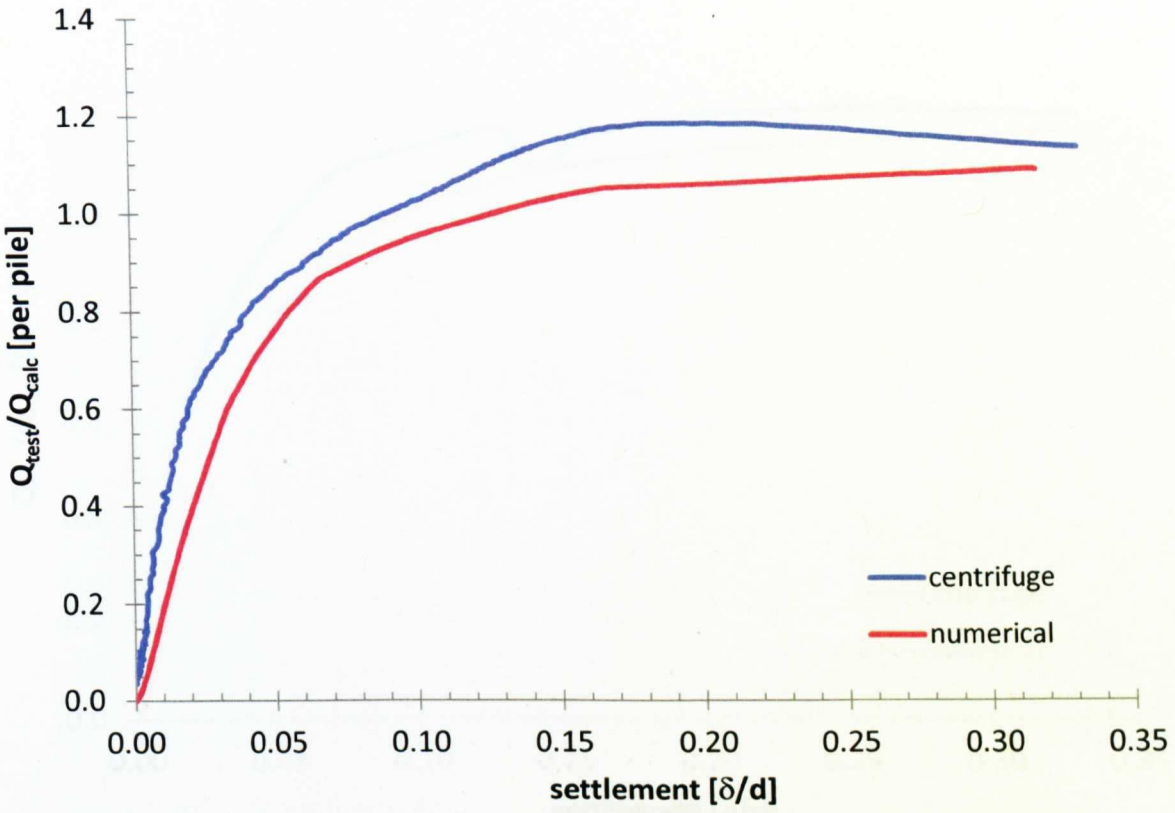

Figure 8.07 Q_{test}/Q_{calc} vs settlement comparison: TS20_2.00

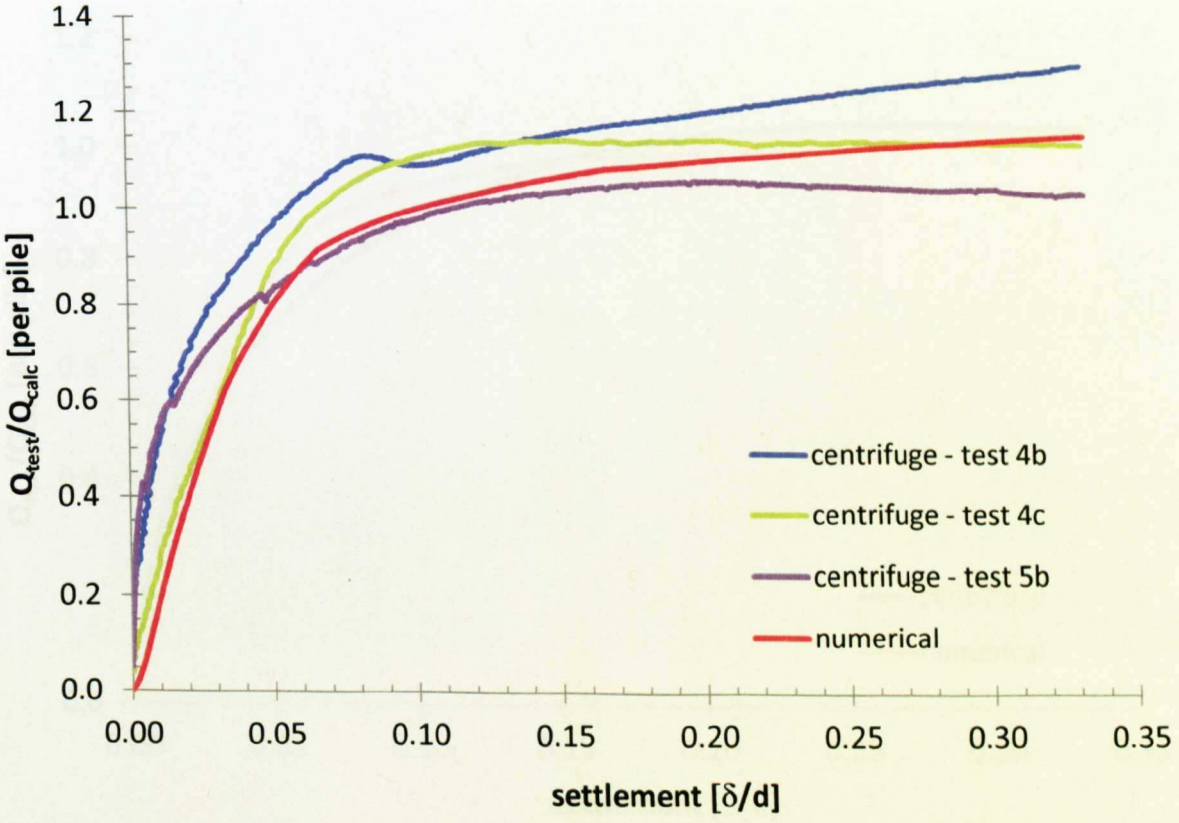

Figure 8.08 Q_{test}/Q_{calc} vs settlement comparison: TS16_2.00

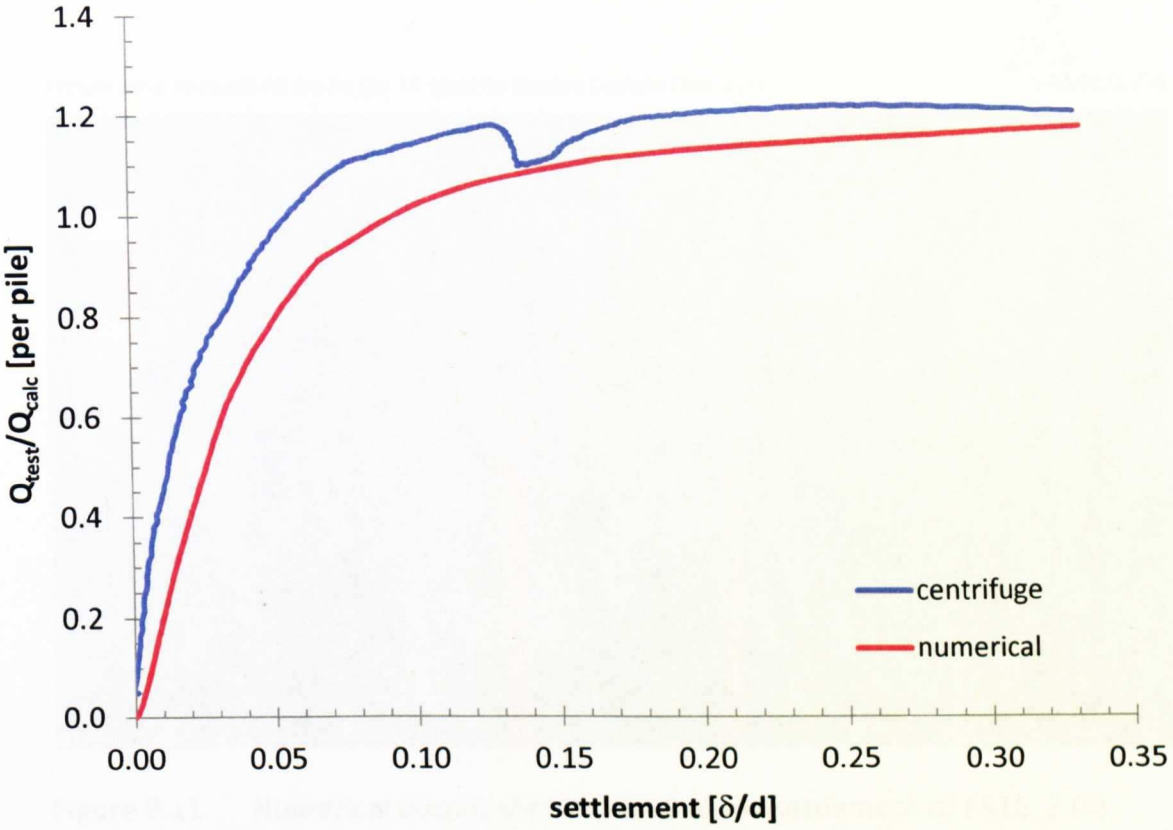

Figure 8.09 Q_{test}/Q_{calc} vs settlement comparison: TC16_2.00

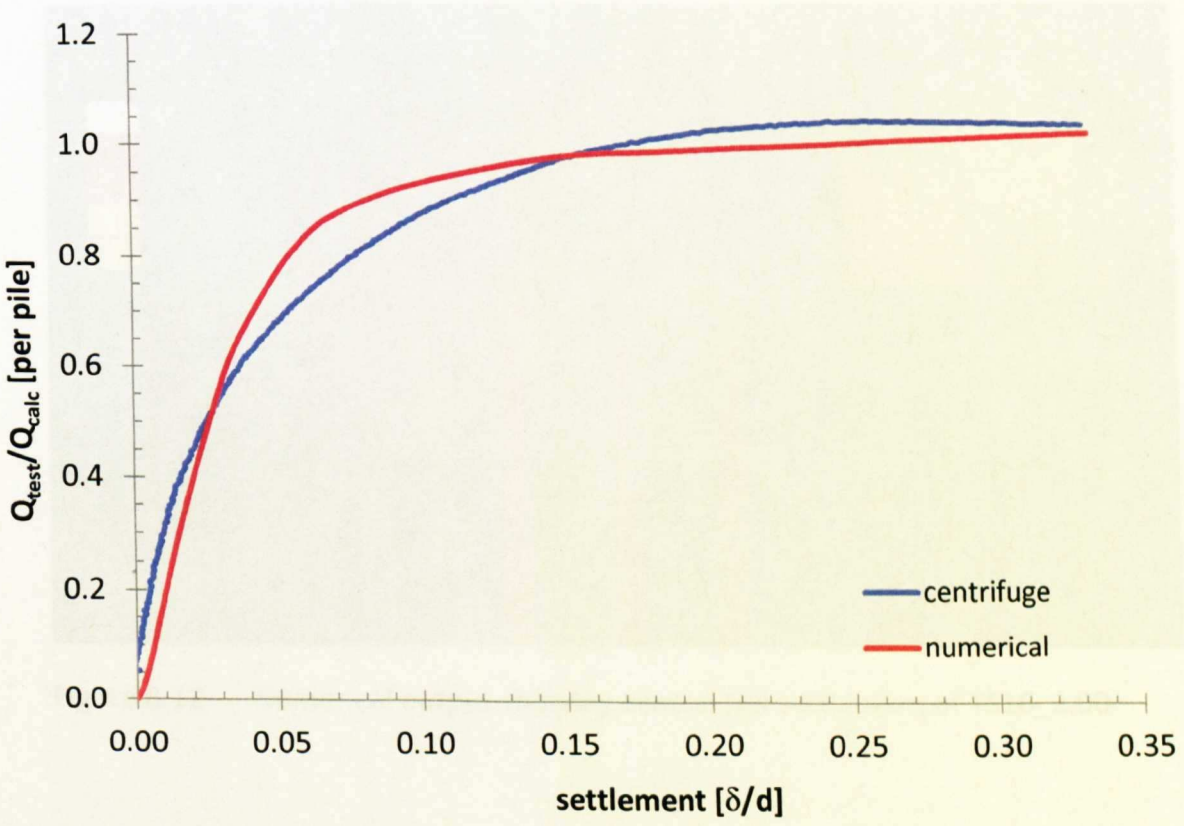

Figure 8.10 Q_{test}/Q_{calc} vs settlement comparison: TC14_1.75

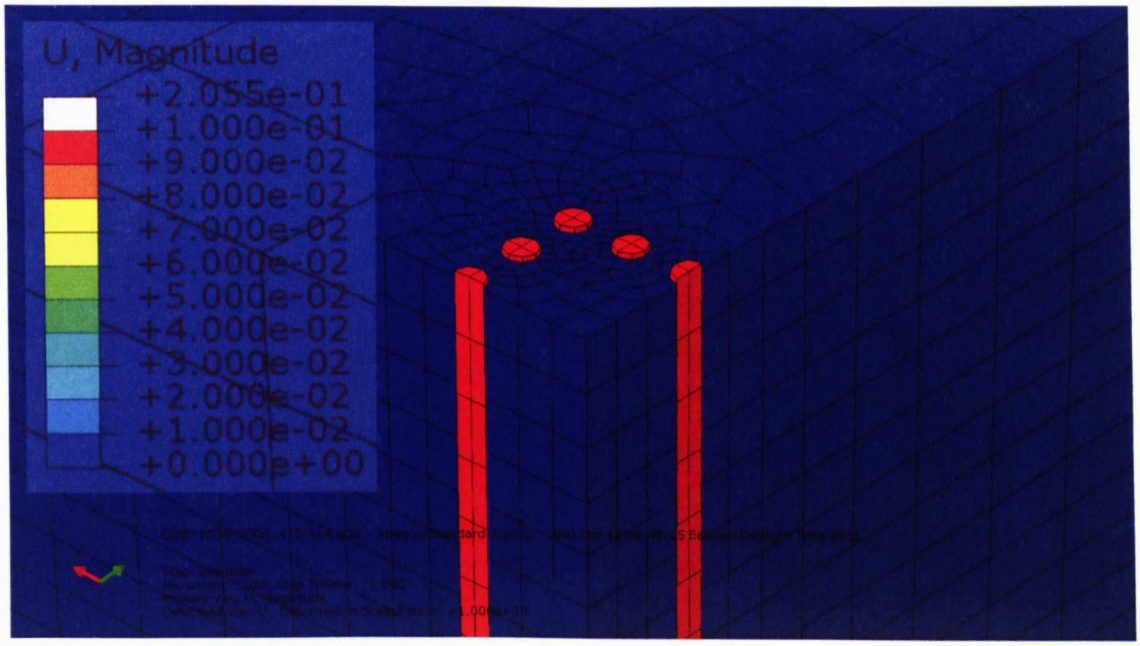

Figure 8.11 Numerical output showing central soil settlement of PS16_2.00

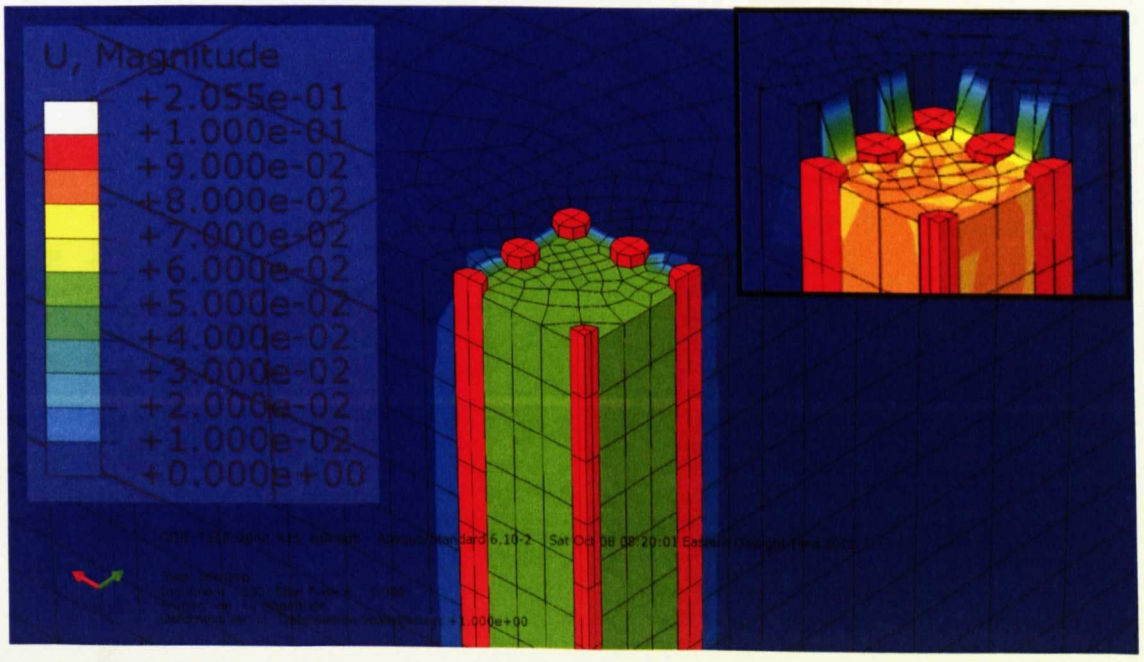

Figure 8.12 Numerical output showing central soil settlement of TS16_2.00

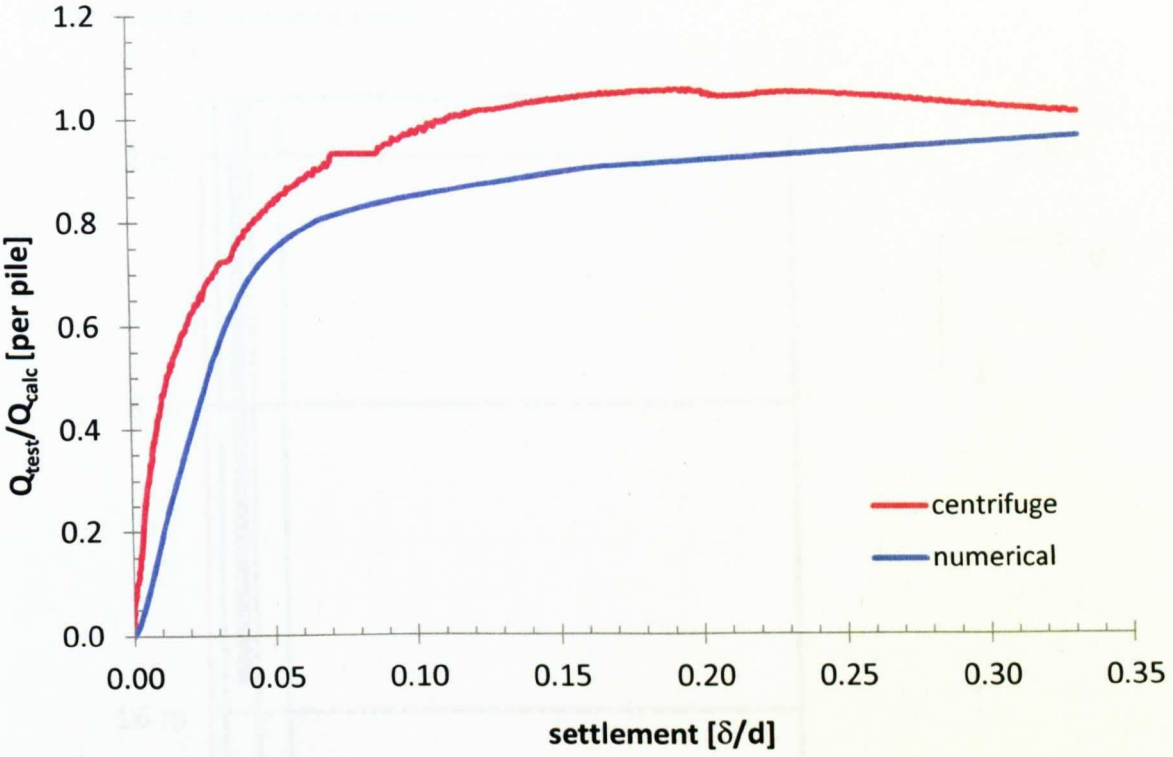

Figure 8.13 Q_{test}/Q_{calc} vs settlement comparison: GS16_2.00

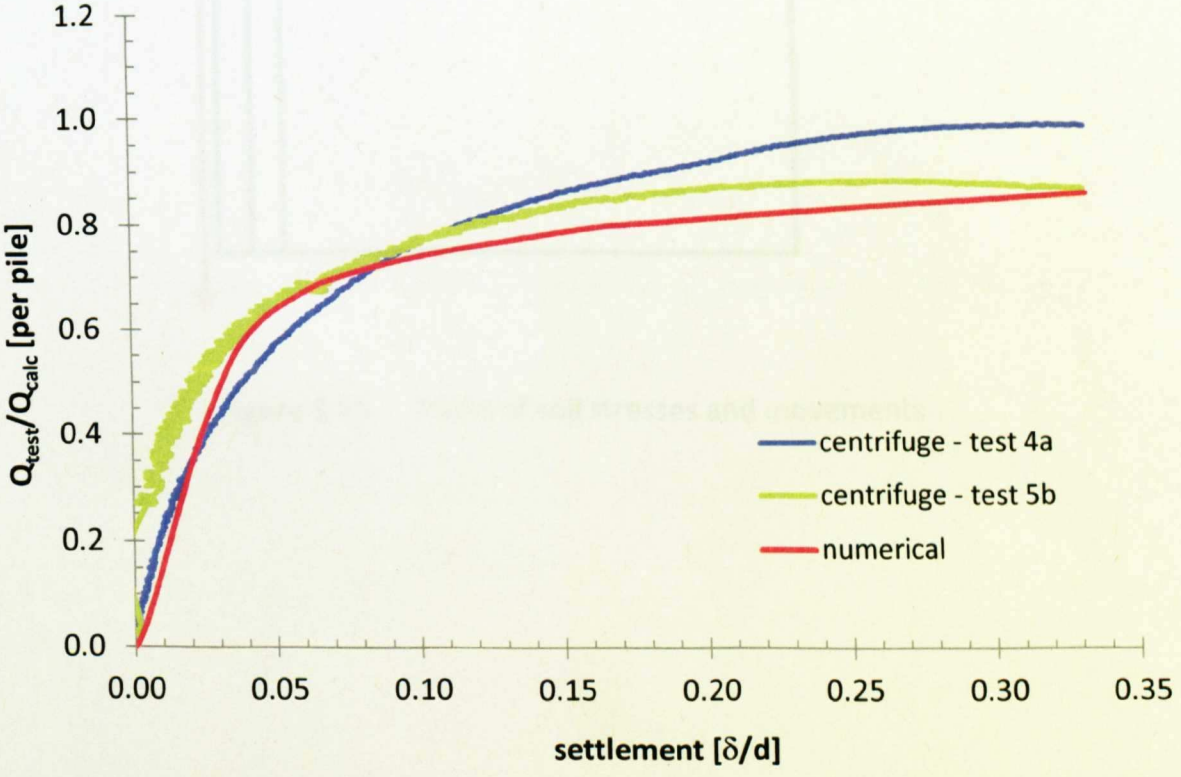

Figure 8.14 Q_{test}/Q_{calc} vs settlement comparison: GS25_2.00

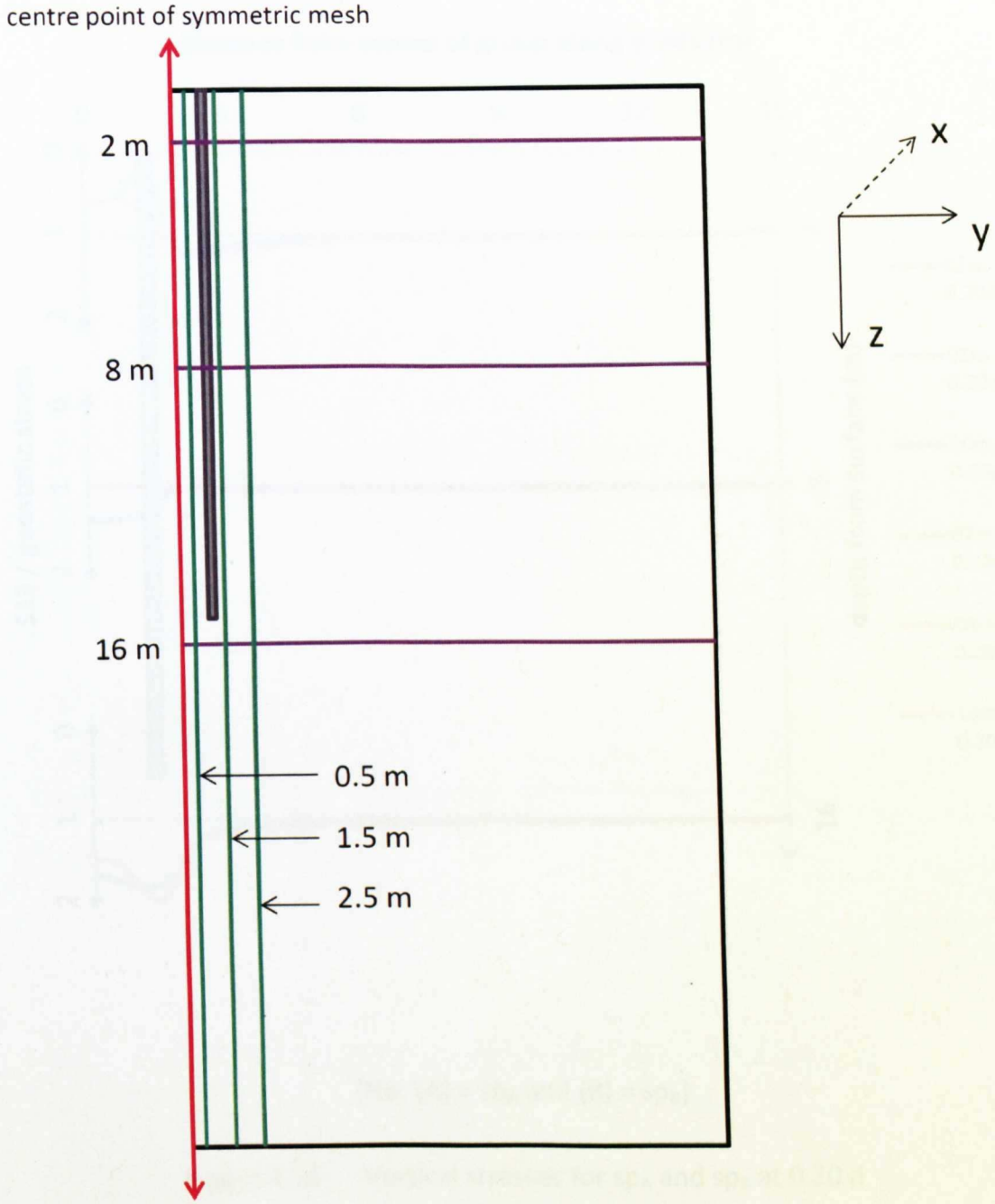

Figure 8.15 Paths of soil stresses and movements

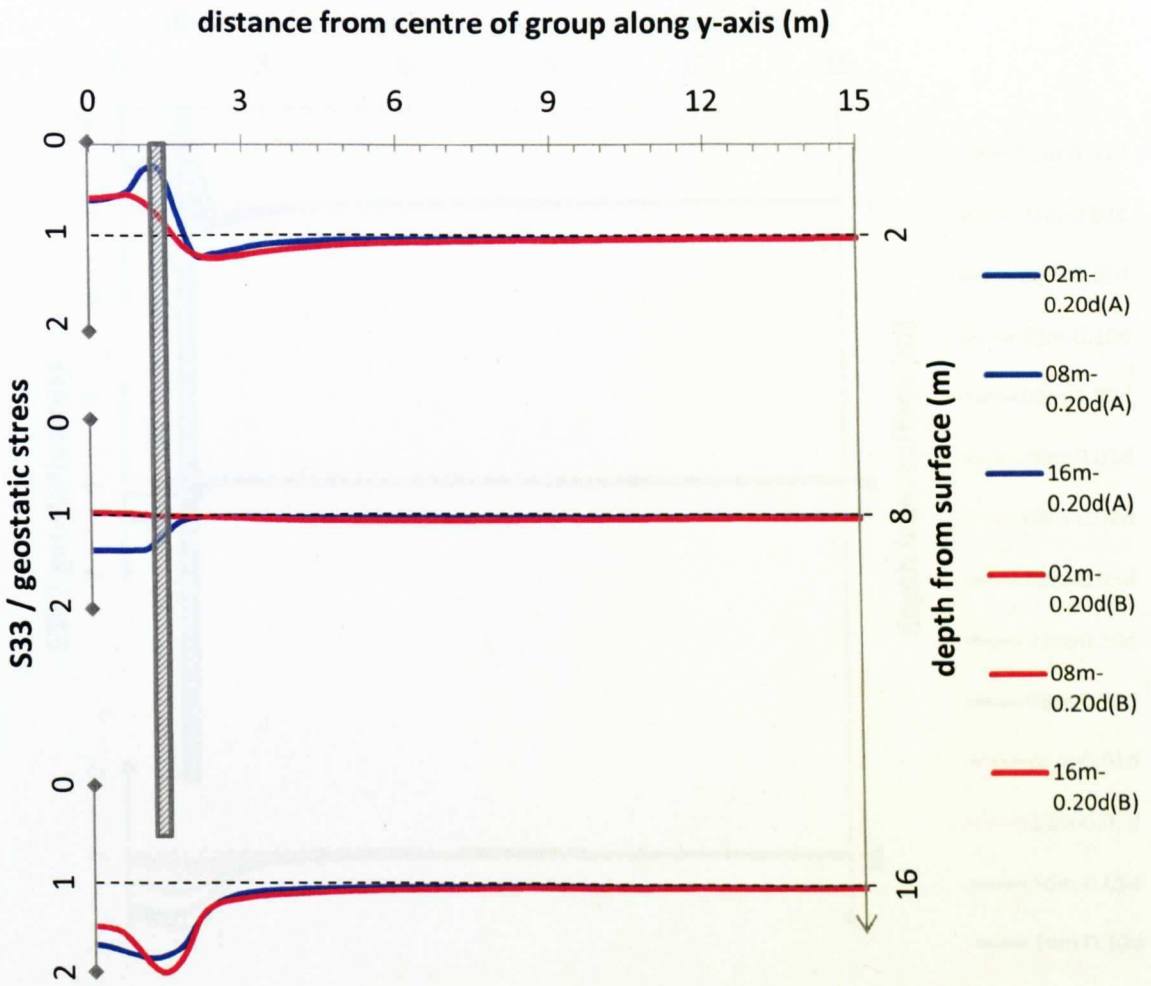

[NB: (A) = sp_A and (B) = sp_B]

Figure 8.16 Vertical stresses for sp_A and sp_B at 0.20 d

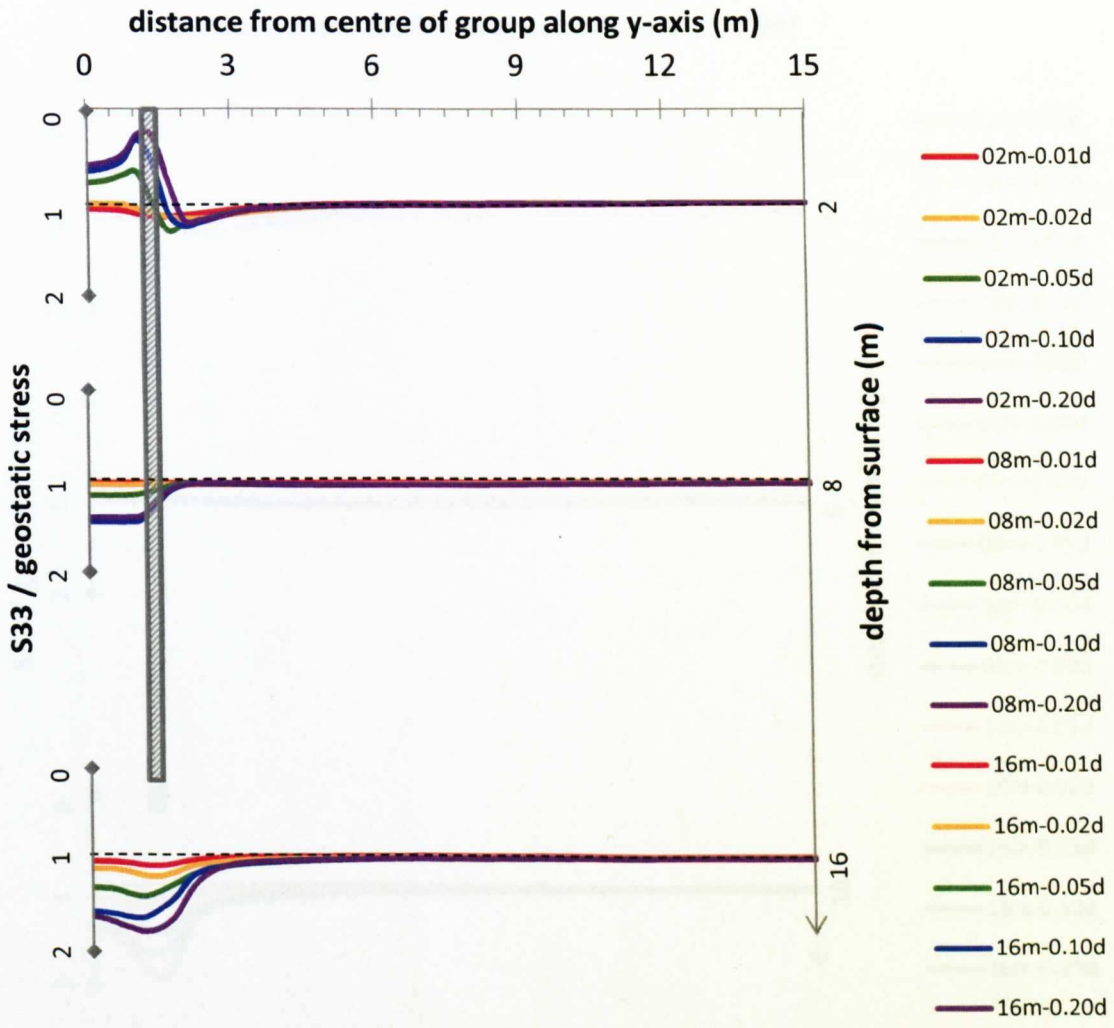

Figure 8.17 Vertical stress change with settlement (sp_A)

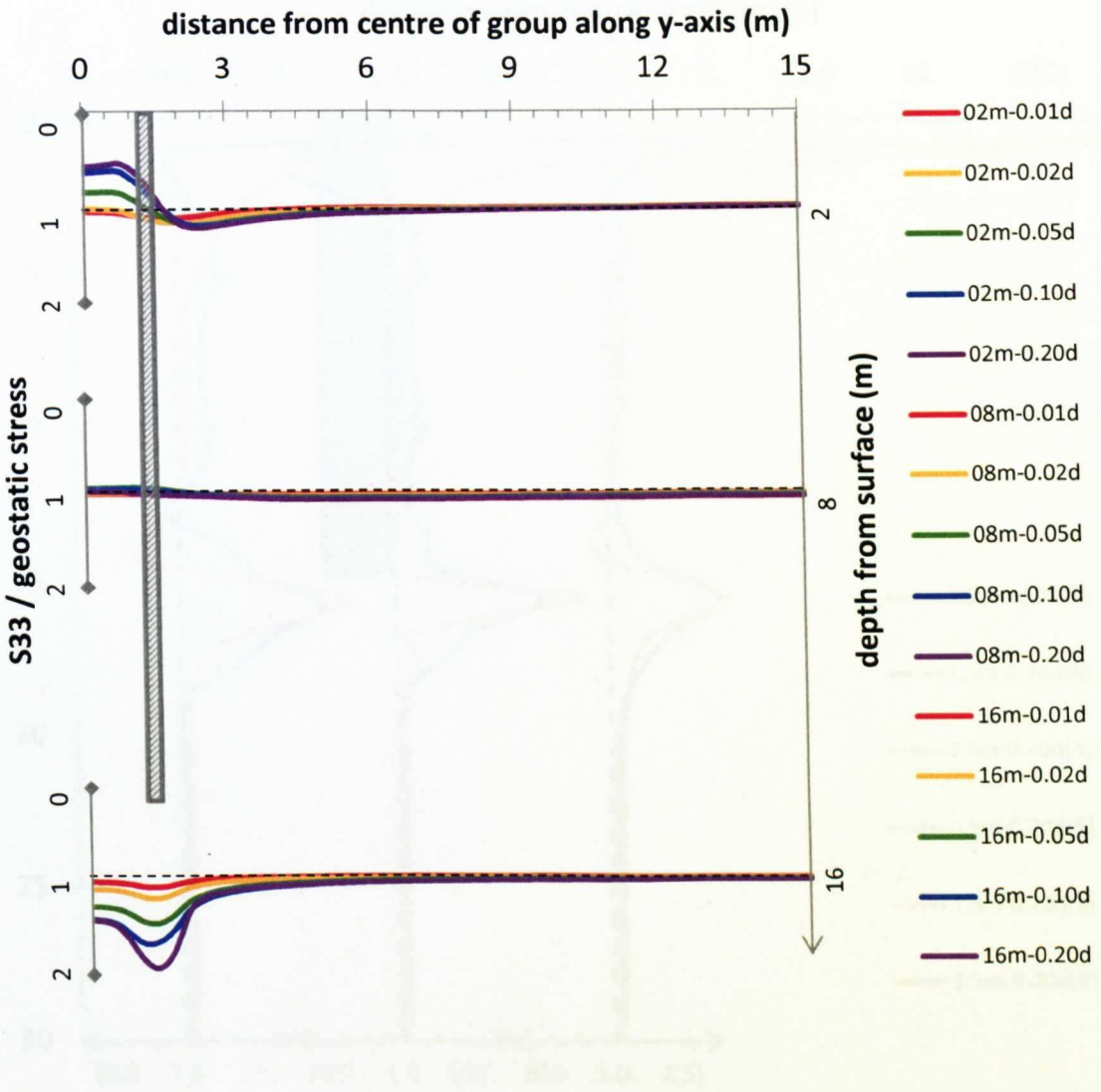

Figure 8.18 Vertical stress change with settlement (sp_B)

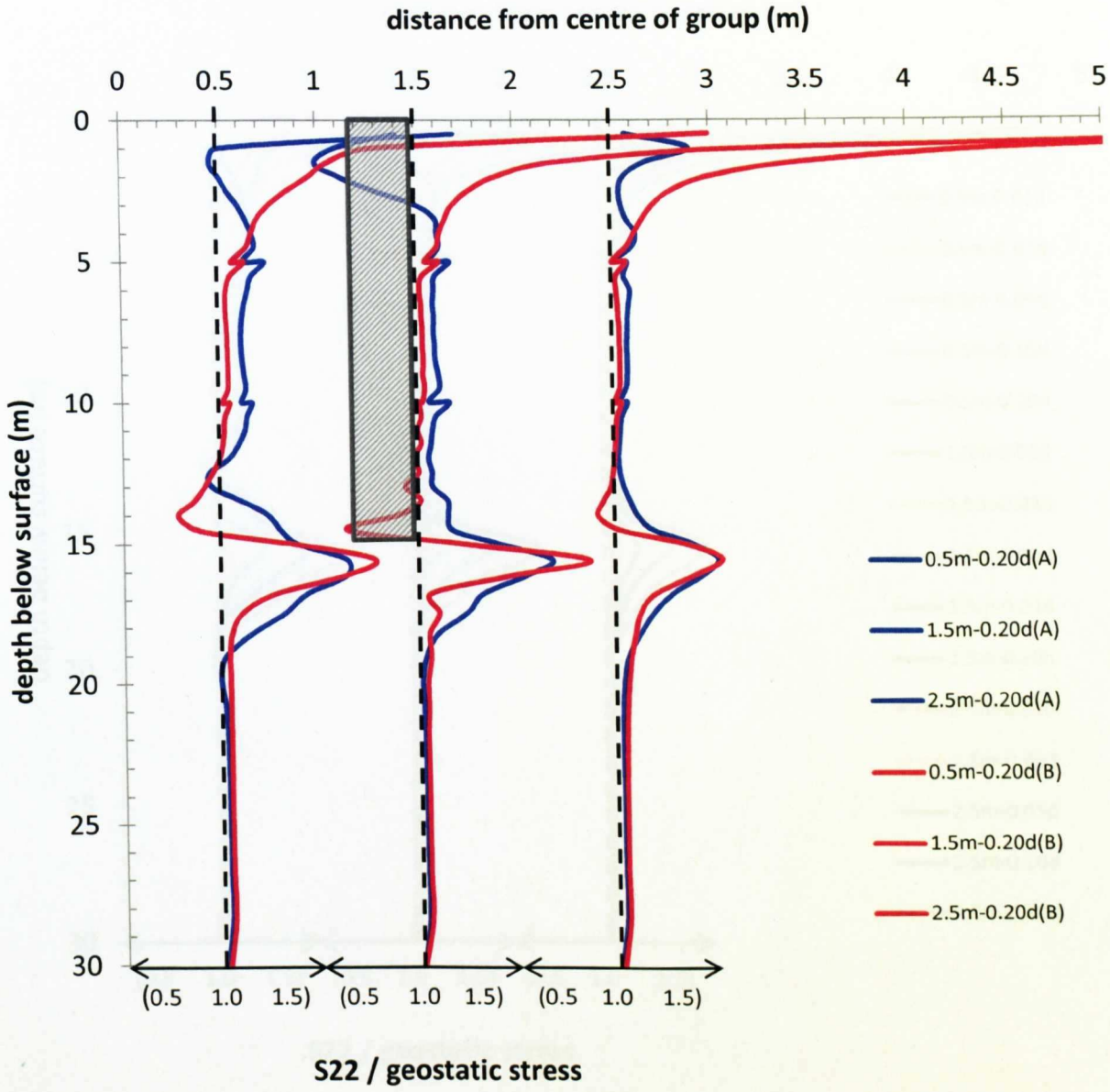

[NB: (A) = sp_A and (B) = sp_B]

Figure 8.19 Horizontal stresses for sp_A and sp_B at 0.20 d

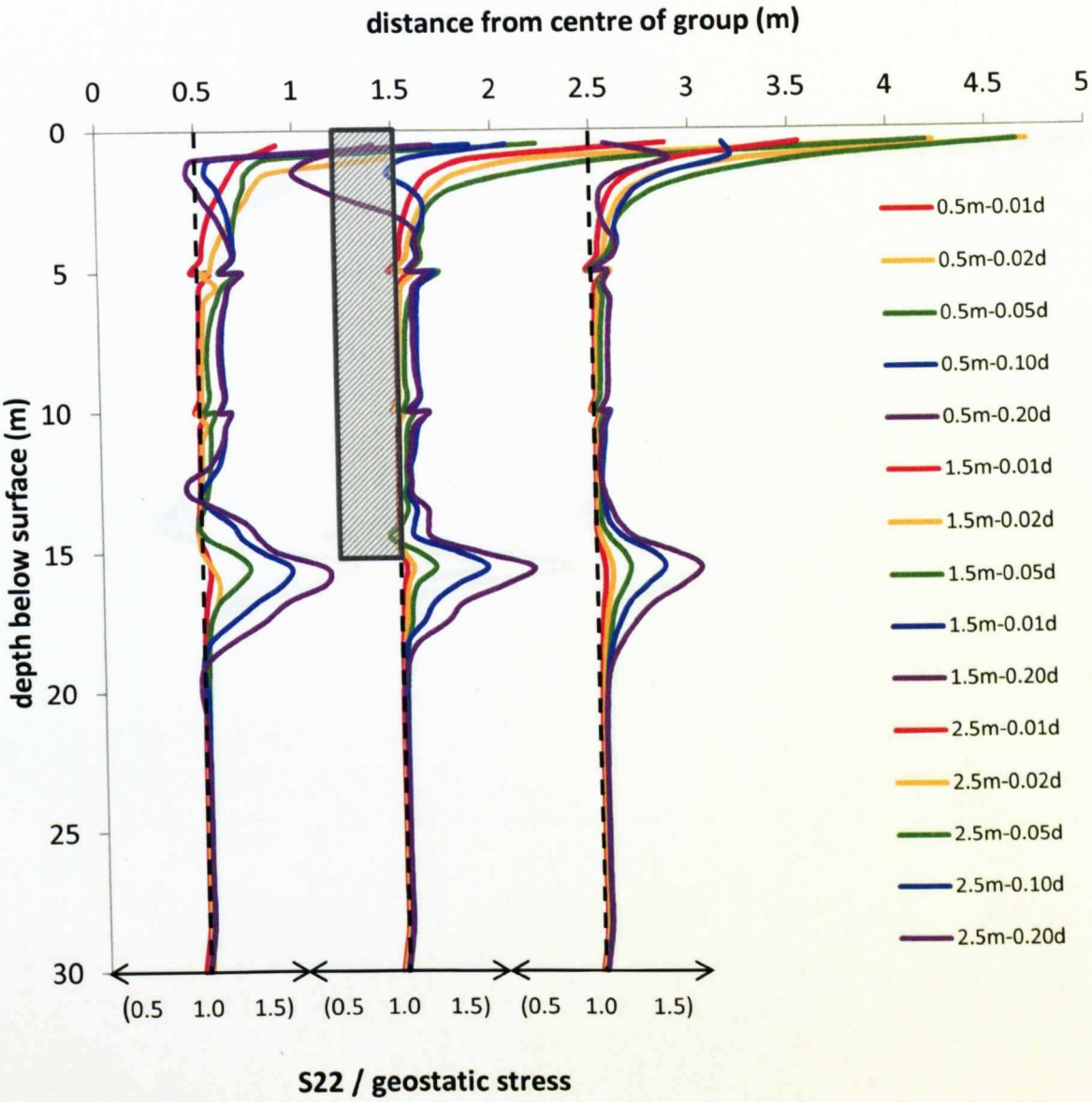

Figure 8.20 Horizontal stress change with settlement (sp_A)

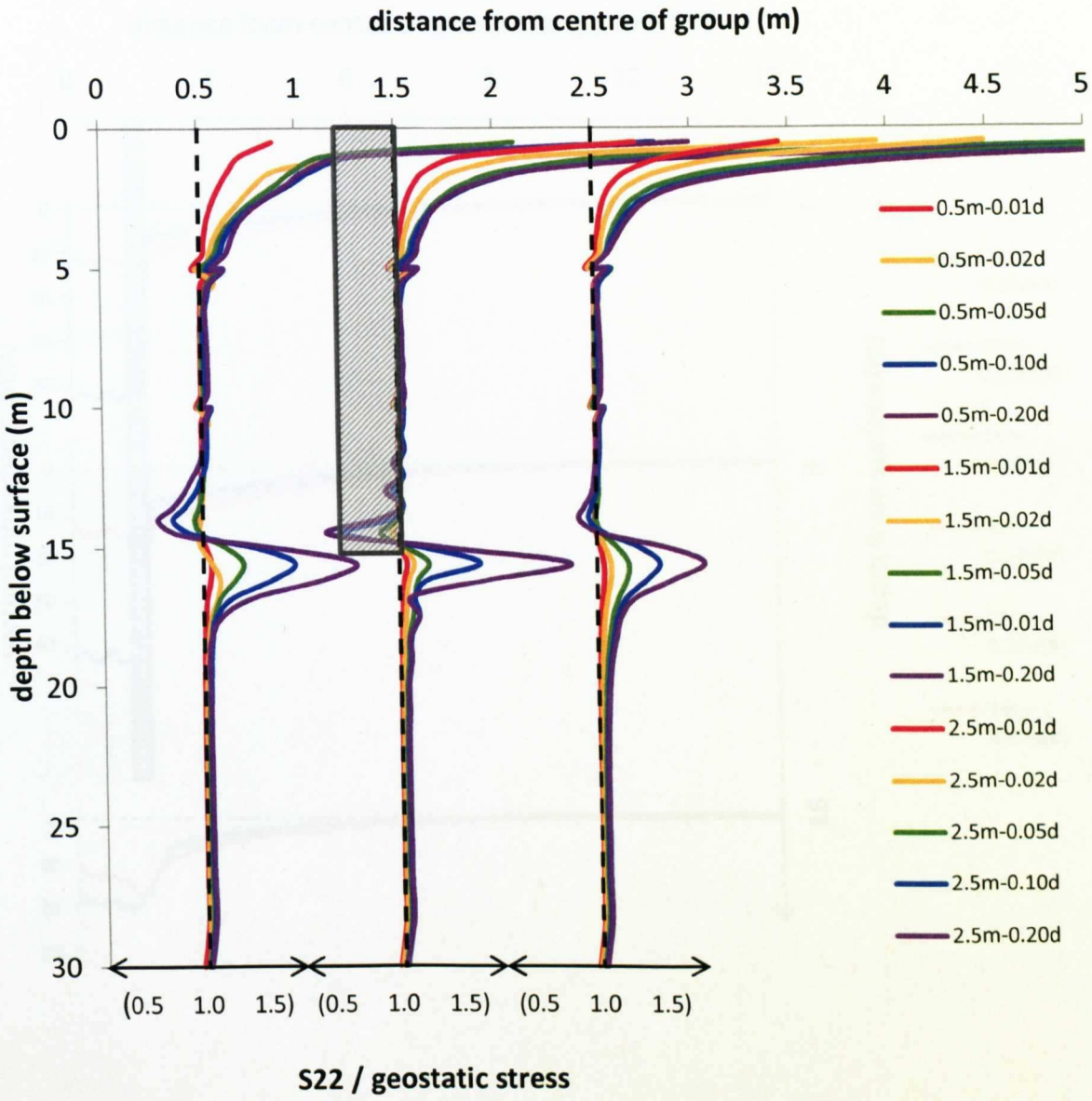

Figure 8.21 Horizontal stress change with settlement (sp_B)

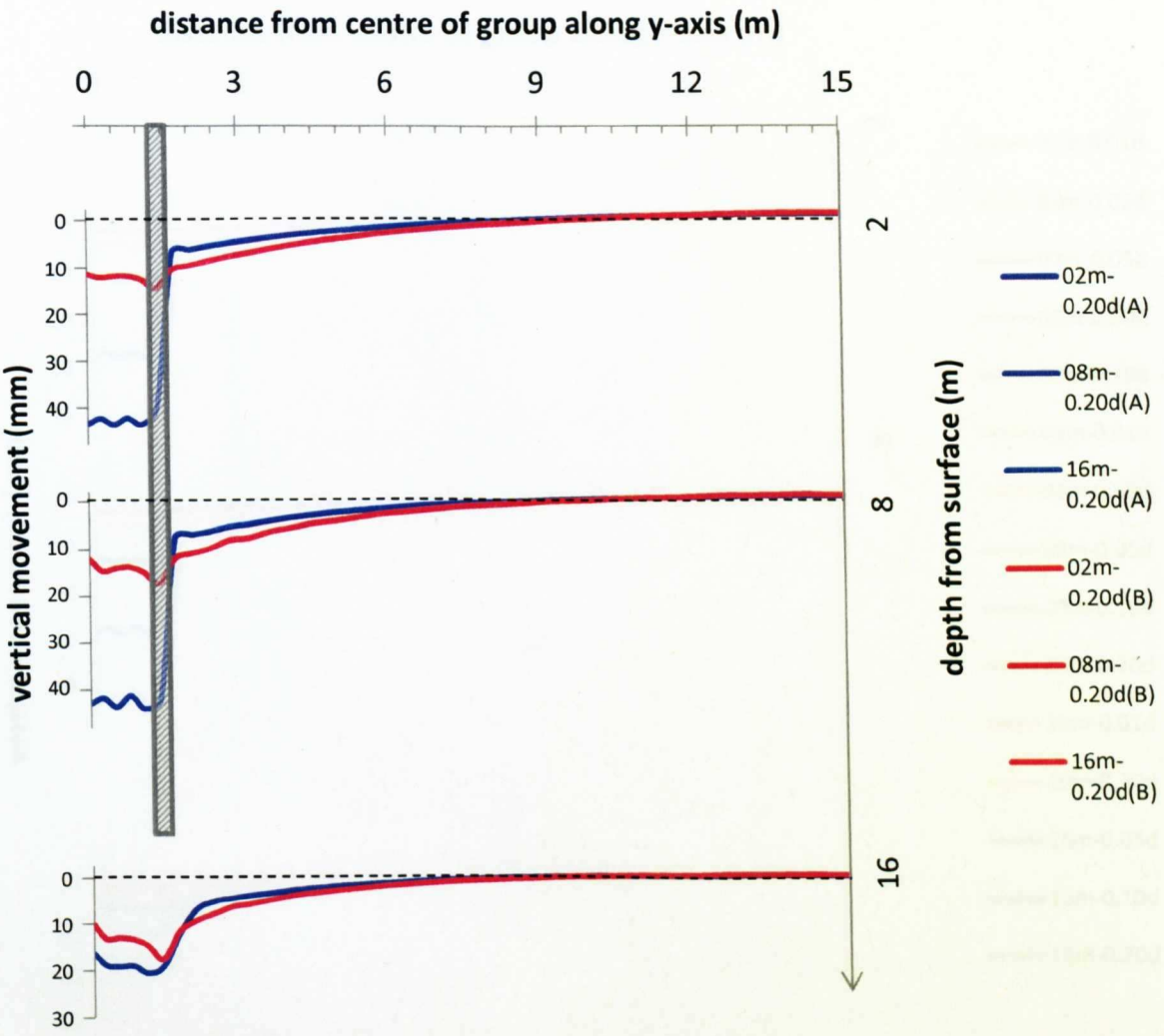

[NB: (A) = sp_A and (B) = sp_B]

Figure 8.22 Vertical soil movements for sp_A and sp_B at 0.20 d

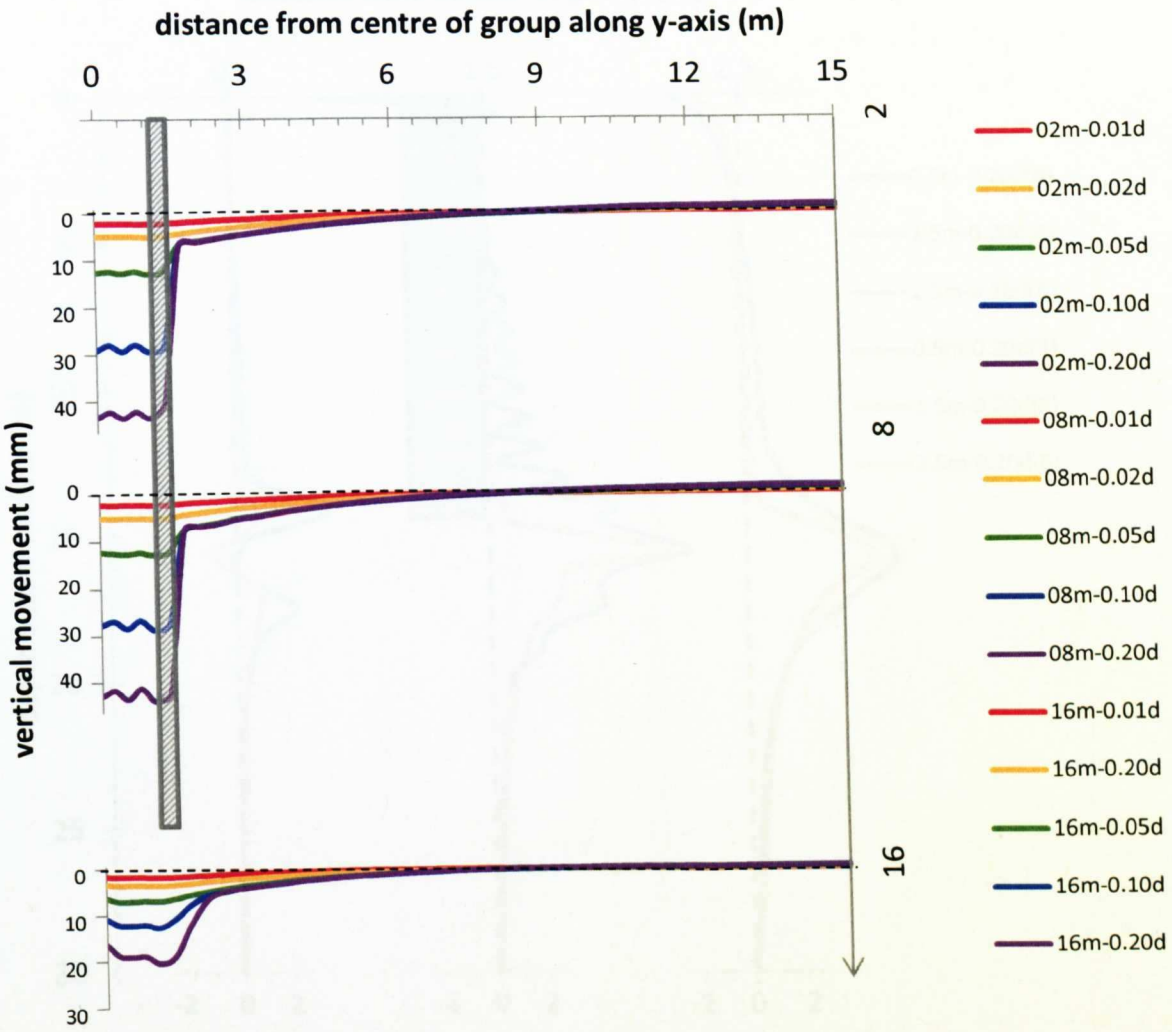

Figure 8.23 Vertical soil movement change with settlement (sp_A)

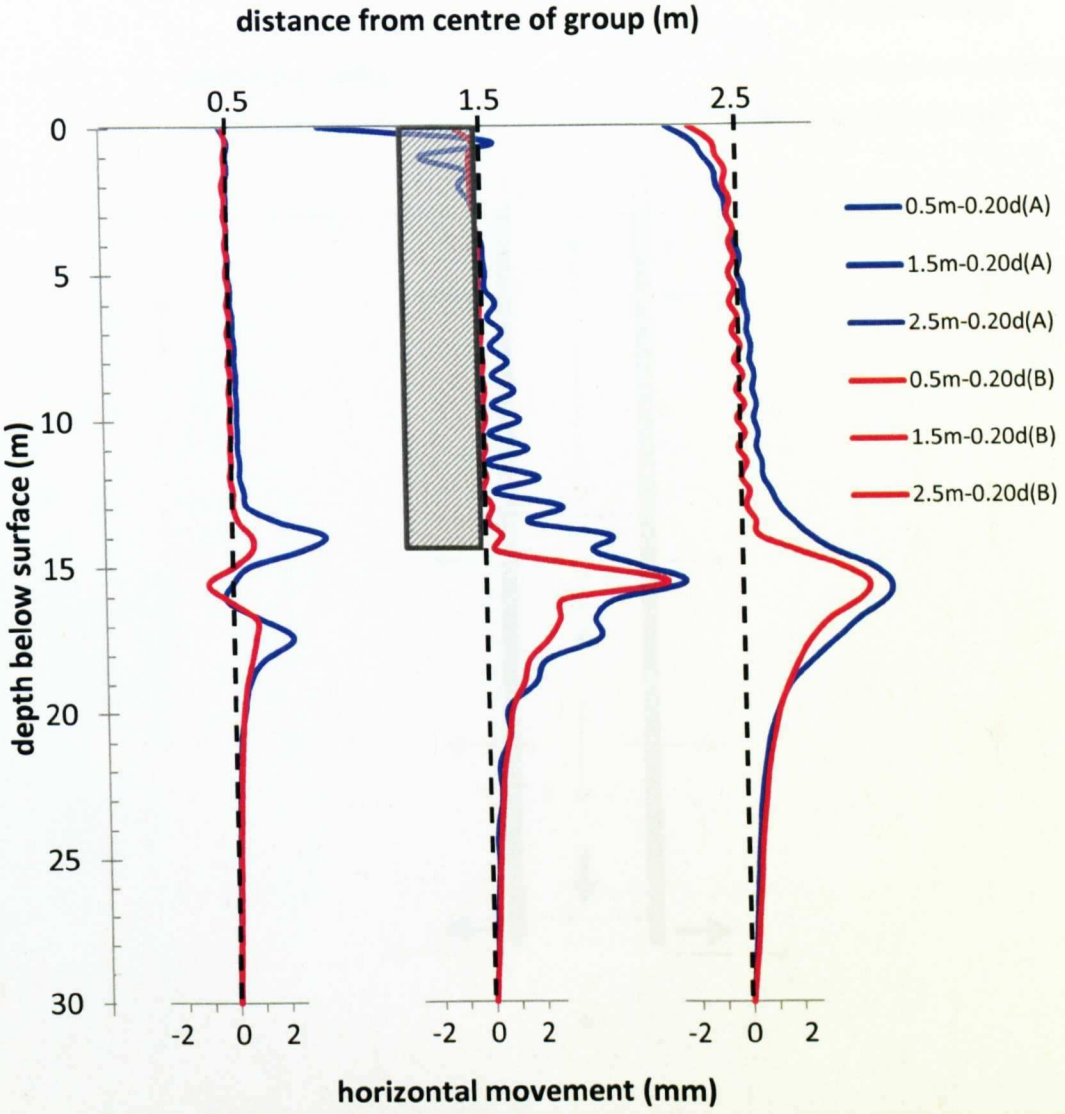

[NB: (A) = sp_A and (B) = sp_B]

Figure 8.24 Horizontal soil movements for sp_A and sp_B at 0.20 d

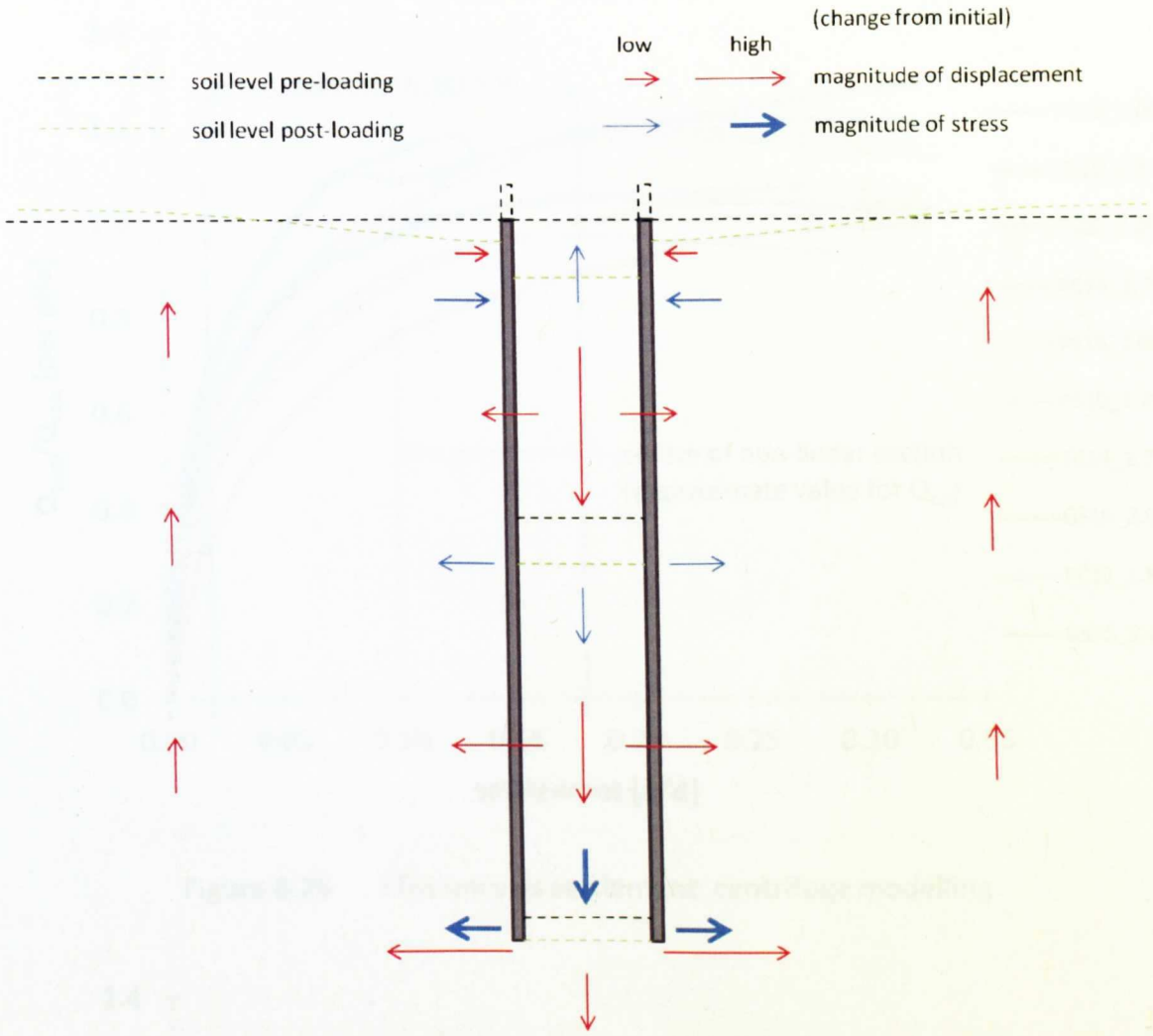

Figure 8.25 Diagram showing the change in soil stresses and movements associated with block failure

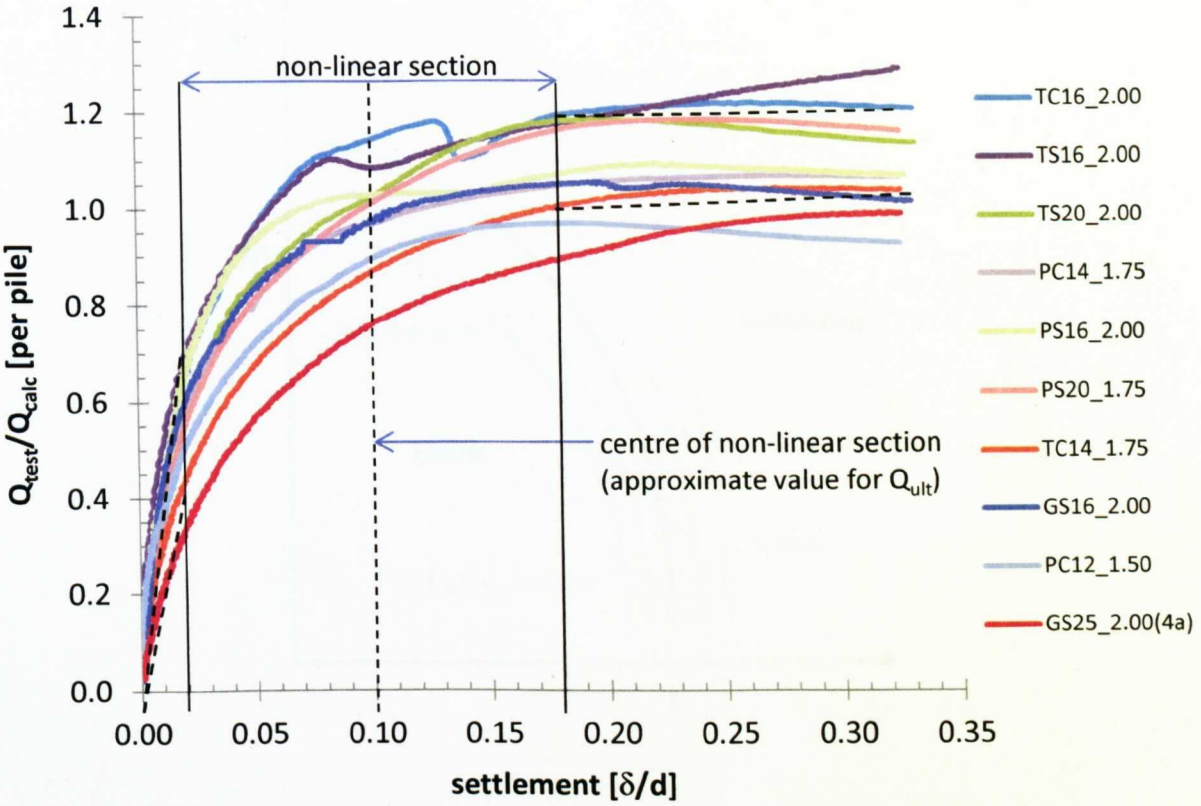

Figure 8.26 Efficiency vs settlement: centrifuge modelling

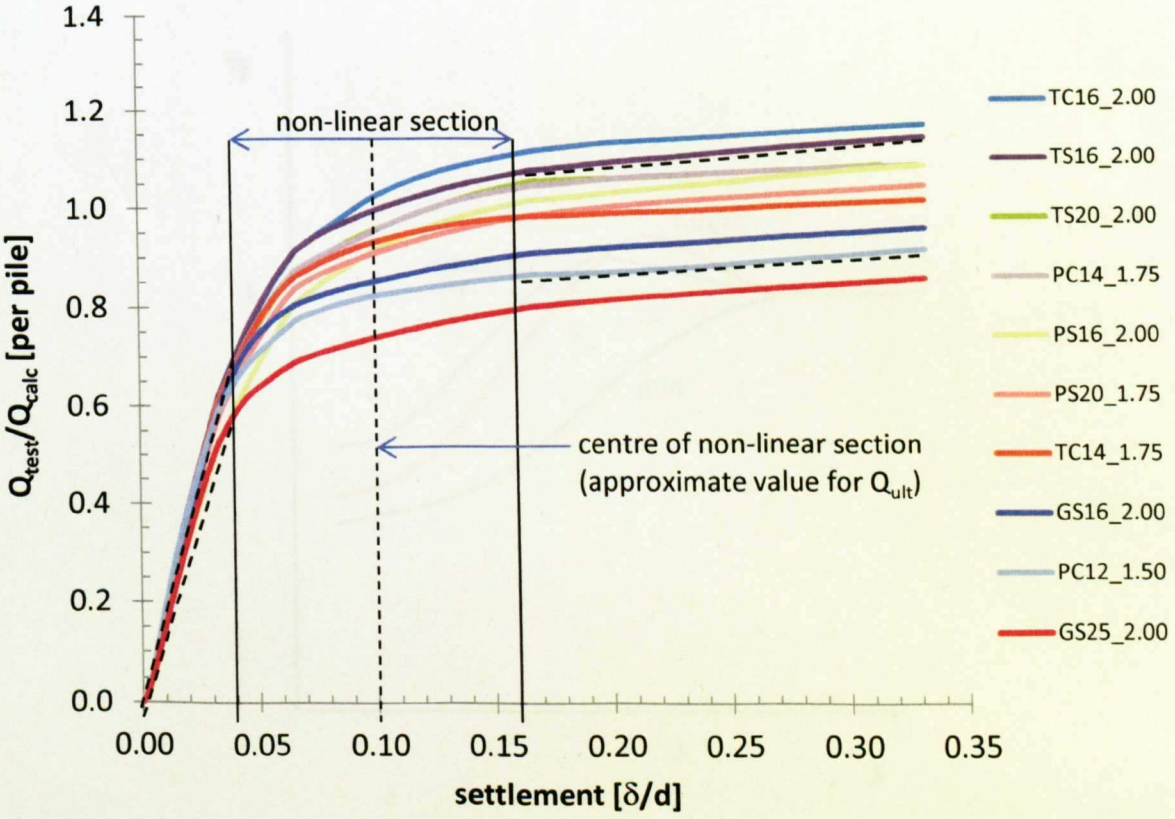

Figure 8.27 Efficiency vs settlement: numerical modelling

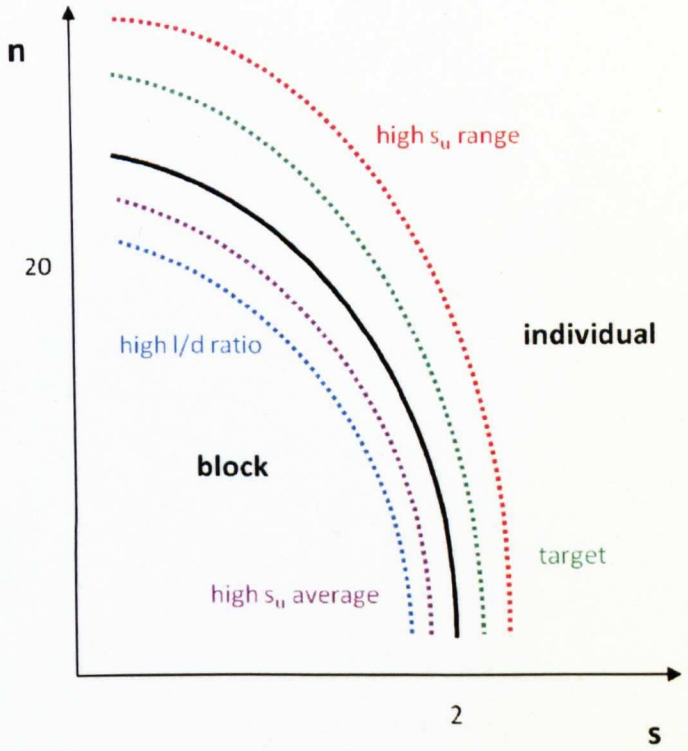

Figure 10.01 General trend showing influences on failure mechanism

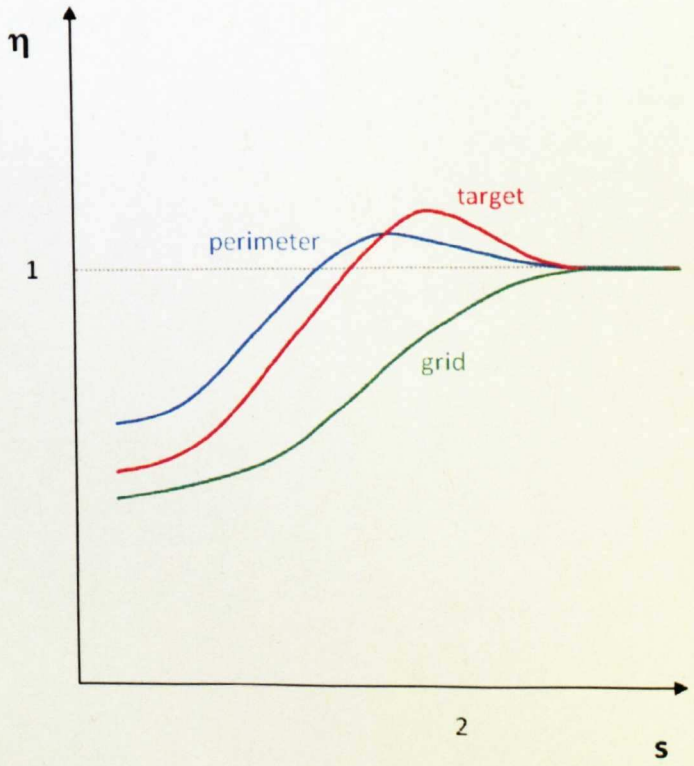

Figure 10.02 General trend of η vs s: for perimeter, target and grid groups